USDA
United States Department of Agriculture

# Forest Health Monitoring: National Status, Trends, and Analysis 2012

Editors Kevin M. Potter Barbara L. Conkling

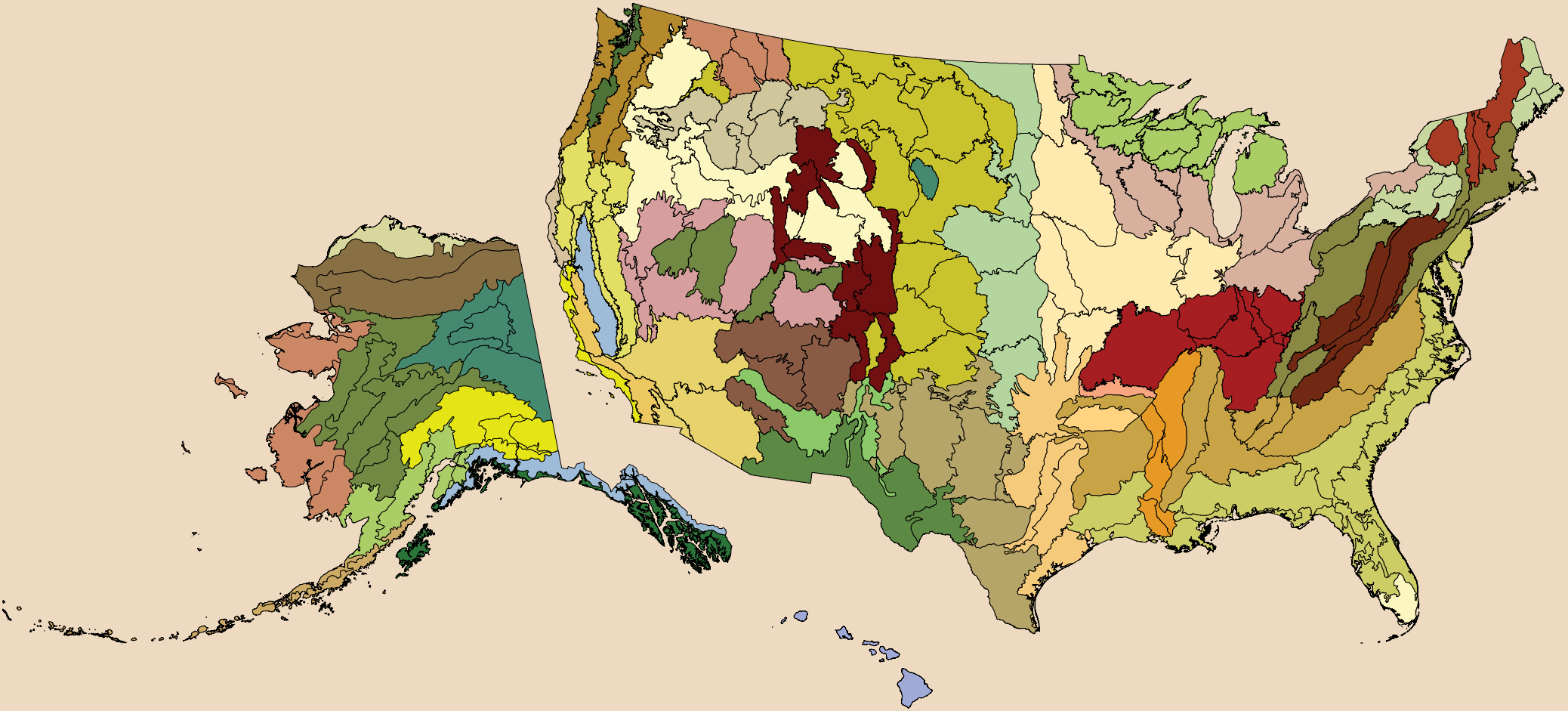

Forest Service
Research & Development
Southern Research Station
General Technical Report SRS-198

Front cover map: Ecoregion provinces and ecoregion sections for the conterminous United States (Cleland and others 2007) and for Alaska (Nowacki and Brock 1995).

Back cover map: Forest cover (green) backdrop derived from Moderate Resolution Imaging Spectroradiometer (MODIS) satellite imagery by the U.S. Forest Service Remote Sensing Applications Center.



September 2014

**Southern Research Station**
200 W.T. Weaver Blvd.
Asheville, NC 28804

www.srs.fs.usda.gov

# Forest Health Monitoring:

## National Status, Trends, and Analysis 2012

Editors

Kevin M. Potter, Research Associate Professor, North Carolina State University, Department of Forestry and Environmental Resources, Raleigh, NC 27695

Barbara L. Conkling, Research Assistant Professor, North Carolina State University, Department of Forestry and Environmental Resources, Raleigh, NC 27695

# ABSTRACT

The annual national report of the Forest Health Monitoring Program of the Forest Service, U.S. Department of Agriculture, presents forest health status and trends from a national or multi-State regional perspective using a variety of sources, introduces new techniques for analyzing forest health data, and summarizes results of recently completed Evaluation Monitoring projects funded through the national Forest Health Monitoring Program. Survey data are used to identify geographic patterns of insect and disease activity. Satellite data are employed to detect geographic clusters of forest fire occurrence. Data collected by the Forest Inventory and Analysis Program of the Forest Service are employed to detect regional differences in tree mortality. Relationships are assessed between macrolichen species richness and forest density, forest connectivity, and land cover. Macrolichen data are also used to investigate the effects of precipitation on indices used to develop nitrogen critical loads. Nine recently completed Evaluation Monitoring projects are summarized, addressing forest health concerns at smaller scales.

**Keywords**—Drought, fire, forest health, forest insects and disease, lichens, tree mortality.

# CONTENTS

# LIST OF FIGURES

*Figures, cont.*

# LIST OF TABLES

# EXECUTIVE SUMMARY

Healthy ecosystems are those that are stable and sustainable, able to maintain their organization and autonomy over time while remaining resilient to stress (Costanza 1992). Healthy forests are vital to our future (Edmonds and others 2011). The Forest Health Monitoring (FHM) Program of the Forest Service, U.S. Department of Agriculture, with cooperating researchers within and outside the Forest Service and with State partners, quantifies the health of U.S. forests (chapter 1). The analyses and results outlined in sections 1 and 2 of this FHM annual national report offer a snapshot of the current condition of U.S. forests from a national or multi-State regional perspective, incorporating baseline investigations of forest ecosystem health, examinations of change over time in forest health metrics, and assessments of developing threats to forest stability and sustainability. For datasets collected annually, analyses are presented from 2011 data. For datasets collected over several years, analyses are presented at a longer temporal scale. Chapters describe new techniques for analyzing forest health data as well as new applications of established techniques. Finally, section 3 of this report presents summaries of results from recently completed Evaluation Monitoring (EM) projects that have been funded through the FHM national Program to determine the extent, severity, causes, or all three, of specific forest health problems (FHM 2012).

Monitoring the occurrence of forest pest and pathogen outbreaks is important at regional scales because of the significant impact insects and disease can have on forest health across landscapes (chapter 2). National insect and disease survey data collected in 2011 by the Forest Health Protection Program of the Forest Service identified 78 different mortality-causing agents on nearly 2.26 million ha in the conterminous United States and 68 defoliating agents on approximately 1.54 million ha. Large geographic hot spots of forest mortality were associated with mountain pine beetle in the West. Hot spots of defoliation were spread throughout the conterminous States, associated with spruce budworm, tent caterpillar, pinyon needle scale, pine butterfly, winter moth, aspen defoliation, and baldcypress leafroller. Spruce beetle was the most important cause of mortality in Alaska, while aspen leaf miner and willow leafblotch miner were identified as the most important defoliating agents there.

Forest fire occurrence outside the historic range of frequency and intensity can result in extensive economic and ecological impacts. The detection of regional patterns of fire occurrence density can allow for the identification of areas at greatest risk of significant impact and for selecting locations for more intensive analysis (chapter 3). In 2011, ecoregions in the Southeast, the Southwest, and Texas experienced the most fires per 100 $km^2$ of

forested area. Geographic hot spots of high fire occurrence density were detected in the Southeast, the Southwest, Idaho, Oklahoma, Oregon, Texas, and Wyoming. Ecoregions in the Midwest, Northwest, Southeast, and Southwest experienced greater fire occurrence density than normal compared with the 10-year mean and accounting for variability over time. Throughout Alaska, all ecoregions experienced low fire occurrence density in 2011 and near-normal or lower-than-normal fire occurrence density compared with the 10-year mean.

Most U.S. forests experience droughts, with varying degrees of intensity and duration between and within forest ecosystems. The duration of a drought event arguably is more critical than its intensity. A standardized drought indexing approach was applied to monthly climate data from 2011 to map drought conditions across the conterminous United States at a fine scale (chapter 4). A swath of moderate-to-extreme drought conditions stretched across the southern portion of the country. North of this area, most of the United States, with the exception of an area near the Great Lakes, experienced a moisture surplus in 2011. Meanwhile, the first drought indexing analysis was conducted for Hawaii, despite the lack of monthly gridded climate data. This analysis found that areas with high variability in moisture are often drier, suggesting the importance of considering long-term moisture regime when assessing the drought conditions in particular areas of Hawaii.

Mortality is a natural process in all forested ecosystems, but high levels of mortality at large scales may indicate that the health of forests is declining. Phase 2 data collected by the Forest Inventory and Analysis (FIA) Program of the Forest Service offer tree mortality information on a relatively spatially intense basis of approximately 1 plot per 6,000 acres (chapter 5). An analysis of FIA plots from 34 States found that the highest ratios of annual mortality to gross growth occurred in ecoregion sections of the Plains States and of Florida. In three ecoregions with the highest mortality relative to growth, the predominant vegetation is grassland and most of the species experiencing the greatest mortality are commonly found in riparian areas. In all ecoregions, the plot-level ratio of average dead tree diameter to average surviving live tree diameter indicated that the trees that died were similar in size to the trees that survived, although some plots with high ratios of dead to live tree diameter existed in most ecoregions.

Using FIA lichen data, species richness of macrolichens from timed samples of fixed-area forested plots (Lichen S) has shown potential to indicate response of forests to climate (in the West) and to air quality (in the East) at large spatial scales (chapter 6). One possible confounding factor is that landscape pattern and intensity of human land use may be correlated with air quality and climate. In several ecoregions, relationships were examined for Lichen S, climate, and air quality with forest density, forest connectivity, and land cover.

The results show that land cover variables are linked to Lichen S, that relationships of land cover variables with climate and air pollution differ among regions, and that land cover is correlated with climate in the West. In the East, results indicated an effect of land cover on Lichen S independent from climate and pollution. Therefore, in the East, land cover variables should be considered for inclusion in investigations of forest ecosystem health and diversity.

The Lichen Communities Indicator is a sensitive indicator of forest health changes caused by air quality, climate change, and other stressors (chapter 7). Lichen community indicator data have been used to investigate climate effects on lichen indices used to develop critical loads for monitoring nitrogen (N) in California's forests. Nonparametric multiplicative regression models were generated for N-sensitive (oligotrophs), moderately sensitive (mesotroph), and N-loving (eutroph) lichen species. All three response indices showed sensitivity to precipitation and a nonlinear interaction between precipitation and N. The negative effect N has on oligotrophs and mesotrophs appears less severe at high-moisture sites. Eutroph abundance, conversely, appears to accumulate more quickly at dry sites for a given level of N deposition. This suggests that climate change and moisture differences among monitoring sites may skew lichen-based estimates of N deposition. It is also possible that dry conditions actually enhance susceptibility to N pollution, meaning it takes less N to extirpate sensitive species. Thus, N response indices used across heterogeneous landscapes must investigate possible interactions with moisture.

Finally, nine recently completed EM projects address a wide variety of forest health concerns at a scale smaller than the national or multi-State regional analyses included in the first sections of the report. These nine EM projects (funded by the FHM Program):

1. Investigated the effects of prescribed fire on upland oak forest ecosystems in the Missouri Ozarks to develop indicators that predict the impact of fire treatments on forest size structure and species composition (chapter 8).

2. Determined the frequencies of decline and mortality of hickory species in the Midwest and Northeast and quantified the relationships between decline and pathogen, insect presence, or both, and among priority land use, soil fertility, and drought, or all three (chapter 9).

3. Evaluated the effects of overstory thinning, prescribed fire, and understory seeding on the restoration of Iowa oak savannas and on understory and overstory indicators of forest health (chapter 10).

4. Measured the progression of laurel wilt disease in Georgia, monitored its impact on redbay and other host plants, and established a methodology to document resulting changes in vegetation composition (chapter 11).

5. Quantified fire fuels in forest stands with high levels of bark beetle-caused mortality in ponderosa pine and Douglas-fir, with or without removal of dead trees, and modeled fire behavior in these stands under severe weather scenarios (chapter 12).

6. Assessed white ash health status in the Allegheny Plateau region using an intensified ash health plot network to enhance existing FIA/FHM data and explore how site characteristics are related to ash decline and mortality patterns (chapter 13).

7. Applied forest inventory data to document patterns of Alaska yellow-cedar occurrence, mortality, and regeneration in the context of climate (chapter 14).

8. Analyzed black walnut crown conditions in Tennessee to determine if symptoms of thousand cankers disease have previously existed and evaluated the effectiveness of the FIA plot network for detecting localized forest health problems (chapter 15).

9. Quantified changes over time in Swiss needle cast severity, tree diameter, total height growth, and live-crown ratio in Douglas-fir in the northern Oregon Cascade Mountains (chapter 16).

The FHM Program, in cooperation with forest health specialists and researchers inside and outside the Forest Service, continues to investigate a broad range of issues relating to forest health using a wide variety of data and techniques. This report presents some of the latest results from ongoing national-scale detection monitoring and smaller scale environmental monitoring efforts by FHM and its cooperators. For more information about efforts to determine the status, changes, and trends in indicators of the condition of U.S. forests, please visit the FHM Web site at www.fs.fed.us/foresthealth/fhm.

## LITERATURE CITED

Costanza, R. 1992. Toward an operational definition of ecosystem health. In: Costanza, R.; Norton, B.G.; Haskell, B.D., eds. Ecosystem health: new goals for environmental management. Washington, DC: Island Press: 239-256.

Edmonds, R.L.; Agee, J.K.; Gara, R.I. 2011. Forest health and protection. Long Grove, IL: Waveland Press. 667 p.

Forest Health Monitoring (FHM). 2012. Program description. Forest Health Monitoring Fact Sheet Series. http://www.fhm.fs.fed.us/fact/. [Date accessed: June 21].

# CHAPTER 1.
## Introduction

Kevin M. Potter

Forests cover a vast area of the United States: 304 million ha, or approximately one-third of the Nation's land area (Smith and others 2009). These forests possess substantial ecological and socioeconomic importance. Both their ecological integrity and their continued capacity to provide goods and services are of concern in the face of a long list of threats, including insect and disease infestation, fragmentation, catastrophic fire, invasive species, and the effects of climate change.

Assessing and monitoring the health of these forests are critical and challenging tasks. The complexity of these tasks is reflected in the Criteria and Indicators for the Conservation and Sustainable Management of Temperate and Boreal Forests (Montréal Process Working Group 1995), which the Forest Service, U.S. Department of Agriculture, uses as a forest sustainability assessment framework (USDA Forest Service 2004, 2011). Although the concept of a healthy forest has universal appeal, forest ecologists and managers have struggled with how exactly to define forest health (Teale and Castello 2011), and they have not agreed on a universally accepted definition.

Most definitions of forest health can be categorized as representing an ecological or a utilitarian perspective (Kolb and others 1994). From an ecological perspective, the current understanding of ecosystem dynamics suggests that healthy ecosystems are those that are able to maintain their organization and autonomy over time while remaining resilient to stress (Costanza 1992) and that evaluations of forest health should emphasize factors that affect the inherent processes and resilience of forests (Kolb and others 1994, Raffa and others 2009, Edmonds and others 2011). On the other hand, the utilitarian perspective holds that a forest is healthy if management objectives are met, and that a forest is unhealthy if not (Kolb and others 1994). Although this definition may be appropriate when a single, unambiguous management objective exists, such as the production of wood fiber or the maintenance of wilderness attributes, the definition is too narrow when multiple management objectives are required (Edmonds and others 2011, Teale and Castello 2011). Teale and Castello (2011) incorporated both ecological and utilitarian perspectives into their two-component definition

of forest health. First, a healthy forest must be sustainable with respect to its size structure, including a correspondence between baseline and observed mortality, and, second, a healthy forest must meet the landowner's objectives, provided these objectives do not conflict with sustainability.

This national report, the 12th in an annual series produced by the Forest Health Monitoring (FHM) Program, attempts to quantify the status of, changes to, and trends in a wide variety of broadly defined indicators of forest health. The indicators described in this report encompass forest insect and disease activity, wildland fire occurrence, drought, tree mortality, and lichen diversity, among others.

This report has three specific objectives. The first objective is to present information about forest health from a national perspective, or from a multi-State regional perspective when appropriate, using data collected by the Forest Health Protection (FHP) and Forest Inventory and Analysis (FIA) Programs of the Forest Service as well as from other sources available at a wide extent. The chapters that present analyses at a national scale or multi-State regional scale are divided between section 1 and section 2 of the report. Section 1 presents results from the analyses of forest health data that are available annually, allowing for the detection of trends over time and changes from one year to the next. Section 2 presents longer term forest health trends in addition to describing new techniques for analyzing forest health data at national or regional scales. Although in-depth interpretation and analysis of specific geographic or ecological regions are beyond the scope of these parts of the report, the chapters in sections 1 and 2 present information that can be used to identify areas that may require investigation at a finer scale.

The second objective of the report is to present new techniques for analyzing forest health data and new applications of established techniques, presented in selected chapters of section 2. Examples in this report are chapter 6, which investigates the relationship of land cover and air quality to a lichen species richness indicator in six large geographic regions, and chapter 7, which investigates climate effects on lichen indices that are used to develop nitrogen critical loads for California forests. In addition, chapter 4, in the first section of the report, includes an innovative analysis of drought patterns in Hawaii, despite the lack

of monthly gridded climate data that was used in that chapter to conduct the annual analysis of drought status across the conterminous United States.

The third objective of the report is to present results of recently completed Evaluation Monitoring (EM) projects funded through the FHM national program. These project summaries, presented in section 3, determine the extent, severity, cause, or all three, of forest health problems (FHM 2012), generally at a finer scale than that addressed by the analyses in sections 1 and 2. Each chapter in section 3 contains an overview of an EM project and key results.

When appropriate throughout this report, authors use the Forest Service revised ecoregions (Cleland and others 2007) as a common, ecologically based spatial framework for their forest health assessments (fig. 1.1). To be specific, when the spatial scale of the data and the expectation of an identifiable pattern in the data are appropriate, authors use ecoregion sections or provinces as assessment units for their analyses. In Bailey's hierarchical system, the two broadest ecoregion scales, domains and divisions, are based on large ecological climate zones, whereas each division is broken into provinces based on vegetation macro features (Bailey 1995). Provinces are further divided into sections, which may be thousands of square kilometers in extent and are expected to encompass regions similar in their geology, climate, soils, potential natural vegetation, and potential natural communities (Cleland and others 1997).

## DATA SOURCES

Forest Service data sources included in this edition of the FHM national report are FIA annualized phase 2 and phase 3 survey data (Bechtold and Patterson 2005, Woodall and others 2010, Woudenberg and others 2010), FHP national insect and disease detection survey forest mortality and defoliation data for 2011, Moderate Resolution Imaging Spectroradiometer (MODIS) Active Fire Detections for the United States database for 2011, and forest cover data developed from MODIS satellite imagery by the Forest Service Remote Sensing Applications Center. Other sources of data are daily weather station data from the U.S. National Climatic Data Center (2012); the Parameter-Elevation Regression on Independent Slopes climate

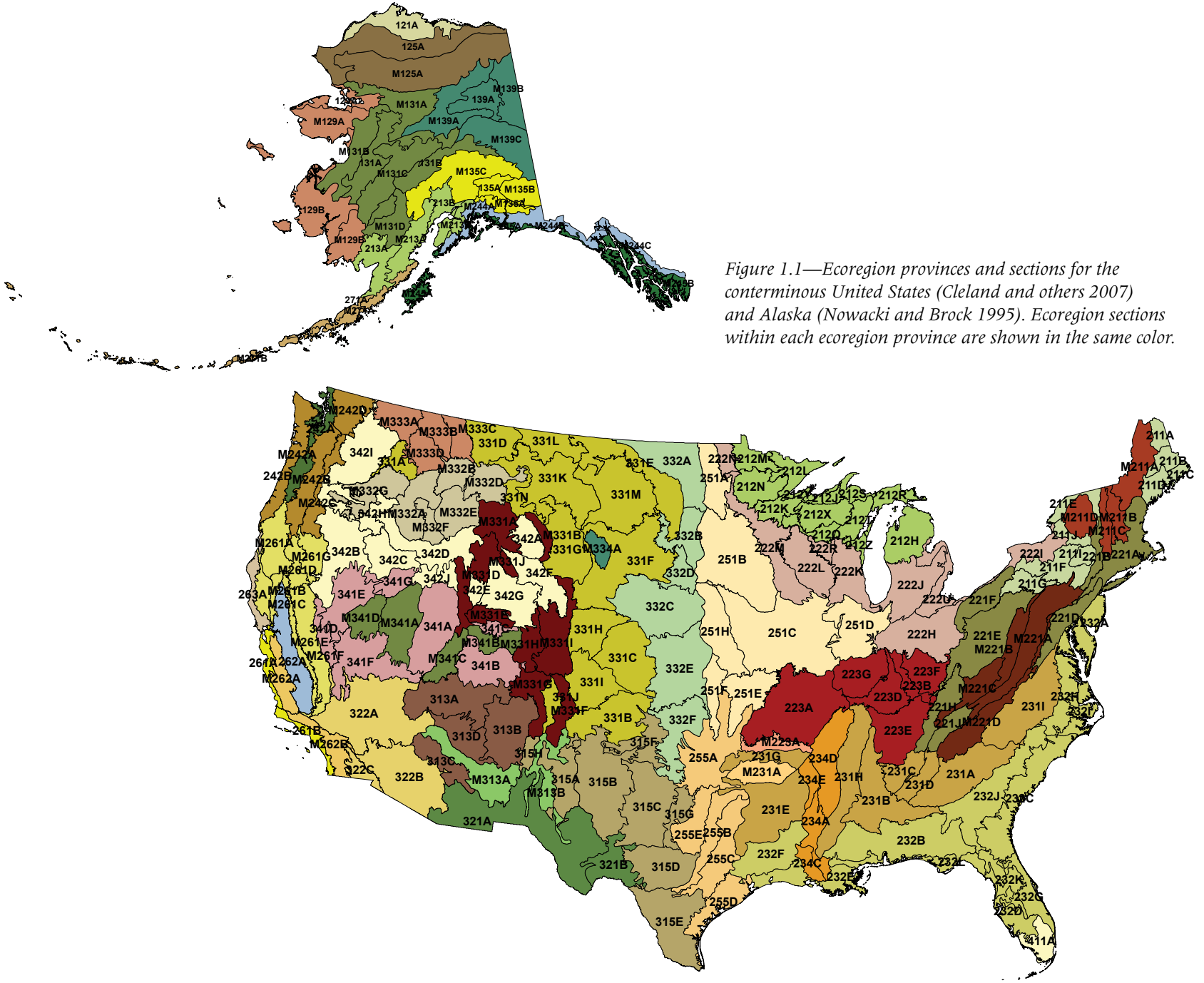


*Figure 1.1—Ecoregion provinces and sections for the conterminous United States (Cleland and others 2007) and Alaska (Nowacki and Brock 1995). Ecoregion sections within each ecoregion province are shown in the same color.*

Alaska Ecoregion Provinces

- Alaska Mixed Forest (213)
- Alaska Range Taiga (135)
- Aleutian Meadow (271)
- Arctic Tundra (121)
- Bering Sea Tundra (129)
- Brooks Range Tundra (125)
- Pacific Coastal Icefields (244)
- Pacific Gulf Coast Forest (245)
- Upper Yukon Taiga (139)
- Yukon Intermontaine Taiga (131)

Conterminous States Ecoregion Provinces

- Adirondack-New England Mixed Forest - Coniferous Forest - Alpine Meadow (M211)
- American Semi-Desert and Desert (322)
- Arizona-New Mexico Mountains Semi-Desert - Open Woodland - Coniferous Forest - Alpine Meadow (M313)
- Black Hills Coniferous Forest (M334)
- California Coastal Chaparral Forest and Shrub (261)
- California Coastal Range Open Woodland - Shrub - Coniferous Forest - Meadow (M262)
- California Coastal Steppe - Mixed Forest - Redwood Forest (263)
- California Dry Steppe (262)
- Cascade Mixed Forest - Coniferous Forest - Alpine Meadow (M242)
- Central Appalachian Broadleaf Forest-Coniferous Forest-Meadow (M221)
- Central Interior Broadleaf Forest (223)
- Chihuahuan Semi-Desert (321)
- Colorado Plateau Semi-Desert (313)
- Eastern Broadleaf Forest (221)
- Everglades (411)
- Great Plains - Palouse Dry Steppe (331)
- Great Plains Steppe (332)
- Intermountain Semi-Desert and Desert (341)
- Intermountain Semi-Desert (342)
- Laurentian Mixed Forest (212)
- Lower Mississippi Riverine Forest (234)
- Middle Rocky Mountain Steppe - Coniferous Forest - Alpine Meadow (M332)
- Midwest Broadleaf Forest (222)
- Nevada-Utah Mountains Semi-Desert - Coniferous Forest - Alpine Meadow (M341)
- Northeastern Mixed Forest (211)
- Northern Rocky Mountain Forest-Steppe - Coniferous Forest - Alpine Meadow (M333)
- Ouachita Mixed Forest-Meadow (M231)
- Outer Coastal Plain Mixed Forest (232)
- Ozark Broadleaf Forest (M223)
- Pacific Lowland Mixed Forest (242)
- Prairie Parkland (Subtropical) (255)
- Prairie Parkland (Temperate) (251)
- Sierran Steppe - Mixed Forest - Coniferous Forest - Alpine Meadow (M261)
- Southeastern Mixed Forest (231)
- Southern Rocky Mountain Steppe - Open Woodland - Coniferous Forest - Alpine Meadow (M331)
- Southwest Plateau and Plains Dry Steppe and Shrub (315)

mapping system data (Daley and Taylor 2000; PRISM Group 2004, 2012); The Rainfall Atlas of Hawaii (Giambelluca and others 2011); the 2001 National Land Cover Database (Homer and others 2007); 1998–2004 average annual wet deposition values for sulfur dioxide, nitrate, and ammonium interpolated for each plot from models using National Atmospheric Deposition Program data (Coulston and others 2004); and version 4.4 of the Community Multiscale Air Quality model (Tonneson and others 2007).

As a major source of data for FHM analyses, the FIA Program deserves detailed description. The FIA Program collects forest inventory information across all forest land ownerships in the United States and maintains a network of more than 125,000 permanent forested ground plots across the conterminous United States and southeastern Alaska, with a sampling intensity of approximately one plot per 2428 ha. FIA phase 2 encompasses the annualized inventory measured on plots at regular intervals, with each plot surveyed every 5 to 7 years in most Eastern States, but with plots in the Rocky Mountain and Pacific Northwest regions surveyed once every 10 years (Reams and others 2005). The standard 0.067-ha plot (fig. 1.2) consists of four 7.315-m radius subplots (approximately 168.6 $m^2$, or 1/24 acre), on which field crews measure trees at least 12.7 cm in diameter. Within each subplot is nested a 2.073-m radius microplot (approximately 13.48 $m^2$, or 1/300 acre), on which crews measure trees smaller than 12.7 cm in diameter. A core-optional variant of the standard design includes four "macroplots," each with a radius of 17.953 m, or approximately 0.1012 ha, that originates at the center of each subplot (Woudenberg and others 2010).

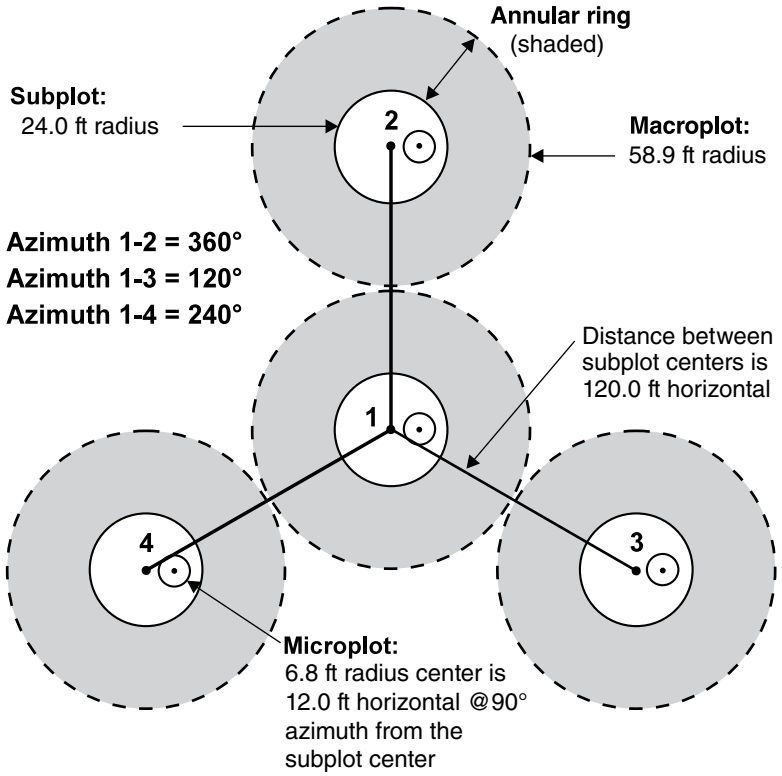


*Figure 1.2—The Forest Inventory and Analysis mapped plot design. Subplot 1 is the center of the cluster with subplots 2, 3, and 4 located 120 feet away at azimuths of 360°, 120°, and 240°, respectively (Woudenberg and others 2010).*

FIA phase 3 plots represent a subset of these phase 2 plots, with one phase 3 plot for every 16 standard FIA phase 2 plots. In addition to traditional forest inventory measurements, data for a variety of important ecological indicators are collected from phase 3 plots, including tree crown condition, lichen communities, down woody material, soil condition, and vegetation structure and diversity, while data on ozone bioindicator plants are collected on a separate grid of plots (Woodall and others 2010, 2011). Most of these additional forest health indicators were measured as part of the FHM Detection Monitoring ground plot system before 2000[1] (Palmer and others 1991).

## THE FOREST HEALTH MONITORING PROGRAM

The national FHM Program is designed to determine the status, changes, and trends in indicators of forest condition annually and covers all forested lands through a partnership encompassing the Forest Service, State foresters, and other State and Federal agencies and academic groups (FHM 2012). The FHM Program uses data from a wide variety of sources, both inside and outside the Forest Service, and develops analytical approaches for addressing forest health issues that affect the sustainability of forest ecosystems. The FHM Program has five major components (fig. 1.3):

- Detection Monitoring—nationally standardized aerial and ground surveys to evaluate status and change in condition of forest ecosystems (sections 1 and 2 of this report).
- Evaluation Monitoring—projects to determine extent, severity, and causes of undesirable changes in forest health identified through Detection Monitoring (section 3 of this report).
- Intensive Site Monitoring—projects to enhance understanding of cause-effect relationships by linking Detection Monitoring to ecosystem process studies and to assess specific issues, such as calcium depletion and carbon sequestration, at multiple spatial scales (section 3 of this report).
- Research on Monitoring Techniques—work to develop or improve indicators, monitoring systems, and analytical techniques, such as urban and riparian forest health monitoring, early detection of invasive species, multivariate analyses of forest health indicators, and spatial scan statistics (section 2 of this report).
- Analysis and Reporting—synthesis of information from various data sources within and external to the Forest Service to produce issue-driven reports on status and change in forest health at national, regional, and State levels (sections 1, 2, and 3 of this report).

[1]U.S. Department of Agriculture Forest Service. 1998. Forest Health Monitoring 1998 field methods guide. Research Triangle Park, NC: U.S. Department of Agriculture Forest Service, National Forest Health Monitoring Program. 473 p. On file with: Forest Health Monitoring Program, 3041 Cornwallis Rd., Research Triangle Park, NC 27709.

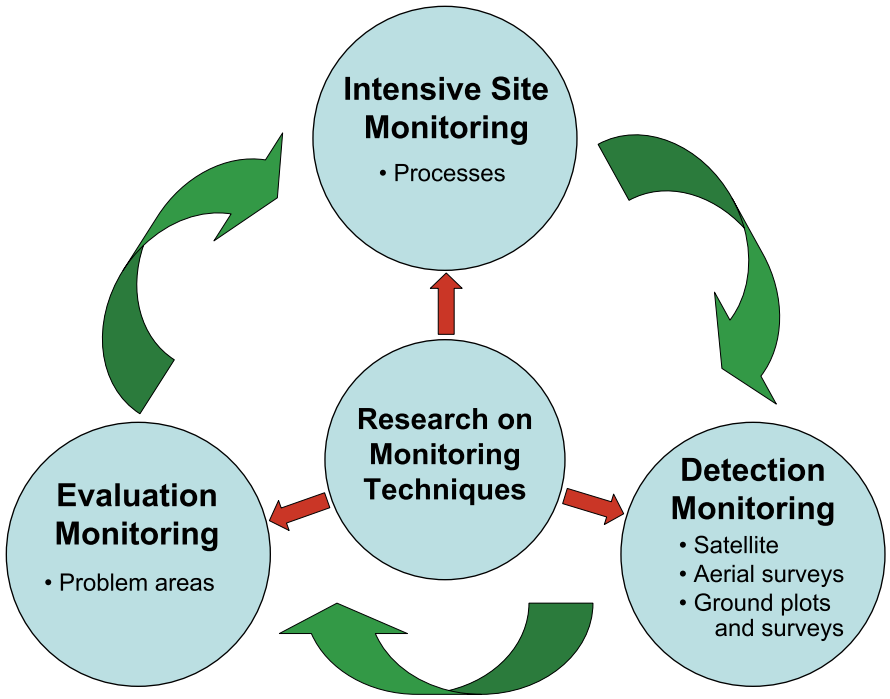


*Figure 1.3—The design of the Forest Health Monitoring (FHM) Program of the Forest Service, U.S. Department of Agriculture (FHM 2003). A fifth component, Analysis and Reporting of Results, draws from the four FHM components shown here and provides information to help support land management policies and decisions.*

In addition to its national reporting efforts, FHM generates regional and State reports. These reports may be produced with FHM partners, both within the Forest Service and in State forestry and agricultural departments. For example, the FHM regions cooperate with their respective State partners to produce the annual Forest Health Highlights report series, available on the FHM Web site at www.fs.fed.us/foresthealth/fhm. Other examples include Steinman (2004) and Harris and others (2011).

The FHM Program and its partners also produce reports and journal articles on monitoring techniques and analytical methods, including forest health data (Smith and Conkling 2004), soils as an indicator of forest health (O'Neill and others 2005), urban forest health monitoring (Cumming and others 2006, 2007; Lake and others 2006), health conditions in national forests (Morin and others 2006), crown conditions (Schomaker and others 2007, Randolph 2010, Randolph and Moser 2009), sampling and estimation procedures for vegetation diversity and structure (Schulz and others 2009), ozone monitoring (Rose and Coulston 2009), establishment of alien-invasive forest insect species (Koch and others 2011), spatial patterns of land cover (Riitters 2011), changes in forest biodiversity (Potter and Woodall 2012), and the overall forest health indicator program (Woodall and others 2010). For more information, visit the FHM Web site at www.fs.fed.us/foresthealth/fhm.

This FHM national report is produced by national forest health monitoring researchers at the Eastern Forest Environmental Threat Assessment Center, which was established under the Healthy Forest Restoration Act to generate

knowledge and tools needed to anticipate and respond to environmental threats. For more information about the research team and about threats to U.S. forests, please visit www.forestthreats.org/about.

## LITERATURE CITED


Bailey, R.G. 1995. Descriptions of the ecoregions of the United States. 2d ed. Misc. Pub. No. 1391, Map scale 1:7,500,000. Washington, DC: U.S. Department of Agriculture Forest Service. 108 p.

Bechtold, W.A.; Patterson, P.L., eds. 2005. The enhanced Forest Inventory and Analysis Program—national sampling design and estimation procedures. Gen. Tech. Rep. SRS-80. Asheville, NC: U.S. Department of Agriculture Forest Service, Southern Research Station. 85 p.

Cleland, D.T.; Avers, P.E.; McNab, W.H. [and others]. 1997. National hierarchical framework of ecological units. In: Boyce, M.S.; Haney, A., eds. Ecosystem management applications for sustainable forest and wildlife resources. New Haven, CT: Yale University Press: 181-200.

Cleland, D.T.; Freeouf, J.A.; Keys, J.E., Jr. [and others]. 2007. Ecological subregions: sections and subsections for the conterminous United States. 1:3,500,000; Albers equal area projection; colored. In: Sloan, A.M., tech. ed. Gen. Tech. Rep. WO-76. Washington, DC: U.S. Department of Agriculture Forest Service. Map, presentation scale. Also as a GIS coverage in ArcINFO format on CD-ROM or at http://fsgeodata.fs.fed.us/other_resources/ecosubregions.html. [Date accessed: March 18, 2011].

Costanza, R. 1992. Toward an operational definition of ecosystem health. In: Costanza, R.; Norton, B.G.; Haskell, B.D., eds. Ecosystem health: new goals for environmental management. Washington, DC: Island Press: 239-256.

Coulston, J.W.; Riitters, K.H.; Smith, G.C. 2004. A preliminary assessment of Montréal Process indicators of air pollution for the United States. Environmental Monitoring and Assessment. 95: 57-74.

Cumming, A.B.; Nowak, D.J.; Twardus, D.B. [and others]. 2007. Urban forests of Wisconsin: pilot monitoring project 2002. NA-FR-05-07. Newtown Square, PA: U.S. Department of Agriculture Forest Service, Northeastern Area State and Private Forestry. 33 p. Low resolution: http://www.na.fs.fed.us/pubs/fhm/pilot/pilot_study_wisconsin_02_lr.pdf . High resolution: http://www.na.fs.fed.us/pubs/fhm/pilot/pilot_study_wisconsin2_02_hr.pdf. [Date accessed: October 19].

Cumming, A.B.; Twardus, D.B.; Smith, W.D. 2006. National Forest Health Monitoring Program, Maryland and Massachusetts street tree monitoring pilot projects. NA-FR-01-06. Newtown Square, PA: U.S. Department of Agriculture Forest Service Northeastern Area, State and Private Forestry. 23 p.

Daly, C.; Taylor, G. 2000. United States average monthly or annual precipitation, temperature, and relative humidity 1961-90. Arc/INFO and ArcView coverages. Corvallis, OR: Oregon State University, Spatial Climate Analysis.

Edmonds, R.L.; Agee, J.K.; Gara, R.I. 2011. Forest health and protection. Long Grove, IL: Waveland Press. 667 p.

Forest Health Monitoring (FHM). 2003. Forest health monitoring: a national strategic plan. http://fhm.fs.fed.us/annc/strategic_plan03.pdf. [Date accessed: June 22, 2012].

Forest Health Monitoring (FHM). 2012. Program description. Forest Health Monitoring Fact Sheets Series. http://www.fhm.fs.fed.us/fact/. [Date accessed: June 21].

Giambelluca, T.W.; Chen, Q.; Frazier, A.G. [and others]. 2011. The rainfall atlas of Hawai'i [web page]. http://rainfall.geography.hawaii.edu. [Date accessed: January 17, 2012].

Harris, J.L., comp.; Region 2 FHP staff. 2011. Forest health conditions, 2009–2010: Rocky Mountain Region (R2). R2-11-RO-31. Golden, CO: U.S. Department of Agriculture Forest Service, Renewable Resources, Forest Health Protection, Rocky Mountain Region. 108 p.

Homer, C.; Dewitz, J.; Fry, J. [and others]. 2007. Completion of the 2001 National Land Cover Database for the conterminous United States. Photogrammetric Engineering and Remote Sensing. 73: 337-341.

Koch, F.H.; Yemshanov, D.; Colunga-Garcia, M. [and others]. 2011. Potential establishment of alien-invasive forest insect species in the United States: where and how many? Biological Invasions. 13: 969-985.

Kolb, T.E.; Wagner, M.R.; Covington, W.W. 1994. Concepts of forest health: utilitarian and ecosystem perspectives. Journal of Forestry. 92: 10-15.

Lake, M.; Marshall, P.; Mielke, M. [and others]. 2006. National Forest Health Monitoring Program monitoring urban forests in Indiana: pilot study 2002, part 1. Analysis of field methods and data collection. Gen. Tech. Rep. NA FR-06-06. Newtown Square, PA: U.S. Department of Agriculture Forest Service, Northeastern Area. http://www.fhm.fs.fed.us/pubs/ufhm/indianaforests02/indianaforests02.html. [Date accessed: November 6, 2007].

Montréal Process Working Group. 1995. Criteria and indicators for the conservation and sustainable management of temperate and boreal forests. http://www.rinya.maff.go.jp/mpci/rep-pub/1995/santiago_e.html. [Date accessed: June 21, 2012].

Morin, R.S.; Liebhold, A.M.; Gottschalk, K.W. [and others]. 2006. Analysis of forest health monitoring surveys on the Allegheny National Forest (1998–2001). Gen. Tech. Rep. NE-339. Newtown Square, PA: U.S. Department of Agriculture Forest Service, Northeastern Research Station. 102 p. http://www.fs.fed.us/ne/newtown_square/publications. [Date accessed: November 6, 2007].

National Climatic Data Center. 2012. Climate data online—monthly surface data (DS3220). http://cdo.ncdc.noaa/pls/plclimprod/somdmain.somdwrapper?datasetabbv= DS3220&countryabbv=&georegionabbv=&forceoutside=. [Date accessed: February 17].

Nowacki, G.; Brock, T. 1995. Ecoregions and subregions of Alaska, EcoMap Version 2.0. 1:5,000,000; colored. Juneau, AK: U.S. Department of Agriculture Forest Service, Alaska Region.

O'Neill, K.P.; Amacher, M.C.; Perry, C.H. 2005. Soils as an indicator of forest health: a guide to the collection, analysis, and interpretation of soil indicator data in the Forest Inventory and Analysis Program. Gen. Tech. Rep. NC-258. St. Paul, MN: U.S. Department of Agriculture Forest Service, North Central Research Station. 53 p.

Palmer, C.J.; Riitters, K.H.; Strickland, T. [and others]. 1991. Monitoring and research strategy for forests—Environmental Monitoring and Assessment Program (EMAP). EPA/600/4-91/012. Washington, DC: U.S. Environmental Protection Agency. 187 p.

Potter, K.M.; Woodall, C.W. 2012. Trends over time in tree and seedling phylogenetic diversity indicate regional differences in forest biodiversity change. Ecological Applications. 22(2): 517-531.

PRISM Group. 2004. 2.5-arcmin (4 km) gridded monthly climate data. http://www.prismclimate.org. [Date accessed: June 20, 2012].

PRISM Group. 2012. 2.5-arcmin (4 km) gridded monthly climate data. ftp://prism.oregonstate.edu//pub/prism/us/grids. [Date accessed: April 23, 2012].

Raffa, K.F.; Aukema, B.; Bentz, B.J. [and others]. 2009. A literal use of "forest health" safeguards against misuse and misapplication. Journal of Forestry. 107: 276-277.

Randolph, K.C. 2010. Equations relating compacted and uncompacted live crown ratio for common tree species in the South. Southern Journal of Applied Forestry. 34(3): 118-123.

Randolph, K.C.; Moser, W.K. 2009. Tree crown conditions in Missouri, 2000–2003. Gen. Tech. Rep. SRS–113. Asheville, NC: U.S. Department of Agriculture Forest Service, Southern Research Station. 11 p.

Reams, G.A.; Smith, W. D.; Hansen, M.H. [and others]. 2005. The Forest Inventory and Analysis sampling frame. In: Bechtold, W.A.; Patterson, P.L., eds. The enhanced Forest Inventory and Analysis Program—national sampling design and estimation procedures. Asheville, NC: U.S. Department of Agriculture Forest Service, Southern Research Station: 11-26.

Riitters, K.H. 2011. Spatial patterns of land cover in the United States: a technical document supporting the Forest Service 2010 RPA Assessment. Gen. Tech. Rep. SRS-136. Asheville, NC: U.S. Department of Agriculture Forest Service, Southern Research Station. 64 p.

Rose, A.K.; Coulston, J.W. 2009. Ozone injury across the Southern United States, 2002–06. Gen. Tech. Rep. SRS–118. Asheville, NC: U.S. Department of Agriculture Forest Service, Southern Research Station. 25 p.

Schomaker, M.E.; Zarnoch, S.J.; Bechtold, W.A. [and others]. 2007. Crown-condition classification: a guide to data collection and analysis. Gen. Tech. Rep. SRS-102. Asheville, NC: U.S. Department of Agriculture Forest Service, Southern Research Station. 78 p.

Schulz, B.K.; Bechtold, W.A.; Zarnoch, S.J. 2009. Sampling and estimation procedures for the vegetation diversity and structure indicator. Gen. Tech. Rep. PNW-GTR-781. Portland, OR: U.S. Department of Agriculture Forest Service, Pacific Northwest Research Station. 53 p.

Smith, W.D.; Conkling, B.L. 2004. Analyzing forest health data. Gen. Tech. Rep. SRS-077. Asheville, NC: U.S. Department of Agriculture Forest Service, Southern Research Station. 33 p. http://www.srs.fs.usda.gov/pubs/gtr/gtr_srs077.pdf. [Date accessed: November 6, 2007].

Smith, W.B.; Miles, P.D.; Perry, C.H.; Pugh, S.A. 2009. Forest resources of the United States, 2007. Gen. Tech. Rep. WO-78. St. Paul, MN: U.S. Department of Agriculture Forest Service, Washington Office. 336 p.

Steinman, J. 2004. Forest health monitoring in the Northeastern United States: disturbances and conditions during 1993–2002. NA-Technical Paper 01-04. Newtown Square, PA: U.S. Department of Agriculture Forest Service, State and Private Forestry, Northeastern Area. 46 p. http://fhm.fs.fed.us/pubs/tp/dist_cond/dc.shtml. [Date accessed: December 8, 2009].

Teale, S.A.; Castello, J.D. 2011. The past as key to the future: a new perspective on forest health. In: Castello, J.D.; Teale, S.A., eds. Forest health: an integrated perspective. New York: Cambridge University Press: 3-16.

Tonnesen, G.; Wang, Z.; Omary, M.; Chien, C.J. 2007. Assessment of nitrogen deposition: modeling and habitat assessment. Sacramento, CA: California Energy Commission, PIER Energy-Related Environmental Research. www.energy.ca.gov/2006publications/CEC-500-2006-032/CEC-500-2006-032.PDF. [Date accessed: June 20, 2012].

U.S. Department of Agriculture (USDA) Forest Service. 2004. National report on sustainable forests—2003. FS-766. Washington, DC: U.S. Department of Agriculture Forest Service. 139 p.

U.S. Department of Agriculture (USDA) Forest Service. 2011. National report on sustainable forests—2010. FS-979. Washington, DC: U.S. Department of Agriculture Forest Service. 134 p.

Woodall, C.W.; Amacher, M.C.; Bechtold, W.A. [and others]. 2011. Status and future of the forest health indicators program of the USA. Environmental Monitoring and Assessment. 177: 419-436.

Woodall, C.W.; Conkling, B.L.; Amacher, M.C. [and others]. 2010. The Forest Inventory and Analysis database: database description and users manual version 4.0 for phase 3. Gen. Tech. Rep. NRS-61. Newtown Square, PA: U.S. Department of Agriculture Forest Service, Northern Research Station. 180 p.

Woudenberg, S.W.; Conkling, B.L.; O'Connell, B.M. [and others]. 2010. The Forest Inventory and Analysis database: database description and users manual version 4.0 for phase 2. Gen. Tech. Rep. RMRS-GTR-245. Fort Collins, CO: U.S. Department of Agriculture Forest Service, Rocky Mountain Research Station. 336 p.

# SECTION 1.
## Analyses of Short-Term Forest Health Data

# CHAPTER 2.

# Large-Scale Patterns of Insect and Disease Activity in the Conterminous United States and Alaska from the National Insect and Disease Survey, 2011

Kevin M. Potter
Jeanine L. Paschke

## INTRODUCTION

The impacts of insects and pathogens on forests vary from natural thinning to extraordinary levels of tree mortality, but the fact that insects and diseases kill trees does not necessarily make them enemies of the forest (Teale and Castello 2011). If disturbances, pests, and diseases are viewed in their full ecological context, then some amount can be considered "healthy" to sustain the structure of the forest (Manion 2003, Zhang and others 2011) by causing the tree mortality that culls weak competitors and releases resources that are needed to support the growth of the surviving trees (Teale and Castello 2011).

Recognizing how much mortality is natural, and how much is excessive, is an important task for forest managers, pathologists, and entomologists, and relates to ecologically based or commodity-based management objectives (Teale and Castello 2011). Diseases and insects cause changes in forest structure and function, species succession, and biodiversity, which may be considered negative or positive depending on management objectives (Edmonds and others 2011).

Analyzing patterns of forest pest infestations, disease occurrences, forest declines, and related biotic stress factors is necessary to monitor the health of forested ecosystems and their potential impacts on forest structure, composition, biodiversity, and species distributions (Castello and others 1995). Introduced nonnative insects and diseases, in particular, can extensively damage the diversity, ecology, and economy of affected areas (Brockerhoff and others 2006, Mack and others 2000). Few forests remain unaffected by invasive species, and their devastating impacts in forests are undeniable, including, in some cases, wholesale changes to the structure and function of an ecosystem (Parry and Teale 2011).

Examining pest occurrences and related stress factors from a landscape-scale perspective is useful, given the regional extent of many infestations and the large-scale complexity of interactions among host distribution, stress factors, and the development of pest outbreaks (Holdenrieder and others 2004). The detection of geographic clusters of disturbance is one such landscape-scale approach that allows for the identification of areas at greater risk of significant impact and for the selection of locations for more intensive monitoring and analysis.

## METHODS

Nationally compiled Forest Health Protection (FHP) low-altitude aerial survey and ground survey data (FHM 2005) can be used to identify forest landscape-scale patterns associated with geographic hot spots of forest insect and disease activity in the conterminous 48 States and to summarize insect and disease activity by ecoregion in Alaska (Potter and Koch 2012, Potter 2012, Potter 2013, Potter and Paschke 2013). In 2011, FHP surveys covered approximately 147.9 million ha of the forested area in the conterminous United States

(58 percent of the total), and 8.0 million ha of Alaska's forested area (15.6 percent of the total) (fig. 2.1).

These surveys identify areas of mortality and defoliation caused by insect and pathogen activity, although some important forest insects (such as emerald ash borer and hemlock woolly adelgid), diseases (such as laurel wilt, Dutch elm disease, white pine blister rust, and thousand cankers disease), and mortality complexes (such as oak decline) are not easily detected or thoroughly quantified through aerial detection surveys. Such pests may attack hosts that are widely dispersed throughout forests with high tree species diversity or may cause mortality or defoliation that is otherwise difficult to detect. A pathogen or insect might be considered a mortality-causing agent in one location and a defoliation-causing agent in another, depending on the level of damage to the forest in a given area and the convergence of stress factors such as drought. In some cases, the identified agents of mortality or defoliation are actually complexes of multiple agents summarized under an impact label related to a specific host tree species (e.g., "subalpine fir mortality" or "aspen defoliation"). In addition, differences in data collection, attribute recognition, and coding procedures among States and regions can complicate the analysis of the data and the interpretation of the results.

The 2011 mortality and defoliation polygons were used to identify the mortality and defoliation agents and complexes found on more than 5000 ha of forest in the conterminous United States in that year and to identify and list the most widely detected defoliation and mortality agents for Alaska. As a result of the insect and disease sketch-mapping process, all quantities are "footprint" areas for the agent or complex, outlining the areas within which the agent or complex is present. Unaffected trees may exist within the footprint, and the amount of damage within the footprint is not reflected in the estimates of forest area affected. The sum of agents and complexes is not equal to the total affected area as a result of reporting multiple agents per polygon in some situations.

A Getis-Ord hot spot analysis (Getis and Ord 1992) was employed in ArcMap 9.2 (ESRI 2006) to identify surveyed forest areas with the greatest exposure to the detected mortality- and defoliation-causing agents and complexes. The Environmental Monitoring and Assessment Program North American hexagon coordinates (White and others 1992) were intensified to develop a lattice of hexagonal cells, of 2500 $km^2$ extent, for the conterminous United States. This cell size allows for analysis at a medium-scale resolution of about the same area as a typical county. The percentage of surveyed forest area in each hexagon exposed to either mortality-causing or defoliation-causing agents was then calculated by masking the surveyed area and mortality and defoliation polygons with a forest cover map (1-$km^2$ resolution), derived from Moderate Resolution Imaging Spectroradiometer (MODIS) satellite imagery by the Forest Service Remote Sensing Applications Center (USDA Forest Service 2008). The percentage

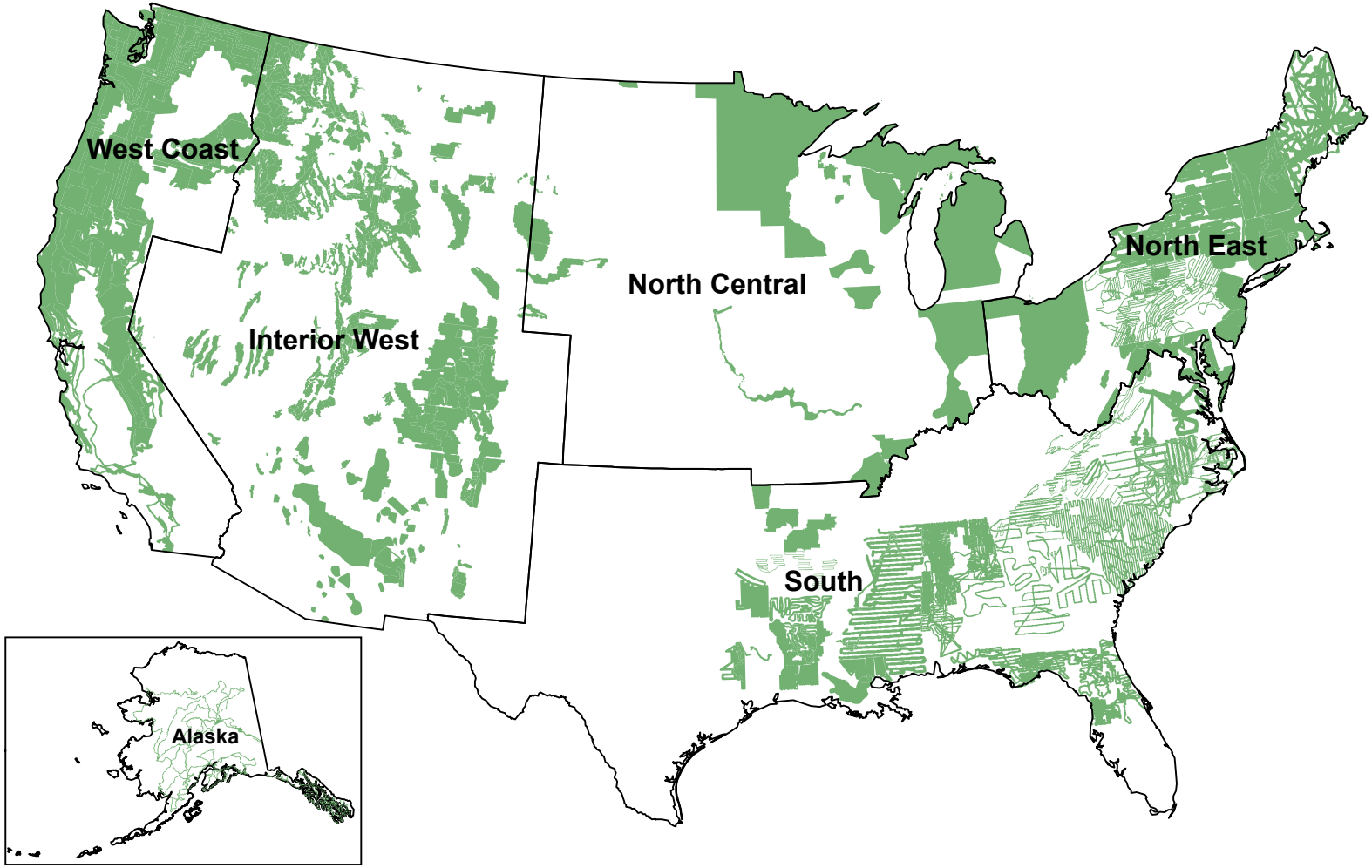


*Figure 2.1—The extent of surveys for insect and disease activity conducted in the conterminous United States and Alaska in 2011. The black lines delineate Forest Health Monitoring regions. (Data source: USDA Forest Service, Forest Health Protection Program.)*

of surveyed forest exposed to mortality or defoliation agents was calculated by dividing the total forest-masked damage area by the forest-masked surveyed area.

The Getis-Ord $G_i^*$ statistic was used to identify clusters of hexagonal cells in which the percentage of surveyed forest exposed to mortality or defoliation agents was higher than expected by chance. This statistic allows for the decomposition of a global measure of spatial association into its contributing factors, by location, and is therefore particularly suitable for detecting nonstationarities in a dataset, such as when spatial clustering is concentrated in one subregion of the data (Anselin 1992).

The Getis-Ord $G_i^*$ statistic for each hexagon summed the differences between the mean values in a local sample, determined by a moving window consisting of each hexagon and its 18 first- and second-order neighbors (the 6 adjacent hexagons and the 12 additional hexagons contiguous to those 6), and the global mean of all the forested hexagonal cells in the conterminous 48 States. It is then standardized as a $z$-score with a mean of 0 and a standard deviation of 1, with values greater than 1.96 representing significant ($p < 0.025$) local clustering of high values and values less than -1.96 representing significant clustering of low values ($p < 0.025$), because 95 percent of the observations under a normal distribution should be within approximately 2 standard deviations of the mean (Laffan 2006). In other words, a $G_i^*$ value of 1.96 indicates that the local mean of the percentage of forest exposed to mortality- or defoliation-causing agents for a hexagon and its 18 neighbors is approximately 2 standard deviations greater than the mean expected in the absence of spatial clustering, whereas a $G_i^*$ value of -1.96 indicates that the local mortality or defoliation mean for a hexagon and its 18 neighbors is approximately 2 standard deviations less than the mean expected in the absence of spatial clustering. Values between -1.96 and 1.96 have no statistically significant concentration of high or low values. In other words, when a hexagon has a $G_i^*$ value between -1.96 and 1.96, it and its 18 neighbors have neither consistently high nor consistently low percentages of forest exposed to mortality- or defoliation-causing agents.

It is worth noting that the threshold values are not exact because the correlation of spatial data violates the assumption of independence required for statistical significance (Laffan 2006). The Getis-Ord approach does not require that the input data be normally distributed because the local $G_i^*$ values are computed under a randomization assumption, with $G_i^*$ equating to a standardized $z$-score that asymptotically tends to a normal distribution (Anselin 1992). The $z$-scores are reliable, even with skewed data, as long as the distance band used to define the local sample around the target observation is large enough to include several neighbors for each feature (ESRI 2006).

The low density of survey data from Alaska in 2011 (fig. 2.1) precluded the use of hot spot analyses for the State. Instead, mortality and defoliation data were summarized by ecoregion

section (Nowacki and Brock 1995), calculated as the percentage of the forest within the surveyed areas affected by agents of mortality or defoliation. For reference purposes, ecoregion sections (Cleland and others 2007) were also displayed on the geographic hot spot maps of the conterminous 48 States.

## RESULTS AND DISCUSSION

The FHP survey data identified 78 different mortality-causing agents on approximately 2.26 million ha across the conterminous United States in 2011, an area slightly larger than that of the combined land area of New Jersey and Rhode Island. (Of these mortality-cause categories, three were "rollups" of multiple agents.) By way of comparison, forests cover about 304 million ha of the conterminous 48 States (Smith and others 2009).

Mountain pine beetle (*Dendroctonus ponderosae*) was the most widespread mortality agent, detected on 1.54 million ha (table 2.1). Other mortality agents and complexes detected across very large areas, each affecting more than 100 000 ha, were five-needle pine decline, spruce beetle (*D. rufipennis*), fir engraver (*Scolytus ventralis*), and subalpine fir (*Abies lasiocarpa*) mortality. Mortality from the western bark beetle group, encompassing 19 different agents in the insect and disease survey data (table 2.2), was detected on a total of more than 2.12 million ha in 2011, a large majority of the total area on which mortality was recorded.

**Table 2.1—Mortality agents and complexes affecting more than 5000 ha in the conterminous United States in 2011**

| Agents/complexes causing mortality, 2011 | Area |
|---|---|
| | *ha* |
| Mountain pine beetle[a] | 1 542 877.2 |
| Five-needle pine decline[a] | 160 423.2 |
| Spruce beetle | 153 570.3 |
| Fir engraver | 128 156.5 |
| Subalpine fir mortality[a] | 122 372.5 |
| Western pine beetle | 82 649.6 |
| Douglas-fir beetle | 64 624.5 |
| Spruce budworm | 46 147.9 |
| Ips | 40 962.0 |
| Bark beetles | 38 585.5 |
| Sudden aspen decline[b] | 18 622.1 |
| Beech bark disease | 13 745.3 |
| Emerald ash borer | 9 245.1 |
| Western balsam bark beetle[c] | 9 129.3 |
| Hemlock decline | 8 125.0 |
| Unknown | 8 011.1 |
| Balsam woolly adelgid | 6 703.0 |
| Decline | 6 142.6 |
| Flatheaded borer | 5 077.3 |
| Other mortality agents (59) | 38 733.9 |
| **Total, all agents** | **2 258 275.6** |

Note: All values are "footprint" areas for each agent or complex. The sum of the individual agents is not equal to the total for all agents because of overlapping damage polygons.

[a] Rollup of multiple agent codes from the Insect and Disease Survey database.

[b] Includes mortality, defoliation, and decline.

[c] Also included in the subalpine fir mortality rollup.

**Table 2.2—Beetle taxa included in the "western bark beetle" group**

| Western bark beetle taxa | Genus and species |
|---|---|
| Douglas-fir beetle | *Dendroctonus pseudotsugae* |
| Fir engraver | *Scolytus ventralis* |
| Flatheaded borer | *Buprestidae* |
| Ips engraver beetles | *Ips* spp. |
| Jeffrey pine beetle | *D. jeffreyi* |
| Mountain pine beetle | *D. ponderosae* |
| Northern spruce engraver beetle | *Ips perturbatus* |
| Roundheaded pine beetle | *D. adjunctus* |
| Silver fir beetle | *Pseudohylesinus sericeus* |
| Spruce beetle | *D. rufipennis* |
| Tip beetles | *Pityogenes* spp. |
| Western balsam bark beetle | *Dryocoetes confusus* |
| Western cedar bark beetle | *Phloeosinus punctatus* |
| Western pine beetle | *Dendroctonus brevicomis* |
| Bark beetles | Nonspecific |

In addition, the survey identified 68 defoliation agents affecting about 2.84 million ha across the conterminous United States in 2011, an area slightly smaller than the land area of New Hampshire and Delaware combined. (Of these defoliation-cause categories, 4 were "rollups" of multiple agents.) The most widespread defoliators were western and eastern spruce budworms (*Choristoneura occidentalis* and *C. fumiferana*), affecting 1.95 million ha (table 2.3). Tent caterpillars (*Malacosoma* spp.), pinyon needle scale (*Matsucoccus acalyptus*), and pine butterfly (*Neophasia menapia*) each affected more than 100 000 ha.

The Forest Health Monitoring (FHM) Program Interior West region (as defined by the FHM

**Table 2.3—Defoliation agents and complexes affecting more than 5000 ha in the conterminous United States in 2011**

| Agents/complexes causing defoliation, 2011 | Area |
|---|---|
| | *ha* |
| Spruce budworm (eastern and western)[a] | 1 954 235.3 |
| Tent caterpillars[a] | 284 609.0 |
| Pinyon needle scale | 260 652.0 |
| Pine butterfly | 101 339.6 |
| Douglas-fir tussock moth | 47 875.0 |
| Winter moth | 36 791.0 |
| Aspen defoliation[b] | 36 043.9 |
| Needlecast | 35 602.0 |
| Baldcypress leafroller | 17 694.3 |
| Unknown | 12 676.1 |
| Larch casebearer | 12 404.2 |
| Larch needle blight | 10 522.3 |
| Birch leaf fungus | 10 106.4 |
| Jack pine budworm | 8 507.2 |
| Large aspen tortrix | 8 411.0 |
| Larger elm leaf beetle | 7 619.3 |
| Western hemlock looper | 7 570.6 |
| Unknown defoliator | 6 737.5 |
| Oak worms | 6 266.7 |
| Larch needle cast | 5 552.0 |
| Pinyon sawfly | 5 358.6 |
| Other defoliation agents (46) | 48 592.1 |
| **Total, all agents** | **2 837 254.8** |

Note: All values are "footprint" areas for each agent or complex. The sum of the individual agents is not equal to the total for all agents because of overlapping damage polygons.

[a] Rollup of multiple agent codes from the Insect and Disease Survey database.

[b] Includes mortality, defoliation, and decline.

Program) had, by far, the largest area on which mortality-causing agents were detected in 2011, approximately 1.72 million ha (table 2.4). A large majority of mortality within that area was associated with mountain pine beetle, although spruce beetle, subalpine fir mortality, and five-needle pine decline were also important mortality agents and complexes.

The Getis-Ord analysis detected the three largest and most clustered hot spots of mortality exposure in the Interior West region (fig. 2.2). The most intense was centered on the M331I-Northern Parks and Ranges ecoregion section of north-central Colorado and south-central Wyoming and included much of M331H-North Central Highlands and Rocky Mountains and M331G-Southern Central Highlands. This hot spot, not surprisingly, was associated with extensive mountain pine beetle mortality in lodgepole and ponderosa pine forests. Spruce beetle mortality was also present. Meanwhile, a very large hot spot of mortality exposure, also caused primarily by mountain pine beetle, extended across several ecoregions in central Idaho and western Montana, including M332E-Beaverhead Mountains, M322B-Northern Rockies and Bitterroot Valley, M332D-Belt Mountains, M332A-Idaho Batholith, M332F-Challis Volcanics, and M331A-Yellowstone Highlands. This hot spot overlapped with a third hot spot centered on M331J-Wind River Mountains of Wyoming and that extended into the neighboring M331D-Overthrust Mountains and the Yellowstone Highlands. In addition to mountain pine beetle, five-needle pine decline was a major cause of mortality in this area.

**Table 2.4—The top five mortality agents or complexes for each Forest Health Monitoring region in 2011**

| Mortality agents, 2011 | Area |
|---|---|
| | *ha* |
| **Interior West** | |
| Mountain pine beetle[a] | 1 339 848.3 |
| Spruce beetle | 147 567.0 |
| Subalpine fir mortality[a] | 118 752.1 |
| Five-needle pine decline[a] | 130 800.2 |
| Douglas-fir beetle | 51 964.5 |
| Other mortality agents (18) | 101 196.4 |
| **Total, all agents** | **1 715 790.3** |
| **North Central** | |
| Spruce budworm | 46 147.9 |
| Mountain pine beetle[a] | 26 911.1 |
| Beech bark disease | 13 253.1 |
| Emerald ash borer | 5 708.9 |
| Oak wilt | 1 053.2 |
| Other mortality agents (13) | 1 193.9 |
| **Total, all agents** | **94 268.1** |
| **North East** | |
| Unknown | 6 354.7 |
| Forest tent caterpillar | 4 667.2 |
| Decline | 4 600.5 |
| Gypsy moth | 3 791.2 |
| Emerald ash borer | 3 536.2 |
| Other mortality agents (33) | 7 344.2 |
| **Total, all agents** | **30 013.8** |

| Mortality agents, 2011 | Area |
|---|---|
| | *ha* |
| **South** | |
| Hemlock woolly adelgid | 1 433.5 |
| Southern pine beetle | 88.4 |
| Unknown | 43.8 |
| Ips | 39.9 |
| Bark beetles (nonspecific) | 39.6 |
| Black turpentine beetle | 0.1 |
| **Total, all agents** | **1 645.2** |
| **West Coast** | |
| Mountain pine beetle[a] | 176 117.2 |
| Fir engraver | 121 722.6 |
| Western pine beetle | 59 443.6 |
| Bark beetles (nonspecific) | 38 399.5 |
| Douglas-fir beetle | 12 660.0 |
| Other mortality agents (26) | 45 985.1 |
| **Total, all agents** | **416 558.2** |
| **Alaska** | |
| Spruce beetle | 19 761.2 |
| Alaska yellow-cedar decline | 10 833.9 |
| Northern spruce engraver beetle | 2 675.5 |
| Unspecified mortality | 2 519.8 |
| Western balsam bark beetle | 1.0 |
| **Total, all agents** | **35 791.5** |

Note: The total area affected by other agents is listed at the end of each section. All values are "footprint" areas for each agent or complex. The sum of the individual agents may not equal the total for all agents because of overlapping damage polygons.

[a] Rollup of multiple agent codes in the Insect and Disease Survey database.

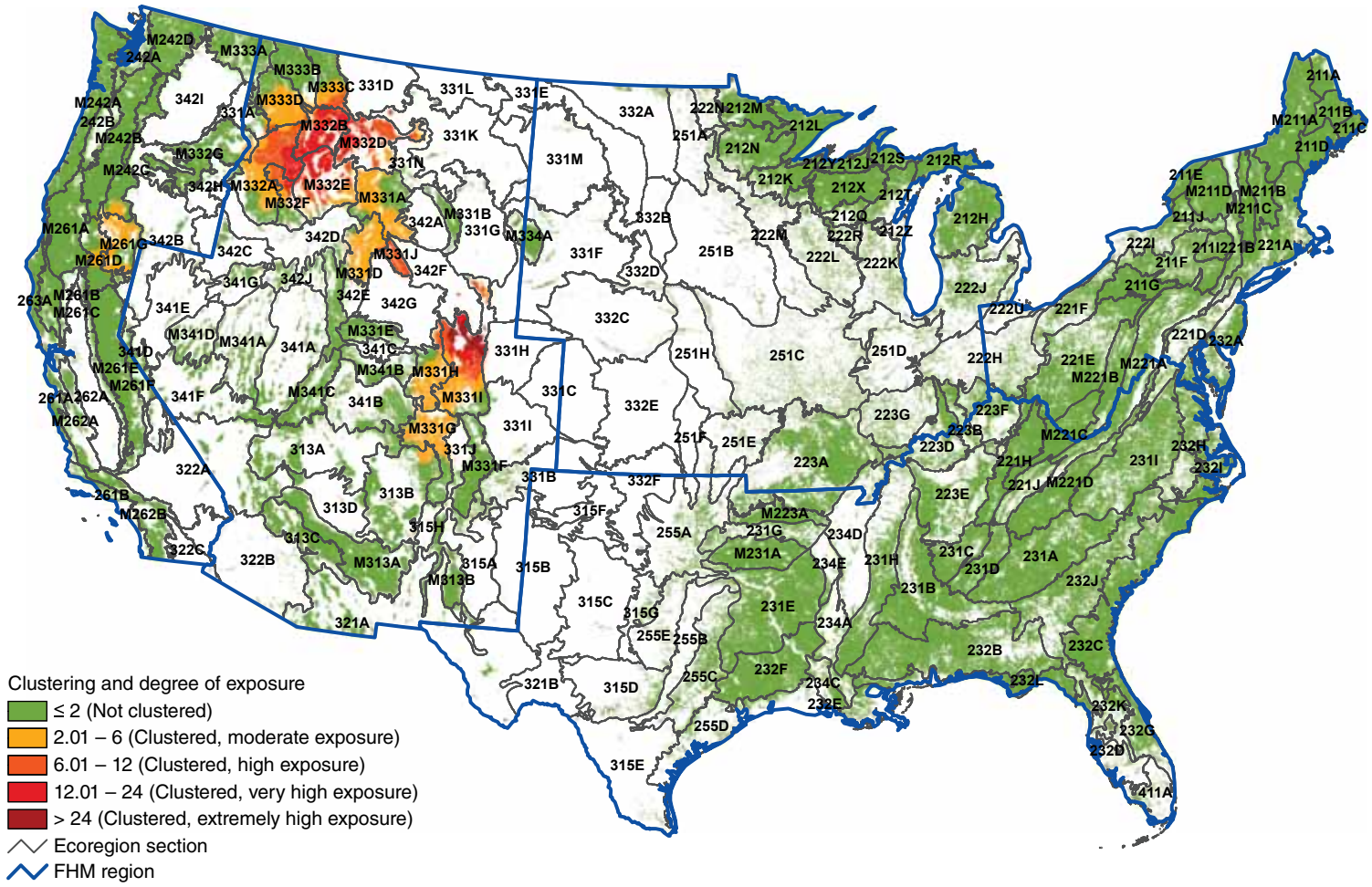


*Figure 2.2—Hot spots of exposure to mortality-causing insects and diseases in 2011. Values are Getis-Ord $G_i^*$ scores, with values > 2 representing significant clustering of high percentages of forest area exposed to mortality agents. (No areas of significant clustering of low percentages of exposure, <-2, were detected.) The gray lines delineate ecoregion sections (Cleland and others 2007); the blue lines delineate Forest Health Monitoring regions. Background forest cover is derived from MODIS imagery by the USDA Forest Service Remote Sensing Applications Center. (Data source: USDA Forest Service, Forest Health Protection Program.)*

Mountain pine beetle was also a leading cause of mortality in the West Coast region, where mortality-causing agents and complexes were recorded on nearly 417 000 ha (table 2.4). Several other types of bark beetles, including fir engraver and western pine beetle (*D. brevicomis*), were also important causes of mortality in this region. These bark beetles, especially mountain pine beetle and fir engraver, were associated with a relatively low-intensity geographic hot spot of mortality in northeastern California and south-central Oregon (fig. 2.2). This hot spot encompassed M242C-Eastern Cascades, M261D-Southern Cascades, and M261G-Modoc Plateau.

Mountain pine beetle was the second most widely detected mortality agent in the North Central region, behind spruce budworm. Beech bark disease (*Nectria coccinea*) and emerald ash borer (*Agrilus planipennis*) were also important mortality agents. Mortality-causing agents and complexes were detected on approximately 94 000 ha in the region (table 2.4).

As in the North Central region, no mortality hot spots occurred in the North East and South FHM regions. In the North East, however, mortality was recorded on 30 000 ha, with forest tent caterpillar (*Malacosoma disstria*) the most widely named causal agent. In the South, mortality was detected on 1600 ha, with hemlock woolly adelgid (*Adelges tsugae*) the most commonly reported agent (table 2.4). In addition, record-setting drought in Texas, much of Louisiana, and other areas in the South, often associated with pests such as pine engraver beetles, contributed to widespread, often scattered mortality of pines and hardwoods, which occurred in late summer and early fall (Alabama Forestry Commission 2012, Louisiana Department of Agriculture and Forestry 2012, Texas Forest Service 2012) and was largely undocumented by routine detection surveys.

As with mortality, the Interior West FHM region encompassed the greatest area on which defoliating agents and complexes were detected in 2011, about 1.9 million ha (table 2.5). Western spruce budworm was the most widely detected defoliator in the region, but pinyon needle scale was also important. A large complex of geographic hot spots of defoliation, contained mostly in Idaho and Montana, was associated with western spruce budworm in the Interior West in 2011 (fig. 2.3). This complex of hot spots included:

- A large and intense hot spot centered on M333D-Bitterroot Mountains and extending into M333A-Okanogan Highland, M333B-Flathead Valley, and M333C-Northern Rockies.
- Another large and intense hot spot centered on M332A-Idaho Batholith and M332F-Challis Volcanics and extended into M332E-Beaverhead Mountains.
- A large hot spot taking in M332D-Belt Mountains and extending into M332B-Northern Rockies and Bitterroot Valley, M333C-Northern Rockies, and M331A-Yellowstone Highlands.

**Table 2.5—The top five defoliation agents or complexes for each Forest Health Monitoring region in 2011**

| Defoliation agents, 2011 | Area |
|---|---|
| | *ha* |
| **Interior West** | |
| Western spruce budworm | 1 515 696.6 |
| Pinyon needle scale | 258 016.0 |
| Douglas-fir tussock moth | 43 655.9 |
| Aspen defoliation[a] | 32 745.7 |
| Needlecast | 32 565.8 |
| Other defoliation agents (24) | 51 870.3 |
| **Total, all agents** | **1 906 426.2** |
| **North Central** | |
| Spruce budworm | 116 499.7 |
| Forest tent caterpillar | 32 207.7 |
| Jack pine budworm | 8 507.2 |
| Large aspen tortrix | 7 771.8 |
| Larch casebearer | 4 627.2 |
| Other defoliation agents (12) | 15 711.7 |
| **Total, all agents** | **183 226.1** |
| **North East** | |
| Winter moth | 36 791.0 |
| Birch leaf fungus | 10 106.4 |
| Forest tent caterpillar | 6 913.3 |
| Loopers | 4 444.6 |
| Unknown | 2 469.9 |
| Other defoliation agents (19) | 9 021.2 |
| **Total, all agents** | **68 791.6** |
| **South** | |
| Forest tent caterpillar | 238 265.5 |
| Baldcypress leafroller | 17 694.3 |
| Larger elm leaf beetle | 7 619.3 |
| Oak worms | 6 266.7 |
| Unknown | 4 265.2 |
| Other defoliation agent (1) | 4.9 |
| **Total, all agents** | **256 519.7** |
| **West Coast** | |
| Western spruce budworm | 321 545.6 |
| Pine butterfly | 101 022.2 |
| Larch casebearer | 7 777.0 |
| Ponderosa pine sawfly | 4 640.2 |
| Douglas-fir tussock moth | 4 219.1 |
| Other defoliation agents (16) | 16 406.5 |
| **Total, all agents** | **422 291.1** |
| **Alaska** | |
| Defoliators (nonspecific) | 81 412.3 |
| Aspen leaf miner | 56 312.3 |
| Willow leafblotch miner | 25 829.4 |
| Hemlock sawfly | 4 514.0 |
| Spruce aphid | 1 665.7 |
| Other defoliation agents (5) | 2 977.4 |
| **Total, all agents** | **166 660.8** |

Note: The total area affected by other agents is listed at the end of each section. All values are "footprint" areas for each agent or complex. The sum of the individual agents may not equal the total for all agents because of overlapping damage polygons.

[a] Includes mortality, defoliation, and decline.

An additional defoliation hot spot associated mostly with western spruce budworm, along with some aspen defoliation, occurred in northern New Mexico and southern Colorado, mostly in M331G-South Central Highlands, M331F-Southern Parks and Rocky Mountain Range, 313B-Navajo Canyonlands, and 331J-Northern Rio Grande Basin (fig. 2.3). Finally, a hot spot in Nevada was caused by pinyon needle scale extending across forested parts of M341D-West Great Basin and Mountains, 341F-Southeastern Great Basin, M341A-East Great Basin and Mountains, and 341D-Mono.

Western spruce budworm was also the most important defoliator in the West Coast region, accounting for the majority of the 422 000 ha of defoliation detected there. Pine butterfly was the second leading defoliation agent; no other agent or complex was nearly as widespread as these two (table 2.5). The more intense of the two defoliation hot spots in the region was caused by infestations of western spruce budworm and pine butterfly in M332G-Blue Mountains and 342H-Blue Mountains Foothills of Oregon (fig. 2.3). Western spruce budworm was the cause of a second hot spot in M333A-Okanogan Highland and M242D-Northern Cascades of northern Washington.

Spruce budworm was similarly the leading defoliator detected in the North Central region, recorded on about 117 000 ha of the 183 000 ha of defoliation. It was followed in extent by forest tent caterpillar (table 2.5). Jack pine budworm (*C. pinus*) and spruce budworm

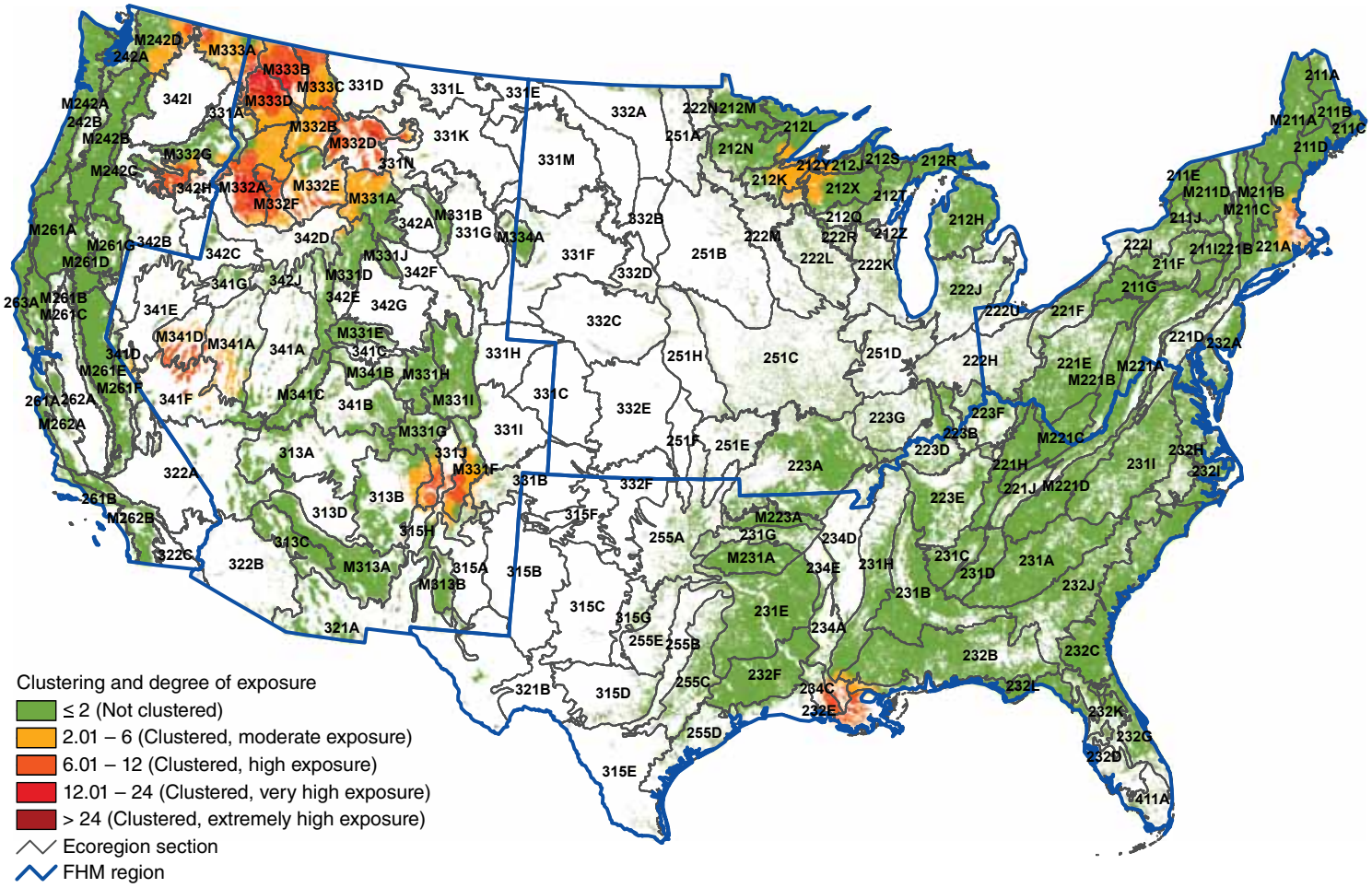


*Figure 2.3—Hot spots of exposure to defoliation-causing insects and diseases in 2011. Values are Getis-Ord $G_i^*$ scores, with values > 2 representing significant clustering of high percentages of forest area exposed to defoliation agents. (No areas of significant clustering of low percentages of exposure, <-2, were detected.) The gray lines delineate ecoregion sections (Cleland and others 2007); the blue lines delineate Forest Health Monitoring regions. Background forest cover is derived from MODIS imagery by the USDA Forest Service Remote Sensing Applications Center. (Data source: USDA Forest Service, Forest Health Protection Program.)*

were the assigned causal agents associated with the region's defoliation hot spot in 212K-Western Superior Uplands, 212L-Northern Superior Uplands, 212Q-North Central Wisconsin Uplands, 212X-Northern Highlands, 212Y-Southwest Lake Superior Clay Plain, and 212J-Southern Superior Uplands (fig. 2.3).

The single defoliation hot spot in the North East FHM region, meanwhile, was caused by winter moth (*Operophtera brumata*) in 221A-Lower New England; winter moth was the most commonly detected defoliation agent in the region, found on 37 000 ha of 69 000 ha on which defoliation was recorded (table 2.5). Birch leaf fungus (*Septoria betulae*) was the second most widely detected defoliator.

Forest tent caterpillar was by far the leading defoliating agent in the South region, detected on 238 000 ha of the 257 000 ha on which defoliation was detected (table 2.5). An intense hot spot was caused by forest tent caterpillar and baldcypress leafroller (*Archips goyerana*) in southern Louisiana, in 234C-Atchafalaya and Red River Alluvial Plains, 234A-Southern Mississippi Alluvial Plain, and 232E-Louisiana Coastal Prairie and Marshes.

In 2011, five mortality-causing agents and complexes were reported for Alaska, affecting approximately 36 000 ha (table 2.4). Alaska contains about 51.3 million ha (126.9 million acres) of forest (Smith and others 2009).

Spruce beetle was the most widely detected mortality agent, affecting about 20 000 ha of forest, mostly in the south-central part of the State. Yellow-cedar (*Chamaecyparis nootkatensis*) decline was the second most widely detected mortality agent, found on about 11 000 ha in the Alaska panhandle. Northern spruce engraver beetle (*Ips perturbatus*) was detected on about 3000 ha of forest, mostly in the central and east-central parts of the State. The ecoregions with the highest percentage of surveyed forest affected by mortality agents (fig. 2.4) were M129A-Seward Mountains of east-central Alaska (1.61 percent), and M213A-Northern Aleutian Range and 213B-Cook Inlet Lowlands of south-central Alaska (1.50 and 1.00 percent, respectively).

The study detected 10 defoliation agents and complexes on nearly 167 000 ha (table 2.5) in Alaska during 2011. For nearly half of that area, approximately 81 000 ha, nonspecific defoliators were the assigned cause of defoliation. Aspen leaf miner (*Phyllocnistis populiella*) was detected on 56 000 ha, mostly in the eastern and central parts of Alaska. The next most important defoliator in 2011 was willow leafblotch miner (*Micrurapteryx salicifoliella*), found on nearly 26 000 ha. Hemlock sawfly (*Neodiprion tsugae*) was observed on about 4500 ha, and spruce aphid (*Elatobium abietinum*) was found on less than 2000 ha.

The Alaska ecoregion with the highest proportion of surveyed forest affected by defoliation was M212B-Kenai Mountains in the south-central part of the State, with 4.48 percent (fig. 2.5). Other ecoregions with relatively high levels of defoliation detection were in east-central Alaska, including 139A-Yukon Flats

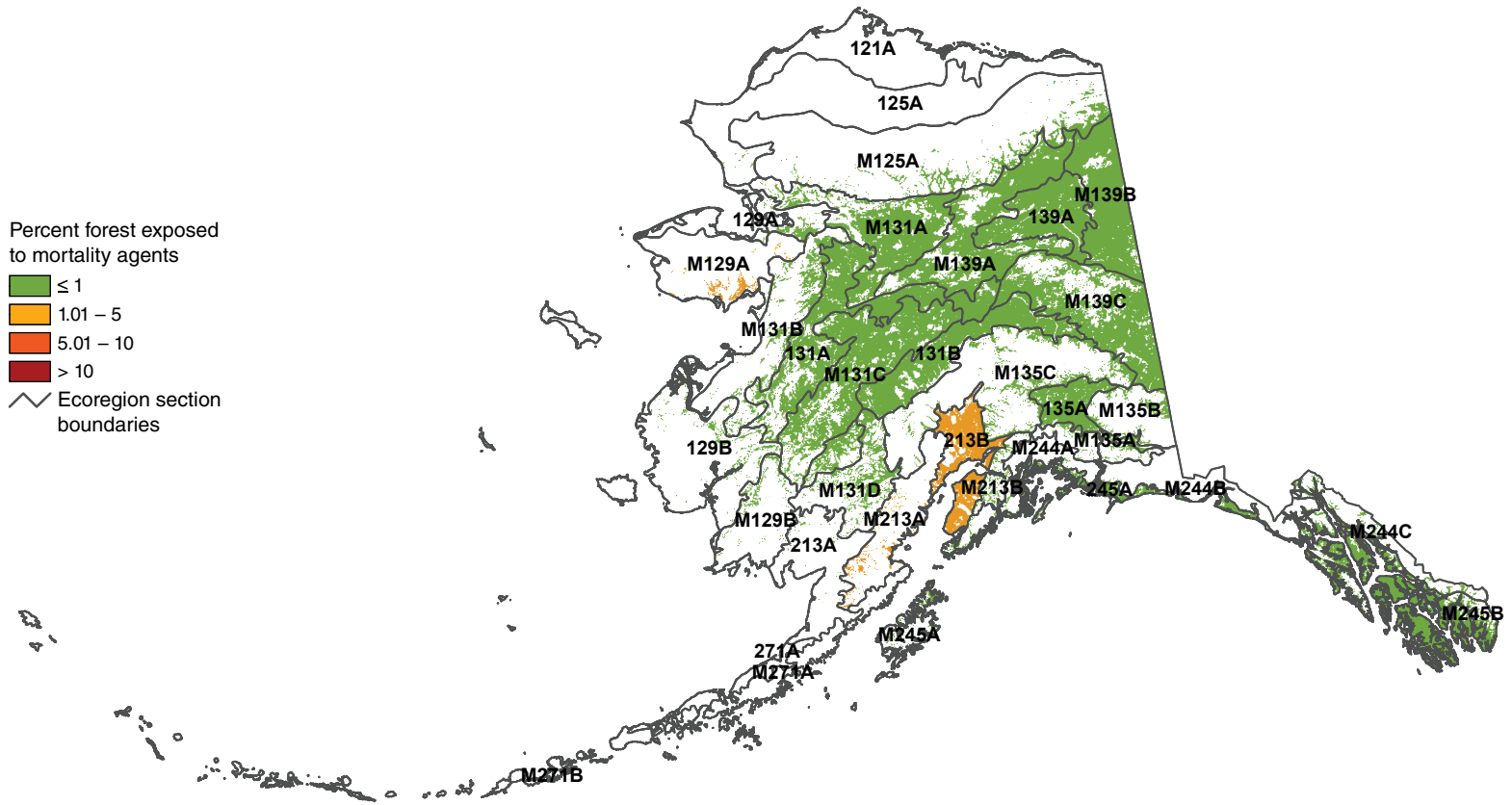


*Figure 2.4—Percent of surveyed forest in Alaska ecoregion sections exposed to mortality-causing insects and diseases in 2011. The gray lines delineate ecoregion sections (Nowacki and Brock 1995). Background forest cover is derived from MODIS imagery by the USDA Forest Service Remote Sensing Applications Center. (Data source: USDA Forest Service, Forest Health Protection Program.)*

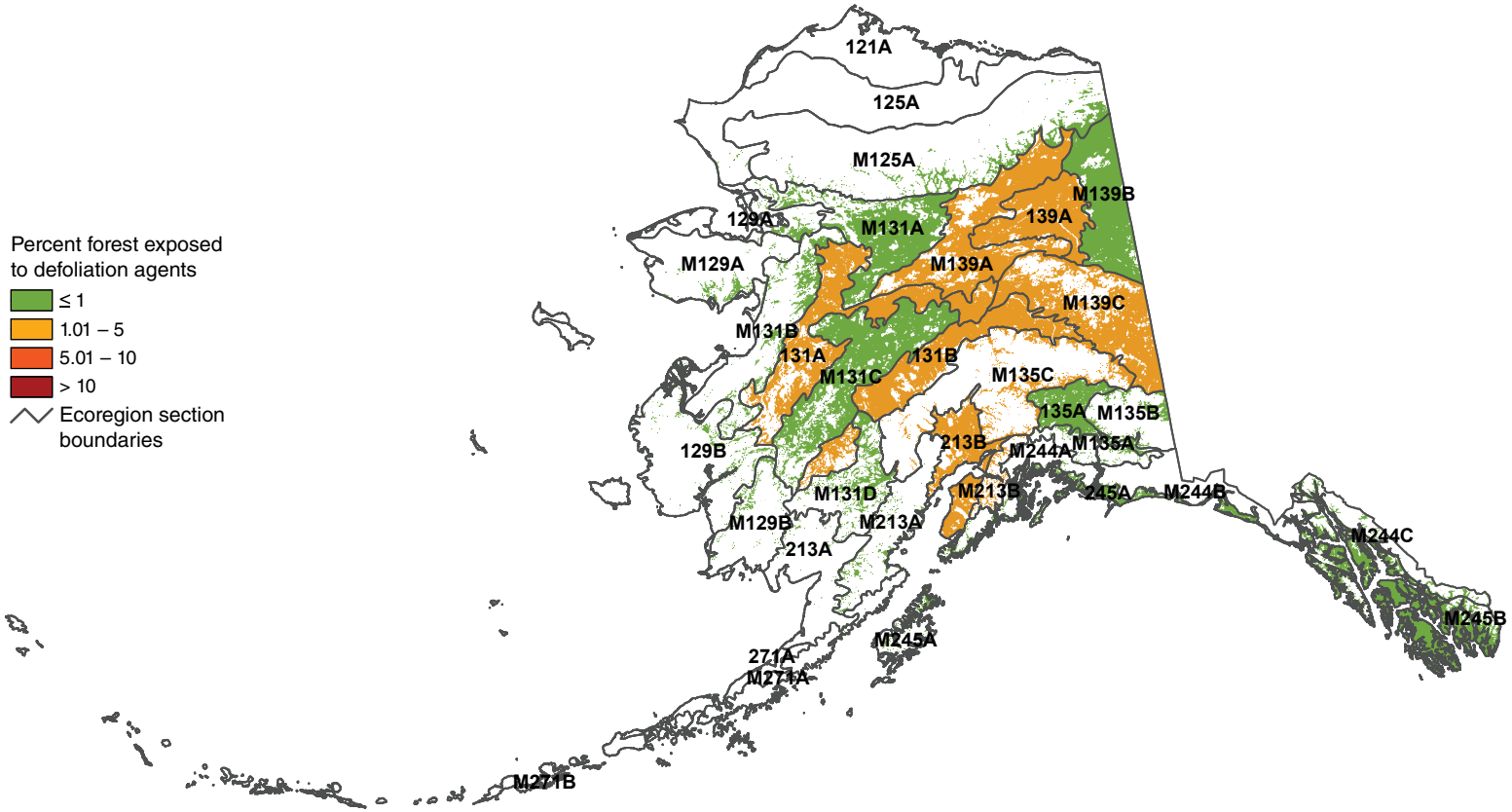


*Figure 2.5—Percent of surveyed forest in Alaska ecoregion sections exposed to defoliation-causing insects and diseases in 2011. The gray lines delineate ecoregion sections (Nowacki and Brock 1995). Background forest cover is derived from MODIS imagery by the USDA Forest Service Remote Sensing Applications Center. (Data source: USDA Forest Service, Forest Health Protection Program.)*

section, with 3.37 percent; M139C-Dawson Range, with 3.24 percent; and M135C-Alaska Range, with 2.28 percent.

Continued monitoring of insect and disease outbreaks across the United States will be necessary for determining appropriate followup investigation and management activities. Because of the limitations of survey efforts to detect certain important forest insects and diseases, the pests and pathogens discussed in this chapter do not include all the biotic forest health threats that should be considered when making management decisions and budget allocations. As these analyses demonstrate, however, large-scale assessments of mortality and defoliation exposure, including geographical hot spot detection analyses, offer a potentially useful approach for prioritizing geographic areas where the concentration of monitoring and management activities would be most effective.

## LITERATURE CITED


Alabama Forestry Commission. 2012. Alabama forest health highlights 2011. http://fhm.fs.fed.us/fhh/fhh_11/AL_FHH_2011.pdf. [Date accessed: June 7].

Anselin, L. 1992. Spatial data analysis with GIS: an introduction to application in the social sciences. Tech. Rep. 92-10. Santa Barbara, CA: National Center for Geographic Information and Analysis. 53 p.

Brockerhoff, E.G.; Liebhold, A.M.; Jactel, H. 2006. The ecology of forest insect invasions and advances in their management. Canadian Journal of Forest Research. 36(2): 263-268.

Castello, J.D.; Leopold, D.J.; Smallidge, P.J. 1995. Pathogens, patterns, and processes in forest ecosystems. Bioscience. 45(1): 16-24.

Cleland, D.T.; Freeouf, J.A.; Keys, J.E., Jr. [and others]. 2007. Ecological subregions: sections and subsections for the conterminous United States. 1:3,500,000; Albers equal area projection; colored. In: Sloan, A.M., tech. ed. Gen. Tech. Rep. WO-76. Washington, DC: U.S. Department of Agriculture Forest Service. Also as a GIS coverage in ArcINFO format on CD-ROM or at http://fsgeodata.fs.fed.us/other_resources/ecosubregions.html. [Date accessed: March 18, 2011].

Edmonds, R.L.; Agee, J.K.; Gara, R.I. 2011. Forest health and protection. Long Grove, IL: Waveland Press. 667 p.

ESRI. 2006. ArcMap 9.2. Redlands, CA: Environmental Systems Research Institute.

Forest Health Monitoring (FHM). 2005. Aerial survey geographic information system handbook: sketchmaps to digital geographic information. U.S. Department of Agriculture Forest Service, State and Private Forestry, Forest Health Protection. http://www.fs.fed.us/foresthealth/technology/pdfs/GISHandbook_body_apndxA-C.pdf. [Date accessed: May 7, 2013].

Getis, A.; Ord, J.K. 1992. The analysis of spatial association by use of distance statistics. Geographical Analysis. 24(3): 189-206.

Holdenrieder, O.; Pautasso, M.; Weisberg, P.J.; Lonsdale, D. 2004. Tree diseases and landscape processes: the challenge of landscape pathology. Trends in Ecology & Evolution. 19(8): 446-452.

Laffan, S.W. 2006. Assessing regional scale weed distributions, with an Australian example using *Nassella trichotoma*. Weed Research. 46(3): 194-206.

Louisiana Department of Agriculture and Forestry. 2012. Louisiana forest health highlights 2011. http://fhm.fs.fed.us/fhh/fhh_11/LA_FHH_2011.pdf. [Date accessed: June 7].

Mack, R.N.; Simberloff, D.; Lonsdale, W.M. [and others]. 2000. Biotic invasions: causes, epidemiology, global consequences, and control. Ecological Applications. 10(3): 689-710.

Manion, P.D. 2003. Evolution of concepts in forest pathology. Phytopathology. 93: 1052-1055.

Nowacki, G.; Brock, T. 1995. Ecoregions and subregions of Alaska, EcoMap Version 2.0. 1:5,000,000; colored. Juneau, AK: U.S. Department of Agriculture Forest Service, Alaska Region.

Parry, D.; Teale, S.A. 2011. Alien invasions: the effects of introduced species on forest structure and function. In: Castello, J.D.; Teale, S.A., eds. Forest health: an integrated perspective. New York: Cambridge University Press: 115-162.

Potter, K.M. 2012. Large-scale patterns of insect and disease activity in the conterminous United States and Alaska from the national insect and disease detection survey database, 2007 and 2008. In: Potter, K.M.; Conkling, B.L., eds. Forest health monitoring 2009 national technical report. Gen. Tech. Rep. SRS-167. Asheville, NC: U.S. Department of Agriculture Forest Service, Southern Research Station: 63-78.

Potter, K.M. 2013. Large-scale patterns of insect and disease activity in the conterminous United States and Alaska from the national insect and disease detection survey, 2009. In: Potter, K.M.; Conkling, B.L., eds. Forest health monitoring: national status, trends, and analysis 2010. Gen. Tech. Rep. SRS-176. Asheville, NC: U.S. Department of Agriculture Forest Service, Southern Research Station: 15-29.

Potter, K.M.; Koch, F.H. 2012. Large-scale patterns of insect and disease activity in the conterminous United States and Alaska, 2006. Potter, K.M.; Conkling, B.L., eds. Forest health monitoring 2008 national technical report. Gen. Tech. Rep. SRS-158. Asheville, NC: U.S. Department of Agriculture Forest Service, Southern Research Station: 63-72.

Potter, K.M.; Paschke, J.L. 2013. Large-scale patterns of insect and disease activity in the conterminous United States and Alaska from the national insect and disease detection survey database, 2010. In: Potter, K.M.; Conkling, B.L., eds. Forest health monitoring: national status, trends, and analysis 2011. Gen. Tech. Rep. SRS-185. Asheville, NC: U.S. Department of Agriculture Forest Service, Southern Research Station: 15-28.

Smith, W.B.; Miles, P.D.; Perry, C.H.; Pugh, S.A. 2009. Forest resources of the United States, 2007. Gen. Tech. Rep. WO-78. St. Paul, MN: U.S. Department of Agriculture Forest Service, Washington Office. 336 p.

Teale, S.A.; Castello, J.D. 2011. Regulators and terminators: the importance of biotic factors to a healthy forest. In: Castello, J.D.; Teale, S.A., eds. Forest health: an integrated perspective. New York: Cambridge University Press: 81-114.

Texas Forest Service. 2012. Texas forest health highlights 2011. http://fhm.fs.fed.us/fhh/fhh_11/TX_FHH_2011.pdf. [Date accessed: June 7].

U.S. Department of Agriculture (USDA) Forest Service. 2008. National forest type data development. http://svinetfc4.fs.fed.us/rastergateway/forest_type/. [Date accessed: May 13].

White, D.; Kimerling, A.J.; Overton, W.S. 1992. Cartographic and geometric components of a global sampling design for environmental monitoring. Cartography and Geographic Information Systems. 19(1): 5-22.

Zhang, L.; Rubin, B. D.; Manion, P.D. 2011. Mortality: the essence of a healthy forest. In: Castello, J.D.; Teale, S.A., eds. Forest health: an integrated perspective. New York: Cambridge University Press: 17-49.

# CHAPTER 3.

# Large-Scale Patterns of Forest Fire Occurrence in the Conterminous United States and Alaska, 2011

Kevin M. Potter

## INTRODUCTION

Free-burning fire has been a constant ecological presence on the American landscape, the expression of which has changed as new climates, peoples, and land uses have become predominant (Pyne 2010). It is an important ecological mechanism that shapes the distributions of species, maintains the structure and function of fire-prone communities, and is a significant evolutionary force (Bond and Keeley 2005). As a ubiquitous disturbance agent operating at many spatial and temporal scales, wildland fire is a key abiotic factor in forest health, and even large, intense fires that cause extensive tree mortality can play a role in maintaining healthy ecosystems (Lundquist and others 2011). In some ecosystems, wildland fires have been essential for regulating processes that maintain forest health, while fires have created forest health problems in other ecosystems (Edmonds and others 2011).

Fire outside the historic range of frequency and intensity can have extensive economic and ecological impacts. As a result of intense suppression efforts during most of the 20th century, the land area burned annually decreased from approximately 16–20 million ha (40–50 million acres) in the early 1930s to about 2 million ha (5 million acres) in the 1970s (Vinton 2004). In some regions, plant communities are undergoing rapid compositional and structural changes as a result of fire suppression (Nowacki and Abrams 2008). At the same time, fires have become larger, more intense, and more damaging because of the accumulation of fuels (Pyne 2010). Current fire regimes on more than half of the forested area in the conterminous United States have been either moderately or significantly altered from historical regimes, potentially altering key ecosystem components such as species composition, structural stage, stand age, canopy closure, and fuel loadings (Schmidt and others 2002). Understanding inherent fire regimes is essential to properly assessing the impact of fire on forest health because changes to historical fire regimes can alter forest developmental patterns, including the establishment, growth, and mortality of trees (Lundquist and others 2011).

Fire suppression, and the introduction of nonnative plants in particular, has dramatically altered fire regimes (Barbour and others 1999). In addition, changes in fire intensity and recurrence could result in decreased forest resilience and persistence (Lundquist and others 2011), and fire regimes altered by global climate change could cause large-scale shifts in vegetation spatial patterns (McKenzie and others 1996).

Quantifying and monitoring broad-scale patterns of fire occurrence across the United States can help provide a fuller understanding of the ecological and economic impacts of fire and of the appropriate management and prescribed use of fire. To be specific, large-scale assessments of fire occurrence can help identify areas where specific management activities may be useful, or where research into the ecological and socioeconomic impacts of fires may be necessary.

## METHODS

Annual monitoring and reporting of active wildland fire events using the Moderate Resolution Imaging Spectroradiometer (MODIS) Active Fire Detections for the United States ("MODIS Active Fire") database (USDA Forest Service 2012) enables analysts to spatially display and summarize fire occurrences (Coulston and others 2005; Potter 2012a, 2012b; Potter 2013a, 2013b). Fire occurrences are defined as the satellite detection of wildland fire in a 1-$km^2$ pixel for 1 day in a given year. The data are derived using the MODIS Rapid Response System (Justice and others 2002) from the thermal infrared bands of imagery collected daily by two satellites at a resolution of 1 $km^2$, with the center of a pixel recorded as a fire occurrence when the satellites' MODIS sensors identify the presence of a fire at the time of image collection (USDA Forest Service 2012). The data represent only whether a fire was active because the MODIS sensors do not differentiate between a hot fire in a relatively small area (0.01 $km^2$, for example) and a cooler fire over a larger area (1 $km^2$, for example). The MODIS Active Fire Detections database does well at capturing large fires, but it may underrepresent rapidly burning, small, and low-intensity fires as well as fires in areas with frequent cloud cover (Hawbaker and others 2008).

The number of fire occurrences per 100 $km^2$ (10 000 ha) of forested area was determined for each ecoregion section in the conterminous 48 States (Cleland and others 2007) and Alaska (Nowacki and Brock 1995) for 2011. This forest fire occurrence density measure was calculated after screening out wildland fires on nonforested pixels using a forest cover layer derived from MODIS imagery by the Forest Service Remote Sensing Applications Center (USDA Forest Service 2008). The total number of forest fire occurrences across the conterminous States and Alaska was also calculated.

The 2011 fire-occurrence density value for each ecoregion was then compared with the mean fire density values for the first 10 full years of MODIS Active Fire data collection (2001–10). To be specific, the difference of the 2011 value and the previous 10-year mean for an ecoregion was divided by the standard deviation across the previous 10-year period, assuming normal distribution of fire density over time in the ecoregion. The result for each ecoregion was a standardized *z*-score, which is a dimensionless quantity describing the degree of deficit or excess of fire-occurrence density in the ecoregion in 2011 relative to all of the previous years for which data have been collected, accounting for the variability in the previous years. The *z*-score is the number of standard deviations between the observation and the mean of the previous observations. Approximately 68 percent of observations would be expected within 1 standard deviation of the mean, and 95 percent expected within 2 standard deviations. Near-normal conditions are classified as those within a single standard deviation of the mean, although such a threshold is somewhat arbitrary.

In addition, a Getis-Ord hot spot analysis (Getis and Ord 1992) in ArcMap 9.2 (ESRI 2006) was employed to identify forested areas in the conterminous 48 States with higher-than-expected fire-occurrence density in 2011. The spatial units of analysis were cells of about 2500 $km^2$ from a hexagonal lattice of the conterminous United States, intensified from Environmental Monitoring and Assessment Program North America hexagon coordinates (White and others 1992). This cell size allows for analysis at a medium-scale resolution of approximately the same area as a typical county. Fire-occurrence density values for each hexagon were quantified as the number of forest fire occurrences per 100 $km^2$ of forested area within the hexagon.

The Getis-Ord $G_i^*$ statistic was used to identify clusters of hexagonal cells with fire-occurrence density values higher than expected by chance. This statistic allows for the decomposition of a global measure of spatial association into its contributing factors, by location, and is therefore particularly suitable for detecting nonstationarities in a dataset, such as when spatial clustering is concentrated in one subregion of the data (Anselin 1992).

Briefly, $G_i^*$ sums the differences between the mean values in a local sample, determined in this case by a moving window of each hexagon and its 18 first- and second-order neighbors (the 6 adjacent hexagons and the 12 additional hexagons contiguous to those 6), and the global mean of all the forested hexagonal cells in the conterminous 48 States. $G_i^*$ is standardized as a $z$-score with a mean of 0 and a standard deviation of 1, with values greater than 1.96 representing significant local clustering of higher fire-occurrence densities ($p < 0.025$) and values less than -1.96 representing significant clustering of lower fire-occurrence densities ($p < 0.025$), because 95 percent of the observations under a normal distribution should be within approximately 2 standard deviations of the mean (Laffan 2006). Values between -1.96 and 1.96 have no statistically significant concentration of high or low values; a hexagon and its 18 neighbors, in other words, have a range of both high and low numbers of fire occurrences per 100 $km^2$ of forested area. It is worth noting that the threshold values are not exact because the correlation of spatial data violates the assumption of independence required for statistical significance (Laffan 2006). The Getis-Ord approach does not require that the input data be normally distributed because the local $G_i^*$ values are computed under a randomization assumption, with $G_i^*$ equating to a standardized $z$-score that asymptotically tends to a normal distribution (Anselin 1992). The $z$-scores are reliable, even with skewed data, as long as the distance band is large enough to include several neighbors for each feature (ESRI 2006).

## RESULTS AND DISCUSSION

The MODIS Active Fire Detections database captured 77,892 wildland forest fire occurrences across the conterminous United States in 2011, approximately 46 percent more than in 2010 (53,309) and the third highest number since the first full year of MODIS data was collected in 2001 (fig. 3.1). It is also higher than the 48,862 mean annual forest fire occurrences during the previous 10 full years of data collection. The database captured only 343 forest fire occurrences in Alaska in 2011, the second fewest since 2001 and a small fraction of the previous 10-year annual mean of 14,736.

The increase in total number of fire occurrences across the conterminous States is consistent with the official wildland fire statistics, which show a 155-percent increase in the overall area burned nationally between 2010 (1 385 127 ha) and 2011 (3 525 365 ha) (National Interagency Coordination Center 2012).

In 2011, the 321A-Chihuahuan Desert Basin and Range ecoregion section in west Texas and southern New Mexico and Arizona and the 315G-Eastern Rolling Plains ecoregion section in north-central Texas were the highly forested ecoregions with the highest wildland forest fire-occurrence density (32.8 and 28.2 fires per 100 $km^2$ of forest, respectively) (fig. 3.2). Immediately north of the Basin and Range ecoregion, the M313A-White Mountains-San Francisco Peaks-Mogollon Rim ecoregion experienced 18.7 fire occurrences per 100 $km^2$ of forest.

In the Southeast, meanwhile, 232C-Atlantic Coastal Flatwoods had a high density of fire occurrences (13.6 per 100 $km^2$ of forest). Several neighboring ecoregions also had a relatively high fire-occurrence density, including 232G-Florida Coastal Lowlands-Atlantic (10.3 per 100 $km^2$), 232B-Gulf Coastal Plains and Flatwoods (9.2 per 100 $km^2$), 232I-Northern Atlantic Coastal Flatwoods (8.4 per 100 $km^2$), and 232K-Florida Coastal Plains Central Highlands (8.2 per 100 $km^2$).

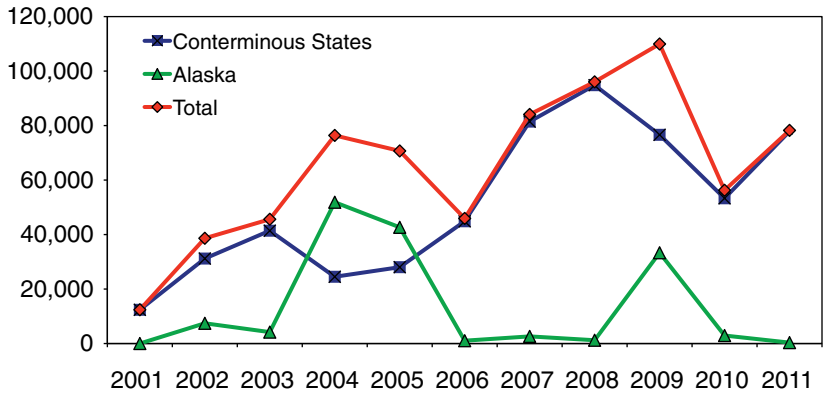


*Figure 3.1—Forest fire occurrences detected by MODIS from 2001 to 2011 for the conterminous United States, for Alaska, and for the two regions combined. (Data source: USDA Forest Service, Remote Sensing Applications Center.)*

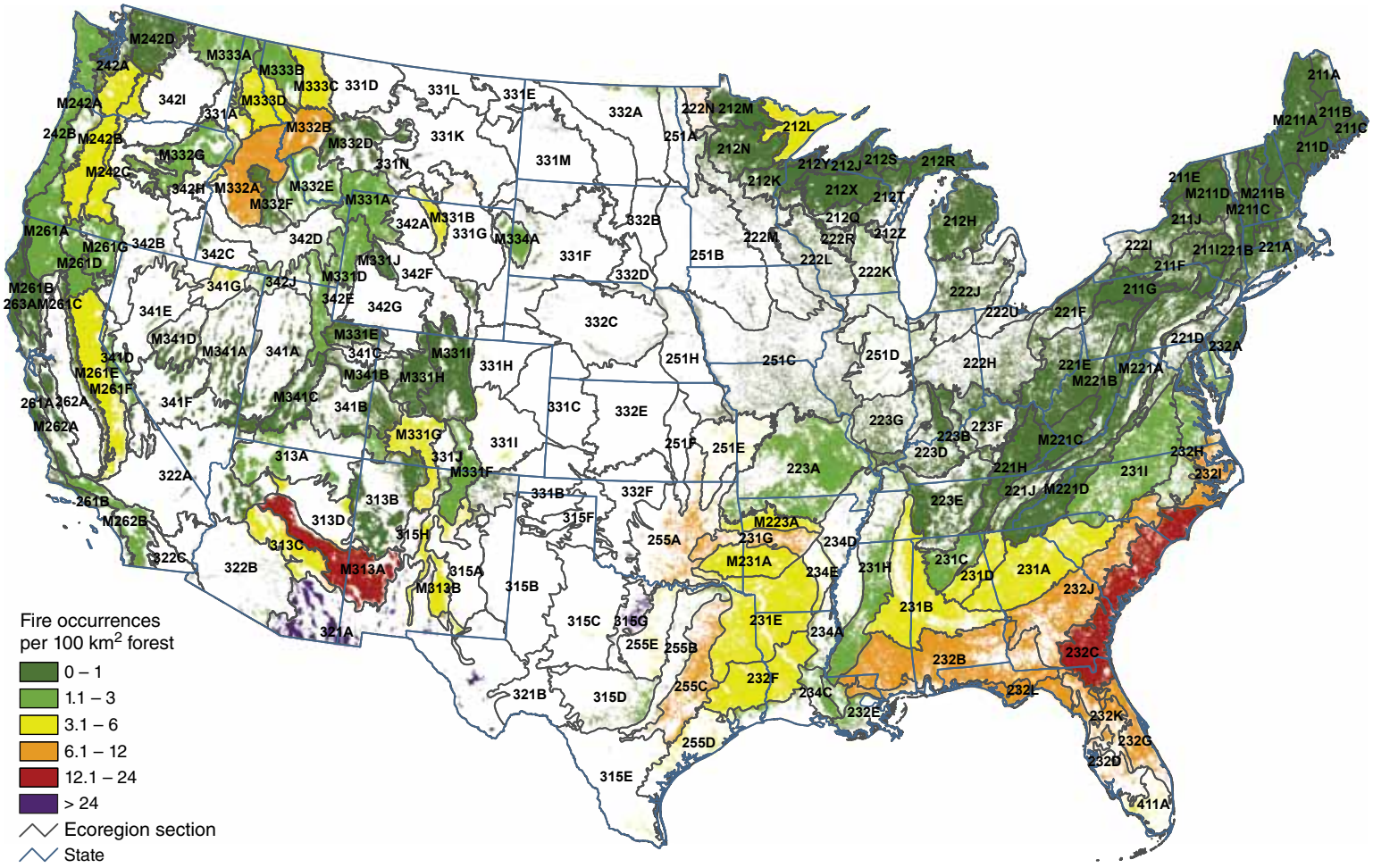


*Figure 3.2—The number of forest fire occurrences, per 100 km$^2$ (10 000 ha) of forested area, by ecoregion section in the conterminous United States for 2011. The gray lines delineate ecoregion sections (Cleland and others 2007). Forest cover is derived from MODIS imagery by the USDA Forest Service Remote Sensing Applications Center. (Source of fire data: USDA Forest Service, Remote Sensing Applications Center.)*

Ecoregions in the south-central States of Arkansas and Oklahoma also experienced relatively high fire densities, including 231G-Arkansas Valley (9.4 fire occurrences per 100 $km^2$) and 255A-Cross Timbers and Prairie (9.2 per 100 $km^2$). Nearby, the 255C-Oak Woods and Prairie ecoregion of east Texas had 6.6 fires per 100 $km^2$ of forest.

Fire occurrences in the West, outside of New Mexico and Arizona, were relatively few compared with the occurrences in recent years. The only two highly forested ecoregions with relatively high densities of fire occurrences were in Idaho and western Montana: M332B-Northern Rockies and Bitterroot Valley and M332A-Idaho Batholith, with 10.8 and 7.3 fires per 100 $km^2$ of forest, respectively. In the North, 222N-Lake Agassiz-Aspen Woodlands in northern Minnesota saw a relatively high fire-occurrence density for its region, 6.7 per 100 $km^2$ of forest.

In Alaska, where very few fire occurrences were detected, all ecoregions experienced fewer than 0.5 fires per 100 $km^2$ of forest (fig. 3.3). The M139C-Dawson Range ecoregion had the highest fire-occurrence density, with only 0.3 fires per 100 $km^2$ of forest.

Contrasting short-term (1-year) wildland forest fire occurrence with longer term trends is possible by comparing these results for each ecoregion section with the results for the first 10 full years of MODIS Active Fire data collection (2001–10). In general, most of the Appalachian, Central Rocky Mountain, Mid-Atlantic, Midwestern, and Northeastern regions experienced fewer than 1 fire per 100 $km^2$ of forest during that period, with means higher in the Northern Rocky Mountain, Pacific, Southeast, and Southwest regions (fig. 3.4A). Heavily forested areas that have experienced the most fires, on average, were located near the California coast and in central Idaho (mean annual fire-occurrence densities of 6.1 to 12.0 per 100 $km^2$). Ecoregions with the greatest variation in fire-occurrence densities over time were also located along the California coast and in central Idaho, with moderate variation in the M261E-Sierra Nevada of California ecoregion and in north-central Washington and western Montana (fig. 3.4B). Lesser degrees of variation occurred throughout the Rocky Mountains and in the Southeast, with the lowest degree of variation apparent in the Midwest and Northeast.

In 2011, ecoregion sections in the Midwest, Northwest, Southeast, and Southwest experienced greater fire-occurrence density than normal compared with the 10-year mean and accounting for variability over time (fig. 3.4C). Several of these ecoregions had the highest fire-occurrence densities in 2011, including 321A-Basin and Range, M313A-White Mountains-San Francisco Peaks-Mogollon Rim, 315G-Eastern Rolling Plains, and 232C-Atlantic Coastal Flatwoods. Others had moderate fire-occurrence densities in 2011 that still deviated

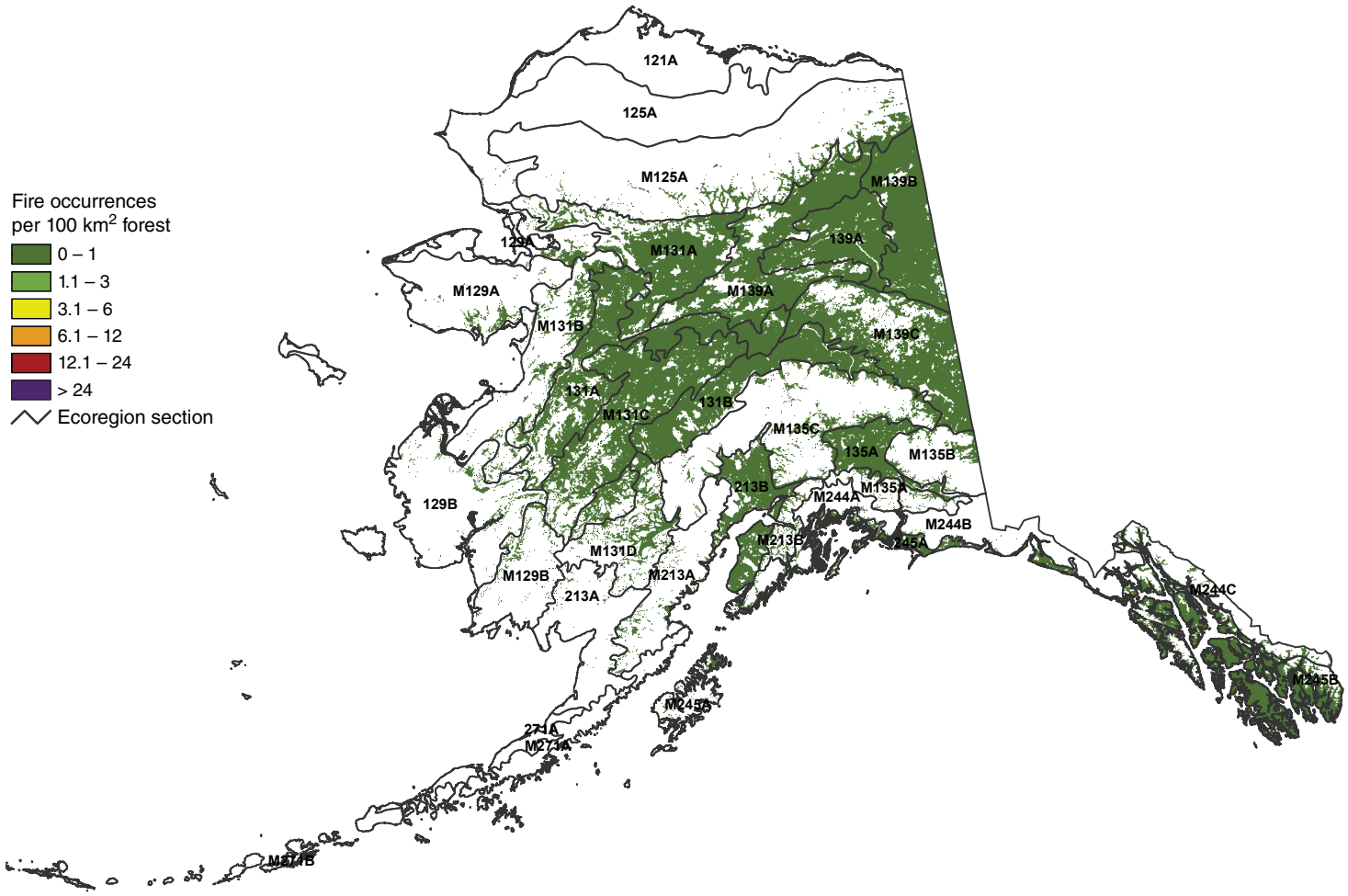


*Figure 3.3—The number of forest fire occurrences, per 100 km$^2$ (10 000 ha) of forested area, by ecoregion section in Alaska for 2011. The gray lines delineate ecoregion sections (Nowacki and Brock 1995). Forest cover is derived from MODIS imagery by the USDA Forest Service Remote Sensing Applications Center. (Source of fire data: USDA Forest Service, Remote Sensing Applications Center.)*

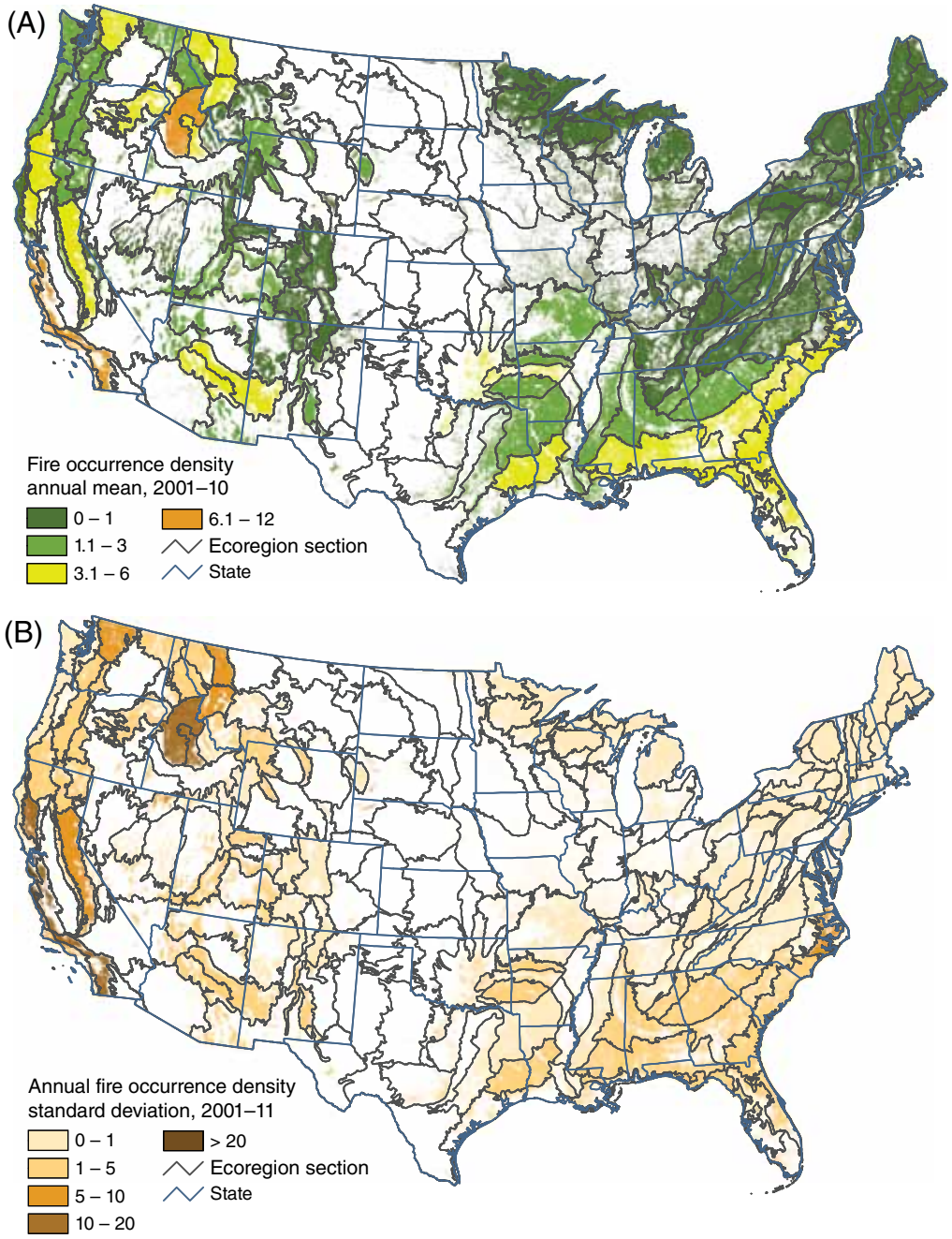


considerably from the previous 10-year mean, including 212L-Northern Superior Uplands of Minnesota; M331G-South-Central Highlands of Colorado and New Mexico; 231E-Mid-Coastal Plains-Western of east Texas, northern Louisiana, and southern Arkansas; and M231A-Ouachita Mountains and 231G-Arkansas Valley of Oklahoma and Arkansas.

Perhaps more interesting is the fact that some ecoregions had relatively low fire-occurrence densities in 2011 that were still considerably higher than the longer term mean. These ecoregions include 231H-Coastal Plains-Loess of Mississippi, Tennessee, and Kentucky; 231C-Southern Cumberland Plateau of northern Alabama; 251D-Central Till Plains and Grand Prairies of Illinois and Indiana; and M341D-Western Great Basin and Mountains of central Nevada (fig. 3.4C). Conversely, some ecoregions with high relative fire-occurrence densities in 2011 did not deviate much from the longer term mean when considering temporal variability,

*Figure 3.4—(A) Mean number and (B) standard deviation of forest fire occurrences, per 100 km$^2$ (10 000 ha) of forested area from 2001 to 2010, by ecoregion section within the conterminous United States. (C) Degree of 2011 fire occurrence density excess or deficiency by ecoregion relative to 2001–10 and accounting for variation over that time. The gray lines delineate ecoregion sections (Cleland and others 2007). Forest cover is derived from MODIS imagery by the U.S. Forest Service Remote Sensing Applications Center. (Source of fire data: USDA Forest Service, Remote Sensing Applications Center.)* *(continued to next page)*

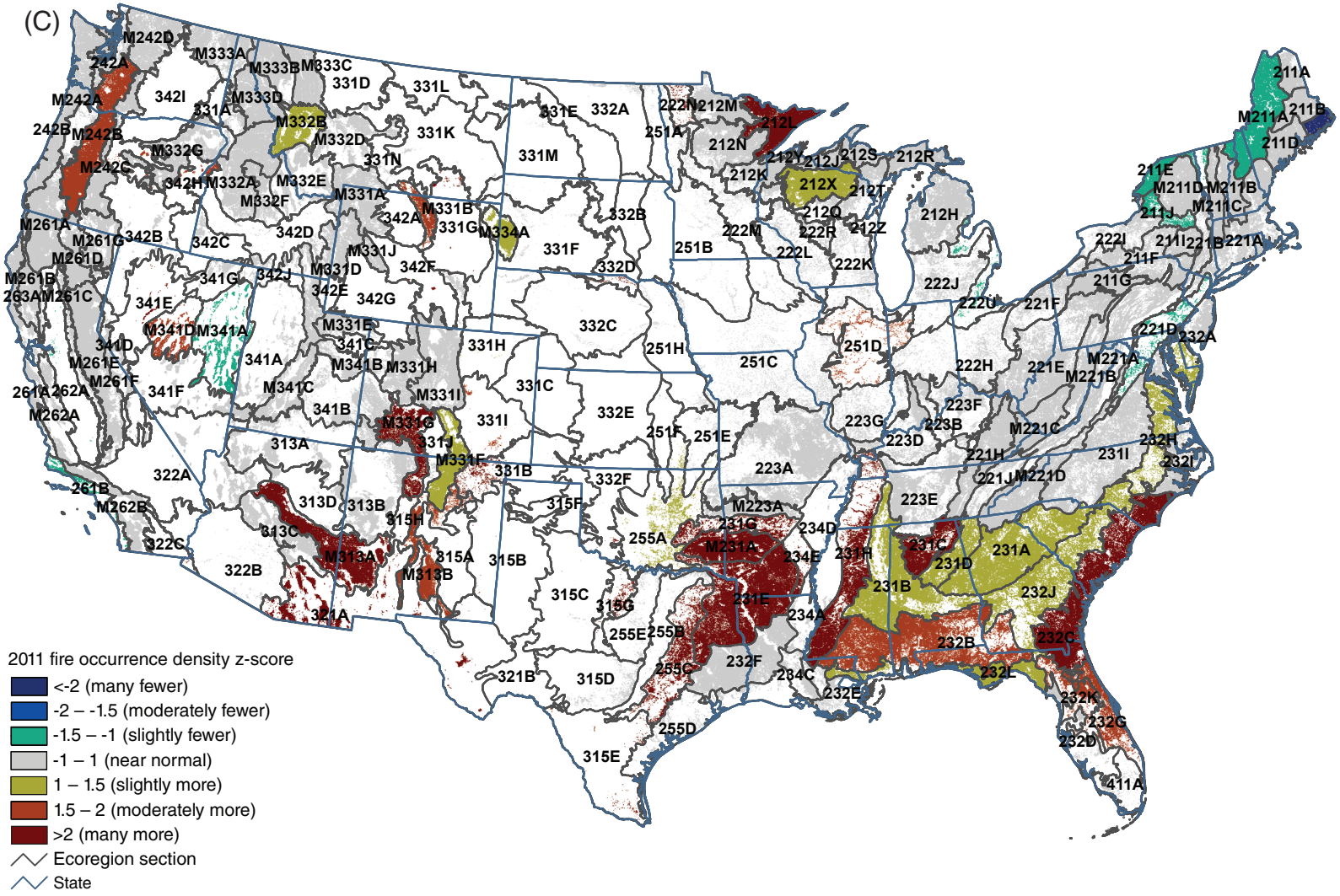


*Figure 3.4 (continued)—(A) Mean number and (B) standard deviation of forest fire occurrences, per 100 km$^2$ (10 000 ha) of forested area from 2001 to 2010, by ecoregion section within the conterminous United States. (C) Degree of 2011 fire occurrence density excess or deficiency by ecoregion relative to 2001–10 and accounting for variation over that time. The gray lines delineate ecoregion sections (Cleland and others 2007). Forest cover is derived from MODIS imagery by the USDA Forest Service Remote Sensing Applications Center. (Source of fire data: USDA Forest Service, Remote Sensing Applications Center.)*

including M332A-Idaho Batholith and several neighboring ecoregions, M261E-Sierra Nevada of California, and 232I-Northern Atlantic Coastal Flatwoods of eastern North Carolina.

A handful of ecoregions in the West and in the Northeast, meanwhile, had lower fire-occurrence densities in 2011 compared with the longer term mean. Most had relatively low long-term means and standard deviations, including 211C-Fundy Coastal and Interior and M211A-White Mountains of Maine, 211E-St. Lawrence and Champlain Valley and 211J-Tug Hill Plateau-Mohawk Valley of northern New York, and M341A-East Great Basin and Mountains of eastern Nevada (fig. 3.4C). One ecoregion, 261B-Southern California Coast, had a lower fire-occurrence density in 2011 compared with a relatively high long-term mean.

In Alaska, meanwhile, the highest mean annual fire-occurrence density between 2001 and 2010 occurred in the east-central and central parts of the State (fig. 3.5A), in the 139A-Yukon Flats and M139A-Ray Mountains ecoregions, with moderate mean fire-occurrence density in neighboring areas. Many of those same areas experienced the greatest degree in variability during the 10-year period (fig. 3.5B). In 2011, only two ecoregions were outside the range of near-normal fire-occurrence density compared with the mean of the previous 10 years and accounting for variability. The M135B-Wrangell Mountains ecoregion, an area in southeast Alaska, had a greater-than-normal fire-occurrence density, and 139A-Yukon Flats, in east-central Alaska, had a lower-than-normal fire-occurrence density (fig. 3.5C).

While summarizing fire-occurrence data at the ecoregion scale allows for the quantification of fire-occurrence density across the country, a geographical hot spot analysis can offer insights into where, at a finer scale, fire occurrences are concentrated. In 2011, the most intense geographical hot spots of fire density within the conterminous States existed in the Southwestern and Southeastern States, with less intense hot spots existing in the Northwest (fig. 3.6). In the Southwest, intense geographic hot spots occurred in the 321A-Chihuahuan Desert Basin and Range section of southwestern New Mexico and southeastern Arizona and in the M313A-White Mountains-San Francisco Peaks-Mogollon Rim section of western New Mexico and eastern Arizona.

Less intense geographic hot spots of fire-occurrence density in the region were detected in 315G-Eastern Rolling Plains of north-central Texas; 315D-Edwards Plateau, 255B-Blackland Prairie, and 255C-Oak Woods and Prairie of east Texas; 321A-Chihuahuan Desert Basin and Range of west Texas; 255A-Cross Timbers and Valley, 231G-Arkansas Valley, and M231A-Ouchita Mountains of eastern Oklahoma; and M331G-South-Central Highlands, M313B-Sacramento-Monzano Mountains, and M331F-Southern Parks and Rocky Mountain Range of north-central New Mexico (fig. 3.6).

In the Southeast, a 2011 high-intensity hot spot of fire-occurrence density occurred

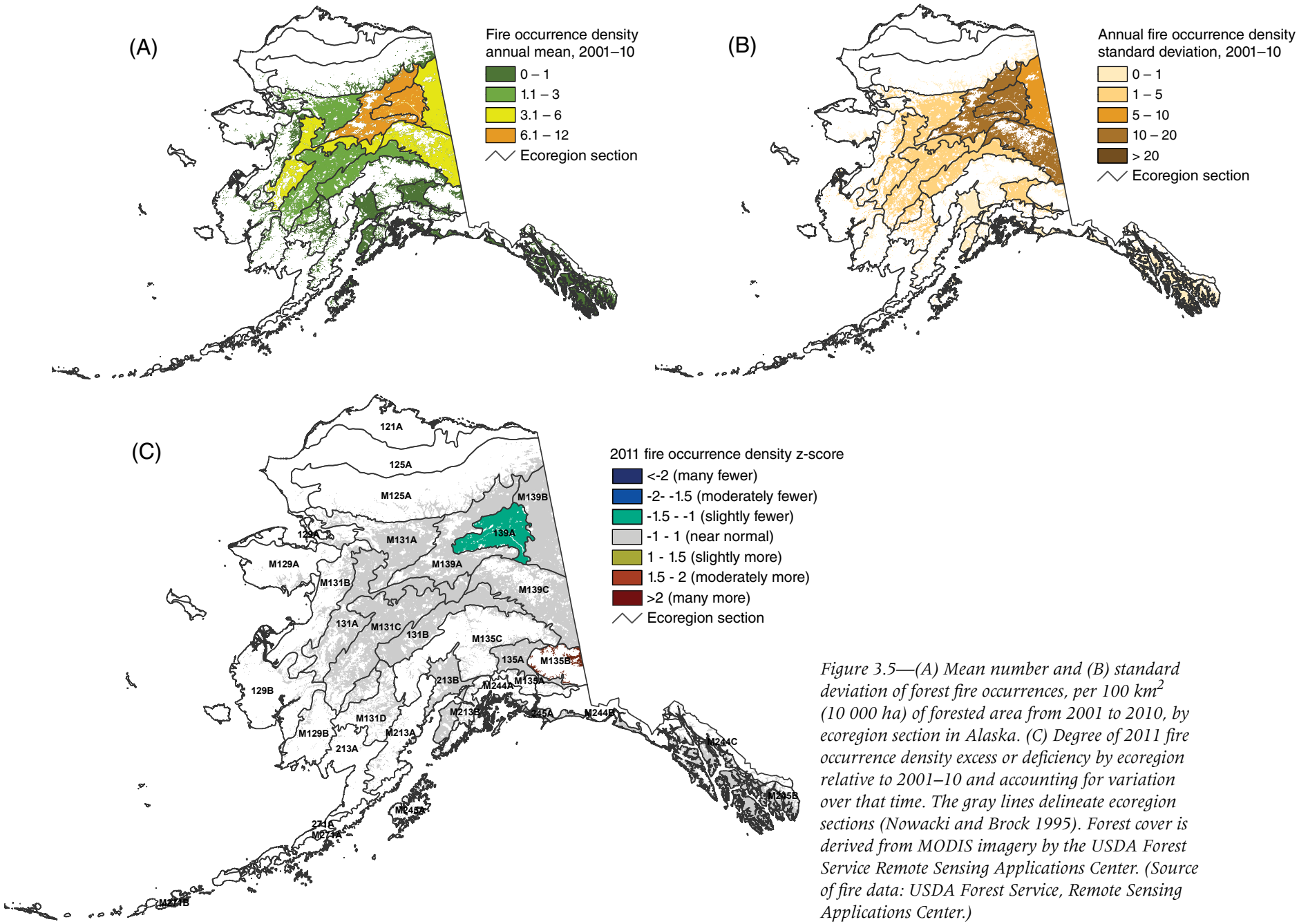


*Figure 3.5—(A) Mean number and (B) standard deviation of forest fire occurrences, per 100 km$^2$ (10 000 ha) of forested area from 2001 to 2010, by ecoregion section in Alaska. (C) Degree of 2011 fire occurrence density excess or deficiency by ecoregion relative to 2001–10 and accounting for variation over that time. The gray lines delineate ecoregion sections (Nowacki and Brock 1995). Forest cover is derived from MODIS imagery by the USDA Forest Service Remote Sensing Applications Center. (Source of fire data: USDA Forest Service, Remote Sensing Applications Center.)*

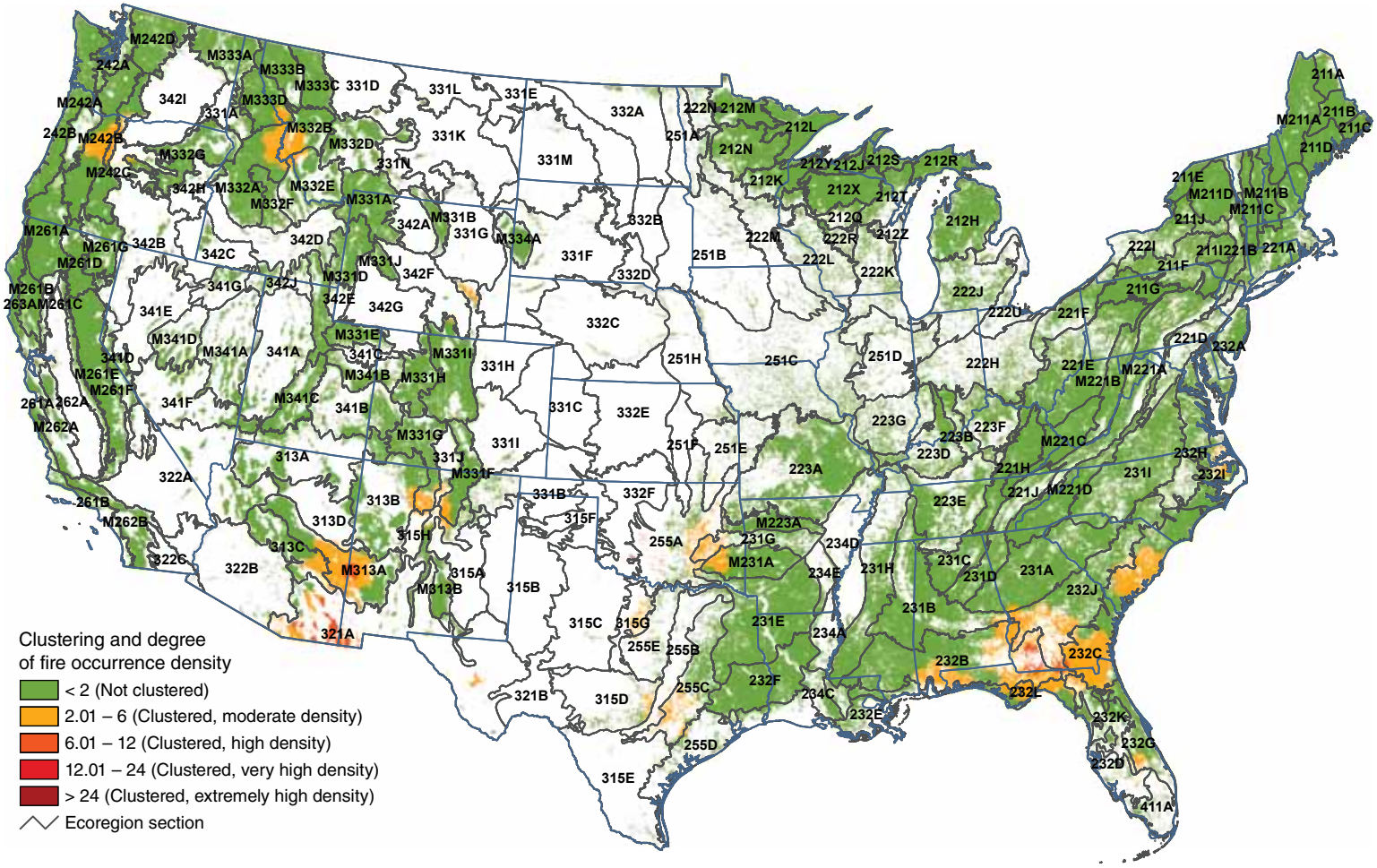


*Figure 3.6—Hot spots of fire occurrence across the conterminous United States for 2011. Values are Getis-Ord $G_i^*$ scores, with values > 2 representing significant clustering of high fire occurrence densities. (No areas of significant clustering of low fire occurrence densities, <-2, were detected.) The gray lines delineate ecoregion sections (Cleland and others 2007). Background forest cover is derived from MODIS imagery by the USDA Forest Service Remote Sensing Applications Center. (Source of fire data: USDA Forest Service, Remote Sensing Applications Center.)*

in 232B-Gulf Coastal Plains and Flatwoods, 232J-Southern Atlantic Coastal Plains and Flatwoods, 232L-Gulf Coastal Lowlands, and 232C-Atlantic Coastal Flatwoods of southeastern Alabama, southern Georgia, and north-central Florida. Less intense geographic hot spots were detected in the Southeast, in 232B-Gulf Coastal Plains and Flatwoods of southern Alabama and western Florida, 232C-Atlantic Coastal Flatwoods of South Carolina, 232I-Northern Atlantic Coastal Flatwoods of eastern North Carolina, and 232G-Florida Coastal Lowlands-Atlantic and 232D-Florida Coastal Lowlands-Gulf of southern Florida.

A handful of other low-intensity geographic hot spots of fire occurrence were detected in the Northwest and the Interior West:

- M242B-Western Cascades and M242C-Eastern Cascades of north-central Oregon.
- M332A-Idaho Batholith, M333D-Bitterroot Mountains, M332B-Northern Rockies and Bitterroot Valley, and M323E-Beaverhead Mountains of eastern Idaho and western Montana.
- M331I-Northern Parks and Ranges of southeastern Wyoming.

The results of these geographic analyses are intended to offer insights into where fire occurrences have been concentrated spatially in a given year and compared with previous years but are not intended to quantify the severity of a given fire season. While ecological impact and forest health relating to fire and other abiotic disturbances are scale-dependent properties that in turn depend on management objectives (Lundquist and others 2011), information about the concentration of fire occurrences may be useful for identifying areas for management activities and for conducting followup investigations related to the ecological and socioeconomic impacts of fires that may be outside the range of historic frequency.

## LITERATURE CITED


Anselin, L. 1992. Spatial data analysis with GIS: an introduction to application in the social sciences. Tech. Rep. 92-10. Santa Barbara, CA: National Center for Geographic Information and Analysis. 53 p.

Barbour, M.G.; Burk, J.H.; Pitts, W.D. [and others]. 1999. Terrestrial plant ecology. Menlo Park, CA: Addison Wesley Longman. 649 p.

Bond, W.J.; Keeley, J.E. 2005. Fire as a global 'herbivore': the ecology and evolution of flammable ecosystems. Trends in Ecology & Evolution. 20(7): 387-394

Cleland, D.T.; Freeouf, J. A., Keys, J.E., Jr. [and others]. 2007. Ecological subregions: sections and subsections for the conterminous United States. 1:3,500,000; Albers equal area projection; colored. In: Sloan, A.M., tech. ed. Gen. Tech. Rep. WO-76. Washington, DC: U.S. Department of Agriculture Forest Service. Also as a GIS coverage in ArcINFO format on CD-ROM or at http://fsgeodata.fs.fed.us/other_resources/ecosubregions.html. [Date accessed: March 18, 2011].

Coulston, J.W.; Ambrose, M.J.; Riitters, K.H.; Conkling, B.L. 2005. Forest Health Monitoring 2004 national technical report. Gen. Tech. Rep. SRS-90. Asheville, NC: U.S. Department of Agriculture Forest Service, Southern Research Station. 81 p.

Edmonds, R.L.; Agee, J.K.; Gara, R.I. 2011. Forest health and protection. Long Grove, IL: Waveland Press. 667 p.

ESRI. 2006. ArcMap 9.2. Redlands, CA: Environmental Systems Research Institute.

Getis, A.; Ord, J.K. 1992. The analysis of spatial association by use of distance statistics. Geographical Analysis. 24(3): 189-206.

Hawbaker, T.J.; Radeloff, V.C.; Syphard, A.D. [and others]. 2008. Detection rates of the MODIS active fire product. Remote Sensing of Environment. 112: 2656-2664.

Justice, C.O.; Giglio, L.; Korontzi, S. [and others]. 2002. The MODIS fire products. Remote Sensing of Environment. 83(1-2): 244-262.

Laffan, S.W. 2006. Assessing regional scale weed distributions, with an Australian example using *Nassella trichotoma*. Weed Research. 46(3): 194-206.

Lundquist, J.E.; Camp, A.E.; Tyrrell, M.L. [and others]. 2011. Earth, wind and fire: abiotic factors and the impacts of global environmental change on forest health. In: Castello, J.D.; Teale, S.A., eds. Forest health: an integrated perspective. New York: Cambridge University Press: 195-243.

McKenzie, D.; Peterson, D.L.; Alvarado, E. 1996. Predicting the effect of fire on large-scale vegetation patterns in North America. Res. Pap. PNW-RP-489. U.S. Department of Agriculture Forest Service, Pacific Northwest Research Station. 38 p.

National Interagency Coordination Center. 2012. Wildland fire summary and statistics annual report: 2011. http://www.predictiveservices.nifc.gov/intelligence/2011_statssumm/intro_summary.pdf. [Date accessed: February 24, 2012].

Nowacki, G.; Brock, T. 1995. Ecoregions and subregions of Alaska, EcoMap Version 2.0. 1:5,000,000; colored. Juneau, AK: U.S. Department of Agriculture Forest Service, Alaska Region.

Nowacki, G.J.; Abrams, M.D. 2008. The demise of fire and "mesophication" of forests in the Eastern United States. BioScience. 58(2): 123-138.

Potter, K.M. 2012a. Large-scale patterns of forest fire occurrence in the conterminous United States and Alaska, 2005-07. In: Potter, K.M.; Conkling, B.L., eds. Forest Health Monitoring 2008 national technical report. Gen. Tech. Rep. SRS-158. Asheville, NC: U.S. Department of Agriculture Forest Service, Southern Research Station: 73-83. Chapter 5.

Potter, K.M. 2012b. Large-scale patterns of forest fire occurrence in the conterminous United States and Alaska, 2001-08. In: Potter, K.M.; Conkling, B.L., eds. Forest health monitoring 2009 national technical report. Gen. Tech. Rep. SRS-167. Asheville, NC: U.S. Department of Agriculture Forest Service, Southern Research Station: 151-162. Chapter 9.

Potter, K.M. 2013a. Large-scale patterns of forest fire occurrence in the conterminous United States and Alaska, 2009. In: Potter, K.M.; Conkling, B.L., eds. Forest health monitoring: national status, trends, and analysis 2010. Gen. Tech. Rep. SRS-176. Asheville, NC: U.S. Department of Agriculture Forest Service, Southern Research Station: 31-38. Chapter 3.

Potter, K.M. 2013b. Large-scale patterns of forest fire occurrence in the conterminous United States and Alaska, 2010. In: Potter, K.M.; Conkling, B.L., eds. Forest health monitoring 2011 national technical report: national status, trends, and analysis 2011. Gen. Tech. Rep. SRS-185. Asheville, NC: U.S. Department of Agriculture Forest Service, Southern Research Station: 29-39. Chapter 3.

Pyne, S.J. 2010. America's fires: a historical context for policy and practice. Durham, NC: Forest History Society. 91 p.

Schmidt, K.M.; Menakis, J.P.; Hardy, C.C. [and others]. 2002. Development of coarse-scale spatial data for wildland fire and fuel management. Gen. Tech. Rep. RMRS-GTR-87. Fort Collins, CO: U.S. Department of Agriculture Forest Service, Rocky Mountain Research Station. 41 p.

U.S. Department of Agriculture (USDA) Forest Service. 2008. National forest type data development. http://svinetfc4.fs.fed.us/rastergateway/forest_type/. [Date accessed: May 13].

U.S. Department of Agriculture (USDA) Forest Service. 2012. MODIS active fire mapping program: fire detection GIS data. http://activefiremaps.fs.fed.us/gisdata.php. [Date accessed: January 11].

Vinton, J.V., ed. 2004. Wildfires: issues and consequences. Hauppauge, NY: Nova Science Publishers. 127 p.

White, D.; Kimerling, A.J.; Overton, W.S. 1992. Cartographic and geometric components of a global sampling design for environmental monitoring. Cartography and Geographic Information Systems. 19(1): 5-22.

# CHAPTER 4.

# Drought Patterns in the Conterminous United States and Hawaii

Frank H. Koch
William D. Smith
John W. Coulston

## INTRODUCTION

Droughts are common in virtually all U.S. forests, but their frequency and intensity vary widely both between and within forest ecosystems (Hanson and Weltzin 2000). Forests in the Western United States generally exhibit a pattern of annual seasonal droughts. Forests in the Eastern United States tend to exhibit one of two prevailing patterns: random occasional droughts, typical of the Appalachian Mountains and of the Northeast, or frequent late-summer droughts, typical of the southeastern Coastal Plain and the eastern edge of the Great Plains (Hanson and Weltzin 2000). For plants, a reduction in basic growth processes (i.e., cell division and enlargement) is the most immediate response to drought; photosynthesis, which is less sensitive than these basic processes, decreases slowly at low levels of drought stress but begins to decrease more sharply when the stress becomes moderate to severe (Kareiva and others 1993, Mattson and Haack 1987). Drought makes some forests more susceptible to infestations of tree-damaging insects and diseases (Clinton and others 1993, Mattson and Haack 1987). Furthermore, drought may increase wildland fire risk by impeding decomposition of organic matter and reducing the moisture content of downed woody materials and other potential fire fuels (Clark 1989, Keetch and Byram 1968, Schoennagel and others 2004).

Notably, forests appear to be relatively resistant to short-term drought conditions (Archaux and Wolters 2006), although individual tree species differ in their responses (Hinckley and others 1979, McDowell and others 2008). The duration of a drought event is arguably more significant than its intensity (Archaux and Wolters 2006); for example, multiple consecutive years of drought (2 to 5 years) are more likely to result in high tree mortality than a single dry year (Guarín and Taylor 2005, Millar and others 2007). This suggests that a comprehensive characterization of drought impact in forested areas should include analysis of moisture conditions in the United States during relatively long (i.e., multiyear) time windows.

In the Forest Health Monitoring (FHM) 2010 national report, we outlined a new methodology for mapping drought conditions across the conterminous United States (Koch and others 2013a). As in previous work related to this topic (Koch and others 2012a, 2012b), a primary objective of this new methodology was to provide forest managers and researchers with drought-related spatial datasets that are finer scale than products available from such sources as the National Climatic Data Center (2007) or the U.S. Drought Monitor Program (Svoboda and others 2002). The primary inputs are gridded climate data (i.e., monthly raster maps of precipitation and temperature over a 100-year period) created with the Parameter-Elevation

Regression on Independent Slopes (PRISM) climate mapping system (Daly and others 2002). A pivotal aspect of our new methodology is a standardized drought indexing approach that enables us to directly compare, for any given location of interest, its moisture status during different time windows, regardless of their length. For example, the FHM 2010 national report includes a comparison of national drought maps for 2009, the 3-year window 2007–09, and the 5-year window 2005–09 (Koch and others 2013a).

One of our main goals for the present analysis was to apply this methodology to the most currently available climate data (i.e., the monthly PRISM data through 2011). In turn, our results are intended to complement the results of similar analyses performed for the 2010 and 2011 FHM national reports, which were based on PRISM data through 2009 and 2010, respectively (Koch and others 2013a, 2013b). Thus, the current analysis represents a third time step in what we expect to be an ongoing annual record of drought status across the conterminous United States. In addition, we performed a separate analysis of drought patterns in Hawaii. Briefly, we developed 1-, 3-, and 5-year drought map products as data support for insect and disease risk mapping efforts in the State. However, unlike for the conterminous United States, we did not have monthly gridded climate data (i.e., PRISM data) of Hawaii as a foundation for our analysis. Therefore, we generated these grids ourselves through spatial interpolation of weather station observations recorded in Hawaii during an 88-year (1920-2007) period. Details about the interpolation process are provided in this chapter, along with a discussion of some highlights of our analytical results for the State.

## METHODS

We acquired monthly PRISM grids for total precipitation, mean daily minimum temperature, and mean daily maximum temperature for the conterminous United States from the PRISM group Web site (PRISM Group 2012). When we performed our analyses, gridded datasets were available for all years from 1895 to 2011. However, the grids for May through December 2011 were only provisional versions (i.e., the PRISM group had not yet released finalized grids for these months). For the current analyses, we treated these provisional grids as if they were the final versions. The spatial resolution of the grids was approximately 4 km (cell area = 16 $km^2$); for future applications and to ensure better compatibility with other spatial datasets, all output grids were resampled to a spatial resolution of approximately 2 km (cell area = 4 $km^2$) using a nearest neighbor approach.

## Potential Evapotranspiration Maps

As in our previous drought mapping efforts (Koch and others 2012a, 2012b, 2013a, 2013b), we adopted an approach in which a moisture index value for each location of interest (i.e., each grid cell in a map of the conterminous United States) was calculated based on both precipitation and potential evapotranspiration (*PET*) values for that location during the period of interest. *PET* measures the loss of soil moisture through plant uptake and transpiration (Akin 1991). It does not measure actual moisture loss, but rather the loss that would occur under ideal conditions (i.e., if there was no possible shortage of moisture for plants to transpire) (Akin 1991, Thornthwaite 1948). The ratio between precipitation and *PET* subsequently provides a fuller accounting of a location's water balance than precipitation alone.

To complement the available PRISM monthly precipitation grids, we computed corresponding monthly *PET* grids using Thornthwaite's formula (Akin 1991, Thornthwaite 1948):

$$PET_m = 1.6 L_{lm} \left(10 \frac{T_m}{I}\right)^a \qquad (1)$$

where

$PET_m$ = the potential evapotranspiration for a given month $m$ in cm

$L_{lm}$ = a correction factor for the mean possible duration of sunlight during month $m$ for all locations (i.e., grid cells) at a particular latitude $l$ [see table V in Thornthwaite (1948) for a list of $L$ correction factors by month and latitude]

$T_m$ = the mean temperature for month $m$ in degrees C

$a$ = an exponent calculated as $a = 6.75 \times 10^{-7} I^3 - 7.71 \times 10^{-5} I^2 + 1.792 \times 10^{-2} I + 0.49239$ [see appendix I in Thornthwaite (1948) regarding the empirical derivation of $a$]

$I$ = an annual heat index, calculated as $I = \sum_{m=1}^{12} \left(\frac{T_m}{5}\right)^{1.514}$ where

$T_m$ = the mean temperature for each month $m$ of the year

To implement equation 1 spatially, we created a grid of latitude values for determining the $L$ adjustment for any given grid cell (and any given month) in the conterminous United States. We calculated the mean monthly temperature grids as the mean of the corresponding PRISM daily minimum and maximum monthly temperature grids.

## Moisture Index Maps

We used the precipitation (*P*) and *PET* grids to generate baseline moisture index grids for the past 100 years (i.e., 1912–2011) for the conterminous United States. We used a moisture index, *MI′*, described by Willmott and Feddema (1992), with the following form:

$$MI' = \begin{cases} P/PET - 1 & , \quad P < PET \\ 1 - PET/P & , \quad P \geq PET \\ 0 & , \quad P = PET = 0 \end{cases} \qquad (2)$$

where

*P* = precipitation

*PET* = potential evapotranspiration

(*P* and *PET* must be in equivalent measurement units, e.g., mm)

This set of equations yields a dimensionless index scaled between -1 and 1. A key reason for using this particular equation set is that it ensures that *MI′* is centered at zero, with values below zero indicating moisture deficit and values greater than zero indicating moisture surplus. *MI′* can be calculated for any period but is commonly calculated on an annual basis using summed *P* and *PET* values (Willmott and Feddema 1992). An alternative to this summation approach is to calculate *MI′* from monthly *P* and *PET* values and then, for a given time window of interest, calculate its moisture index as the mean of the *MI′* values for all months in the window. This "mean-of-months" approach limits the ability of short-term peaks in either *P* or *PET* to negate corresponding short-term deficits, as would happen under a summation approach.

For each year in our study period (i.e., 1912–2011), we used the mean-of-months approach to calculate moisture index grids for three different time windows: 1 year ($MI_1'$), 3 years ($MI_3'$), 5 years ($MI_5'$). Briefly, the $MI_1'$ grids are the mean of the 12 monthly *MI′* grids for each year in the study period, the $MI_3'$ grids are the mean of the 36 monthly grids from January 2 years prior through December of the target year, and the $MI_5'$ grids are the mean of the 60 consecutive monthly *MI′* grids from January 4 years prior to December of the target year. For example, for the year 2011, the $MI_1'$ grid is the mean of the monthly *MI′* grids from January to December 2011, the $MI_3'$ grid is the mean of grids from January 2009 to December 2011, and the $MI_5'$ grid is the mean of the grids from January 2007 to December 2011.

## Annual and Multiyear Drought Maps

To determine degree of departure from typical moisture conditions, we first created a normal grid, $MI_{i\,norm}'$ for each of our three time windows, representing the mean of the 100 corresponding moisture index grids (i.e., the $MI_1'$, $MI_3'$, or $MI_5'$ grids, depending on the window; see fig. 4.1). We also created a standard deviation grid, $MI_{i\,SD}'$, for each time window, calculated from the window's 100 individual moisture index grids as well as its $MI_{i\,norm}'$ grid.

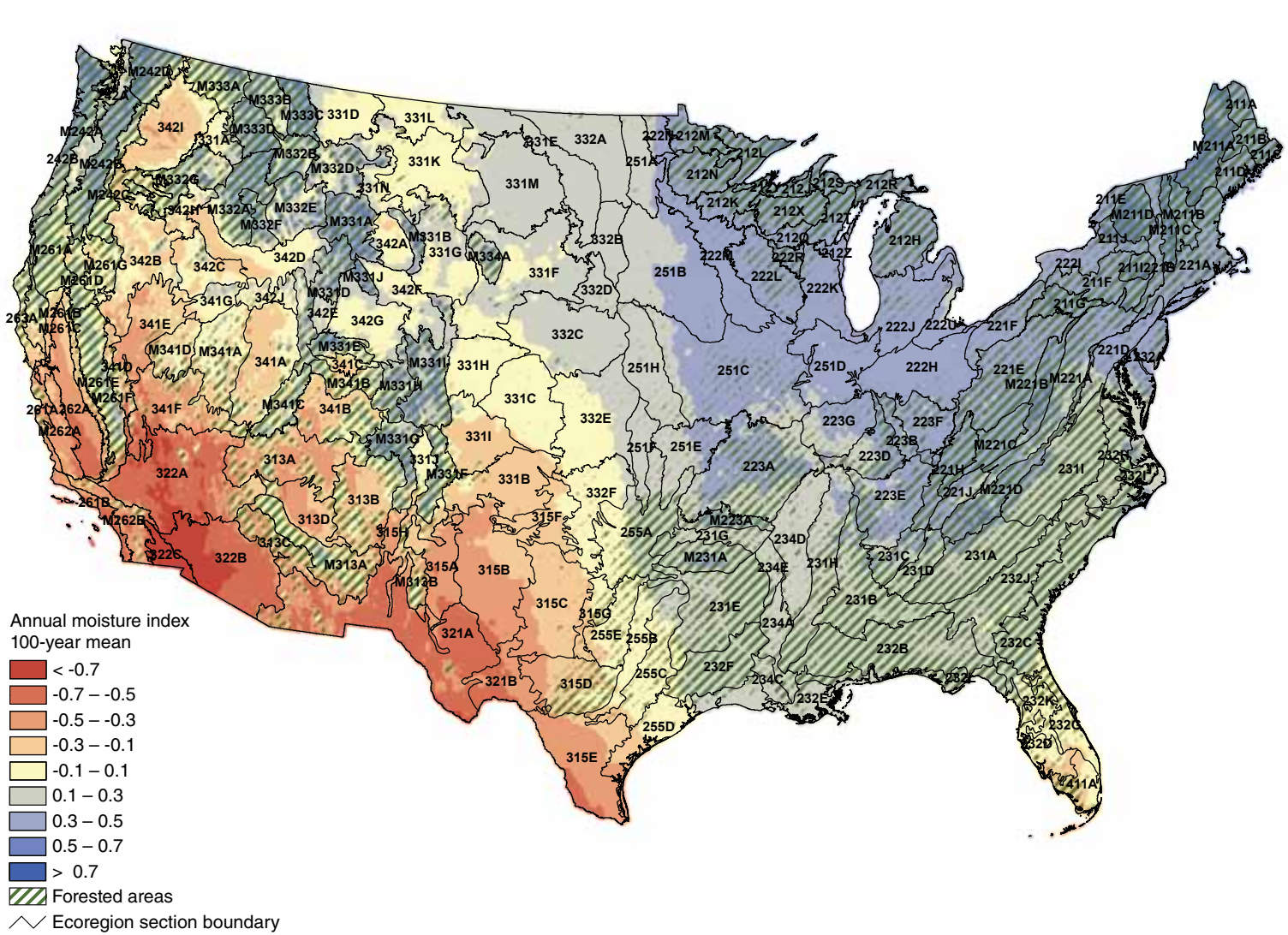


*Figure 4.1—The 100-year (1912–2011) mean annual moisture index, or* $\mathrm{MI}_1{}'_{\mathrm{norm}}$ *for the conterminous United States. Ecoregion section (Cleland and others 2007) boundaries and labels are included for reference. Forest cover data (overlaid green hatching) is derived from MODIS imagery by the USDA Forest Service Remote Sensing Applications Center. (Data source: PRISM Group, Oregon State University.)*

We subsequently calculated moisture difference *z*-scores (*MDZ*s) for each time window using these derived datasets:

$$MDZ_{ij} = \frac{MI_i' - MI_{i\ norm}'}{MI_{i\ SD}'} \qquad (3)$$

where

$i$ = the analytical time window (1, 3, or 5 years)

$j$ = a particular target year in our 100-year study period (i.e., 1911-2011)

*MDZ*s may be classified in terms of degree of moisture deficit or surplus (table 4.1). The classification scheme includes categories (e.g., severe drought or extreme drought) like those associated with the Palmer Drought Severity Index (Palmer 1965). Importantly, because of the standardization in equation 3, the breakpoints between categories remain the same regardless of the size of the time window of interest. For comparative analysis, we generated classified *MDZ* maps of the conterminous United States, based on all three time windows, for the target year 2011 (figs. 4.2, 4.3, and 4.4). Because our analysis focused on drought (i.e., moisture deficit) rather than surplus conditions, we combined the four moisture surplus categories from table 4.1 into a single category for map display.

**Table 4.1—Moisture difference *z*-score (*MDZ*) value ranges for nine wetness and drought categories, along with each category's approximate theoretical frequency of occurrence**

| *MDZ* score value range | Category | Frequency |
|---|---|---|
| | | % |
| < -2 | Extreme drought | 2.3 |
| -2 to -1.5 | Severe drought | 4.4 |
| -1.5 to -1 | Moderate drought | 9.2 |
| -1 to -0.5 | Mild drought | 15.0 |
| -0.5 to 0.5 | Near-normal conditions | 38.2 |
| 0.5 to 1 | Mild moisture surplus | 15.0 |
| 1 to 1.5 | Moderate moisture surplus | 9.2 |
| 1.5 to 2 | Severe moisture surplus | 4.4 |
| > 2 | Extreme moisture surplus | 2.3 |

## Drought map products for Hawaii

Because a historical record of monthly gridded climate data was unavailable for Hawaii, we generated monthly grids of total precipitation and average temperature through spatial interpolation of observations at weather stations distributed across the State. Several well-documented spatial interpolation methods include inverse distance weighting, spline, and the geostatistical procedure known as "kriging." All these methods similarly predict values for a variable of interest at unsampled locations based on the values recorded at nearby known locations. Kriging, in particular, makes its predictions by exploiting the underlying spatial structure of the variable, i.e., the spatial dependence or autocorrelation between

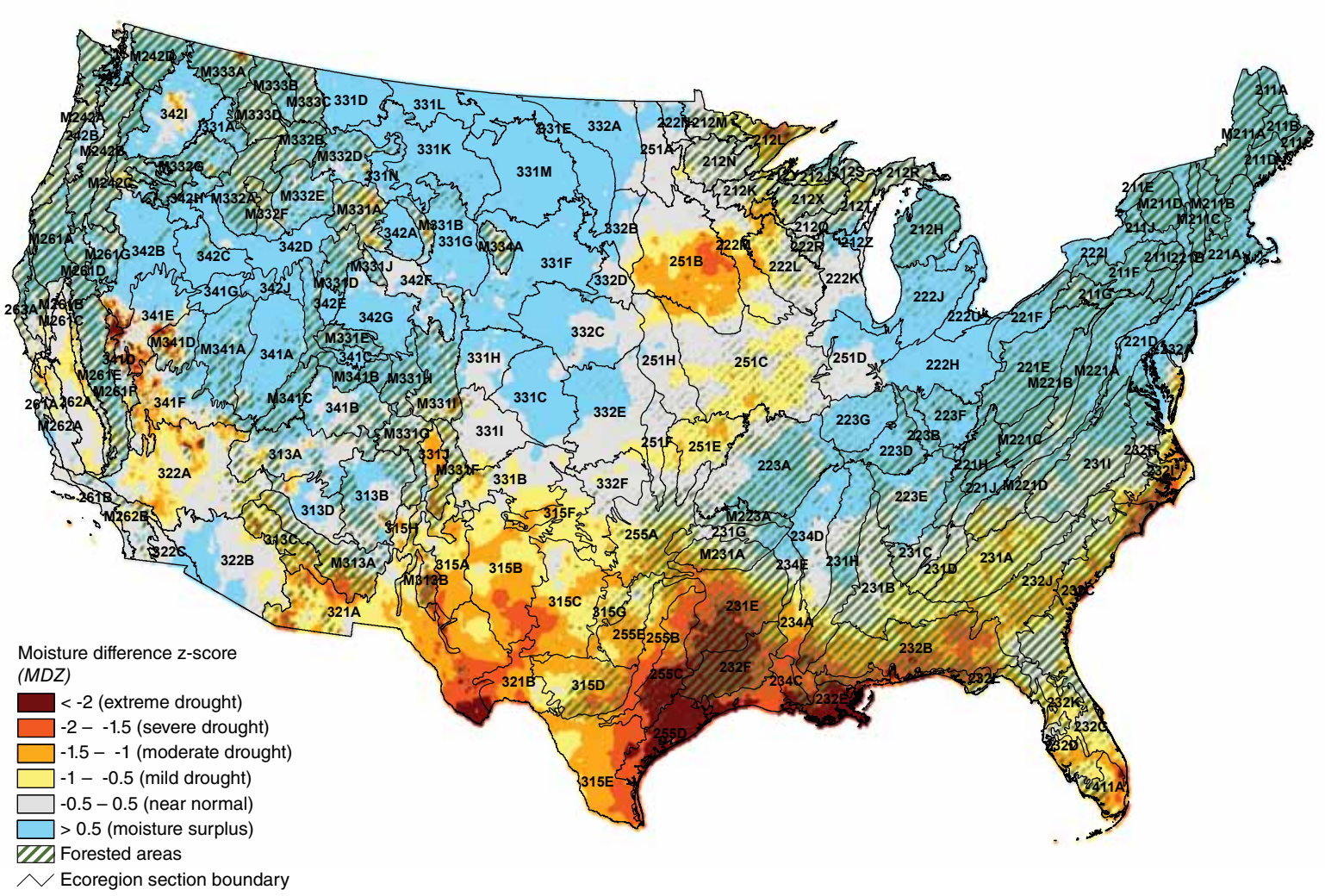


*Figure 4.2—The 2011 annual (i.e., 1-year) moisture difference* z-score, or MDZ, *for the conterminous United States. Ecoregion section (Cleland and others 2007) boundaries and labels are included for reference. Forest cover data (overlaid green hatching) is derived from MODIS imagery by the USDA Forest Service Remote Sensing Applications Center. (Data source: PRISM Group, Oregon State University.)*

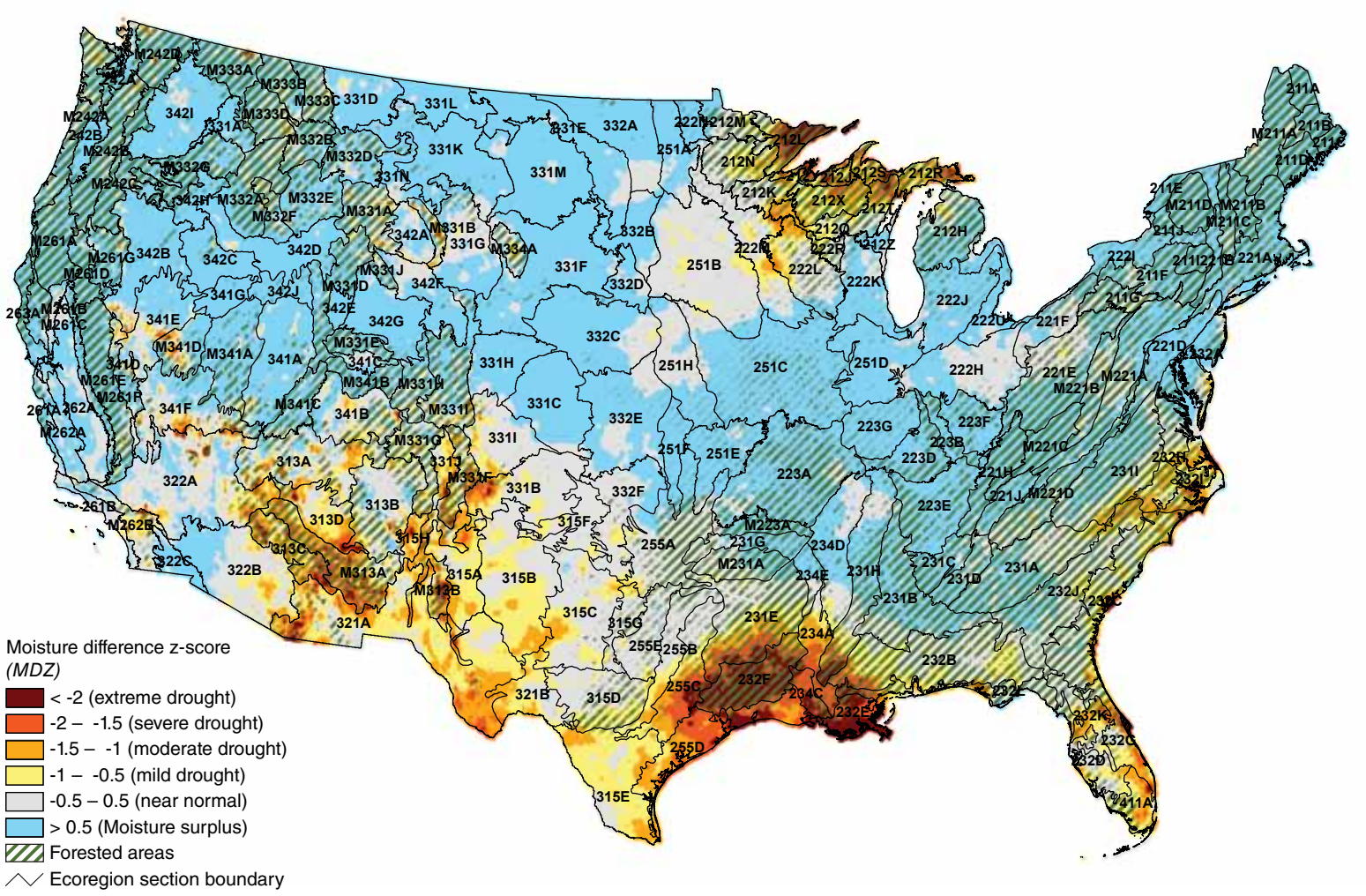


*Figure 4.3—The 2009–11 (i.e., 3-year) moisture difference* z-score, *or* MDZ, *for the conterminous United States. Ecoregion section (Cleland and others 2007) boundaries are included for reference. Forest cover data (overlaid green hatching) is derived from MODIS imagery by the USDA Forest Service Remote Sensing Applications Center. (Data source: PRISM Group, Oregon State University.)*

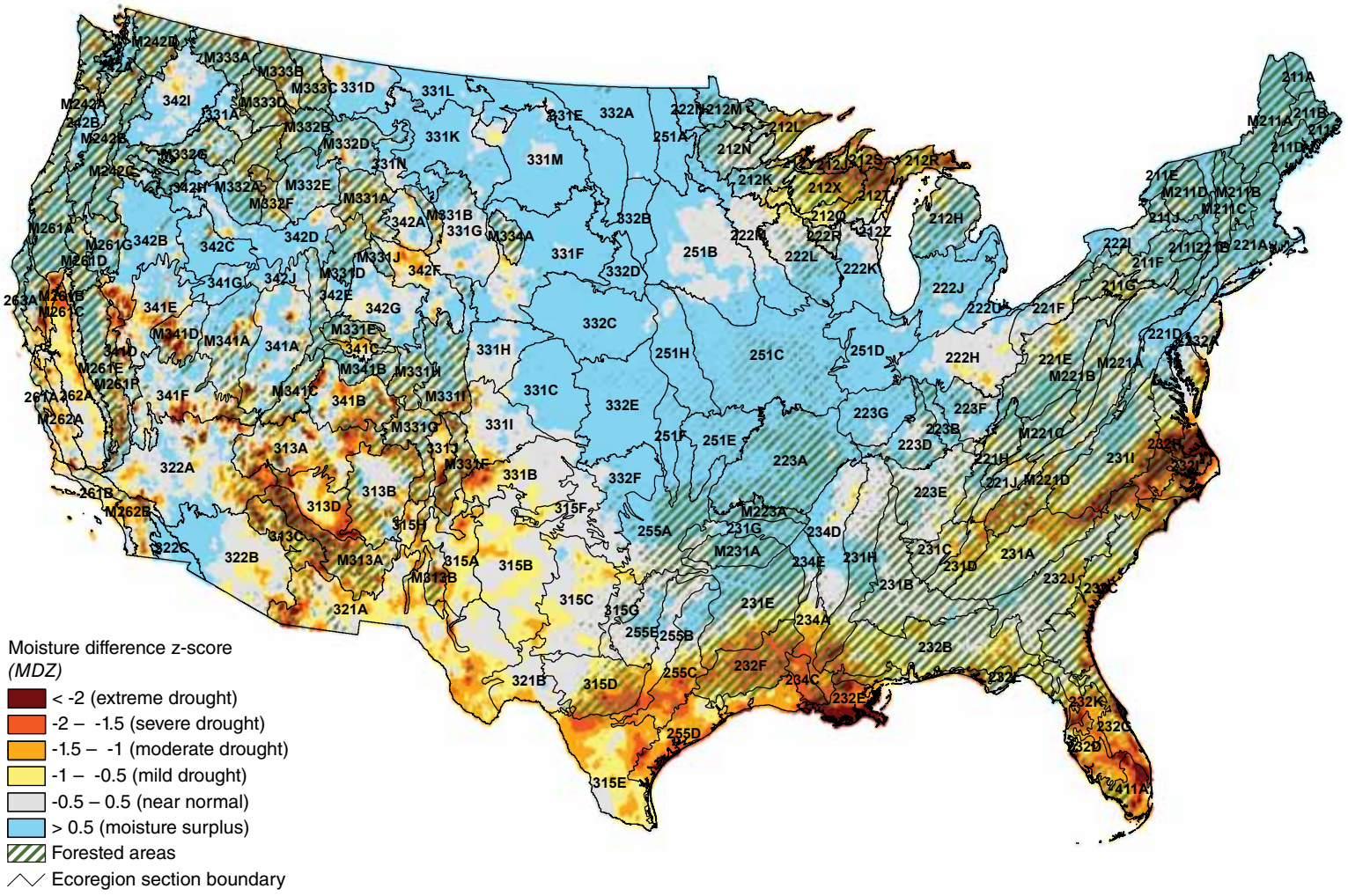


*Figure 4.4—The 2007–11 (i.e., 5-year) moisture difference* z-score, *or* MDZ, *for the conterminous United States. Ecoregion section (Cleland and others 2007) boundaries are included for reference. Forest cover data (overlaid green hatching) is derived from MODIS imagery by the USDA Forest Service Remote Sensing Applications Center. (Data source: PRISM Group, Oregon State University.)*

neighboring locations (Goovaerts 2000). This structure may be quantified using an empirical semivariogram constructed from pairs of known locations that comprise a sample of the variable (Cressie 1993). A model semivariogram (e.g., a spherical or exponential model) is fitted to the empirical semivariogram, which is then used to calculate "kriging weights" that are applied to a set of nearby known points in order to estimate the value at an unsampled location (Phillips and others 1992).

Cokriging is a multivariate version of kriging; the values for a variable of interest at unsampled locations are still estimated from neighboring known locations but, in this case, using values of one or more covariates as well as the variable of interest. This requires quantification of the spatial structure of each covariate (commonly done using additional semivariograms) as well the variables' cross-correlations or cross-covariance (Phillips and others 1992). Although this adds computational complexity, cokriging is especially suited to cases in which the target variable has been only sparsely sampled in space but a highly correlated covariate (or covariates) has been sampled more intensively. Elevation, which is often densely and regularly sampled, is a common covariate. For instance, elevation data have been used in cokriging of both precipitation (Hevesi and others 1992) and air temperature (Ishida and Kawashima 1993) from relatively sparse networks of observations. We applied ordinary cokriging (Cressie 1993, Goovaerts 1998), using elevation values drawn from a digital elevation model (DEM), to construct monthly grids of total precipitation and mean temperature for Hawaii.

Our source for precipitation data was *The Rainfall Atlas of Hawai'i* (Giambelluca and others 2011), which provided regular sets of rain gauge observations for each month from January 1920 until December 2007. The atlas assembled these data from a variety of sources, including the Office of the State Climatologist, the U.S. National Climatic Data Center (NCDC), the U.S. Geological Survey (USGS), and a variety of smaller rain gauge networks. Furthermore, because the rain gauges in these networks had different periods of operation, the researchers who constructed the atlas dataset employed a process of "gap-filling" (i.e., statistically estimating precipitation values for rain gauges that were not operational at a particular point in time) in order to improve spatial coverage. As a result, we were able to perform our interpolations based on more than 1,000 precipitation observations in any given month and year. These observations were distributed across all of the major Hawaiian Islands except Ni'ihau, which was therefore omitted from our analyses.

We acquired monthly mean temperature data for Hawaii from the NCDC (National Climatic Data Center 2012a). Over the period of interest (January 1920 to December 2007), the average number of temperature observations available each month was 46 (minimum = 28, maximum = 69). Although there were considerably more

observations of precipitation than temperature in any given month, temperature is less spatially variable (Gómez and others 2008) and so may be interpolated more reliably from fewer data. Regarding elevation, the USGS had previously developed a 30-m resolution DEM for Hawaii. To reduce computation time, however, we resampled the original DEM to a resolution of 240 m (using the cubic convolution method). We used this resampled DEM in all of our interpolations.

We performed cokriging of precipitation and temperature separately for each month of the study period. We set up the interpolations for each variable as batch processes, which we executed using the Geostatistical Analyst extension of the ArcGIS software package (ESRI 2010). Each month, all model semivariogram (i.e., the stable semivariogram model; see Johnston and others 2003) parameters for elevation and the target variable, as well as the cross-covariance, were automatically refitted using the weighted least squares approach (Cressie 1993). Before calculating these parameters, we removed either a first-order (temperature) or second-order (precipitation) trend from the climate data to minimize macroscale variation. We did not detrend the elevation data. After calculating the semivariograms and cross-covariance, we used circular search windows (with the optimal radial distance recalculated each month) to define neighborhoods of sampled locations used in predicting values at unsampled locations. In summary, predicted values were based on from 2 to 5 observations of the target variable (i.e., either temperature or precipitation) and up to 20 elevation observations. (Trials with different neighborhoods revealed only minor changes in prediction estimates.) The output interpolated grids had a spatial resolution of 2 km (cell area = 4 $km^2$).

After completing the cokriging operations, we used the interpolated grids to develop drought-related map products for Hawaii in a manner similar to our procedure for the conterminous United States. First, we used the temperature grids to develop *PET* grids for each month in our study period (see equation 1). Next, we applied the monthly *PET* grids and corresponding *P* grids to develop baseline moisture index grids for the 1-year, 3-year, and 5-year time windows (i.e., $MI_1'$, $MI_3'$, and $MI_5'$ grids; see equation 2). From these moisture index grids, we calculated $MI_{i\,norm}'$ and $MI_{i\,SD}'$ grids for each time window, which we then used to create a full set of classified *MDZ* maps for the study period (see equation 3). The only noteworthy difference between our analyses for the conterminous United States and Hawaii is that we had a total of 88 years (i.e., 1920–2007) of available data for the latter, as opposed to more than 110 years for the former. This meant that we had to calculate the $MI_{1\,norm}'$ and $MI_{1\,SD}'$ grids for Hawaii (and the corresponding *MDZ* maps) based on an 88-year window. Moreover, because we did not have additional years of data before 1920, we were limited to an 86-year (1922–2007) window

for $MI_{3\,norm}'$, $MI_{3\,SD}'$, and the corresponding *MDZ* maps, as well as an 84-year (1924–2007) window for $MI_{5\,norm}'$, $MI_{3\,SD}'$, and their corresponding maps.

To investigate long-term drought patterns in Hawaii, we created a series of four drought frequency grids by overlaying the annual (i.e., 1-year) *MDZ* maps and subsequently calculating, for each map cell, the proportion of years out of 88 that the cell exhibited the following conditions: at least mild drought (*MDZ* < -0.5), at least moderate drought (*MDZ* < -1), at least severe drought (*MDZ* < -1.5), and extreme drought (*MDZ* < -2). We adopted a similar approach for the 3- and 5-year drought windows. Briefly, we overlaid the appropriate set of *MDZ* grids and counted the number of times (out of 86 and 84, respectively) in which grid cell values indicated at least mild, at least moderate, at least severe, or extreme drought conditions. We then divided these counts by the matching value (i.e., 86 or 84) to estimate 3- and 5-year drought frequencies in the outlined drought categories.

## RESULTS AND DISCUSSION

### Conterminous United States

The 100-year (1912–2011) mean annual moisture index, or $MI_{1\,norm}'$, grid (fig. 4.1) provides a relatively long-term historical overview of climatic regimes across the conterminous United States. (Because the 100-year $MI_{3\,norm}'$ and $MI_{5\,norm}'$ grids were very similar to the mean $MI_{1\,norm}'$ grid, they are not shown here.) Wet climates ($MI' > 0$) are typical throughout the Eastern United States, especially the Northeast. Southern Florida—in particular ecoregion sections 232C-Florida Coastal Lowlands-Atlantic, 232D-Florida Coastal Lowlands-Gulf, and 411A-Everglades—appears to be, perhaps surprisingly, the driest region of the Eastern United States. Although this region usually receives a high level of *P*, this is counteracted by a high level of *PET*, resulting in negative *MI*′ values. The apparent dryness of southern Florida (i.e., where high *P* is offset by high *PET*) arises from very different circumstances than those observed in the driest parts of the Western United States, especially the Southwest (e.g., sections 322A-Mojave Desert, 322B-Sonoran Desert, and 322C-Colorado Desert), where *PET* is very high but *P* levels are very low. In fact, dry climates ($MI' < 0$) are common across much of the Western United States because of generally lower precipitation than in the East. Yet, mountainous areas in the central and northern Rocky Mountains and in the Pacific Northwest are relatively wet; for example, ecoregion sections M242A-Oregon and Washington Coast Ranges, M242B-Western Cascades, M331G-South-Central Highlands, and M333C-Northern Rockies. This may be partially shaped by high levels of winter snowfall in these regions.

Figure 4.2 shows the annual (i.e., 1-year) *MDZ* map for 2011 for the conterminous United States. Its most distinctive feature is a nearly continuous swath of moderate-to-extreme drought conditions stretching across the southern portion of the country.

The western end of this swath is essentially defined by a cluster of areas with extreme drought (*MDZ* < -2) conditions in ecoregion sections 341D-Mono, 341E-Northern Mono, and M341D-West Great Basin and Mountains; however, only in the latter section do these conditions appear to affect forested areas. The eastern end of the swath is demarcated by an area of moderate to extreme drought along the southeast Atlantic coast, especially in the northern portion of ecoregion section 232C-Atlantic Coastal Flatwoods and the adjacent portion of section 232I-Northern Atlantic Coastal Flatwoods.

The swath includes three sizeable and contiguous "hot spots" of extreme drought. The largest of these hot spots encompasses much of ecoregion sections 231E-Mid Coastal Plains-Western, 232F-Coastal Plains and Flatwoods-Western Gulf, 255C-Oak Woods and Prairie, and the sparsely forested section 255D-Central Gulf Prairie and Marshes. The second largest hot spot includes most of the eastern portion of section 232E-Louisiana Coastal Prairie and Marshes, but it also extends into two more heavily forested sections, 234C-Atchafalaya and Red River Alluvial Plains and 232L-Gulf Coastal Lowlands. Finally, another hot spot occupies the southeastern tip of section 321A-Chihuahuan Desert Basin and Range and extends into the adjacent section 321B-Stockton Plateau. (The area in question is largely unforested.) Taken together, these three hot spots—along with neighboring areas of moderate to severe drought—comprise an expansive region of intense drought conditions that spans the States of Texas and Louisiana. Both States, especially Texas, had historically dry years in 2011. Furthermore, both States experienced record heat during the summer months (National Climatic Data Center 2012b).

North of this swath, most of the United States experienced a moisture surplus in 2011. In the Northeastern United States, there were isolated occurrences of mild drought, but the droughts were extremely limited in extent (i.e., encompassing no more than a few adjacent map cells). The northern Rocky Mountain and Pacific Northwest regions contained some larger pockets of moderate to extreme drought, perhaps most notably in the forested ecoregion sections M331A-Yellowstone Highlands and M333A-Okanogan Highland as well as the largely unforested section 342I-Columbia Basin. These examples notwithstanding, the northern Rockies and Pacific Northwest had precipitation levels far above normal through the first half of 2011, which offset drier-than-normal conditions in some portions of these regions during the latter half of the year (National Climatic Data Center 2012b).

A fairly extensive area of moderate to severe drought was centered on (largely unforested) section 251B-North Central Glaciated Plains. To the north of this area, in the heavily forested western Great Lakes region, there was a pronounced drought hot spot (moderate to extreme drought) in section 212L-Northern Superior Uplands. This represents a departure from 2010, when this region experienced record dryness (National Climatic Data Center 2011)

and many other nearby ecoregion sections (e.g., 212S-Northern Upper Peninsula) also exhibited extreme drought conditions.

Whereas the single-year *MDZ* map in figure 4.2 represents the most recent annual snapshot of moisture conditions across the conterminous United States, the 3-year (fig. 4.3) and 5-year (fig. 4.4) *MDZ* maps depict recent short-term trends in these conditions. For instance, the Southwestern United States has been regularly subject to intense and widespread droughts during the past two decades (Groisman and Knight 2008; Mueller and others 2005; National Climatic Data Center 2010, 2011; O'Driscoll 2007). The persistence of these conditions is partially illustrated by the 3-year and 5-year *MDZ* maps, which both depict numerous areas of severe to extreme drought distributed across this region. A couple of interesting exceptions exist, however; for example, the western portion of ecoregion section 322B-Sonoran Desert and most of section 322C-Colorado Desert display a moisture surplus in the 1-, 3-, and 5-year maps. (The two sections are virtually unforested.)

In addition, the 3- and 5-year *MDZ* maps depict severe to extreme drought conditions along the same section of the Gulf Coast (i.e., in eastern Texas and Louisiana) as highlighted by the 2011 annual map. Because forests in this region may not be as well adapted to drought as those in the Southwest, these conditions might represent a more immediate threat to forest health. In contrast, the drought hot spot observed in the Great Lakes region during 2011 (i.e., in ecoregion section 212L; see fig. 4.2) is small compared with the drought-affected areas depicted in the region by the 3- and 5-year *MDZ* maps. Thus, although drought stress may also be a persistent problem for forests in the Great Lakes region, at least a recent improvement in regional moisture conditions may have positive implications for affected forests.

In some geographic regions, the 5-year *MDZ* map (fig. 4.4) displays more extensive or severe drought conditions than the 3-year *MDZ* map (fig. 4.3). This difference may indicate short-term temporal fluctuations in a long-term pattern of persistent drought for the region of interest, as is the case in the Southwestern United States. It may be explained alternatively by the occurrence of especially intense drought conditions during the early years of the 5-year *MDZ* window (i.e., 2007–08 for the current 2011 analysis). For instance, a part of the Southeastern United States (i.e., in sections 231I-Central Appalachian Piedmont, 232H-Middle Atlantic Coastal Plain and Flatwoods, and 232I-Northern Atlantic Coastal Plain and Flatwoods) exhibits comparatively worse drought conditions in the 5-year *MDZ* map than in the 3-year map; a historically exceptional drought that occurred during 2007 (O'Driscoll 2007) likely explains this discrepancy, as well as a similarly observable difference in central to southern Florida. Thus, while the 1-year, 3-year, and 5-year *MDZ* maps together provide a fairly comprehensive short-term overview, it may also be important to consider a particular region's longer term drought history when assessing the current health of its forests.

## Hawaii

With the exception of Kaho'olawe, which is relatively flat, the major islands of Hawaii (fig. 4.5) display rugged topography, often transitioning quickly from coastal lowlands to inland mountains along steep elevation gradients. The largest island, Hawai'i, is dominated by the volcanoes Mauna Kea and Mauna Loa, both of which approach 14,000 feet in elevation; the volcano Haleakala on the island of Maui rises to approximately 10,000 feet. Each of these volcanoes is encircled by a subalpine zone (6,000 to 6,500 feet in elevation) that features certain shrub communities that extend above treeline, which is approximately 8,200 feet (Cordell and others 2000, Cuddihy 1989). A true alpine ecological zone exists only on the high slopes of Mauna Kea and Mauna Loa (Cuddihy 1989).

The major islands of Hawaii all exhibit a similar, concentric pattern of vegetation distribution (Noguchi 1992). A key factor behind this pattern (fig. 4.6) is the influence of northeasterly trade winds, which interact with the islands' mountains to create dramatic variations in precipitation levels (Cuddihy 1989, Noguchi 1992). The winds essentially bring moisture across the windward (i.e., northeastern) sides of the islands; in turn, as elevation increases and air temperature decreases, this moisture is released as rainfall. Due to this effect, some windward locations receive more than 15 times the rainfall observed

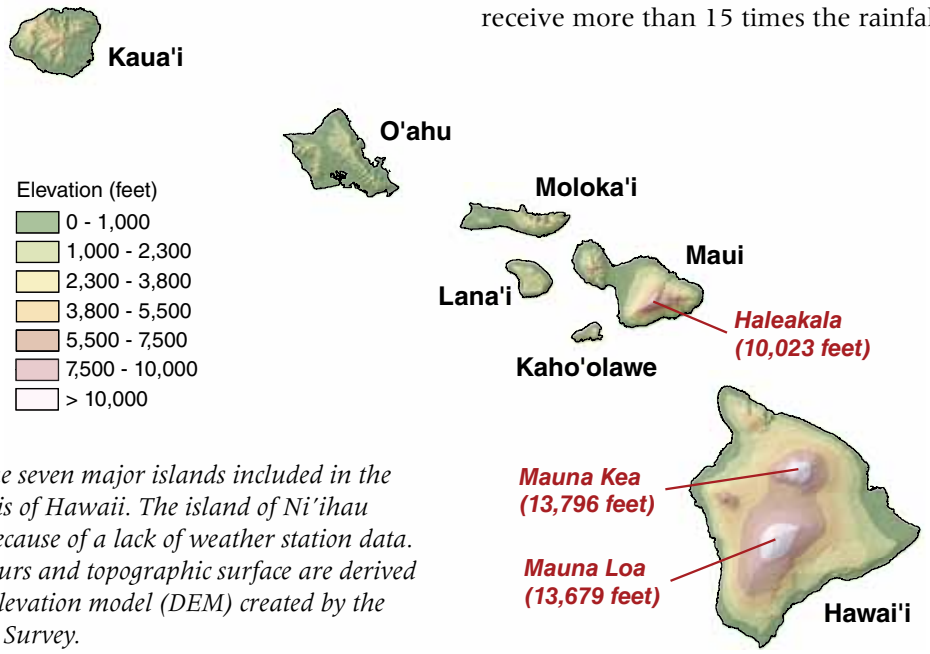


*Figure 4.5—The seven major islands included in the drought analysis of Hawaii. The island of Ni'ihau was excluded because of a lack of weather station data. Elevation contours and topographic surface are derived from a digital elevation model (DEM) created by the U.S. Geological Survey.*

over the open ocean near Hawaii (Loope and Giambelluca 1998). For instance, the peaks and upper slopes of Kaua'i, O'ahu, and Moloka'i are extremely wet, supporting dense forests. In contrast, leeward (i.e., southwestern) slopes and low-lying areas of the islands, because they are in the rain shadows of the mountains, are typically dominated by grasslands, or, in some cases, woodlands (i.e., tree cover between 10 and 50 percent) and shrublands (Cuddihy 1989). The limited forest cover on Kaho'olawe and Lana'i is likewise explained by the fact that both islands lie in the rain shadow of Maui (Chu and others 2009, Cuddihy 1989). A departure from this general windward-leeward trend is the Kona (i.e., west-southwest) coast of Hawai'i, where a distinctive pattern of onshore sea breezes results in some unique weather behavior; in short, this area is wet enough to support a narrow band of forests near the coastline (Chu and others 2009, Cuddihy 1989). In addition, on Maui and on Hawai'i, a temperature inversion layer between 5,900 and 7,900 feet prevents moisture-laden air masses from rising above this elevation zone (Juvik and Nullet 1994, Noguchi 1992). As a result, the upper slopes of Mauna Kea, Mauna Loa, and Haleakala are extremely dry and nearly devoid of vegetation.

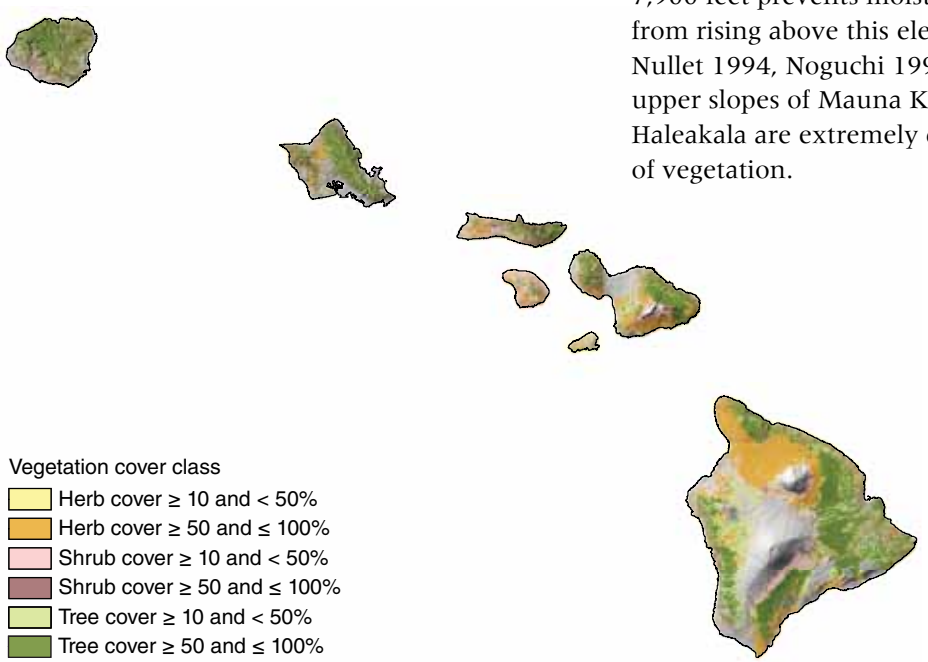


*Figure 4.6—The vegetation of Hawaii, categorized according to the percentage cover of the predominant life form (i.e., herb, shrub, or tree). Agricultural, developed, and barren areas have been omitted. Underlying topographic surface is derived from a digital elevation model (DEM) created by the U.S. Geological Survey. (Data source: LANDFIRE.)*

The long-term (i.e., 88-year) mean annual moisture index, or $MI_{1\,norm}'$, grid for Hawaii (fig. 4.7) is consistent with the vegetation distribution pattern shown in figure 4.6: the windward slopes of the islands are moderate to very wet ($MI' > 0.3$), while leeward and high-elevation areas—other than Hawai'i's Kona coast—are moderate to extremely dry ($MI' < -0.3$). Most of the areas with dense (≥ 50 percent) tree cover exhibit positive $MI'$ values, although patches of "dry forest" (with negative $MI'$ values) are distributed throughout the islands (Cuddihy 1989). The grid ($MI_{1\,SD}'$) showing the long-term standard deviation of the annual moisture index is not shown; to summarize it briefly, dry leeward areas usually display high levels of variability in the index, while wet windward areas typically display low levels of variability. One exception is a very dry ($MI' < -0.7$) area along the northwestern coast of the island of Hawai'i, which likewise exhibits low variability.

Drought has been a chronic problem for Hawaii (Chu 1989). Significantly, drought conditions in the State appear to be linked to the El Niño-Southern Oscillation (ENSO) cycle, with dry conditions tending to emerge in El

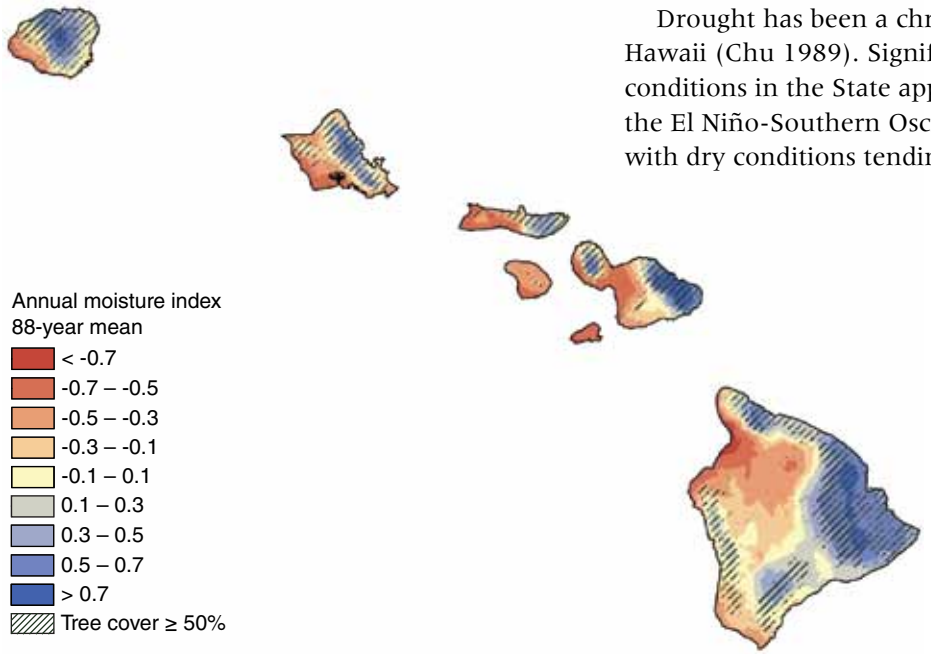


*Figure 4.7—The mean annual moisture index, or* $\mathrm{MI}_{1}{}'_{\mathrm{norm}}$ *for Hawaii based on 88 years (1920–2007) of available data. To enhance display, the* $\mathrm{MI}_{1}{}'_{\mathrm{norm}}$ *map was resampled to 240-m resolution using the cubic convolution method. Tree cover map (overlaid green hatching) was developed by LANDFIRE (see fig. 4.6). (Data sources: Giambelluca and others 2011, National Climatic Data Center 2012a.)*

Niño years and to last into the immediately following years, while La Niña years typically bring wet conditions (Chu 1989, 1995; Chu and Chen 2005). Furthermore, because the ENSO cycle operates on a fluctuating time scale of 2 to 8 years (Chu and Chen 2005), droughts—and likewise, moisture surpluses—occur rather frequently. On a broader (i.e., interdecadal) time scale, the Pacific Decadal Oscillation (PDO) signal has also shown a negative influence on Hawaiian rainfall. Chu and Chen (2005) described an epoch of low rainfall that lasted from the mid-1970s until 2001 but that came after a similarly long epoch (i.e., almost 28 years) of high rainfall.

A time series of annual (i.e., 1-year) *MDZ* maps (fig. 4.8) depicts the dynamic moisture conditions that occurred in Hawaii between the late 1970s and mid-1980s, i.e., in the early portion of the "dry" epoch reported by Chu and Chen (2005). (The corresponding 3-year and 5-year *MDZ* maps are not shown.) The first map in the series (fig. 4.8A), which depicts conditions during 1979, shows only scattered areas of moderate or worse drought, primarily limited to O'ahu and Kaua'i. Although 1979 is not documented as either an El Niño or La Niña year, the presence of moisture surplus conditions across much of the State may reflect a protracted period of heavy rainfall that occurred in January and February 1979, especially on Hawai'i (Jayawardena and others 2012). In contrast, the 1981 map (fig. 4.8B) shows extensive areas of moderate to extreme drought on Maui and Hawai'i, coinciding with an El Niño event that began in 1980 and continued into the next year (Chu and Chen 2005). The 1983 map (fig. 4.8C) depicts large regions of extreme drought on Hawai'i, O'ahu, and Kaua'i and at least moderate drought conditions across most of the major islands. An exceptionally strong El Niño event, with record-low rainfall, occurred in 1982–83; the severity of the event prompted officials to impose strict water rationing in parts of the State during subsequent years (Chu 1989, Loope and Giambelluca 1998). By 1985, which was a La Niña year (Chu and Chen 2005), most of Hawaii had returned to near normal or surplus moisture conditions, with small pockets of moderate to severe drought appearing on Hawai'i and Kaua'i (fig. 4.8D).

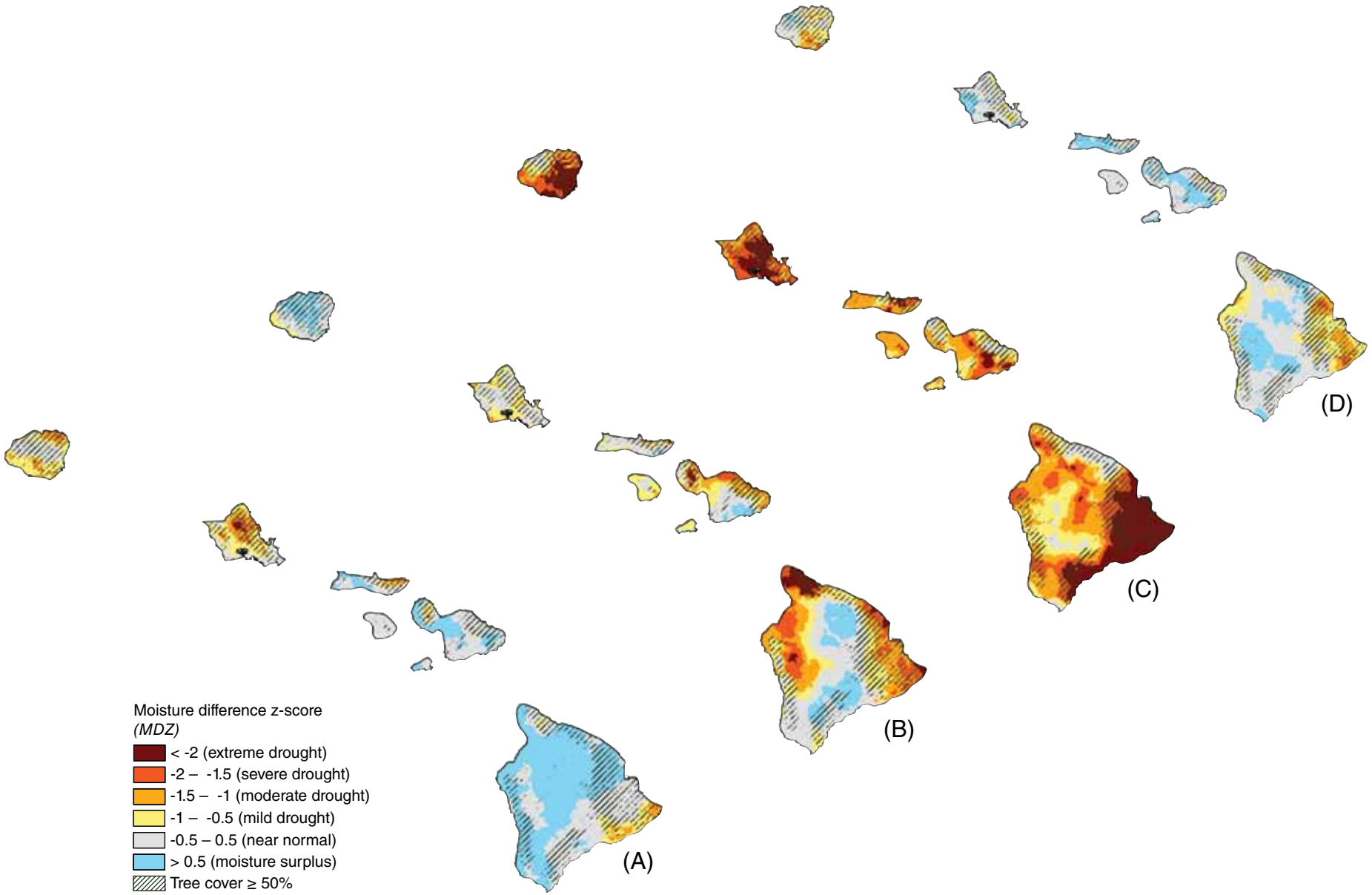


*Figure 4.8—Chronological sequence of annual (i.e., 1-year) moisture difference* z*-score, or* MDZ*, maps for Hawaii: (A) 1979, (B) 1981, (C) 1983, and (D) 1985. To enhance display, the* MDZ *maps were resampled to 240-m resolution using the cubic convolution method. Tree cover map (overlaid green hatching) was developed by LANDFIRE (see fig. 4.6). (Data sources: Giambelluca and others 2011, National Climatic Data Center 2012a.)*

Because the ENSO and PDO cycles operate at such large geographic scales, one might expect little variation among the individual islands of Hawaii in terms of drought frequency. This is largely affirmed by a set of maps (fig. 4.9) depicting the frequencies at which certain levels of drought intensity (see table 4.1) occur across the State. (The maps depict annual drought frequencies; the 3- and 5-year drought frequency maps have been omitted.) When considered as a group, the maps straightforwardly show that as drought intensity increases, the frequency of occurrence tends to decrease. A more subtle yet still important point is that the range of variation in the frequency values is fairly small within each map. For example, in the map depicting frequency of mild or worse drought conditions (fig. 4.9A), the frequencies are mostly in the 0.20 to 0.40 range, while in the map depicting the frequency of moderate or worse drought conditions (fig. 4.9B), they are in the 0.10 to 0.25 range. Furthermore, in the map depicting the frequency of extreme drought (fig. 4.9D), the frequencies are rarely above 0.05. Nevertheless, an interesting pattern emerges despite the limited variability. In figure 4.9A, and figure 4.9B to a lesser degree, there appears to be a slightly higher frequency of drought conditions on the leeward side of most islands, which is to be expected given the importance of the trade winds to the overall moisture regime. In the map depicting the frequency of at least severe drought conditions (fig. 4.9C), however, this pattern is reversed: the frequencies tend to be slightly higher on the windward sides of the islands or, more simply, in areas that are normally wet (see fig. 4.7). To some extent, figure 4.9D also displays this pattern. This apparent switch in the frequency pattern probably relates to our depiction of drought as a standardized departure from normal conditions. In equation 3, a map cell's $MDZ_{ij}$ value depends on the cell's long-term normal moisture index ($MI'_{norm}$) value and its standard deviation ($MI'_{SD}$). Under this approach, locations where the amount of moisture is stable through time (i.e., areas with low $MI'_{SD}$) are more sensitive to small departures from average conditions, such that a small negative difference between the $MI'_{norm}$ (i.e., the long-term normal) value and the $MI'$ value for a particular year of interest can translate to a relatively low $MDZ$ value for that year. In the case of Hawaii, these low-variability areas tend to be wetter. Conversely, areas where the amount of moisture is highly variable through time (i.e., areas with high $MI'_{SD}$) are far less sensitive, so it may require a relatively large difference between $MI'_{norm}$ and the $MI'$ value for the target year to achieve a low $MDZ$ value. In Hawaii, these high-variability areas are often drier. This suggests that, ultimately, it is important to consider the long-term moisture regime (fig. 4.7) when assessing the impact of reported drought conditions in particular areas of Hawaii.

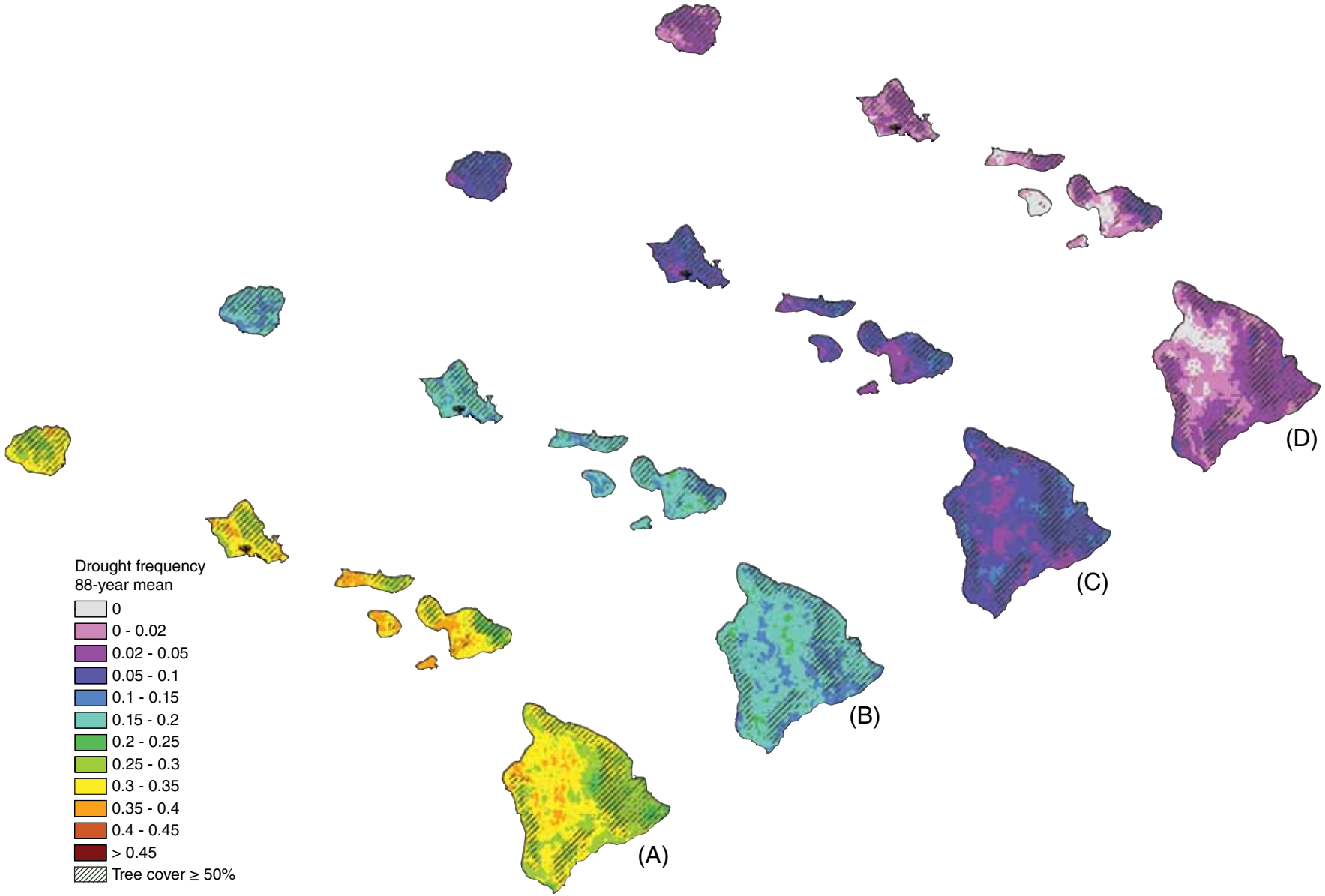


*Figure 4.9—One-year drought frequency maps for Hawaii: frequency of (A) at least mild drought (*MDZ < -0.5*), (B) at least moderate drought (*MDZ < -1*), (C) at least severe drought (*MDZ < -1.5*), and (D) extreme drought (*MDZ < -2*). To enhance display, the frequency maps were resampled to 240-m resolution using the cubic convolution method. Tree cover map (overlaid green hatching) was developed by LANDFIRE (see fig. 4.6). (Data sources: Giambelluca and others 2011, National Climatic Data Center 2012a.)*

## Future efforts

If the appropriate spatial data (i.e., high-resolution maps of precipitation and temperature) continue to be available for public use, we expect to produce our 1-, 3-, and 5-year *MDZ* maps of the conterminous United States as a regular yearly component of national-scale forest health reporting. Unfortunately, a similar goal for the State of Hawaii is probably impractical given the potential lack of contemporary weather data and the need to create our own gridded datasets via spatial interpolation. Nevertheless, we anticipate returning to the topic of drought in Hawaii at some point in time. One particular aspect that may be worth further investigation is our choice of spatial interpolation method; for example, we may want to compare datasets generated via cokriging with results from other interpolation methods that do not employ semivariogram estimation. In any case, it is important for users to interpret and compare the *MDZ* drought maps presented here cautiously. Although the maps use a standardized index scale that applies regardless of the size of the time window, it should also be understood that, for instance, an extreme drought that persists over a 5-year period has substantially different forest health implications than an extreme drought over a 1-year period. In future work, we hope to provide forest managers and other decisionmakers with better quantitative evidence regarding some of these relationships between drought and forest health.

## LITERATURE CITED


Akin, W.E. 1991. Global patterns: climate, vegetation, and soils. Norman, OK: University of Oklahoma Press. 370 p.

Archaux, F.; Wolters, V. 2006. Impact of summer drought on forest biodiversity: what do we know? Annals of Forest Science. 63: 645-652.

Chu, P.-S. 1989. Hawaiian drought and the Southern Oscillation. International Journal of Climatology. 9: 619-631.

Chu, P.-S. 1995. Hawaii rainfall anomalies and El Niño. Journal of Climate. 8: 1697-1703.

Chu, P.-S.; Chen, H. 2005. Interannual and interdecadal rainfall variations in the Hawaiian Islands. Journal of Climate. 18: 4796-4813.

Chu, P.-S.; Zhao, X.; Ruan, Y.; Grubbs, M. 2009. Extreme rainfall events in the Hawaiian Islands. Journal of Applied Meteorology and Climatology. 48: 502-516.

Clark, J.S. 1989. Effects of long-term water balances on fire regime, north-western Minnesota. Journal of Ecology. 77: 989-1004.

Cleland, D.T.; Freeouf, J.A.; Keys, J.E., Jr. [and others]. 2007. Ecological subregions: sections and subsections for the conterminous United States. 1:3,500,000; Albers equal area projection; colored. In: Sloan, A.M., tech. ed. Gen. Tech. Rep. WO-76. Washington, DC: U.S. Department of Agriculture Forest Service. Also as a GIS coverage in ArcINFO format on CD-ROM or at http://fsgeodata.fs.fed.us/other_resources/ecosubregions.html. [Date accessed: May 9, 2011].

Clinton, B.D.; Boring, L.R.; Swank, W.T. 1993. Canopy gap characteristics and drought influences in oak forests of the Coweeta Basin. Ecology. 74(5): 1551-1558.

Cordell, S.; Goldstein, G.; Melcher, P.J.; Meinzer, F.C. 2000. Photosynthesis and freezing avoidance in ohia (*Metrosideros polymorpha*) at treeline in Hawaii. Arctic, Antarctic, and Alpine Research. 32(4): 381-387.

Cressie, N.A.C. 1993. Statistics for spatial data. New York: John Wiley & Sons. 900 p.

Cuddihy, L.W. 1989. Vegetation zones of the Hawaiian Islands. In: Stone, C.P.; Stone, D.B., eds. Conservation biology in Hawaii. Honolulu: University of Hawaii Press: 27-37.

Daly, C.; Gibson, W.P.; Taylor, G.H. [and others]. 2002. A knowledge-based approach to the statistical mapping of climate. Climate Research. 22: 99-113.

ESRI. 2010. ArcGIS. Version 10.0. Redlands, CA: Environmental Systems Research Institute.

Giambelluca, T.W.; Chen, Q.; Frazier, A.G. [and others]. 2011. The rainfall atlas of Hawai'i. http://rainfall.geography.hawaii.edu. [Date accessed: January 17, 2012].

Goovaerts, P. 1998. Ordinary cokriging revisited. Mathematical Geology. 30(1): 21-41.

Goovaerts, P. 2000. Geostatistical approaches for incorporating elevation into the spatial interpolation of rainfall. Journal of Hydrology. 228: 113-129.

Gómez, J. D.; Etchevers, J.D.; Monterroso, A.I. [and others]. 2008. Spatial estimation of mean temperature and precipitation in areas of scarce meteorological information. Atmósfera 21:35-56.

Groisman, P.Y.; Knight, R.W. 2008. Prolonged dry episodes over the conterminous United States: new tendencies emerging during the last 40 years. Journal of Climate. 21: 1850-1862.

Guarín, A.; Taylor, A.H. 2005. Drought triggered tree mortality in mixed conifer forests in Yosemite National Park, California, USA. Forest Ecology and Management. 218: 229-244.

Hanson, P.J.; Weltzin, J.F. 2000. Drought disturbance from climate change: response of United States forests. The Science of the Total Environment. 262: 205-220.

Hevesi, J.A.; Istok, J.D.; Flint, A.L. 1992. Precipitation in mountainous terrain using multivariate geostatistics. Part I: structural analysis. Journal of Applied Meteorology. 31: 661-676.

Hinckley, T.M.; Dougherty, P.M.; Lassoie, J.P. [and others]. 1979. A severe drought: impact on tree growth, phenology, net photosynthetic rate, and water relations. American Midland Naturalist. 102(2): 307-316.

Ishida, T.; Kawashima, S. 1993. Use of cokriging to estimate surface air temperature from elevation. Theoretical and Applied Climatology. 47: 147-157.

Jayawardena, I.M.S.; Chen, Y.-L.; Nash, A.J.; Kodama, K. 2012. A comparison of three prolonged periods of heavy rainfall over the Hawaiian Islands. Journal of Applied Meteorology and Climatology. 51: 722-744.

Johnston, K.; Ver Hoef, J.M.; Krivoruchko, K.; Lucas, N. 2003. Using ArcGIS geostatistical analyst. Redlands, CA: Environmental Systems Research Institute. 300 p.

Juvik, J.O.; Nullet, D. 1994. A climate transect through tropical montane rain forest in Hawaii. Journal of Applied Meteorology. 33: 1304-1312.

Kareiva, P. M.; Kingsolver, J.G.; Huey, B.B, eds. 1993. Biotic interactions and global change. Sinauer Associates, Inc., Sunderland, MA. 559 p.

Keetch, J.J.; Byram, G.M. 1968. A drought index for forest fire control. Res. Pap. SE-38. Asheville, NC: U.S. Department of Agriculture Forest Service, Southeastern Forest Experiment Station. 33 p.

Koch, F.H.; Coulston, J.W.; Smith, W.D. 2012a. High-resolution mapping of drought conditions. In: Potter, K.M.; Conkling, B.L., eds. Forest health monitoring 2008 national technical report. Gen. Tech, Rep. SRS-158. Asheville, NC: U.S. Department of Agriculture Forest Service, Southern Research Station: 45-62.

Koch, F.H.; Coulston, J.W.; Smith, W.D. 2012b. Mapping drought conditions using multi-year windows. In: Potter, K.M.; Conkling, B.L., eds. Forest health monitoring 2009 national technical report. Gen. Tech. Rep. SRS-167. Asheville, NC: U.S. Department of Agriculture Forest Service, Southern Research Station: 163-178. Chapter 10.

Koch, F.H.; Smith, W.D.; Coulston, J.W. 2013a. An improved method for standardized mapping of drought conditions. In: Potter, K.M.; Conkling, B.L., eds. Forest health monitoring: national status, trends, and analysis 2010. Gen. Tech. Rep. SRS-176. Asheville, NC: U.S. Department of Agriculture Forest Service, Southern Research Station: 67-82. Chapter 6.

Koch, F.H.; Smith, W.D.; Coulston, J.W. 2013b. Recent drought conditions in the conterminous United States. In: Potter, K.M.; Conkling, B.L., eds. Forest health monitoring: national status, trends, and analysis 2011. Gen. Tech. Rep. SRS-185. Asheville, NC: U.S. Department of Agriculture Forest Service, Southern Research Station: 41-56. Chapter 4.

Loope, L.L.; Giambelluca, T.W. 1998. Vulnerability of island tropical montane cloud forests to climate change, with special reference to East Maui, Hawaii. Climatic Change. 39: 503-517.

Mattson, W.J.; Haack, R.A. 1987. The role of drought in outbreaks of plant-eating insects. BioScience. 37(2): 110-118.

McDowell, N.; Pockman, W.T.; Allen, C.D. [and others]. 2008. Mechanisms of plant survival and mortality during drought: why do some plants survive while others succumb to drought? New Phytologist. 178: 719-739.

Millar, C.I.; Westfall, R.D.; Delany, D.L. 2007. Response of high-elevation limber pine (*Pinus flexilis*) to multiyear droughts and 20th-century warming, Sierra Nevada, California, USA. Canadian Journal of Forest Research. 37: 2508-2520.

Mueller, R.C.; Scudder, C.M.; Porter, M.E. [and others]. 2005. Differential tree mortality in response to severe drought: evidence for long-term vegetation shifts. Journal of Ecology. 93: 1085-1093.

National Climatic Data Center. 2007. Time bias corrected divisional temperature-precipitation-drought index. Documentation for dataset TD-9640. http://www1.ncdc.noaa.gov/pub/data/cirs/drought.README. [Date accessed: July 20, 2010].

National Climatic Data Center. 2010. State of the climate—drought—annual report 2009. http://www.ncdc.noaa.gov/sotc/2009/13. [Date accessed: May 12, 2011].

National Climatic Data Center. 2011. State of the climate—drought—annual report 2010. http://www.ncdc.noaa.gov/sotc/drought/2010/13. [Date accessed: May 10].

National Climatic Data Center. 2012a. Climate data online—monthly surface data (DS3220). http://cdo.ncdc.noaa/pls/plclimprod/somdmain. somdwrapper?datasetabbv=DS3220& countryabbv=&georegionabbv=&forceoutside=. [Date accessed: February 17].

National Climatic Data Center. 2012b. State of the climate—drought—annual report 2011. http://www.ncdc.noaa.gov/sotc/drought/2011/13. [Date accessed: April 26].

Noguchi, Y. 1992. Vegetation asymmetry in Hawaii under the trade wind regime. Journal of Vegetation Science. 3: 223-230.

O'Driscoll, P. 2007. A drought for the ages: from the dried lake beds of Florida to the struggling ranches of California, a historic lack of rain is changing how Americans live. USA Today. June 8: 1A.

Palmer, W.C. 1965. Metereological drought. Res. Pap. No. 45. Washington, DC: U.S. Department of Commerce, Weather Bureau. 58 p.

Phillips, D.L.; Dolph, J.; Marks, D. 1992. A comparison of statistical procedures for spatial analysis of precipitation in mountainous terrain. Agricultural and Forest Meteorology. 58: 119-141.

PRISM Group. 2012. 2.5-arcmin (4 km) gridded monthly climate data. ftp://prism.oregonstate.edu//pub/prism/us/grids. [Date accessed: April 23, 2012].

Schoennagel, T.; Veblen, T.T.; Romme, W.H. 2004. The interaction of fire, fuels, and climate across Rocky Mountain forests. BioScience. 54(7): 661-676.

Svoboda, M.; LeComte, D.; Hayes, M. [and others]. 2002. The drought monitor. Bulletin of the American Meteorological Society. 83(8): 1181-1190.

Thornthwaite, C.W. 1948. An approach towards a rational classification of climate. Geographical Review. 38(1): 55-94.

Willmott, C.J.; Feddema, J.J. 1992. A more rational climatic moisture index. Professional Geographer. 44(1): 84-87.

# CHAPTER 5.

# Tree Mortality

Mark J. Ambrose

## INTRODUCTION

Tree mortality is a natural process in all forest ecosystems. Extremely high mortality, however, can also be an indicator of forest health issues. On a regional scale, high mortality levels may indicate widespread insect or disease problems. High mortality may also occur if a large proportion of the forest in a particular region is made up of older, senescent stands.

In early Forest Health Monitoring (FHM) national reports (2001–04), mortality was analyzed using FHM and Forest Inventory and Analysis (FIA) phase 3 data. Those data spanned a relatively long period (for some States, up to 12 years), but the sample was not spatially intense (approximately 1 plot per 96,000 acres). In the 2007 FHM national report (Ambrose 2011), the same method was applied to FIA phase 2 (P2) data, which were more spatially intense (approximately 1 plot per 6,000 acres) but came from the relatively small number of States in the Eastern United States where repeated plot measurements had been taken. In the 2008 through 2011 reports, the method was applied to successively larger areas, using increasing numbers of plots. For this report, the repeated P2 data cover much of the Central and Eastern United States, and for some States include data from a third cycle of measurements (i.e., a third measurement of the plots).

The mission of FHM is to monitor, assess, and report on the status, changes, and long-term trends in forest ecosystem health in the United States (USDA Forest Service, Forest Health Monitoring Program 1994). Thus, the aim of this mortality analysis contrasts with how mortality might be approached in other reports, such as FIA State reports or State Forest Health Highlights. The approach to mortality presented here seeks to detect mortality patterns that might reflect subtle changes to fundamental ecosystem processes (due to such large-scale factors as air pollution, global climate change, or fire-regime change) that transcend individual tree species-pest/pathogen interactions. Sometimes, however, the proximate cause of mortality may be discernable. In such cases, the cause of mortality is reported, both because it is of interest in and of itself to many readers and because understanding such proximate causes of mortality *might* provide insight into whether the mortality is within the range of natural variation or reflects more fundamental changes to ecological processes.

At this point, a mortality baseline is still being established for most of the United States. To discern trends in mortality rates, at least three complete cycles of FIA data are required. With the data currently available, it is only possible to do a spatial comparison of ecoregions and identify regions of higher than average mortality (relative to growth) for further study.

## DATA

FIA P2 inventory data are collected using a rotating panel sample design (Bechtold and Patterson 2005). Field plots are divided into spatially balanced panels, with one panel being measured each year. A single cycle of

measurements consists of measuring all panels. This "annualized" method of inventory was adopted, State by State, beginning in 1999. Any analysis of mortality requires data collected at a minimum of two points in time from any given plot. Therefore, mortality analysis was possible for areas where data from repeated plot measurements using consistent sampling protocols were available (i.e., where one cycle of measurements had been completed and at least one panel of the next cycle had been measured, and where there had been no changes to the protocols affecting measurement of trees or saplings). Once all P2 plots have been remeasured in a State, mortality estimates generally will be based on a sample intensity of approximately 1 plot per 6,000 acres of forest.[1] At this time, however, not all plots have been remeasured in all the States included in this analysis. When not all plots have been remeasured, mortality estimates are based on a lower effective sample intensity. Table 5.1 shows the 34 States from which consistent repeated P2 measurements were available, the period spanned by the data, and the effective sample intensity. Additional measurements of any plot, beyond the minimum of two required for a single mortality estimate, improve the mortality estimate. At present, third plot measurements have been taken in some States (table 5.1). The States included in this analysis as well as and the forest cover within those States are shown in figure 5.1.

[1] In some States, more intensive sampling has been implemented. See table 5.1 for details.

**Table 5.1—States from which repeated Forest Inventory and Analysis phase 2 measurements were available, the time period spanned by the data, and the effective sample intensity (based on plot density and on proportion of plots that had been remeasured) in the available datasets**

| Time period | States | Effective sample intensity | Proportion of plots measured three times |
|---|---|---|---|
| 1999–2010 | IN, MO | 1 plot per 6,000 acres[a] | 1/5 |
| 1999–2010 | MN, WI | 1 plot per 3,000 acres[b] | 1/5 |
| 1999–2010 | ME | 1 plot per 6,000 acres | 2/5 |
| 2000–2011 | IA | 1 plot per 6,000 acres | 2/5 |
| 2000–2010 | MI | 1 plot per 2,727 acres[c] | 1/11 |
| 2000–2010 | AR, PA | 1 plot per 6,000 acres | 1/5 |
| 2000–2010 | VA | 1 plot per 7,500 acres | 0 |
| 2001–2011 | AL | 1 plot per 7,000 acres | 0 |
| 2001–2011 | TX[d] | 1 plot per 6,000 acres | 3/5 |
| 2001–2010 | GA, IL, KS, NE, ND, SD, TN | 1 plot per 6,000 acres[e] | 0 |
| 2001–2010 | OH | 1 plot per 7,500 acres | 0 |
| 2002–2010 | KY, SC | 1 plot per 7,500 acres | 0 |
| 2002–2010 | NH, NY | 1 plot per 10,000 acres | 0 |
| 2002–2010 | FL | 1 plot per 15,000 acres | 0 |
| 2003–2010 | CT, MA, VT | 1 plot per 10,000 acres | 0 |
| 2003–2010 | RI | 1 plot per 5,000 acres[b] | 0 |
| 2003–2010 | NC | 1 plot per 21,000 acres | 0 |
| 2004–2010 | DE | 1 plot per 7,500 acres[b] | 0 |
| 2004–2010 | MD, NJ, WV | 1 plot per 15,000 acres | 0 |

[a] In Indiana and Missouri, the phase 2 (P2) inventory was done at twice the standard Forest Inventory and Analysis (FIA) sample intensity, approximately 1 plot per 3,000 acres, on national forest lands and at the standard intensity, 1 plot per 6,000 acres, on all other lands.
[b] In Delaware, Minnesota, Rhode Island, and Wisconsin, the P2 inventory was done at twice the standard FIA sample intensity, approximately 1 plot per 3,000 acres.
[c] In Michigan, the P2 inventory was done at triple the standard FIA sample intensity, approximately one plot per 2,000 acres, for three of the five inventory panels.
[d] Annualized growth and mortality data were only available for eastern Texas.
[e] In Illinois, the P2 inventory was done at triple the standard FIA sample intensity, approximately 1 plot per 2,000 acres, on national forest lands and at the standard intensity on all other lands.

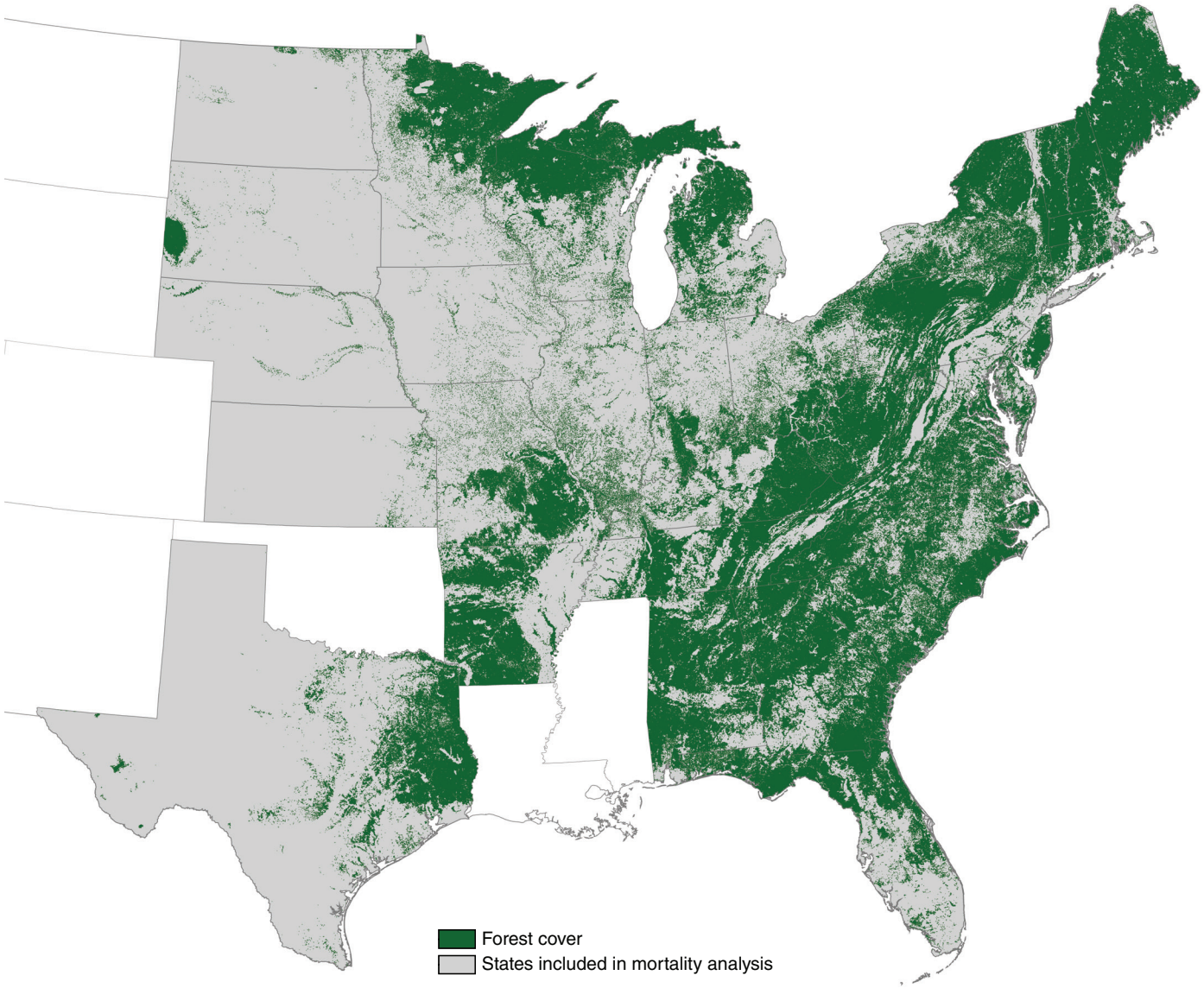


*Figure 5.1—Forest cover in the States where mortality was analyzed. Forest cover was derived from Advanced Very High Resolution Radiometer satellite imagery (Zhu and Evans 1994).*

Because the data used here are collected using a rotating panel design and all available annualized data are used, most of the data used in this mortality analysis were also used in the analysis presented in the previous FHM national report. Using the data in this way, it would be very unusual to see any great changes in mortality patterns from one annual report to the next. It is important nevertheless to look at mortality patterns every year so as not to miss detecting mortality patterns that may be indicative of forest health problems as soon as they may become discernible.

## METHODS

FIA P2 tree (≥5 inches d.b.h) and sapling (1 inch ≥ d.b.h. > 5 inches) data were used to estimate average annual tree mortality in terms of tons of biomass per acre. The data were obtained from the public FIA Database - version 5.1 (USDA Forest Service, Forest Inventory and Analysis Program 2012). The biomass represented by each tree was calculated by FIA and provided in the FIA Database (USDA Forest Service, Forest Inventory and Analysis program 2011). To compare mortality rates across forest types and climate zones, the ratio of annual mortality to gross growth (MRATIO) is used as a standardized mortality indicator (Coulston and others 2005a). Gross growth rate and mortality rate, in terms of tons of biomass per acre, were independently calculated for each ecoregion section (Cleland and others 2007, McNab and others 2007) using a mixed modeling procedure, wherein plot-to-plot variability is considered a random effect and time is a fixed effect. The mixed modeling approach has been shown to be particularly efficient for estimation using data in which not all plots have been measured over identical time intervals (Gregoire and others 1995). In the estimation procedure, within-plot temporal correlation was based on a covariance matrix modeled using a Toeplitz matrix. MRATIOs were then calculated from the growth and mortality rates. For details on the method, see appendix A—Supplemental Methods in the Forest Health Monitoring 2001 National Technical Report (Coulston and others 2005b) and appendix A—Supplemental Methods in the Forest Health Monitoring 2003 National Technical Report (Coulston and others 2005c).

In addition, the ratio of average dead tree diameter to average surviving live tree diameter (DDLD ratio) was calculated for each plot where mortality occurred. Low DDLD ratios (much < 1) usually indicate competition-induced mortality typical of young, vigorous stands, and high ratios (much > 1) indicate mortality associated with senescence or some external factors such as insects, disease, or severe drought stress (Smith and Conkling 2004). Intermediate DDLD ratios can be hard to interpret because a variety of stand conditions can produce such DDLD values. The DDLD ratio is most useful for analyzing mortality in regions that also have high MRATIOs. High DDLD values in regions with very low MRATIOs may indicate small areas experiencing high mortality of large trees or locations where the death of a single large tree (such as a remnant pine in a young hardwood stand) has produced a deceptively high DDLD.

To further analyze tree mortality, the number of stems and the total biomass of trees that died also were calculated by species within each ecoregion. Identifying the tree species experiencing high mortality in an ecoregion is a first step in identifying what forest health issue may be affecting the forests. Although determining particular causal agents associated with all the observed mortality is beyond the scope of this report, often there are well-known insects and pathogens that are "likely suspects" once the affected tree species are identified.

A biomass-weighted mean mortality age was also calculated by ecoregion and species. For each species experiencing mortality in an ecoregion, the mean stand age was calculated, weighted by the dead biomass on the plot. This value gives a rough indicator of the average age of the stands in which trees died. The age of individual trees may differ significantly, however, from the age assigned to a stand by FIA field crews, especially in mixed-species stands. When the age of trees that die is relatively low compared with the age at which trees of a particular species usually become senescent, it suggests that some pest, pathogen, or other forest health problem may be affecting the forest.

## RESULTS AND DISCUSSION

The MRATIO values are shown in figure 5.2. The MRATIO can be large if an over-mature forest is senescing and losing a cohort of older trees. If forests are not naturally senescing, a high MRATIO (>0.6) may indicate high mortality due to some acute cause (insects or pathogens) or due to generally deteriorating forest health conditions. An MRATIO value >1 indicates that mortality exceeds growth, and live standing biomass is actually decreasing.

The highest MRATIO occurred in ecoregion section 331F-Western Great Plains (MRATIO = 1.47) in South Dakota and Nebraska, where mortality actually exceeded growth. Other areas of high mortality relative to growth were sections 332D-North-Central Great Plains, also in South Dakota and Nebraska (MRATIO = 0.65), and 411A-Everglades in Florida (MRATIO = 0.86). Table 5.2 shows the tree species experiencing the greatest mortality in those ecoregions.

The results of the analysis of the relative sizes of trees that died to those that lived, the DDLD ratio, are shown in table 5.3. The DDLD ratio is a plot-level indicator, so I obtained summary statistics for the ecoregions where mortality relative to growth was highest. In all cases the mean and median DDLDs were rather close to 1, meaning that the trees that died were similar in size to the trees that survived. However, there were some plots with extremely high DDLD values. Interestingly, the same pattern of mean and median DDLD close to 1 and some high DDLD values was observed in nearly all ecoregions, regardless of the overall mortality level.

In two of the ecoregion sections exhibiting highest mortality relative to growth (331F-Western Great Plains and 332D-North-

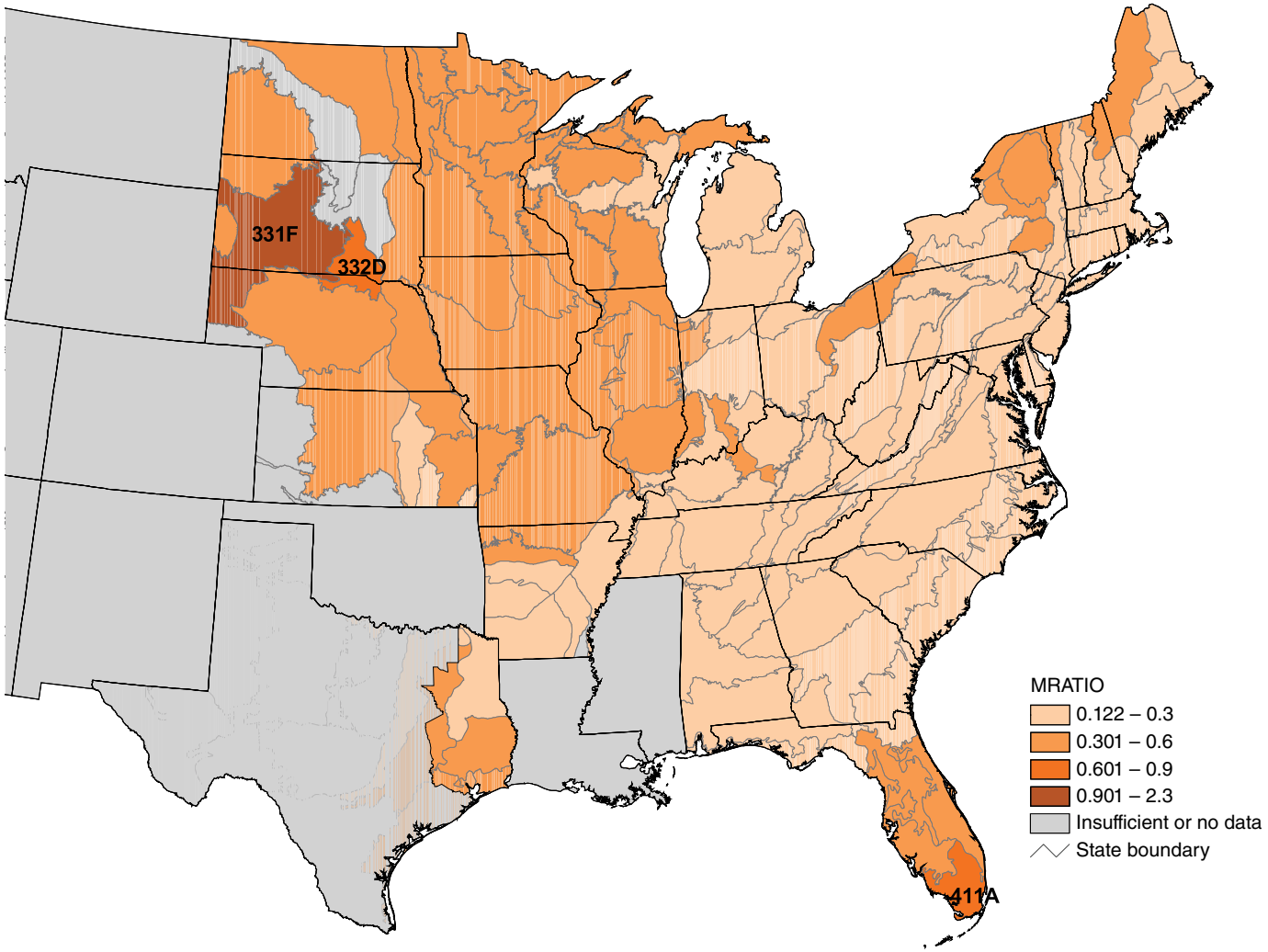


*Figure 5.2—Tree mortality expressed as the ratio of annual mortality of woody biomass to gross annual growth in woody biomass, or MRATIO, by ecoregion section (Cleland and others 2007). The labelled ecoregions are discussed in the text. (Data source: USDA Forest Service, Forest Inventory and Analysis Program.)*

**Table 5.2—Tree species responsible for at least 5 percent of the mortality (in terms of biomass) for ecoregions where the ratio of annual mortality to gross growth (MRATIO) was ≥ 0.60**

| Ecoregion section | MRATIO | Tree species | Percent of total ecoregion mortality biomass | Mean age of dead trees[a] | Species percent mortality | |
|---|---|---|---|---|---|---|
| | | | | | Biomass | Stems |
| 331F-Western Great Plains | 1.47 | Ponderosa pine *(Pinus ponderosa)* | 58.72 | 59 | 6.21 | 12.13 |
| | | Green ash *(Fraxinus pennsylvanica)* | 20.53 | 42 | 19.82 | 19.36 |
| | | Eastern cottonwood *(Populus deltoides)* | 5.38 | 85 | 3.96 | 3.33 |
| 332D-North-Central Great Plains | 0.65 | Bur oak *(Quercus macrocarpa)* | 29.35 | 74 | 4.73 | 5.05 |
| | | Hackberry *(Celtis occidentalis)* | 19.33 | 60 | 11.91 | 0.78 |
| | | Green ash *(F. pennsylvanica)* | 15.26 | 77 | 13.21 | 17.32 |
| | | Ponderosa pine *(Pinus ponderosa)* | 10.91 | 59 | 8.17 | 31.58 |
| | | American elm *(Ulmus americana)* | 9.61 | 57 | 7.67 | 9.76 |
| | | Boxelder *(Acer negundo)* | 6.78 | 53 | 49.28 | 40.00 |
| | | Eastern redcedar *(Juniperus virginiana)* | 5.35 | 43 | 2.70 | 5.04 |
| 411A-Everglades | 0.86 | Slash pine *(Pinus elliotii)* | 61.28 | 22 | 19.80 | 45.58 |
| | | Pondcypress *(Taxodium ascendens)* | 15.70 | 22 | 5.58 | 6.78 |
| | | Red maple *(A. rubrum)* | 8.53 | 55 | 39.82 | 4.69 |
| | | Melaleuca *(Melaleuca quinquenervia)* | 5.22 | 16 | 28.83 | 59.51 |

[a] Ages are estimated from the stand age as determined by the Forest Inventory and Analysis field crew. It is possible, especially in mixed-species stands, that the age of individual trees that died differed significantly from the stand age.

**Table 5.3—Dead diameter live diameter ratios for ecoregion sections where the ratio of annual mortality to gross growth (MRATIO) was ≥ 0.60**

| Ecoregion section | Mean DDLD | Maximum DDLD | Median DDLD | Minimum DDLD |
|---|---|---|---|---|
| 331F-Western Great Plains | 0.97 | 3.29 | 0.91 | 0.08 |
| 332D-North-Central Great Plains | 0.89 | 1.83 | 0.96 | 0.29 |
| 411A-Everglades | 1.23 | 3.63 | 1.18 | 0.11 |

DDLD = dead diameter live diameter.

Central Great Plains), the predominant vegetation is grassland (see the forest cover in fig. 5.1), and there were relatively few forested plots measured (92 plots in region 331F and 52 plots in region 332D). Tree growth rates in these regions (especially in 331F) are quite low, so the high MRATIOs are due to a combination of low growth and high mortality. Much of the forest in these sections is riparian forest, and, indeed, most of the species experiencing greatest mortality (table 5.2) are commonly found in riparian areas. The one exception was high ponderosa pine mortality in ecoregion section 331F-Western Great Plains. Ponderosa pine is

not a riparian species, but like the riparian tree species, it only occurs in a relatively small area of the ecoregion; it occurs only on discontinuous mountains, plateaus, canyons, and breaks in the plains (Burns and Honkala 1990a).

DDLD values vary widely within each of these sections. There is a small number of plots with high DDLDs, and these plots represent most of the biomass that died in these sections. However, on many of these plots the overall level of mortality is relatively low, as would be the case when remnant larger trees die, leaving young, vigorous stands behind. Tree growth is generally slow in these ecoregion sections because of naturally dry conditions. Where the number of sample plots is small and tree growth is slow, care must be taken in interpreting mortality relative to growth over short time intervals.

In ecoregion section 331F-Western Great Plains, where the MRATIO was highest (MRATIO = 1.47), by far the largest amount of biomass that died was ponderosa pine (table 5.2); however, this represented a relatively small proportion of the ponderosa pine in the ecoregion. This pine mortality may be related to mountain pine beetle (*Dendroctonus ponderosae*). There was an ongoing pine beetle outbreak in the adjacent Black Hills (South Dakota Department of Agriculture 2011), and mountain pine beetle mortality was reported in western Nebraska (Nebraska Forest Service 2011). Green ash, which made up only half as much of the ecoregion mortality as ponderosa pine, suffered a much larger loss of the total ash stock (about 20 percent of both biomass and stems). This suggests that ash may have suffered from much more serious forest health issues than pine in this ecoregion.

In ecoregion section 332D-North-Central Great Plains, five species experienced the highest total mortality in terms of biomass and together represent about 75 percent of the mortality in the ecoregion: bur oak, hackberry, green ash, and ponderosa pine, (table 5.2[1] ). Of these, hackberry and green ash suffered the greatest proportional loss of biomass (11.91 and 13.21 percent, respectively). The relatively high mean age of the dead trees suggests that the mortality is at least partially due to senescence of older stands. In the case of hackberry, the mortality in terms of biomass (11.91 percent) was much higher than the mortality in terms of number of stems (0.78 percent), which means that the trees that died were a relatively small number of very large trees. Three other species, American elm, boxelder, and eastern redcedar account for an additional 22 percent of the mortality in the ecoregion. Of these, boxelder suffered extremely high relative mortality (49.28 percent of biomass and 40.00 percent of stems). The average age of the dead boxelder was 53 years, while the species on average only live to about 60 (Burns and Honkala 1990b), so, again, the species mortality is likely related to senescence of older stands.

[1] The species mortality values reported for ecoregion 332D-North-Central Great Plains are exactly the same as those reported in the 2011 Forest Health Monitoring national report. This ecoregion is mostly grassland. There were only three additional forested plots in the additional year of data included in this year's analysis, and no mortality occurred on those plots.

One might be tempted to suspect the invasive emerald ash borer as the cause of the ash mortality in sections 331F–Western Great Plains and 332D-North-Central Great Plains. However, this insect pest had not yet been reported in or near these regions (USDA Forest Service and others, N.d.; Nebraska Forest Service 2011).

Although it has a very different climate, ecoregion 411A-Everglades, like the plains ecoregions previously discussed, contains a relatively small proportion of forest (only 41 forested plots for the analysis). Most of the ecoregion is a grassland that is flooded for much of the year. Trees in the ecoregion only occur on hardwood hammocks, "upland" pine forest, cypress swamps, and coastal mangrove forests. The two tree species representing most of the mortality in the Everglades, slash pine and pondcypress, occur in different ecosystems within the ecoregion, so very different factors are likely responsible for the mortality. The species having the highest mortality was slash pine, representing 61 percent of the mortality (by biomass) in the ecoregion. About 46 percent of slash pine stems died, but only 20 percent of the slash pine biomass died. The mean stand age of the dead trees was relatively low (22 years), so much of the mortality was smaller, younger trees, and might be competition-induced. Researchers in Florida are investigating southern pine beetle, which affects slash pine. However, these research and monitoring efforts are focused in northern Florida, not in most of the area identified here as experiencing high mortality (Florida Department of Agriculture and Consumer, Division of Forestry 2010). Pondcypress represented about 16 percent of the mortality in the region. This mortality also occurred in relatively young stands (average of 22 years old). No particular pondcypress forest health issues have been reported.

Red maple accounted for about 9 percent of the mortality in the Everglades. The red maple stands with mortality were older than those of pine or cypress (55 years). About 5 percent of red maples stems died, but they represented about 40 percent of the red maple biomass, so larger, older red maple trees were dying.

One of the species having high mortality in the Everglades is melaleuca. This is an invasive exotic species that has created ecological problems in south Florida. Two insects were introduced into Florida in 1997 and 2002 as biological control agents for melaleuca. Research indicates that these insects have resulted in melaleuca mortality and reduced seed production (Tipping and others 2009, 2012). The observed melaleuca mortality is likely due to these introduced insects, and, in this case, increased mortality is a positive development.

The mortality patterns shown in these analyses do not immediately suggest large-scale forest health issues. Mortality is rather low in most of the areas for which data are available. The areas of highest mortality occur in the mostly riparian forests of Great Plains ecoregions. A common characteristic of all the ecoregions having high mortality is that they are on the margins of land suitable for forest

growth, being mostly very dry (Great Plains ecoregions) or very wet (the Everglades). As a result, the implications of the high mortality are unclear. Trees growing in these marginal situations may be especially susceptible to new or changed biotic or abiotic stressors. Yet, because of the small number of forested plots used to analyze these ecoregions, the mortality may be due to highly localized phenomena. Therefore, further study of the health of these forests may be warranted.

## LITERATURE CITED


Ambrose, M.J. 2013. Mortality. In: Potter, K.M.; Conkling, B.L., eds. Forest Health Monitoring: national status, trends, and analysis 2011. Gen. Tech. Rep. SRS-185. Asheville, NC: U.S. Department of Agriculture Forest Service, Southern Research Station: 59-68.

Ambrose, M.J. 2011.Mortality. In: Ambrose, M.J.; Conkling, B.L., eds. Forest Health Monitoring 2007 national technical report. Gen. Tech. Rep. SRS-147. Asheville, NC: U.S. Department of Agriculture Forest Service, Southern Research Station: 97-105.

Bechtold, W.A.; Patterson, P.L., eds. 2005. The enhanced Forest Inventory and Analysis program—national sampling design and estimation procedures. Gen. Tech. Rep. SRS-80. Asheville, NC: U.S. Department of Agriculture Forest Service, Southern Research Station. 85 p.

Burns, R.M.; Honkala, B.H. 1990a. Silvics of North America: 1, conifers. Agric. Handb. 654. Washington, DC: U.S. Department of Agriculture Forest Service. 675 p.

Burns, R.M.; Honkala, B.H. 1990b. Silvics of North America: 2, hardwoods. Agric. Handb. 654. Washington, DC: U.S. Department of Agriculture Forest Service. 877 p.

Cleland, D.T.; Freeouf, J.A.; Keys, J.E., Jr. [and others]. 2007. Ecological subregions: sections and subsections for the conterminous United States. 1:3,500,000; Albers equal area projection; colored. In: Sloan, A.M., tech. ed. Gen. Tech. Rep. WO-76. Washington, DC: U.S. Department of Agriculture Forest Service. Also as a GIS coverage in ArcINFO format on CD-ROM or at http://fsgeodata.fs.fed.us/other_resources/ecosubregions.html. [Date accessed: March 18, 2011].

Coulston, J.W.; Ambrose, M.J.; Stolte, K.S. [and others]. 2005a. Criterion 3—health and vitality. In: Conkling, B.L.; Coulston, J.W.; Ambrose, M.J., eds. Forest Health Monitoring 2001 national technical report. Gen. Tech. Rep. SRS-81. Asheville, NC: U.S. Department of Agriculture Forest Service, Southern Research Station. 203 p.

Coulston, J.W.; Smith, W.D.; Ambrose, M.J. [and others]. 2005b. Appendix A—supplemental methods. In: Conkling, B.L.; Coulston, J.W.; Ambrose, M.J., eds. Forest Health Monitoring 2001 national technical report. Gen. Tech. Rep. SRS-81. Asheville, NC: U.S. Department of Agriculture Forest Service, Southern Research Station. 203 p.

Coulston, J.W.; Ambrose, M.J.; Riitters, K.H. [and others]. 2005c. Appendix A—supplemental methods. In: Forest Health Monitoring 2003 national technical report. Gen. Tech. Rep. SRS-85. Asheville, NC: U.S. Department of Agriculture Forest Service, Southern Research Station. 97 p.

Florida Department of Agriculture and Consumer Services, Division of Forestry. 2010. Florida forest health highlights 2010. 3 p. http://fhm.fs.fed.us/fhh/sregion.shtml. [Date accessed: June 2, 2012].

Gregoire, T.G.; Schabenberger, O.; Barret, J.P. 1995. Linear modeling of irregularly spaced, unbalanced, longitudinal data from permanent plot measurements. Canadian Journal of Forest Research. 25: 137 156.

McNab, W.H.; Cleland, D.T.; Freeouf, J.A. [and others], comps. 2007. Description of ecological subregions: sections of the conterminous United States [CD-ROM]. Gen. Tech. Rep. WO-76B. Washington, DC: U.S. Department of Agriculture Forest Service. 80 p.

Nebraska Forest Service. 2011. Nebraska forest health highlights 2011. 5 p. http://fhm.fs.fed.us/fhh/ncregion.shtml. [Date accessed: June 1, 2012].

Smith, W.D.; Conkling, B.L. 2004. Analyzing forest health data. Gen. Tech. Rep. SRS-77. Asheville, NC: U.S. Department of Agriculture Forest Service, Southern Research Station. 35 p.

South Dakota Department of Agriculture. 2011. South Dakota forest health highlights 2011. Pierre, SD: South Dakota Department of Agriculture, Division of Resource Conservation and Forestry. 4 p. http://fhm.fs.fed.us/fhh/ncregion.shtml/. [Date accessed: June 1, 2012].

Tipping , P.W.; Martin, M.R.; Nimmoa, K.R. [and others]. 2009. Invasion of a West Everglades wetland by *Melaleuca quinquenervia* countered by classical biological control. Biological Control. 38: 73-78.

Tipping , P.W.; Martin, M.R.; Pierce, R. [and others]. 2012. Post-biological control invasion trajectory for *Melaleuca quinquenervia* in a seasonally inundated wetland. Biological Control. 60: 163-168.

U.S. Department of Agriculture (USDA) Forest Service, Forest Health Monitoring program. 1994. Forest Health Monitoring: a national strategic plan. Research Triangle Park, NC: U.S. Department of Agriculture Forest Service, Forest Health Monitoring program. 13 p.

U.S. Department of Agriculture (USDA) Forest Service, Forest Inventory and Analysis program. 2011. The forest inventory and analysis database: database description and users manual version 5.1 for phase 2. Washington: U.S. Department of Agriculture Forest Service. http://fia.fs.fed.us/library/database-documentation/. [Date accessed: April 4].

U.S. Department of Agriculture (USDA) Forest Service, Forest Inventory and Analysis program. 2012. FIA DataMart FIADB version 5.1 (Online database). Washington: U.S. Department of Agriculture Forest Service. http://apps.fs.fed.us/fiadb-downloads/datamart.html/. [Date accessed: March 27].

U.S. Department of Agriculture (USDA) Forest Service; Michigan State University; Purdue University; Ohio State University. [N.d.]. Emerald ash borer: Where is EAB? http://www.emeraldashborer.info/surveyinfo.cfm.[Date accessed: June 29, 2011].

Zhu, Z.; Evans, D.L. 1994. U.S. forest types and predicted percent forest cover from AVHRR data. Photogrammetric Engineering and Remote Sensing. 60: 525-531.

# SECTION 2.

## Analyses of Long-Term Forest Health Trends and Presentations of New Techniques

# CHAPTER 6.

# Links between Land Cover and Lichen Species Richness at Large Scales in Forested Ecosystems across the United States

Susan Will-Wolf
Randall S. Morin
Mark J. Ambrose
Kurt Riitters
Sarah Jovan

## INTRODUCTION

Lichen community composition is well known for exhibiting response to air pollution, and to macroenvironmental and microenvironmental variables. Lichens are useful indicators of air quality impact, forest health, and forest ecosystem integrity across the United States (McCune 2000, reviews in Nimis and others 2002, USDA Forest Service 2007). Recent studies suggest lichen composition of a forested area can also be affected by the proportion of forest in the nearby landscape, at least at relatively small scales (Stofer and others 2006; Will-Wolf and others 2002, 2010, 2011b). A lichen is a close symbiotic relationship of a fungus (mostly Ascomycota) with green algae, cyanobacteria ("blue-green algae"), or both. The fungus provides a stable environment for the algae to live, while the algae provide the fungus with energy from photosynthesis. A macrolichen can be detached from its substrate and is large enough to see easily. Lichens grow on tree trunks and branches, on rocks, and on soil where vascular plants are sparse.

The Forest and Inventory Analysis (FIA) Program monitors the status of forests nationwide on a national grid of permanent plots (Woodall and others 2011). Lichen data were collected on an interspersed subset of this grid; they are suitable primarily for evaluating large-scale patterns and trends in forest health. Lichen data are collected using standard protocols (USDA Forest Service 2011) that have remained unchanged since they were first implemented in 1994 under the Forest Health Monitoring (FHM) Program. The number of macrolichen species found at a forested plot, referred to here as Lichen S, is an index for lichen species richness available from FIA data. Lichen S has been recommended as an indicator for the condition of the surrounding forested ecosystem across both large and small geographic areas (McCune 2000).

Lichen S is a general indicator for the condition of forested ecosystems. Because it does not depend on a particular species composition (that changes between different geographic regions), Lichen S is a consistent variable across the entire country that can be compared among regions. FIA lichen data are available for public download (at http://apps.fs.fed.us/fiadb-downloads/datamart.html), representing almost two-thirds of forested areas across the conterminous United States, probably the most extensive (but with relatively low spatial intensity) quantitative lichen dataset in the world.

Will-Wolf and others (2011a) found that Lichen S has potential to indicate broad-scale response of forests to climate (stronger in the Western United States) and to air quality (stronger in the Eastern United States) in both East and West regions and in several subregions of each large region. In that earlier study, we did not consider the influence of nearby land cover pattern. We later hypothesized that air

pollution and climate variables may well be correlated with land cover pattern near plots when evaluated across these large regions. If such relationships occur, information on Lichen S variation with nearby land cover is needed to support accurate interpretation of the relationship between Lichen S and pollution or climate.

The purpose of this study was to investigate whether the inclusion of land cover variables improved models for explaining variation in Lichen S as compared with the previous study. We investigated this possibility by exploring with the same data used by Will-Wolf and others (2011a) the relationships of Lichen S, climate, and air quality with new land cover variables for a subset of six geographic areas from the earlier study. We selected our analysis tools to maximize comparability of results among regions and robustness of conclusions, at the cost of lower statistical power for individual results.

Our general questions for this project were:

- How are land cover variables related to Lichen S across large regions?
- How are land cover variables related to environmental variables and each other?
- What implications do these relationships have for interpreting effects of both environment and nearby land cover on Lichen S? Can general recommendations be suggested for analyses?
- Does inclusion of land cover variables improve models to explain Lichen S?

## METHODS

### Study area

For this project, we selected six of the regions defined in Will-Wolf and others (2011a) for the conterminous United States based on Bailey's ecoregions (Bailey 1989, Cleland and others 2005) (fig. 6.1). We include the entire East and West regions, plus two subregions within each region. In each region, one subregion is mountainous and the other subregion has less relief. The region described hereafter as "West all" includes all plots from west of the area in figure 6.1 with no data; "W Sierras" is the Sierras/Coast Mountains subregion, including lowlands; "W CO Plateau" is the Colorado Plateau/S Dry Mountains subregion with less relief. The region described hereafter as "East all" includes all plots from east of the area in figure 6.1 with no data; "E Adiron" is the Adirondacks mountainous subregion; "E Decid" is the Eastern Deciduous subregion with less relief.

### Lichen data

We used lichen data compiled by Will-Wolf and others (2011a) for the six regions described above—2,482 unique plots. These data were the single most recent FIA (or FHM) sample for each plot surveyed 1994–2002 in the conterminous United States; sample year thus varied by plot. Lichen S is the number (count data) of species on a plot from a timed (up to 2-hour) survey of macrolichens on all easily accessible woody substrates in a 0.379-ha (0.937-acre) plot by trained nonspecialists, with species identification by specialists. Lichen data are from the "forest

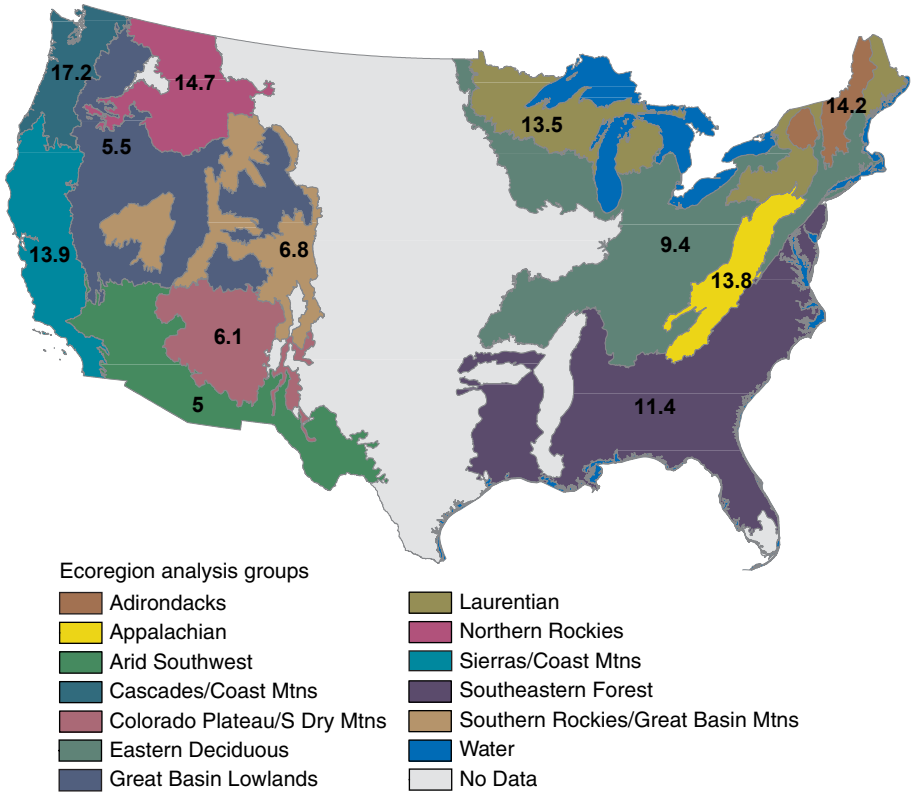


*Figure 6.1—Ecoregion groups from Will-Wolf and others (2011a), based on Bailey's ecoregion provinces (Bailey 1989, Cleland and others 2005). For this project, the "West all" region includes all ecoregion groups west of the large pale gray area with no data, and the "East all" region includes all ecoregion groups east of this same area. Some ecoregion groups include parts of States with no Forest Inventory and Analysis lichen data. Printed numbers are the average for each ecoregion of Lichen S, the number of macrolichen species found per plot. Note the greater variation in average Lichen S among groups in the West.*

health" (phase 3) subset of FIA plots (Woodall and others 2010), whose average density is 1 plot/39 072 ha (per 96,000 acres).

## Explanatory variables

Five land cover variables were developed for neighborhoods of five sizes for each plot (table 6.1). A neighborhood is defined as a square geographic area centered on the approximate coordinates (see next paragraph) for each plot with sides facing the cardinal directions. Within each neighborhood, land cover measurements were taken from the 2001 National Land Cover Database (NLCD) land cover map, which portrays 16 land cover types at a spatial resolution of 30 m (0.09 ha/square pixel; Homer and others 2007). We evaluated forest density (*Fden*), forest connectivity (*Fcon*), and the percentage of pixels in three types of generalized land cover—natural (including seminatural; *pctNt*), agricultural (*pctAg*), and developed (*pctDv*)—to represent the type and degree of human modification within a neighborhood. *Fcon* for a plot is determined by counting the total number of pixel edges (within the neighborhood) that have a forest pixel on at least one side, then calculating the percentage of those edges that have forest pixels on both sides (Riitters and others 2007); higher values of *Fcon* indicate less forest fragmentation. A neighborhood with no forest cover pixels is assigned *Fcon* = 0; connectivity cannot be calculated there, but it is certainly less than for a neighborhood with one forest cover pixel, where *Fcon* = 1. Plot neighborhoods with no forest cover pixels do occur in our data; a clearcut plot

in forest land use (FIA definition) may coincide with a pixel interpreted in NLCD coverage as having no forest cover. Both *Fden* and *Fcon* were measured as continuous variables, then were converted to ordinal indices for our analyses. The three land cover variables related to human modification (*pctNt*, *pctAg*, and *pctDv*) were derived from previously prepared national maps of the categorical "landscape mosaic" tripolar classification model (Riitters 2011, Riitters and others 2007). For that model, "natural" land cover is any land cover not specifically classified as developed (human structures) or agricultural. Ordinal variables with eight numerical values representing the range 0 to 100 percent of each target cover class in the landscape were created from the model categories. Thus, all five land cover metrics are unitless, ordinal indices with a higher index value for more cover of that type or more forest connectivity. There are correlations among the five variables for a given plot; for instance, *Fden* represents a subset of the pixels represented by *pctNt* for the same area, and values for the same variable at different neighborhood sizes are correlated. We added size code (table 6.1) as a suffix to a variable name to indicate the size of the neighborhood. For instance, *Fden4* is forest density evaluated across a neighborhood size of 590.5 ha. Size code 1 has been reserved for a smaller neighborhood size of 4.41 ha for a planned later study to be compared with this project. Each of the three largest neighborhood sizes is 9 times larger than the next lower size. The largest neighborhood size might share a substantial minority of its pixels with the neighborhood of a plot in an adjacent FIA grid cell, making values for plots in adjacent cells potentially not strictly independent at this size. We estimate up to 20 percent of plots in our data are in a grid cell immediately adjacent to another grid cell with a plot.

We used data compiled for Will-Wolf and others (2011a) for the environmental and plot variables defined in that study. Geographic location for each plot was represented by approximate longitude (*long*) and approximate latitude (*lat*) as in the public online FIA databases, and by elevation (*elev*) from field Global Positioning System coordinates (Woudenberg and others 2010). Use of the public location data allows our study to serve as a model broadly relevant to scientists outside FIA; exact plot locations are private by law and are available only through special agreements. The geographic variables are indirect indicators of climate at a plot as well as of other possible factors linked to geographic location; relationship to direct climate variables and other possible factors differs for each region and subregion. Forest structure within a plot was represented by total live tree basal area (*tBA*), and percentage of *tBA* in softwoods, conifers, or both (*pctSoft*); the latter is also a general indicator of variability in lichen substrates at a plot. Location and forest structure variables were extracted from FIA and legacy databases.

Air pollution is represented by 1998–2004 average annual wet deposition values for sulfur dioxide ($SO_2^{--}$), nitrate ($NO_3^-$), and ammonium ($NH_4^+$) (geographic pattern of $NO_3^-$ deposition illustrated in Will-Wolf and others 2011a)

**Table 6.1—Definition of land cover variables and the neighborhoods across which they were evaluated**

| Landscape variables | | | | | | |
|---|---|---|---|---|---|---|
| Name (variables) | Definition | | | | National Land Cover Database classes | Range of values |
| Forest density *(Fden)* | Index for percentage of pixels in the neighborhood that were forest cover | | | | 41, 42, 43, 90 | 1–22[a] |
| Forest connectivity *(Fcon)* | Index for percentage of all forest cover pixel edges that were forest-to-forest edges | | | | 41, 42, 43, 90 | 0–22[a] |
| Percentage natural *(pctNt)* | Index for percentage of natural to seminatural land cover | | | | 11, 12, 31, 41, 42, 43, 52, 71, 90, 95 | 0–22[b] |
| Percentage agricultural *(pctAg)* | Index for percentage of agricultural land cover | | | | 81, 82 | 0–22[b] |
| Percentage developed *(pctDv)* | Index for percentage of developed land cover | | | | 21, 22, 23, 24 | 0–22[b] |
| Neighborhoods | | | | | | |
| Size | 4.41 ha | 15.21 ha | 65.61 ha | 590.5 ha | 5314 ha | 47 830 ha |
| Size code | 1 | 2 | 3 | 4 | 5 | 6 |

Note: All values are ordinal, unitless numbers representing ranges of percentages.

[a] Value 1 represents exactly 0 percent; 22 represents exactly 100 percent. The 20 values (from 2 through 21) represent approximately equal divisions of the 1- through 99-percent range. For *Fcon*, the value 0 represents a landscape with no forest cover pixels; see text.

[b] Value 0 represents exactly 0 percent; 22 represents exactly 100 percent. The 6 intermediate values represent roughly equal divisions of the 1- to 99-percent range.



interpolated for each plot from models using National Atmospheric Deposition Program data (Coulston and others 2004). These modeled variables represent average background pollution in the general region; they do not capture variability over time or spatial variation from either local point sources or diffuse semilocal pollution "hot spot." $SO_2^{--}$ and $NO_3^-$ are strongly correlated with each other in our datasets (Will-Wolf and others 2011a), so $NO_3^-$ represents both acidic pollution variables for most analyses (tables 6.2, 6.3, 6.4, and 6.5). Our pollution variables adequately represent total background air pollution in Eastern States, but they underestimate total background pollution in Western States, where dry deposition is an important contributor (Fenn and others 2003). Wet deposition estimates represent relative air pollution loads well within East regions and reasonably well within West regions (better in the wetter parts of the West). They do not well represent the relative air pollution loads between the East and West, because dry deposition contributes so much more to total pollution in the West.

**Table 6.2—West region and groups: Spearman correlations of land cover variables with Lichen S at the neighborhood size with strongest correlation**

| Variables | West all n = 1,397 | W Sierras n = 254 | W CO Plateau n = 151 |
|---|---|---|---|
| *Fden* | max rho = **+ 0.416** with *Fden6* | max rho = + 0.187 with *Fden6* | max rho = **+ 0.572** with *Fden6* |
| *Fcon* | max rho = + 0.262 with *Fcon6* | NS | max rho = + 0.518 with *Fcon6* |
| *pctNt* | max rho = – 0.204 with *pctNt4* | max rho = – 0.294 with *pctNt4* | NS |
| *pctAg* | max rho = + 0.205 with *pctAg4* | max rho = + 0.294 with *pctAg5* | NS |
| *pctDv* | max rho = + 0.204 with *pctDv4* | max rho = **+ 0.301** with *pctDv4* | NS |

n = sample size, "max" = "maximum." NS = nonsignificant. See text and Table 6.1 for definitions of variable acronyms. Note: The rho value for the strongest correlation in each region is in bold. Correlations with rho < ± 0.40 are considered weak. For the smallest n, rho = ± 0.30 is significant at $p \leq 0.0005$, though the correlation represents less than 10 percent of the variation in Lichen S. For rho > 0.447, at least 20 percent of variation is represented by the correlation.

**Table 6.3—West region and subregions: intercorrelations of variables featuring *Fden* and *pctAg***

| Regions/subregions | *Fden* and similar variables | *pctAg* and similar variables | Environmental variables |
|---|---|---|---|
| West all | n = 1,397 | | |
| Correlations[a] | *Fden*: rho = + 0.611 with *precip*, – 0.453 with *mxJul* at *Fden6*. (*Fcon* similar pattern but weaker.) | *pctAg*: weak negative correlation with *elev* max at *pctAg5*. (*pctNt* similar patterns but weaker, signs opposite.) | Intercorrelations of environmental variables: all rho < 0.600. |
| W Sierras | n = 254 | | |
| Correlations[a] | *Fden*: weak negative correlation with pollution, max at *Fden6*; rho = + 0.742 with *precip*, + 0.509 with *tBA* at *Fden6*. (*Fcon* similar pattern but weaker.) | *pctAg*: weak positive correlation with pollution, max at *pctAg4*; rho = – 0.494 with *elev* at *pctAg4*. (*PctNt* similar pattern but weaker, signs opposite.) | Pollutants intercorrelated, correlated with *long, lat,* all rho > 0.600; *elev, mxJul, pctSoft* all intercorrelated rho > 0.600. |
| W CO Plateau | n = 151 | | |
| Correlations[a] | *Fden*: rho = + 0.417 with $SO_2^{--}$, + 0.562 with $NO_3^-$, + 0.633 with *elev*, + 0.765 with *precip*, – 0.752 with *mxJul*, + 0.427 with *tBA*, – 0.431 with *pctSoft*, all at *Fden6*. (*Fcon* similar pattern but weaker.) | *pctAg*: weak positive correlation with pollution, max at *pctAg4*; rho = – 0.494 with *elev* at *pctAg4*. (*PctNt* similar pattern but weaker, signs opposite.) | $NO_3^-$, *elev*, *mxJul* intercorrelated rho > 0.600. |

n = sample size, "max" = "maximum." See text and Table 6.1 for definitions of variable acronyms.
Note: The strongest Spearman correlations of *Fden* and *pctAg* with environmental variables are listed when absolute value of rho ≥ 0.40 ($p < 0.0005$; at least 16 percent of variation explained). Weaker results are described; "much weaker" indicates correlations were > 0.150 weaker. Selected correlations between environmental variables (rho > 0.60) are summarized in parentheses in the far right column from Will-Wolf and others (2011a). Weaker correlations are not mentioned.

[a] For absolute value of rho > 0.447, at least 20 percent of variation is represented by the correlation; for absolute value of rho ≤ 0.60, 36 percent or less of variation is represented. Correlations not mentioned are very weak to random.

**Table 6.4—East region and subregions: Spearman correlations of land cover variables with Lichen S at the neighborhood size with strongest correlation**

| Variables | East all n = 1,085 | E Adiron n = 152 | E Decid n = 264 |
|---|---|---|---|
| *Fden* | max rho = + 0.370 with *Fden6* | NS | max rho = + 0.428 with *Fden6* |
| *Fcon* | max rho = + 0.311 with *Fcon6* | NS | max rho = + 0.383 with *Fcon5* |
| *pctNt* | max rho = **+ 0.410** with *pctNt6* | max rho = **+ 0.333** with *pctNt4* | max rho = **+ 0.440** with *pctNt6* |
| *pctAg* | max rho = – 0.355 with *pctAg6* | max rho = **– 0.332** with *pctAg4* | max rho = – 0.342 with *pctAg6* |
| *pctDv* | max rho = – 0.264 with *pctDv4* | max rho = – 0.307 with *pctDv4* | max rho = – 0.282 with *pctDv6* |

n = sample size, "max" = "maximum." NS = nonsignificant. See text and Table 6.1 for definitions of variable acronyms.
Note: The rho value for the strongest correlation in each region is in bold, plus a second almost equal for one region. Correlations with rho < ± 0.40 are considered weak For the smallest n, rho = ± 0.30 is significant at $p \leq 0.0005$, though the correlation represents less than 10 percent of the variation in Lichen S. For rho > 0.447, at least 20 percent of variation is represented by the correlation.

**Table 6.5—East region and subregions: intercorrelations of variables featuring *Fden* and *pctAg***

| Regions/subregions | *Fden* and similar variables | *pctAg* and similar variables | Environmental variables |
|---|---|---|---|
| East all | n = 1,085 | | |
| Correlations[a] | *Fden*: weak negative correlations with $NH_4^+$. (*Fcon* similar pattern but weaker.) | *pctAg*: rho = + 0.456 with $NH_4^+$, weak positive with $SO_2^{--}$, $NO_3^-$, all max at *pctAg6*. (*pctNt* similar pattern slightly weaker, signs opposite.) | Intercorrelations of environmental variables: all rho < 0.600. |
| E Adiron | n = 152 | | |
| Correlations[a] | *Fden*: rho = + 0.558 with *elev* at *Fden4*. (*Fcon* similar pattern but weaker.) | *pctAg*: rho = + 0.447 with $SO_2^{--}$, – 0.498 with *elev*, max at *pctAg5*; rho = – 0.521 with *lat*, + 0.536 with *minJan*, max at *pctAg4*. (*pctNt* similar pattern slightly weaker, signs opposite.) | Pollutants strongly intercorrelated, correlated with *long*, *lat*, *minJan*, all rho > 0.600; *long*, *lat*, *minJan*, all intercorrelated rho > 0.600. |
| E Decid | n = 264 | | |
| Correlations[a] | *Fden*: rho = – 0.601 with $NH_4^+$ at *Fden6*, weak positive correlations with *long*. (*Fcon* similar pattern but weaker.) | *pctNt*: rho = – 0.585 with $NH_4^+$ at *pctNt6*. *pctAg*: rho = + 0.684 with $NH_4^+$ at *pctAg6*. | $NH_4^+$ correlated with *long*, rho > 0.60.0 |

n = sample size, "max" = "maximum." See text and Table 6.1 for definitions of variable acronyms.

Note: Spearman correlations of *Fden* and *pctAg* with environmental variables are listed when absolute values of rho ≥ 0.40 ($p < 0.0005$; at least 16 percent of variation explained). Weaker results are described; "much weaker" indicates correlations were > 0.150 weaker. Strength (not sign) of selected intercorrelations between environmental variables (absolute value of rho > 0.60) summarized from Will-Wolf and others (2011a) in the far right column. Weaker correlations are not mentioned.

[a] For absolute value of rho > 0.447, at least 20 percent of variation is represented by the correlation; for absolute value of rho ≤ 0.60, 36 percent or less of variation is represented. Correlations not mentioned are very weak to random.

Climate is represented by average annual precipitation (*precip*), average minimum January temperature (*minJan*), and average maximum July temperature (*mxJul*); each is the 1971–2000 30-year average interpolated for each plot from the Climate Source model (PRISM: Daly and Taylor 2000). Pollution modeled as wet deposition is much higher and varies more widely in the East, and climate varies much more widely in the West (appendices in Will-Wolf and others 2011a).

The full suite of explanatory variables as described above was available for each plot included in the analyses. The numbers of plots for each analysis are reported in tables 6.2 through 6.5.

## Analysis methods

Our analyses were organized to evaluate these preliminary hypotheses:

- Nearby land cover is correlated with Lichen S across large regions.
- In the West, land cover variables are correlated with climate variables.
- In the East, land cover variables are correlated with pollution variables.
- The relationships of land cover variables to environmental variables, and thus the interpretations of their relationships with Lichen S, vary by region.
- Regression models to explain variation in Lichen S are improved when land cover variables are included.

As with Will-Wolf and others (2011a), we found that few of the pairwise scatterplots we examined for variables showed linear relationships. We did not quantitatively evaluate whether parametric assumptions were met for each analysis or what specific data transformations might be most appropriate for each variable. Instead we applied a single data transformation as needed (see next paragraph) to address all such issues.

We calculated Pearson product-moment (parametric) correlations (r) and Spearman rank (nonparametric) correlations (rho) to evaluate the first four hypotheses, and we developed linear regression models with both original and ranked data to evaluate the fifth hypothesis. Rank transformation, the recommended option for standard analysis of FIA lichen data (Will-Wolf 2010), compensates for many different data distribution issues with count, ordinal, and continuous data (Yandell 1997) that affect analysis. It also equalizes data ranges for independent variables, which is useful for avoiding possible bias in regression models from differently scaled variables. Data were always ranked so that higher rank corresponded to higher original value for the variable. All analyses were performed in SPSS for Windows (Release 16.0.1 © SPSS, Inc. 1989–2007).

Many correlations between explanatory variables, as well as between those and Lichen S, were examined to determine which variables were most informative. We report the strongest correlations of Lichen S and environmental

variables with land cover variables and briefly summarize correlations between environmental variables. We discuss only correlations with absolute value of r or rho ≥ 0.40 ($p < 0.0005$ for the smallest sample size used) to highlight the potentially most ecologically important (beyond merely statistically significant) relationships. For correlation strength (sign ignored) > 0.447, a minimum of about 20 percent of variation is represented by the correlation; for correlation strength ≤ 0.60, about 36 percent or less of variation is explained by the correlation.

Many linear regression models were developed for each geographic region, primarily with hand selection of variables and forced simultaneous entry; all reported models were developed this way. Each land cover variable was entered into a particular model at only one neighborhood size. All land cover variables were tested for each region, but a final model was not required to include a land cover variable. Multiple independent variables that had correlations stronger than 0.60 were not entered into the same regression model; instead alternate models were developed. Multiple alternate regression models were examined. Only variables that were significant at $p < 0.05$ were retained in a model. We made these conservative choices for model development to avoid overestimating the significance of a model; the lower power of our analyses was an acceptable cost. We report the single strongest (highest $R^2$) regression model that met our development criteria, unless there were two similarly strong alternate models. All of our "independent" variables including land cover variables are estimated and subject to error, not exact and fixed as assumed for regression models. This is likely to be the case in all large-scale ecological analyses for practical reasons, and should be considered when interpreting predictive models.

## RESULTS

Spearman correlations were often stronger than Pearson correlations, suggesting data may not meet assumptions for parametric statistical tests in those cases. Similarly, many regression models using ranked data were stronger than equivalent models using raw data. For consistency, we report Spearman correlations and regression models using ranked data, except as specifically noted. Our conservative criteria for reporting correlations and for entering variables into regression models mean the patterns we do report are quite robust.

Among land cover variables, percentage of forest cover (*Fden*) in West regions and percentage of natural to seminatural land cover (*pctNt*) in East regions usually had the strongest correlations (+/-) with Lichen S (tables 6.2 and 6.4). Percentage of a neighborhood in agricultural land (*pctAg*) or developed land (*pctDv*) each had the strongest (+/-) correlation with Lichen S in one region. Connectivity of forest cover (*Fcon*) gave results similar to percentage of forest cover, but weaker. As we expected, percentage of forest, percentage of natural to seminatural land cover, and connectivity of forest were positively correlated

in each region, whereas all three were negatively correlated with proportion of agricultural land (statistics not reported). Percentage in developed land usually had weak positive correlations with percentage in agricultural land and was mostly random regarding other land cover variables. We focused on percentage in forest cover and percentage in agricultural land to report relationships of land cover with environmental variables (tables 6.3 and 6.5).

In the West region and both West subregions, land cover variables had relatively strong correlations with climate and related environmental variables (table 6.3). For the East, in contrast, only in the mountainous Adirondacks subregion did land cover variables have relatively strong correlations with climate and related variables (table 6.5). Correlations between land cover variables and pollution variables were relatively weak in the West and slightly stronger in the East. The strongest such correlation, of *pctAg6* with $NH_4^+$ in the Eastern Deciduous subregion, explained almost 50 percent of variation (table 6.5). Correlations between environmental variables that affected interpretation of other statistical relationships varied quite widely among regions; some areas had few or no strong correlations, but others had many strong relationships (tables 6.3 and 6.5).

We found two different patterns for effect of neighborhood size on land cover variables. For percentage of agricultural land and developed land, the strength of several correlations with Lichen S and environmental variables peaked at neighborhood sizes of 590.5 ha or 5314 ha. For percentage of forest and related forest cover variables (*Fcon* and *pctNt*), this happened only twice. Identification of a neighborhood size at which a correlation is strongest helps focus the search for a mechanism causing the inferred effect. For *Fden* and related land cover variables most of the time and for all land cover variables at least some of the time the strength of correlations increased continuously with neighborhood size, lending little help to the search for underlying causes.

All four West regression models included climate variables; only two included land cover variables. Land cover variables were included in the best regression model for region West all:

R-Lichen S = 946.322 - 0.569*R-*elev* + 0.316*R-*Fden6* - 0.195*R-*mxJul* + 0.077*R-*pctAg5* (1)

where

$R^2 = 0.472$
$p < 0.0005$
n = 1,397.

In this region, the land cover variables were more strongly linked to climate-related factors than to pollution variables (table 6.3). Model (1) suggests that climate and human-modified landscape pattern have more influence than pollution on Lichen S in region West all. Land cover variables were not included in the best regression model for the W Sierras subregion:

$$\text{R-Lichen S} = 207.119 - 0.519*\text{R-}elev - 0.268*\text{R-}NH_4^+ + 0.162*\text{R-}tBA \quad (2)$$

where

$R^2 = 0.330$
$p < 0.0005$
n = 254.

Land cover variables were much more strongly linked to climate-related variables than to pollution variables in this region (table 6.3). Model (2) indicates that climate, pollution, and forest structure have more influence than landscape pattern on Lichen S in the W Sierras subregion. There were two equally strong regression models for the W CO Plateau subregion; one included a land cover variable and the other did not:

$$\text{R-Lichen S} = 42.092 + 0.374*\text{R-}NO_3^- + 0.292*\text{R-}precip - 0.176*\text{R-}pctSoft \quad (3)$$

where

$R^2 = 0.404$
$p < 0.0005$
n = 151.

$$\text{R-Lichen S} = 48.461 + 0.327*\text{R-}NO_3^- + 0.298*\text{R-}Fden6 - 0.210*\text{R-}pctSoft \quad (4)$$

where

$R^2 = 0.403$
$p < 0.0005$
n = 151.

*Fden* and $NO_3^-$ were both strongly linked to climate-related variables (table 6.3), and pollution is relatively low in this subregion (Will-Wolf and others 2011a). It is possible that neither pollution nor landscape configuration has an independent influence on Lichen S here; separating their impact from climate will require more detailed studies. Models (3) and (4) suggest Lichen S increases with more pollution. This unexpected result is another indication that in the W CO Plateau subregion, variable $NO_3^-$ may indirectly represent some climate factor, rather than the direct influence of pollution.

All three East models included both pollution and land cover variables; two also included variables linked to climate. Despite the stronger single correlations of land cover variable *pctNt*

with Lichen S in East regions (table 6.5), *Fden* (two regions) and *pctAg* (one region) were the land cover variables entered into the best East regression models. The best regression model for region East all was:

$$\text{R-Lichen S} = 591.290 - 0.435*\text{R-}NO_3^- + 0.345*\text{R-}Fden6 \quad (5)$$

where

$R^2 = 0.324$
$p < 0.0005$
n = 1,085.

Land cover variables were not strongly correlated with either climate-related or pollution variables in this region (table 6.5). Model (5) suggests that pollution and landscape pattern have more influence than climate on Lichen S in the region East all. For the E Adiron subregion, models with original data were stronger than those with ranked data (strongest model with ranked data had $R^2 = 0.324$); the only one of our models for which this was the case:

$$\text{Lichen S} = 30.920 - 0.506*NO_3^- - 0.204*pctAg4 - 0.180*elev \quad (6)$$

where

$R^2 = 0.375$
$p < 0.0005$
n = 152.

Model (6) suggests that pollution, climate, and landscape pattern all influence Lichen S in the E Adiron subregion. Geographic variables *lat* and *long* were strongly correlated with both climate and $NO_3^-$ in this dataset (table 6.5). The effect of urban and industrial pollution on climate may thus be overestimated, with $NO_3^-$ indirectly representing a climate variable in model (6). This E Adiron model, developed using original rather than ranked data, is more subject to bias from data distribution and other data issues than are other models. The best regression model for subregion E Decid was:

$$\text{R-Lichen S} = 137.761 + 0.534*\text{R-}Fden6 - 0.297*\text{R-}NO_3^- - 0.278*\text{R-}long \quad (7)$$

where

$R^2 = 0.323$
$p < 0.0005$
n = 264.

Neither longitude nor land cover variables were strongly correlated with climate variables

in this subregion (table 6.5). Thus, model (7) clearly suggests that landscape pattern and urban and industrial air pollution have more influence than does climate on Lichen S here. Because $NH_4^+$ is strongly correlated with *long* as well as with *Fden6*, the influence of agricultural air pollution is probably represented indirectly in the model.

We found that most of our final linear regression models developed using our very conservative data treatment and analysis choices were stronger ($R^2$ higher by 0.04 to 0.10) than the comparable models reported in Will-Wolf and others (2011a) that used original data and less conservative model development choices, even when a land cover variable was not included in our final model. This is additional evidence that nonstandard distributions of original data probably reduced the power of regression models using the original data. Only for the E Adiron subregion was our best model no stronger than the model for that subregion in the earlier study (Will-Wolf and others 2011a). Best regression models are somewhat stronger for the West (explaining 33 to 47 percent of variation) than for the East (explaining 32 to 38 percent of variation).

## DISCUSSION

Our first hypothesis, that pattern of nearby land cover is linked to Lichen S, is supported at least minimally; a minimum of about 10 percent of the variation in Lichen S is explained by correlation with at least one estimate for nearby land cover in each region. Lichen S is a general index for the condition of a forest lichen community; it is likely that variation in lichen species composition will be even more strongly correlated with neighboring land cover. Our results suggest more intensive studies of the relationship between neighboring land cover and the condition of forests are likely to improve our understanding of impacts on forest health. Regression models for the East support the importance of landscape variables to explain Lichen S more clearly than do models for the West, even though East models are weaker overall than are West models. The land cover variables that we measured have the greatest potential usefulness in the three East regions, and the least potential usefulness in the West Sierras subregion.

Our second hypothesis, that nearby land cover strongly reflects the influence of climate in the West, is supported. In the two West subregions, land cover variables do not clearly improve regression models, while for "West all" they do appear to improve regression models.

These results reflect that local landscape patterns are strongly correlated with climate on forests in the West. More intensive studies should be designed at smaller spatial scales to separate the effects of neighboring land cover from the effects of climate on forest lichens. Such studies will probably use data on abundance of individual species at each site rather than just number of lichen species at a site. They will be required to support conclusions about whether landscape pattern independently affects the condition of forest lichen communities in the West.

Our third hypothesis, that nearby land cover strongly reflects the influence of pollution in the East, is not supported. Correlations of land cover variables with modeled background pollution in the East are mostly moderate to weak. The one exception is for the mountainous Adirondacks region, where pollution is also correlated with climate; possible indirect links of land cover with climate could mean the link between pollution and land cover is overestimated for this region. In the East, landscape variables do improve regression models for all three regions, though interpretation is sometimes difficult. It thus appears that in the East landscape variables contribute information to explaining patterns of lichen species richness, potentially independent of pollution and climate. Lichen S does appear to have some potential as an indicator for condition of forests in the Eastern Deciduous Forest subregion when land cover variables are included, in contrast to our earlier analyses (Will-Wolf and others 2011a) that did not include neighboring land cover.

Our fourth hypothesis, that relationships of land cover variables with Lichen S and with environmental variables differ strongly between regions, is supported. No single landscape variable appears the best to use in all cases. Indices for percentage of forest cover or percentage of natural to seminatural land cover in a neighborhood were often most strongly correlated with Lichen S. The index for percentage of forest cover was most frequently included in the best regression model, even when it was not the land cover variable having the strongest correlation with Lichen S. The indices for percentage of agricultural land or of developed land also sometimes had strong relationships with Lichen S. Correlations of land cover variables with individual climate and pollution variables differed enough between regions that no general recommendations are made; several standard land cover variables should be tested in each new region. We do conclude from this study that land cover composition (represented by indices for percentage of forest, natural and seminatural, or agricultural) may be more important than forest fragmentation (represented by our index of forest connectivity) to explain variation in Lichen S. We also observed that at these large spatial scales our index for percentage of developed land was usually not as useful as other land cover variables.

Our fifth hypothesis, that inclusion of land cover variables improves models to explain variation in Lichen S, is supported for the East but not for the West. In the East, including land cover improves regression models for all three regions tested, and thus helps to explain patterns in lichen species richness independent of pollution and climate. Our failure to demonstrate the usefulness of land cover variables in the West is, however, not conclusive. More intensive studies across smaller geographic areas in West regions more affected by human land use, as well as the use of data reflecting lichen species composition rather than merely species counts, might find that nearby land cover independently affects the condition of forest lichen communities in those circumstances.

For most of our land cover variables, we could not identify neighborhood sizes associated with the strongest correlations. Strength of correlation often increased continuously to the maximum size, at which neighborhoods for plots in adjacent sample grid cells may overlap and possibly inflate the strength of the correlation. The neighborhood sizes at which correlations of Lichen S with our index for percentage of agricultural land peaked are often smaller than the maximum, suggesting a particular scale of impact. That area is still much larger than the area across which a similar land cover variable had the strongest correlations with lichen community composition in a more intensive study (Will-Wolf and others 2005). This means our study provides limited support to focus on possible mechanisms even as it highlights the importance of exploring further the impact of land cover pattern on forest lichen communities. The impact of land cover pattern can itself be considered a proxy for more direct causes such as altered disturbance regime, dispersal limitations, competition from invaders, or alterations in other regional ecological processes (Sillett and others 2000, Stofer and others 2006, Werth and others 2006).

Several additional studies are suggested by our results. One is to evaluate the importance of calculating land cover variables using exact as opposed to approximate plot locations. If the latter approach is found to be adequate, use of public FIA data with approximate plot locations is supported and analyses can be conducted much more easily by a wide variety of investigators. Use of exact plot locations in an additional study would also allow evaluation of a smaller neighborhood size that better corresponds with small scales at which effects of landscape pattern on lichens have been found in other studies (Werth and others 2006, Will-Wolf and others 2005). Another useful addition would be to include an evapotranspiration variable to represent climate in future analyses; this could be particularly helpful for the East, where our simpler climate variables are poorly linked to Lichen S. Yet another useful addition to future studies would be to compare correlations with pollution using dry, wet, and total pollution

deposition, to evaluate which of the pollution deposition variables is most strongly correlated with Lichen S and with land cover variables in different regions. Dry deposition has been shown to be a very important contributor to ground-level pollution in Western States (Fenn and others 2003).

Our study clearly suggests that impact of land cover pattern on forest health indicators should be considered further for analysis of FIA data from Eastern States. The results of this study of large areas using Lichen S, a very general indicator of the condition of lichen communities, suggests likely stronger links between land cover and forest response from investigations with more precise forest health indicators in Eastern States. The strong relationship between land cover pattern and climate at large spatial scales in Western States suggests more research is needed to decide whether independent effects of land cover pattern on forest lichen communities can be identified in the West.

## ACKNOWLEDGMENTS

This research was supported in part by a research grant from the Forest Health Monitoring Program to the University of Wisconsin-Madison for Will-Wolf, by cooperative agreement SRS 06-CA-11330145-079 between the Forest Service and the University of Wisconsin-Madison for Will-Wolf, by project "Forest Health Monitoring, Analysis and Assessment" of research joint venture agreement 07-JV-11330146-134 between the Forest Service and North Carolina State University for Mark Ambrose, by joint venture agreement 08-JV-11261979-349 between the Forest Service and Oregon State University for Sarah Jovan, and by allocation of Forest Service work time for Randall Morin and Kurt Riitters. The research findings are the responsibility of the authors and are not the policy of the Forest Service.

## LITERATURE CITED

Bailey, R.G. 1989. Explanatory supplement to ecoregions map of the continents. Environmental Conservation. 16: 307-309.

Cleland, D.T.; Freeouf, J. A.; Keys, J.E., Jr. [and others]. 2005. Ecological subregions: sections and subsections for the conterminous United States. June 14, 2005 version. Washington, DC: U.S. Department of Agriculture Forest Service. [Map, presentation scale 1:3,500,000; Albers equal area projection; colored].

Cleland, D.T.; Freeouf, J.A.; Keys, J.E., Jr. [and others]. 2007. Ecological subregions: sections and subsections for the conterminous United States. 1:3,500,000; Albers equal area projection; colored. In: Sloan, A.M., tech. ed. Gen. Tech. Rep. WO-76. Washington, DC: U.S. Department of Agriculture Forest Service. Map, presentation scale. Also as a GIS coverage in ArcINFO format on CD-ROM or at http://fsgeodata.fs.fed.us/other_resources/ecosubregions.html. [Date accessed: March 18, 2011].

Coulston, J.W.; Riitters, K.H.; Smith, G.C. 2004. A preliminary assessment of Montreal Process indicators of air pollution for the United States. Environmental Monitoring and Assessment. 95: 57-74.

Daly, C.; Taylor, G. 2000. United States average monthly or annual precipitation, temperature, and relative humidity 1961–90. Arc/INFO and ArcView coverages. Corvallis, OR: Oregon State University, Spatial Climate Analysis Service.

Fenn, M.E.; Haeuber, R.; Tonnesen, G.S. [and others]. 2003. Nitrogen emissions, deposition, and monitoring in the Western United States. BioScience. 53(4): 391-403.

Homer, C.; Dewitz, J.; Fry, J. [and others]. 2007. Completion of the 2001 National Land Cover Database for the conterminous United States. Photogrammetric Engineering and Remote Sensing. 73: 337-341.

McCune, B. 2000. Lichen communities as indicators of forest health. Bryologist. 103: 353-356.

Nimis, P.L.; Scheidegger, C.; Wolseley P., eds. 2002. Monitoring with lichens—monitoring lichens. In: Earth and Environmental Sciences, vol. 7. NATO Science Series. Dordrecht, The Netherlands: Kluwer Academic Publishers. 412 p.

Riitters, K. 2011. Spatial patterns of land cover in the United States: a technical document supporting the Forest Service 2010 Resources Planning Act (RPA) Assessment. General Technical Report SRS-136. Asheville, NC: US Department of Agriculture Forest Service, Southern Research Station. 64 p.

Riitters, K.H.; Wickham, J.D.; Wade, T.G. 2007. An indicator of forest dynamics using a shifting landscape. Mosaic. Ecological Indicators. 9: 107-117.

Sillett, S.C.; McCune, B.; Peck, J.E. [and others]. 2000. Dispersal limitations of epiphytic lichens result in species dependent on old-growth forests. Ecological Applications. 10(3): 789-799.

Stofer, S.; Bergamini, A.; Aragon, G. [and others]. 2006. Species richness of lichen functional groups in relation to land use intensity. Lichenologist. 38(4): 331-353.

U.S. Department of Agriculture (USDA) Forest Service. 2007. Forest Inventory and Analysis (FIA) fact sheet series: lichens community indicator. http://www.fia.fs.fed.us/library/fact-sheets/p3-factsheets/lichen.pdf. [Date accessed: May 8, 2014].

U.S. Department of Agriculture (USDA) Forest Service. 2011. Forest Inventory and Analysis (FIA) Phase 3 field guide – lichens community, version 5.1. http://www.fia.fs.fed.us/library/field-guides-methods-proc/docs/2012/field_guide_p3_5-1_sec21_10_2011.pdf. [Date accessed: May 8, 2014].

Werth, S.; Wagner, H.H.; Gugerli, F. [and others]. 2006. Quantifying dispersal and establishment limitation in a population of an epiphytic lichen. Ecology. 87(8): 2037-2046.

Will-Wolf, S. 2010. Analyzing lichen indicator data in the Forest Inventory and Analysis Program. Gen. Tech. Rep. PNW-GTR-818. Portland, OR: U.S. Department of Agriculture Forest Service, Pacific Northwest Research Station. 61p.

Will-Wolf, S.; Ambrose, M.J.; Morin, R.S. 2011a. Relationship of a lichen species diversity indicator to environmental factors across continental United States. In: Conkling, B.L.; Ambrose, M.J., eds. Forest health monitoring 2007 national technical report. Gen. Tech. Rep. SRS-147. Asheville, NC: U.S. Department of Agriculture Forest Service, Southern Research Station: 25-63.

Will-Wolf, S.; Esseen, P.-A.; Neitlich, P. 2002. Monitoring biodiversity and ecosystem function: forests. In: Nimis, P.L.; Scheidegger, C.; Wolseley P.A., eds. Monitoring with lichens—monitoring lichens. Dordrecht, The Netherlands: Kluwer Academic Publishers: 203-222.

Will-Wolf, S., Makholm, M.M., Roth, J. [and others]. 2005. Lichen bioaccumulation and bioindicator study near Alliant Energy - WPL Columbia Energy Center. Energy Environmental Research Program Final Report. Madison, WI: Division of Energy, Department of Admininistration, State of Wisconsin, and Wisconsin Department of Natural Resources. 57 p. https://focusonenergy.com/sites/default/files/research/willwolflichenlowres_summaryreport.pdf [Accessed May 8, 2014].

Will-Wolf, S.; Nelsen, M.P.; Trest, M.T. 2010. Responses of small foliose lichen species to landscape pattern, light regime, and air pollution from a long-term study in upper Midwest USA. In: Nash, T.H. III; Geiser, L.; McCune, B. [and others], eds. Biology of lichens—symbiosis, ecology, environmental monitoring, systematics, cyber applications. Bibliotheca Lichenologica. 105: 167-182.

Will-Wolf, S.; Nelsen, M.P.; Trest; M.T. 2011b. Does morphological response of four common lichen species to pollution, shade, and landscape pattern predict long-term changes in distribution? In: Bates, S.; Bungartz, F.; Elix, J. [and others], eds. Biomonitoring, ecology, and systematics of lichens: festschrift Thomas H. Nash III. Bibliotheca Lichenologica. 106: 375-386.

Woodall, C.W.; Amacher, M.C.; Bechtold, W.A. [and others]. 2011. Status and future of the forest health indicators program of the USA. Environmental Monitoring and Assessment. 177: 419-436.

Woodall, C.W.; Conkling, B.L.; Amacher, M.C. [and others]. 2010. The Forest Inventory and Analysis database: database description and users manual version 4.0 for phase 3. Gen. Tech. Rep. NRS-61. Newtown Square, PA: U.S. Department of Agriculture Forest Service, Northern Research Station. 180 p.

Woudenberg, S.W.; Conkling, B.L.; O'Connell, B.M. [and others]. 2010. The Forest Inventory and Analysis database: database description and users manual version 4.0 for phase 2. Gen. Tech. Rep. RMRS-GTR-245. Fort Collins, CO: U.S. Department of Agriculture Forest Service, Rocky Mountain Research Station. 336 p.

Yandell, B.S. 1997. Practical data analysis for designed experiments. New York: Chapman & Hall. 437 p.

# CHAPTER 7.

# Climate Effects on Lichen Indicators for Nitrogen

Sarah Jovan

## INTRODUCTION

The Lichen Communities Indicator is a sensitive indicator of forest health changes caused by air quality, climate change, and other stressors. To date, more than 8,000 epiphytic lichen surveys have been collected across the Nation by the Forest Inventory Analysis (FIA) and Forest Health Monitoring (FHM) Programs and their partners (table 7.1; Phelan and others 2012). These data are currently used in several national Forest Service initiatives, including the Chief's Wilderness Challenge, the Watershed Condition Framework, the Terrestrial Ecosystem Condition Framework, and the amended Planning Rule.

The Indicator has been instrumental in developing critical loads (CLs) for nitrogen (N) in North American forests (Pardo and others 2011a). By definition, CLs are the maximum amount of N deposition that a sensitive indicator can tolerate before being "harmed." Regulators and managers use these values to negotiate pollution emissions levels that preserve the function of sensitive ecosystems. For example, the U.S. Environmental Protection Agency used lichen and other CLs to propose the first secondary standards for nitrogen oxide ($NO_x$) pollutants for the United States (EPA 2008), although the standard has not yet been implemented (Pardo and others 2011b). At a smaller scale, land and air managers use CLs to guide pollution permitting near ecosystems of concern.

For lichen CLs, "harm" is typically defined in terms of a shift from N-sensitive species (oligotrophs) to the moderately sensitive mesotrophs or the N-loving eutrophs.

**Table 7.1—Overview of location and timeframe for all Forest Inventory and Analysis-style lichen surveys collected up to 2011**

| Sponsor | FIA region | Number of surveys | On frame? | Years | States |
|---|---|---|---|---|---|
| FIA | IW | 1,856 | Y | 1994–97, 1999–2010 | AZ, CO, ID, MT, NM, NV, UT, WY |
| R6 ARM[a] | IW | 45 | N | 2000, 2003, 2008, 2010 | ID, MT |
| FIA | IW | 68 | N | 2008–11 | ID, MT, WY |
| FIA | North | 97 | N | 1994, 2004 | CT, MA, ME, NH, NY, PA, RI, VT |
| FIA | North | 1,307 | Y | 1994–95, 1998–2005 | CT, DE, IL, IN, OH, MA, MD, ME, MI, MN, NH, NJ, NY, PA, RI, VT, WI, WV |
| FIA | North | 85 | I | 1999–2002 | DE, PA, RI |
| FIA | PNW | 33 | N | 2011 | Interior AK |
| Tongass NF | PNW | 302 | N | 1989–94, 2002–05, 2009, 2011 | AK |
| Chugach NF | PNW | 41 | N | 1993–94 | AK |
| R6 ARM[a] | PNW | 795 | N | 1993–2011 | CA, OR, WA |
| R6 ARM[a] | PNW | 1,698 | I | 1994–2011 | OR, WA |
| FIA | PNW | 1,023 | Y | 1998–2001, 2003–07 | AK, CA, OR, WA |
| FIA | PNW | 255 | N | 1999–2000, 2003–04, 2008–09 | AK, CA, OR, WA |
| FIA | South | 24 | N | 1993 | GA, SC, TN |
| FIA | South | 442 | Y | 1993–95, 1998–99 | AL, GA, NC, SC, TN, VA |

ARM = Air Resources Management; FIA= Forest Inventory and Analysis; IW = Interior West; NF = National Forest; North = Northern; PNW = Pacific Northwest; R6 = Region 6; South = Southern.

[a] Over 2,000 lichen surveys in PNW are provided by the Forest Service, Region 6. For ARM group data, please visit http://gis.nacse.org/lichenair/.

N measurements are compared with response indices, which quantify the dominance or relative abundance of lichens in these N indicator groups (Fenn and others 2008, Geiser and others 2010, Jovan and others 2012). An ideal lichen response index would correlate with N alone, although in practice climate may be a confounding factor to lichen indices applied across mountainous terrain or large geographic areas (Grenon 2012, Jovan and McCune 2004, Will-Wolf and others 2006).

There are many statistical approaches for extracting climate effects from a lichen-N response index (e.g., Geiser and Neitlich 2007, Grenon 2012, Jovan and McCune 2006). Studies focus so much on *correcting* for climate, however, that we rarely investigate the nature of climate interactions with lichen responses to N (although, see Grenon 2012). A better understanding of these interactions will enable the development of multifactored CL models that can cover larger, more climatically heterogeneous landscapes. Likewise, climate change has the potential to skew long-term N trends tracked using lichen-based indicators. Understanding the role of climate will help practitioners detect and correct for these biases.

The purpose of this study was to investigate climate effects on lichen indices used to develop N CLs for California's forests (table 7.2). Lichen Communities Indicator data were combined across dry, oak-dominated forests (fig. 7.1) from the Los Angeles Basin model area (LAB; Jovan and others 2012) and the southern

**Table 7.2—Species list for the study region classified by nitrogen (N) indicator groups used in the lichen-N response indices**

| Genus | Species | Common name | Count | Indicator group |
|---|---|---|---|---|
| *Candelaria* | *concolor* | Candleflame lichen | 80 | Eutroph |
| *Cetraria* | *merrillii* | Blackened thornbush | 8 | Oligotroph |
| *Collema* | *furfuraceum* | Blister tarpaper lichen | 17 | N/A |
| *Collema* | *nigrescens* | Broadleaf tarpaper | 15 | N/A |
| *Evernia* | *prunastri* | Antlered perfume | 43 | Mesotroph |
| *Flavoparmelia* | *caperata* | — | 9 | Mesotroph |
| *Flavopunctelia* | *flaventior* | — | 41 | Mesotroph |
| *Heterodermia* | *leucomela* | Centipede lichen | 4 | N/A |
| *Hypogymnia* | *imshaugii* | Forking bone | 19 | Oligotroph |
| *Hypogymnia* | *inactiva* | Forking bone | 3 | Oligotroph |
| *Hypogymnia* | *physodes* | Monk's hood | 3 | Oligotroph |
| *Leptogium* | *lichenoides* | Tattered vinyl lichen | 6 | N/A |
| *Letharia* | *columbiana* | Wolf lichen | 10 | N/A |
| *Letharia* | *vulpina* | Wolf lichen | 13 | N/A |
| *Melanelixia* | *fuliginosa* | Abraded brown lichen | 5 | Mesotroph |
| *Melanelixia* | *glabra* | Smooth Melanelia lichen | 51 | Mesotroph |
| *Melanelixia* | *subargentifera* | Powdered brown lichen | 9 | Mesotroph |
| *Melanohalea* | *elegantula* | Elegant brown lichen | 12 | Mesotroph |
| *Melanohalea* | *subolivacea* | Eyed brown lichen | 37 | Mesotroph |
| *Niebla* | *cephalota* | Powdery sea-fog lichen | 6 | N/A |
| *Nodobryoria* | *abbreviata* | Tufted foxtail | 2 | Oligotroph |
| *Parmelia* | *hygrophila* | Salted shield | 3 | Mesotroph |
| *Parmelia* | *sulcata* | Powdered shield | 12 | Mesotroph |
| *Parmelina* | *quercina* | — | 31 | N/A |
| *Parmotrema* | *arnoldii* | Powdered scatter-rug | 3 | N/A |
| *Parmotrema* | *austrosinense* | Unwhiskered ruffle lichen | 4 | N/A |

*continued*

**Table 7.2 (continued)—Species list for the study region classified by nitrogen (N) indicator groups used in the lichen-N response indices**

| Genus | Species | Common name | Count | Indicator group |
|---|---|---|---|---|
| *Parmotrema* | *chinense* | Powdered scatter-rug | 11 | N/A |
| *Peltigera* | *collina* | Tree pelt | 4 | N/A |
| *Phaeophyscia* | *hirsuta* | Powdered shadow | 10 | Eutroph |
| *Phaeophyscia* | *orbicularis* | Granulated shadow | 51 | Eutroph |
| *Physcia* | *adscendens* | Hooded rosette | 71 | Eutroph |
| *Physcia* | *aipolia* | Grey-eyed rosette | 28 | Eutroph |
| *Physcia* | *biziana* | Frosted rosette | 39 | Eutroph |
| *Physcia* | *dimidiata* | Frosted rosette | 19 | Eutroph |
| *Physcia* | *stellaris* | Black-eyed rosette | 19 | Eutroph |
| *Physcia* | *tenella* | Fringed rosette | 48 | Eutroph |
| *Physconia* | *americana* | Fancy frost lichen | 36 | Eutroph |
| *Physconia* | *enteroxantha* | Bordered frost lichen | 35 | Eutroph |
| *Physconia* | *fallax* | — | 13 | Eutroph |
| *Physconia* | *isidiigera* | — | 59 | Eutroph |
| *Physconia* | *perisidiosa* | Bordered frost lichen | 50 | Eutroph |
| *Pseudocyphellaria* | *anthraspis* | Dimpled specklebelly | 3 | N/A |
| *Xanthomendoza* | *fallax* | Powdered orange lichen | 22 | Eutroph |
| *Xanthomendoza* | *fulva* | — | 24 | Eutroph |
| *Xanthomendoza* | *galericulata* | — | 8 | Eutroph |
| *Xanthomendoza* | *hasseana* | — | 29 | Eutroph |
| *Xanthomendoza* | *oregana* | — | 49 | Eutroph |
| *Xanthoria* | *candelaria* | Shrubby orange lichen | 8 | Eutroph |
| *Xanthoria* | *parietina* | — | 5 | Eutroph |
| *Xanthoria* | *polycarpa* | Pincushion orange lichen | 54 | Eutroph |
| *Xanthoria* | *tenax* | — | 19 | Eutroph |

— = no common name; N/A= not applicable because species sensitivity to N is poorly understood.

three-fourths of the Greater Central Valley model area (GCV; Jovan and McCune 2005). Lichen communities in these two regions are described by independent models that use the FIA/FHM Lichen Communities Indicator for monitoring N. Within the combined study region, N deposition varies considerably, as do tree species composition, elevation, precipitation, temperature, and dewpoint (table 7.3).

## METHODS

### Sampling design

Lichens were surveyed in the GCV between 1998 and 2003 (n = 71; fig. 7.1), and all LAB plots were surveyed in 2008 (n = 22). Data were combined for all analyses. Survey methods have been described in detail (Woodall and others 2010) but, briefly, a specially trained crew person spends up to 2 hours surveying for epiphytic macrolichens (i.e., excluding crustose and leprose growth forms) within a 0.4-ha plot centered on FIA subplot #1 (fig. 7.2). Most plots in the GCV occur on the systematic FIA phase 3 grid, although 28 plots were established in urban and heavily agricultural areas throughout the region. All LAB plots are "off frame" and are colocated with long-term monitoring sites for air quality and lichens originally established in the mid 1970s (Riddell and others 2011). Each lichen species encountered was assigned a broad abundance code, which follows a logarithmic scale: 1 = Rare (1 to 3 individuals in area), 2 = Uncommon (4 to 10 individuals in area), 3 = Common (> 10 individuals in area but less than half of the boles and branches have that

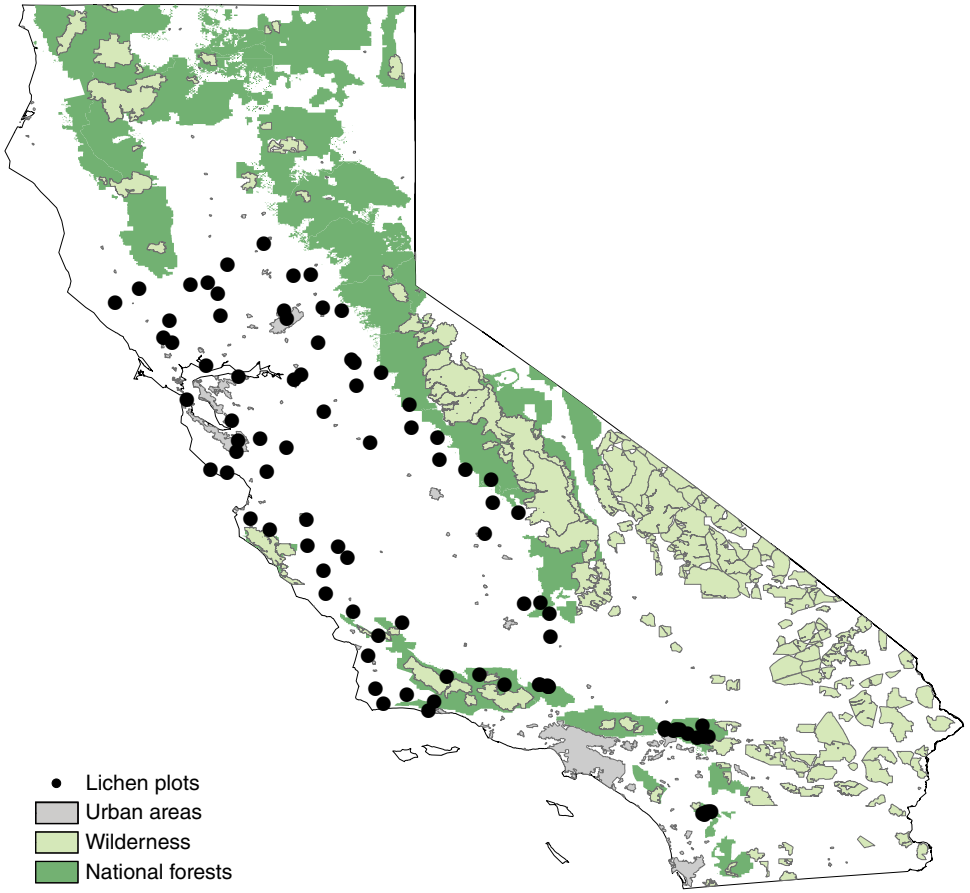


*Figure 7.1—Map of the study region showing approximate locations of Forest Inventory and Analysis plots surveyed for lichens. Greater Central Valley plots all lie north of the Los Angeles metropolitan area.*

**Table 7.3—Variation in environmental variables across the study region and subregions**

| | Average | | Standard deviation | | Range | |
|---|---|---|---|---|---|---|
| Variable | GCV | LAB | GCV | LAB | GCV | LAB |
| Elevation (m) | 397.5 | 1758.9 | 380.5 | 195.0 | 5.4–1650.0 | 1493.0–2327.0 |
| Percent hardwood BA | 0.8 | 0.5 | 0.3 | 0.3 | 0.0–1.0 | 0.1–1.0 |
| Dry $NH_x$ (kg N $ha^{-1}$ $yr^{-1}$ ) | 0.2 | 1.4 | 0.2 | 0.9 | 0.1–1.1 | 0.3–3.5 |
| Dry $NO_x$ (kg N $ha^{-1}$ $yr^{-1}$ ) | 2.6 | 5.7 | 0.8 | 1.8 | 1.1–4.5 | 2.2–9.2 |
| Total N (kg N $ha^{-1}$ $yr^{-1}$ ) | 4.4 | 8.2 | 1.4 | 3.1 | 2.1–8.4 | 3.3–15.6 |
| Max temp. (°C) | 22.5 | 17.9 | 1.8 | 1.2 | 15.7–25.3 | 16.1–19.7 |
| Average temp. (°C) | 15.0 | 11.8 | 1.3 | 1.7 | 10.8–18.1 | 7.8–13.8 |
| Precipitation (mm) | 580.2 | 825.3 | 239.8 | 210.2 | 224.0–1327.0 | 549.3–1150.7 |
| Dew point (°C) | 5.5 | - 0.8 | 2.5 | 2.8 | - 2.9–9.2 | - 6.6–2.2 |

BA = basal area; GCV = Greater Central Valley; LAB = Los Angeles Basin; $NH_x$ = reduced nitrogen; $NO_x$ = oxidized nitrogen.
Note: Hardwood BA was measured in the field. Climate and nitrogen variables ($NH_x$ and $NO_x$) are modeled estimates.

species present), and 4 = Abundant (more than half of boles and branches have the subject species present). Vouchers were collected for each unique species and sent to experts for identification and archiving.

## Analysis

Lichen response indices for oligotrophs, mesotrophs, and eutrophs are based on Jovan (2008), who adapted van Herk's (1999) ammonia ($NH_3$) bioindication indices to fit FIA-style data and West Coast lichen species (table 7.2). An index value for a site is calculated by summing abundance codes for the N indicator group in consideration and relativizing by the summed abundance codes of all lichens found at that site.

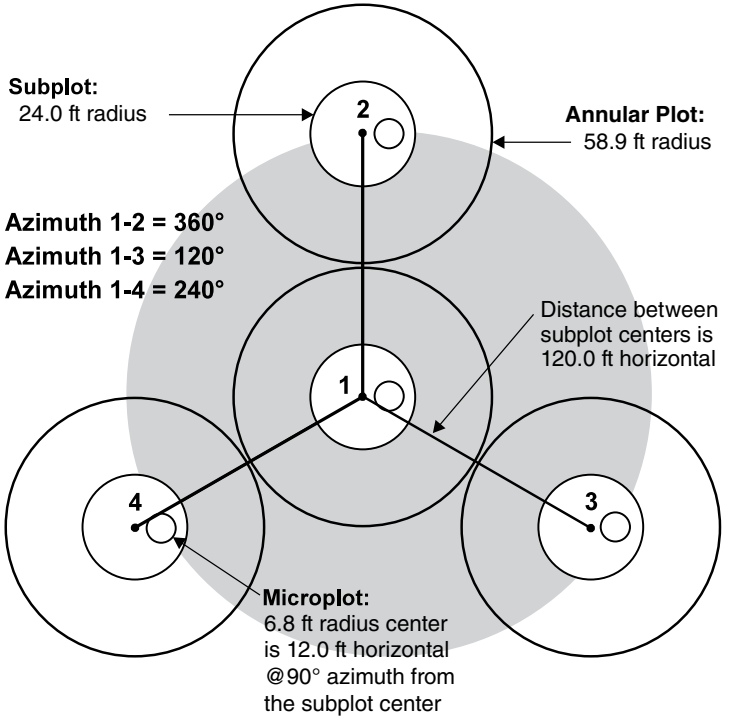


Reprinted from USDA Forest Service. 2011. Forest inventory and analysis national core field guide, volume 1: field data collection procedures for phase 2 plots, version 5.1. USDA Forest Service, Washington Office. Internal report. On file with: USDA Forest Service, Forest Inventory and Analysis, Rosslyn Plaza, 1620 North Kent Street, Arlington, VA 22209.

*Figure 7.2—Diagram of the Forest Inventory and Analysis plot with the 0.4-ha area searched for epiphytic macrolichens overlaid in gray.*

I used HyperNiche 2.2 (McCune and Mefford 2009) to build nonparametric multiplicative regression (NPMR) models for the three lichen response indices. NPMR can resolve complex response surfaces. The model-building process automatically considers possible interactions among all predictors (Lintz and others 2011, McCune 2006). Model building is an iterative search for the best possible combination of predictors given user-defined rules to prevent overfitting. I chose strict settings, requiring a

minimum data-to-predictor ratio of 10 to 1 and a minimum average neighborhood size of 25 plots. I used the local linear estimator to assign weights to observations. This estimator resolved similar but stronger and more parsimonious models than the Gaussian kernel estimator, which is typically favored for modeling species' responses to environmental gradients. Model strength is evaluated using leave-one-out cross validation, yielding an $xR^2$ value that estimates percent variance explained just like a coefficient of determination, but penalized by cross validation. In order to be included in the model, additional predictors were required to improve the variance explained by at least 5 percent. Model significance is evaluated using randomization tests. Confidence bands are determined by bootstrap resampling.

Predictor variables included long-term estimates (1971–2000; 800-m resolution) of average temperature, maximum temperature, dew point temperature, and precipitation extracted from the PRISM model (PRISM Group 2004; table 7.3). Percent basal area of hardwoods was calculated using the variable radius method. Estimates of total N deposition, dry deposition of reduced N ($NH_x$) and dry deposition of oxidized N ($NO_x$) were obtained from version 4.4 of the Community Multiscale Air Quality model (4-$km^2$ resolution). These estimates are based on N emissions inventories and meteorological conditions from 2002. See Tonnesen and others (2007) for more information on model construction and validation.

## RESULTS AND DISCUSSION

The best NPMR models for all three indices included two predictors: precipitation plus one of the N deposition variables (table 7.4; $xR^2$ = 0.48–0.63). Total N deposition was a strong predictor of mesotroph abundance, while oligotrophs and eutrophs appeared more closely correlated with $NO_x$ deposition. Response surfaces show how the proportion of lichens in each of the three indicator groups varies across the full range of precipitation and N values across the study area (fig. 7.3).

There was not a strong direct relationship between precipitation and the N deposition estimates (fig. 7.4). Data points were well spread along the precipitation and N axes, except for a few outliers representing high N and moderately wet plots. A dataset that is well distributed with respect to the important NPMR predictors gives confidence that the model describes real patterns and not just artifacts of the predictors' sampling distributions.

**Table 7.4—Parameters of the best nonparametric multiplicative regression models for each lichen response index**

| Response index | $xR^2$ | Avg. neigh. | Predictor 1 | Tolerance | Predictor 2 | Tolerance |
|---|---|---|---|---|---|---|
| Percent oligotrophs | 0.48 | 26.4 | Dry $NO_x$ | 0.81 | Precipitation | 275.75 |
| Percent mesotrophs | 0.53 | 26 | Total N | 2.67 | Precipitation | 165.45 |
| Percent eutrophs | 0.63 | 26.1 | Dry $NO_x$ | 1.22 | Precipitation | 220.6 |

Avg. neigh. = average neighborhood size; $NO_x$ = oxidized nitrogen.

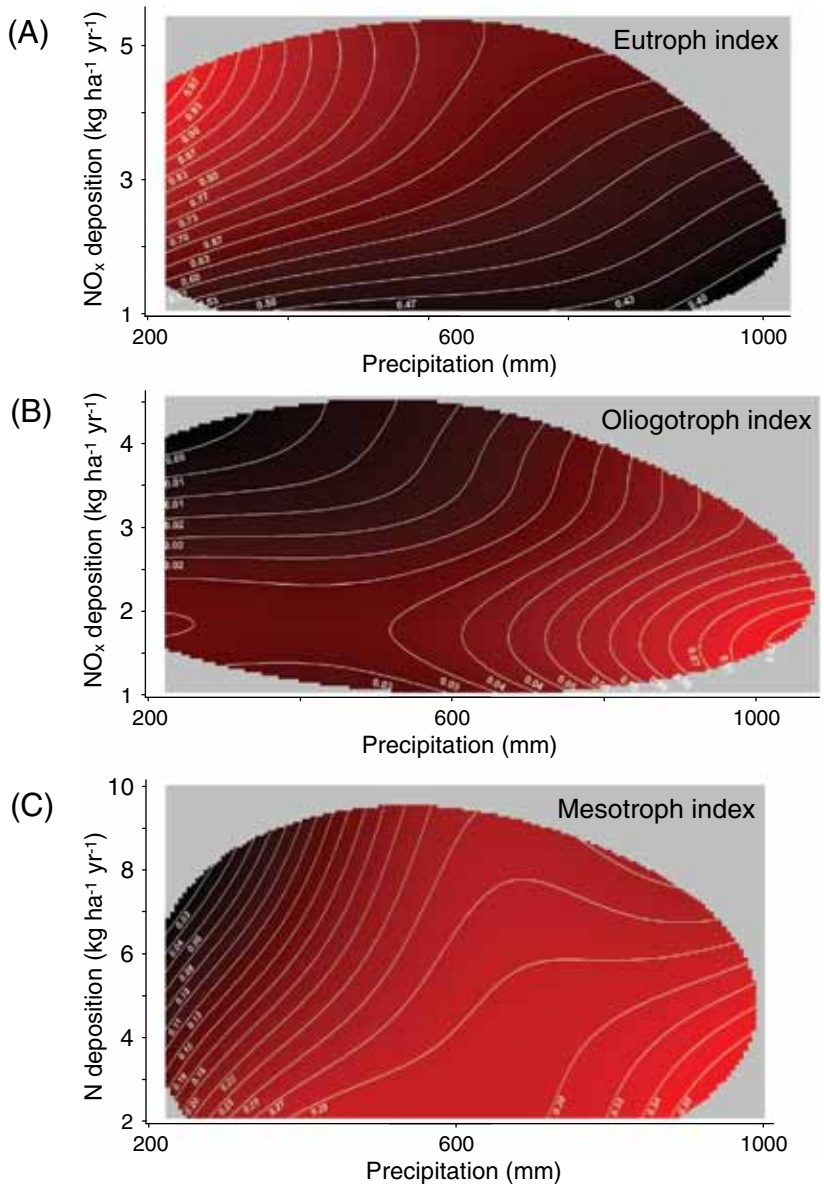


*Figure 7.3—Response surfaces for the three nonparametric multiplicative regression models. White contour lines provide estimates of what proportion of lichen abundance is in eutrophs (A), oligotrophs (B), or mesotrophs (C) at different combinations of precipitation and N deposition.*

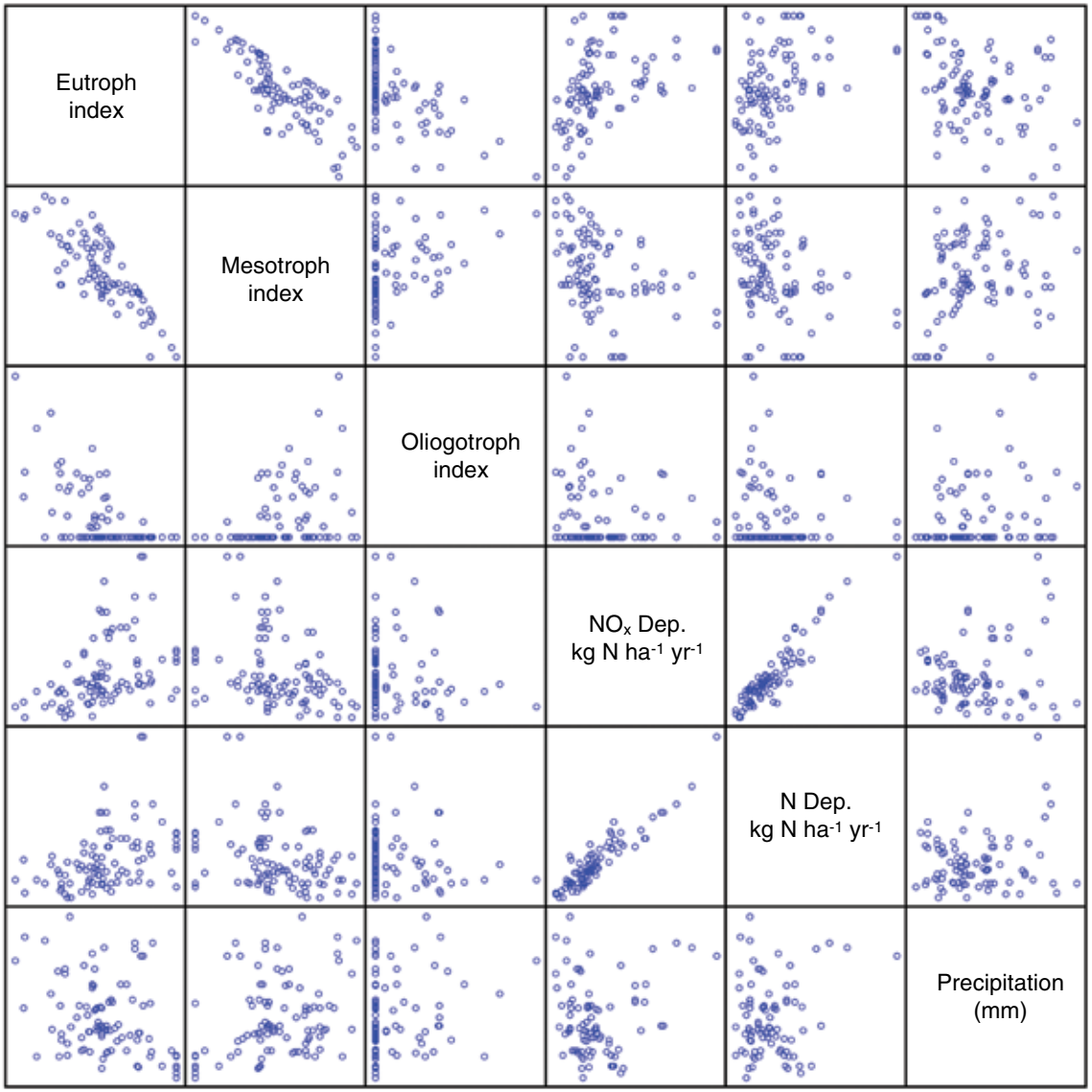


*Figure 7.4—Scatterplot matrix showing 1:1 relationships between response indices and the environmental predictors identified by nonparametric multiplicative regression.*

Precipitation clearly explains different variability in the lichen response indices than do the N deposition variables (fig. 7.4). The $NO_x$ and total N deposition variables, however, were highly correlated with each other. Jovan and others (2012) found that eutrophs in the LAB do not discriminate among N forms, meaning that eutroph abundance links more closely to total N deposition. The results of this study do not necessarily conflict, because the $NO_x$ and total N variables are almost interchangeable (fig. 7.4). Oxidized N is the dominant component of N deposition in both the LAB and the GCV (table 7.3).

The eutroph and oligotroph indices responded oppositely with respect to N and also precipitation (fig. 7.3A and B). Overall lichen communities across the study area were highly eutrophic; under the least favorable conditions for eutrophs in the study area (the wettest and lowest N sites), eutrophs still contributed ≥ 40 percent of lichen abundance. Eutrophic species comprised ≥ 97 percent of lichen abundance at plots that were dry and high in N. By contrast, oligotrophs were sparse in the study region, providing 0 percent to only about 8 percent of lichen abundance under the most favorable conditions for this group (wettest and lowest N sites; fig. 7.3B).

The mesotroph response to N and precipitation was directionally similar to the oligotroph response, suggesting the same preference for wet conditions and low N levels. Mesotrophs made a more substantial contribution to lichen communities, however, ranging from 2 to 36 percent at optimal conditions (fig. 7.3C). The model suggests precipitation has a moderating effect on how the mesotroph index responds to N except, curiously, at sites receiving 400–700 mm. The broadening contour lines in figure 7.3C indicate that mesotroph decline is less severe under these conditions even at the highest deposition levels (~10 kg N/ha/year).

Precipitation also appeared to moderate the oligotroph-N response at all but the lowest levels of precipitation and N deposition (fig. 7.3B). The NPMR model suggested an initial, slight positive effect of N (an increase in oligotroph abundance of < 0.5 percent) with a decline beginning between 1.5 and 2.0 kg N/ha/year. In contrast, more eutrophs tended to accumulate at drier sites than wetter sites for a given level of N.

Nearly all FIA-style lichen studies in the Western United States show some evidence that dry climate and N deposition have similar effects on lichen community composition (Geiser and Neitlich 2007, Geiser and others 2010, Grenon 2012, Jovan 2008, Jovan and McCune 2004, Jovan and McCune 2005, Jovan and McCune 2006), although the consistency of this phenomenon has not been explicitly recognized before now. Can it be concluded, then, that moisture levels affect lichen susceptibility to N level? This is likely because N is a mobile nutrient in the lichen thallus; water delivers

dissolved N pollutants, but a high volume of water also leaches mobile pollutants out of the thallus. Thus, precipitation exerts major control over the concentration of pollution "pulses" received by the lichen.

On the other hand, lichenologists working in Mediterranean and other dry forest types long ago recognized that many of the eutrophs included in this study behave as "xerophytes" (e.g., Barkman 1958, Frati and others 2008) even in the absence of obvious N inputs. Likewise, evidence of the high moisture requirements of oligotrophs is found in several studies (e.g., Geiser and Neitlich 2007, Jovan 2008, Rambo 2010). Thus it is unclear to what degree moisture levels actually modify lichen responses to N as opposed to what degree moisture affects lichen communities in independent but similar ways as N.

The nature of this interaction has important implications for critical loads research and conservation practitioners. It may well be that N-sensitive oligotroph and mesotroph species living in dry habitats are more easily extirpated by N deposition. The vulnerability of these species to extirpation in currently habitable areas may also increase if climate shifts towards drier or hotter conditions.

From an operational standpoint, the importance of precipitation means that moisture differences across monitoring sites can skew N biomonitoring results, making drier habitats appear more polluted than they actually are. Recent research in the LAB shows it is possible to accurately predict annual N deposition levels using only a simple response index, eutroph percent cover (Jovan and others 2012), although sites in that study share a similar moisture regime. The NPMR models developed here suggest that indices designed for larger, more heterogeneous landscapes must explore possible precipitation effects. An index that is both simple and accurate can save forest managers and air quality regulators from costly investments in monitoring instrumentation.

## CONCLUSIONS

Each NPMR response surface revealed interesting nonlinearities (fig. 7.3). Three features of particular note include (1) low $NO_x$ levels seem to have a weak positive effect on oligotroph abundance, (2) mesotrophs appear relatively insensitive to N at midrange precipitation levels, and (3) eutroph abundance appears to accumulate more quickly at dry sites for a given level of N deposition. The first two findings are especially surprising, and supporting observations have not been reported in other lichen-N studies. Further study may reveal that these response features are simply artifacts of model overfitting. It is clear, however, that all three response indices showed some level of sensitivity to precipitation and that the interaction between precipitation and N response is nonlinear. Modeling techniques applied in large-scale lichen bioindication studies for N must be able to accommodate this complexity.

## LITERATURE CITED


Barkman, J.J. 1958. Phytosociology and ecology of cryptogamic epiphytes. Assen, The Netherlands: Koninlijke van Gorcum. 628 p.

Environmental Protection Agency (EPA). 2008. Integrated science assessment for oxides of nitrogen and sulfur—ecological criteria. Tech. Rep. EPA/600/R-08/082F. Research Triangle Park, NC: U.S. Environmental Protection Agency. 898 p.

Fenn, M. E.; Jovan, S.; Yuan,F. [and others]. 2008. Empirical and simulated critical loads for nitrogen deposition in California mixed conifer forests. Environmental Pollution. 155: 492-511.

Frati, L.; Brunialti, G.; Loppi, S. 2008. Effects of reduced nitrogen compounds on epiphytic lichen communities in Mediterranean Italy. Science of the Total Environment. 407: 630-637.

Geiser, L.; Neitlich, P.N. 2007. Air pollution and climate gradients in western Oregon and Washington indicated by epiphytic macrolichens. Environmental Pollution. 145: 203-218.

Geiser, L.H.; Jovan, S.; Glavich, D.A. [and others]. 2010. Lichen-based critical loads for atmospheric nitrogen deposition in western Oregon and Washington forests. Environmental Pollution. 158: 2412-2421.

Grenon, J. 2012. Epiphytic lichens, nitrogen deposition, and climate in the U.S. northern Rocky Mountain States. Bozeman, MT: Montana State University. 166 p. M.S. thesis.

Jovan, S. 2008. Lichen bioindication of biodiversity, air quality, and climate: baseline results from monitoring in Washington, Oregon, and California. Gen. Tech. Rep. PNW-GTR-737. Portland, OR: U.S. Department of Agriculture Forest Service, Pacific Northwest Research Station. 115 p.

Jovan, S.; McCune, B. 2004. Regional variation in epiphytic macrolichen communities in northern and central California forests. The Bryologist. 107: 328-339.

Jovan, S.; McCune, B. 2005. Air-quality bioindication in the greater central valley of California, with epiphytic macrolichen communities. Ecological Applications. 15: 1712-1726.

Jovan, S.; McCune, B. 2006. Using epiphytic macrolichen communities for biomonitoring ammonia in forests of the greater Sierra Nevada. Water, Air, and Soil Pollution. 170: 69-93.

Jovan, S.; Riddell, J.; Padgett, P.; Nash, T. 2012. Eutrophic lichens respond to multiple forms of N: implications for critical levels and critical loads research. Ecological Applications. 22:1910-1922.

Lintz, H.E.; McCune, B.; Gray, A.N.; McCulloh, K.A. 2011. Quantifying ecological thresholds from response surfaces. Ecological Modelling. 222: 427-436.

McCune, B. 2006. Nonparametric habitat models with automatic interactions. Journal of Vegetation Science. 17: 819-830.

McCune, B.; Mefford, M.J. 2009. HyperNiche. Nonparametric multiplicative habitat modeling version 2.20. Gleneden Beach, OR: MjM Software.

Pardo, L.H; Robin-Abbott, M.J.; Driscoll, C.T., eds. 2011a. Assessment of nitrogen deposition effects and empirical critical loads of nitrogen for ecoregions of the United States. Gen. Tech. Rep. NRS-80. Newtown Square, PA: U.S. Department of Agriculture Forest Service, Northern Research Station. 291 p.

Pardo, L.H.; Fenn, M.E.; Goodale, C.L. [and others]. 2011b. Effects of nitrogen deposition and empirical nitrogen critical loads for ecoregions of the United States. Ecological Applications. 21: 3049-3082.

Phelan, J.; Jovan, S.; Schulz, B. [and others]. 2012. Linking biological response to atmospheric nitrogen and sulfur deposition—the potential role of the U.S. Forest Service Forest and Inventory Analysis (FIA) database. Final Report to the Environmental Protection Agency. EP-W-011-029 WA-012. Research Triangle Park, NC: RTI International. [Pages unknown].

PRISM Group. 2004. 2.5-arcmin (4 km) gridded monthly climate data. http://www.prismclimate.org. [Date accessed: June 20, 2012].

Rambo, T.R. 2010. Habitat preferences of an arboreal forage lichen in a Sierra Nevada old-growth mixed-conifer forest. Canadian Journal of Forest Research. 40: 1034-1041.

Riddell, J.; Jovan, S.; Padgett, P.E. [and others]. 2011. Tracking lichen community composition changes due to declining air quality over the last century: the Nash legacy in Southern California. In: Bates, S.T.; Bungartz, F.; Luecking, F. [and others], eds. Biomonitoring, ecology, and systematics of lichens: recognizing the lichenological legacy of Thomas H. Nash III on his 65th birthday. Bibliotheca Lichenologica. 106: 263-267.

Tonnesen, G.; Wang, Z.; Omary, M.; Chien, C.J. 2007. Assessment of nitrogen deposition: modeling and habitat assessment. Sacramento, CA: California Energy Commission, PIER Energy-Related Environmental Research. www.energy.ca.gov/2006publications/CEC-500-2006-032/CEC-500-2006-032.PDF. [Date accessed: June 20, 2012].

van Herk, C.M. 1999. Mapping of ammonia pollution with epiphytic lichens in the Netherlands. Lichenologist. 31: 9-20.

Will-Wolf, S.; Geiser, L.H.; Neitlich, P; Reis, A.H. 2006. Forest lichen communities and environment—how consistent are relationships across scales? Journal of Vegetation Science. 17: 171-184.

Woodall, C.W.; Conkling, B.L.; Amacher, M.C. [and others]. 2010. The Forest Inventory and Analysis database version 4.0: database description and users manual for phase 3. Gen. Tech. Rep. NRS-61. Newtown Square, Pennsylvania: U.S. Department of Agriculture Forest Service, Northern Research Station. 180 p.

Each year, the Forest Health Monitoring (FHM) Program funds a variety of Evaluation Monitoring (EM) projects, which are "designed to determine the extent, severity, and causes of undesirable changes in forest health identified through Detection Monitoring (DM) and other means" (Forest Health Monitoring 2009). In addition, EM projects can produce information about forest health improvements. EM projects are submitted, reviewed, and selected in two main divisions, base EM projects and fire EM projects. More detailed information about how EM projects are selected, the most recent call letter, lists of EM projects awarded by year, and EM project poster presentations can all be found on the FHM Web site: www.fs.fed.us/foresthealth/fhm.

Beginning in 2008, each FHM national report contains summaries of recently completed EM projects. Each summary provides an overview of the project and results and citations for products and other relevant information. The summaries provide an introduction to the kinds of monitoring projects supported by FHM and include enough information for readers to pursue specific interests. Nine project summaries are included in this report.

## LITERATURE CITED

Forest Health Monitoring (FHM). 2009. Evaluation Monitoring. Forest Health Monitoring Fact Sheets Series. http://www.fhm.fs.fed.us/. [Date accessed: June 14, 2012].

# SECTION 3.
# Evaluation Monitoring Project Summaries

# CHAPTER 8.

# Effects of Prescribed Fire on Upland Oak Forest Ecosystems in Missouri Ozarks

## (Project NC-F-06-02)

Zhaofei Fan
Daniel C. Dey

## INTRODUCTION

Fire in the Ozark Highlands was historically used by Native Americans (Guyette and others 2002). Early European settlers continued to burn the landscape to manage livestock forage. In the late 1800s, people began to harvest timber, cutting first pine trees and later oak (Flader 2008). Woodlands eventually succeeded to forests and pine-oak compositions gave way to hardwood-dominated forests as frequent fires and pine logging promoted hardwood regeneration (Record 1910, Sasseen 2003). In the 1930s, fires began being suppressed throughout this area. In the absence of fire, woodlands became forests in structure with the increase in tree density and development of subcanopies. The current oak forest health problems occurring in the Missouri Ozark Highlands are also believed to be related to this long-term fire suppression, shift in species composition, and increased tree density (Hartman and Heumann 2003, Kabrick and others 2008, Shifley and others 2006). Therefore, prescribed fires were reintroduced to restore the oak woodland ecosystem where it occurred historically and to mitigate current health problems that are plaguing oak forests, such as widespread outbreaks of oak decline (Fan and others 2008, Kabrick and others 2008, Spetich and He 2008).

The Chilton Creek Prescribed Burning Project (CCPBP) was initiated by The Nature Conservancy (TNC) in 1996 to study the effects of different fire regimes on promoting the diversity of native species and ecosystem restoration in the Ozark Highlands (Hartman and Heumann 2003). The CCPBP study site is a 1000-ha forest tract that includes one annual burning unit and four random burning units with about a 4-year fire return interval. The primary objectives of the research project were to (1) compare the structural and compositional characteristics of unburned and burned upland oak forests using repeated measures data with treatments ranging from no fire to 8 years of annual burning, and (2) develop indicators, indices, or both that predict the impact of fire treatments on forest size structure and species composition and evaluate the influence of ecological land type (ELT) on forest response.

## METHODS

### Structural and compositional data

In total, 250 0.2-ha permanent plots were installed over the five burning units to monitor the change in forest vegetation. In each plot, overstory trees ≥ 11.5 cm diameter at breast height (d.b.h.) were measured. Midstory trees with d.b.h. less than 11 cm and more than 3.8 cm were measured in four 0.02-ha subplots that were nested within each 0.2-ha plot. Understory trees with d.b.h. less than 3.8 cm were measured in a 0.004-ha subplot that was located in the center of each 0.02-ha subplot. Coverage of herbaceous vegetation and tree seedlings were estimated in four 1-$m^2$ quadrants that were located 6.7 m from the subplot centers at 45°, 135°, 225°, and 315° azimuths. Tree species, d.b.h., crown class, status (dead or live), and d.b.h. per height class (for seedlings and saplings) were recorded or measured.

Data inventory was performed in 1997 (before treatments), and in 2001 and 2007. In addition, corresponding data from 70 0.2-ha plots on the adjacent Missouri Ozark Forest Ecosystem Project (MOFEP) site 9 (measured in 1998, 2002, and 2006) (Shifley and Brookshire 2000) were included to evaluate changes in vegetation where no burning or timber harvesting occurred.

### Prescribed burning

All units were burned in the spring of 1998 to initiate the process of restoring fire. Thereafter, units were burned during the dormant season (usually in March and April) on a randomly selected 1- to 4-year return interval basis, with the exception of Kelly North management unit, which was burned annually. Average total fuel loads ranged from 9.6 to 13.2 mt/ha for any given burn year, and herbaceous and litter fuels accounted for much (40 to 60 percent) of the total tonnage. Air temperatures during most burns were between 16 and 24 °C; winds, in general, were less than 7 km/hour; and relative humidity ranged from 33 to 44 percent. Flame lengths were highly variable but often were in the range of 0.3 to 0.9 m. Rates of spread were also variable, but the fire front usually moved at a rate of 59 to 317 m/hour. Fire temperatures were highest at the fuel surface (ground level), reaching 121 to 316 °C.

### Advance reproduction data

To monitor the response of advance regeneration to the prescribed burning, 26 of the 250 permanent plots were randomly located throughout the five burn units. Individual stems of advance regeneration in a plot were sampled from within a 25.2-m radius of each sampling point. Each stem was permanently marked with a wire stake and metal numbered tag. More than 3,000 stems of various sizes were marked within the 26 plots. Information on species, stem basal diameter 2.5 cm above the ground, total height, d.b.h. (if existing), status (live or dead), and sprout condition (the number of sprouts and the height of the tallest sprout) were recorded. Initial stem measurements were conducted in the fall of 1997, before the first burn. Stems were measured again in 1998, 1999, 2001, and 2007 as the prescribed burn treatments were implemented.

### Forest structural and compositional changes under different fire treatments

Forest composition on the MOFEP and CCPBP sites is a mixture of 50 tree species; however, only a relatively few species are dominant. Eight major tree species (based on importance values [IV])—black oak (23.6 percent), scarlet oak (21.3 percent), white oak (21.2 percent), shortleaf pine (9.0 percent), post oak (6.3 percent), black hickory (4.3 percent), pignut hickory (4.0 percent), and mockernut hickory (4.0 percent)—account for nearly 94 percent of the overstory species. The rest (more than 40 species) are minor species that are sporadically distributed in the forests with an IV of mostly less than 0.2 percent (Shifley and others 2006). Potential forest structural and compositional changes following the fire treatment were evaluated using these major species. Furthermore, it was statistically difficult

to analyze the fire effects at the species level due to the extreme unbalance in sample size (e.g., too small or large sample sizes, missing values). For this reason, the eight major species were further grouped into four functional species groups based on their dominance and bioecological characteristics: white oak group (white oak, post oak), red oak group (black oak, scarlet oak), hickory group (black, pignut, and mockernut hickory), and shortleaf pine. All minor species were grouped into a single group (i.e., the fifth group labeled as other species). This grouping scheme improved the power of statistical analyses and facilitated the explanation of results in analyzing forest- and stand-level compositional changes. All trees were classified into three categories based on the d.b.h. to evaluate forest structural change under different fire treatments: overstory (d.b.h. > 11.5 cm), midstory (3.8 cm < d.b.h. ≤ 11.5 cm), and understory (d.b.h. ≤ 3.8 cm, but height > 1 m). Relative changes in basal area or stem density (for understory) were used in multivariate analysis of variance (MANOVA). The plots under the annual fire, random fire, and no fire regimes were randomly classified into three groups (replicates). Relative changes in basal area or stem density after the fire treatments (i.e., after 4 and 10 years) were calculated as the difference in basal area or stem density between pretreatment and the reinventory years divided by the basal area or stem density of the pretreatment inventory, which ranged from -2.0 to 4.0 for the CCPBP experiment.

## Responses of advance reproduction to fire

To better understand the effects of external factors on advance regeneration after 10 years of burn treatments, the relationship between mortality of advance regeneration and a suite of potential contributing factors was examined. These factors, including fire regimes (treatments), slope, aspect, ELT, stem basal diameter, total height, and species, were analyzed using a nonparametric classification and regression tree (CART) approach (Fan and others 2006). The CART model results indicated that total height and basal diameter are the key factors affecting the mortality rate of the species groups after a long (10-year in this study) period of repeated burns. The logistic regression was then employed to develop the species-specific mortality model for those species with a large sample of advance reproduction stems (> 100). After testing the different combinations of total height and basal diameter, it was finally found that a morphological variable, the ratio of total height to the square of the basal diameter, best predicted the stem mortality probability across most species selected. The Hosmer-Lemeshow test was used to evaluate the performance of the logistic regression model. The logistic regression model was:

$$p = \frac{1}{1 + e^{-(\beta_0 + \beta_1 * HBR)}} \qquad (1)$$

where

$HBR$ = total height/(basal diameter).

## RESULTS AND DISCUSSION

### Structural and compositional change

Total overstory basal areas increased rapidly in both burning units but remained relatively stable in the no-burn unit (MOFEP site 9) from 1997 to 2007 (fig. 8.1). White oak basal areas increased under all treatments, indicating that fire did not change the overstory white oak growth pattern during the 10-year treatment interval. Red oak basal areas increased in both burning units, but decreased in the no-burn unit, suggesting that fire may have a positive influence on the survival or growth of overstory red oak trees in this area, or it is possible that the sites on the CCPBP property were either slightly younger in age than the MOFEP forests or that they had a different management history that left them with lower stocking (fig. 8.1) at the beginning of this study. Under lower stocking, there would be resources to support increases in stand basal area and density in the CCPBP forests compared with the MOFEP stands that were more fully stocked to begin with. Red oaks in the overstory on the CCPBP site had more opportunity to grow in diameter and increase in basal area than at the MOFEP sites. No management disturbances had occurred within 40 years of the initiation of the MOFEP study (Shifley and Brookshire 2000). In contrast, the CCPBP property had been owned by private timber companies until 1991, when it was acquired by TNC. The date of the last timber harvest on the property is unknown, but it is quite possible that it occurred closer to the initiation of this study than was the case on the MOFEP study site, thus explaining the lower initial stand basal area on the CCPBP site.

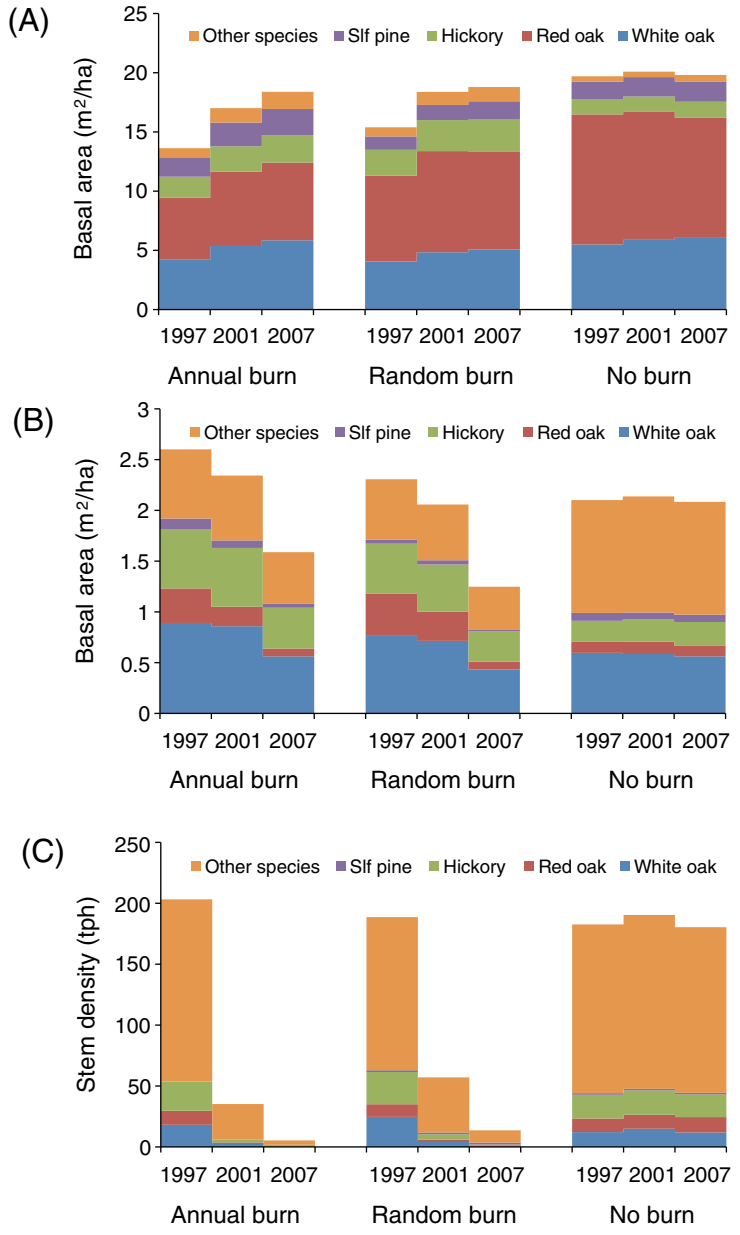


*Figure 8.1—Structural and compositional change of oak forests under different fire treatments: (A) overstory, (B) midstory, and (C) understory.*

Declines in red oak basal area on the no-burn sites may be related to oak decline, which has been occurring throughout the Ozark Highlands (Fan and others 2008, Kabrick and others 2008, Shifley and others 2006, Spetich and He 2008). Red oaks with low annual diameter growth rates, intermediate and suppressed trees in high-density stands, medium-sized dominant trees in high-density stands, and large-diameter dominant red oak trees are at higher risk of dying from oak decline (Shifley and others 2006). Initial stand basal areas on the no-burn MOFEP sites averaged 20 $m^2$/ha, which was higher than that on the CCPBP burn treatments, where basal area ranged from 14 to 15 $m^2$/ha. Changes in density of other species were minor. Hickory basal areas did not change in the no-burn treatment but increased slightly in the two burning treatments. Shortleaf pine basal areas increased slightly in the annual burn treatment but did not change in the no-burn and random burning treatments. Other species basal areas increased slightly under all three treatments.

The MANOVA model indicated significant fire effects ($p < 0.05$) on the relative changes in overstory basal area for both overall and individual species groups in 2001 and 2007. The relative change of overall basal area in overstory by year 2001 was 2.3, 19.5, and 15.3 percent, respectively, and by year 2007 was -7.9, 12.6, and -5.5 percent, respectively, for the unburned control, annual fire, and random fire treatments. The relative increases in basal area for the annual fire and random fire treatments were significantly higher than for the unburned control treatment in both 2001 and 2007. The annual fire treatment caused a significantly higher relative change in basal area than the random fire treatment in both 2001 and 2007. The increase in relative change of basal area by species groups for the annual fire and random fire treatments was three to four times larger than and significantly different from that for the unburned control treatment ($p < 0.05$). In 2001, the relative changes in basal area for the individual species groups ranged from -0.7 to 10.2 percent under the unburned control treatment, 11.3 to 31.7 percent under the annual fire treatment, and 12.4 to 32.1 percent under the random fire treatment. In 2007, the relative changes in basal area for the individual species groups ranged from -8.6 to 19.6 percent under the unburned control treatment, 16.9 to 49.0 percent under the annual fire treatment, and 13.8 to 44.0 percent under the random fire treatment. These findings are confounded because the two fire treatments occurred on sites of initially lower stand basal area that affected the potential for increases in basal area during the course of this study.

Midstory basal areas showed a different trend from changes in the overstory (fig. 8.1). During the period 1997 to 2007, total midstory basal area continually decreased for the annual and random fire treatments but remained stable for the unburned control treatment. The decrease in midstory basal area occurred in all five species groups. The MANOVA model indicated significant fire effects ($p < 0.05$) on the relative change of total midstory basal area in both 2001 and 2007. The relative change of total midstory basal area by year 2001 was 2.4,

-12.9, and -15.5 percent, respectively, and by year 2007 was -0.2, -41.1, and -49.0 percent, respectively, for the unburned control, annual fire, and random fire treatments. The decreases in total midstory basal area for the annual fire and random fire treatments were significantly higher than for the unburned control treatment in both 2001 and 2007, but no significant differences were observed between the two fire treatments. For the individual species groups, the MANOVA model indicated that fire treatments had a significant effect on the relative change in midstory basal areas of all species groups, except for shortleaf pine and white oak in 2001, and of all species groups, except for shortleaf pine, in 2007 compared with the control. Much variability was apparent in the relative changes in the basal area among the fire treatments by species. The red oak group (79 and 82 percent for annual and random burn treatments, respectively) and shortleaf pine (58 and 65 percent for annual and random burn treatments, respectively) experienced the largest reductions.

The patterns of stem density change in the understory were similar to the midstory, except that the reduction was much greater for the annual and random fire treatments (fig. 8.1). The stem density on the burned sites was extremely low after 10 years; following the fire treatments, stem density dropped to less than 20 trees/ha for the annual and random fire treatments. The MANOVA model indicated significant fire effects ($p < 0.05$) on the relative (percent) change in stem density in the understory for all species combined and by individual species and groups in 2001 and 2007. By year 2001, the relative change of stem density in the understory for the unburned control, annual fire, and random fire treatments was 2.8, -83.5, and -74.3 percent, respectively, and was -3.2, -97.0, and -94.1 percent, respectively, by year 2007. Both fire treatments significantly decreased the relative change in stem density in the understory, but no differences in the fire effects were observed between these two fire treatments. In 2007, the MANOVA model indicated no fire effects on the relative change in understory stem density of shortleaf pine. With the exception of shortleaf pine in 2007, both fire treatments significantly decreased the relative change in understory stem density, but no differences in the fire effects were observed between these two fire treatments.

## Responses of advance reproduction to fire

Exploratory analyses indicated that, as the number of prescribed fires increased, species, initial total stem height, and stem basal diameter became increasingly important determinants of mortality and height growth, whereas burning treatment (annual vs. random burn), slope, aspect, ELT, and overstory stocking were not statistically significant by 2007. The simple logistic regression models depicted the impact of initial stem size on mortality of advance reproduction. Interestingly, for several of the major associated species such as hickories (pignut, black, mockernut), blackgum, sassafras, and winged elm, the estimated coefficients for *HBR* were not statistically significant, indicating mortality was less affected by the ratio. For

the oaks, shortleaf pine, flowering dogwood, and the minor species as a whole, however, the *HBR* ratio was a significant determinant of mortality. For these species, *HBR* consistently performed better than initial basal diameter, total height, or a combination of both variables included in the model. In the logistic regression models, oaks, hickories, sassafras, and winged elm had relatively low intercepts compared with shortleaf pine, flowering dogwood, blackgum, and other minor species, suggesting relatively lower mortality in these species as the ratio of stem height to the square of stem basal diameter decreases. The slope of the logistic curves for oaks was steeper than for other associate species, except for shortleaf pine, suggesting that oak mortality was more strongly affected by the *HBR* ratio.

*HBR* is a synthetic parameter derived from the relationship between total height and basal diameter. Basal diameter has been shown to be highly correlated with the size of root systems, especially in oak species (Canadell and Roda 1991, Dey and Parker 1997), and thus *HBR* essentially represents the allocation of biomass and carbohydrate between aboveground and belowground tree components (high *HBR* indicating lower relative belowground allocation, or vice versa). The resultant logistic regression models could be used to predict the mortality of existing advance reproduction prior to the application of multiple fires. After examining the models, we tentatively classified the species into four groups based on their relative slopes and intercepts in the logistic models. These groupings were: (1) species with low intercepts and low slopes representative of black and pignut hickories, sassafras, and winged elm; (2) species with low intercepts and high slopes typical of various oaks and mockernut hickory; (3) species with high intercepts and slopes such as shortleaf pine and flowering dogwood; and (4) species with high intercepts but low slopes such as blackgum and other minor species as a whole. These groupings may represent different functional strategies for tolerating (e.g., vegetative sprouting in species such as oaks, hickories, sassafras, and winged elm) or avoiding (e.g., thick bark in species such as shortleaf pine) fire mortality, or they may indicate a lack of ability to persist in environments of multiple and frequent fires, i.e., the most fire-sensitive and inherently vulnerable species such as flowering dogwood (Dey and Hartman 2005). Species with low slopes and low intercepts, such as hickories, are more resistant to fire-induced mortality, whereas species with high slopes and high intercepts, such as shortleaf pine, are vulnerable to fire. Most oak species have low intercepts and relatively high slopes, indicating that oaks with larger basal diameter will have lower mortality rates but advance reproduction in the smaller size classes is moderately sensitive to fire-induced mortality. This is because oaks have a conservative and effective strategy for persisting in a frequent fire environment. They preferentially allocate biomass to their root system (Dey and Hartman 2005, Dey and Jensen 2002, Johnson and others 2009), which does two things: (1) the belowground plant tissues are insulated from the fire's heat and thus more likely to survive the fire, and (2) the

belowground carbohydrate stores provide energy to fuel rapid growth of new vegetative shoots following topkill.

## CONCLUSIONS

Ten years after initiating burning, fire had little impact on the overstory, but it was effective in reducing the midstory basal area by > 40 percent and the understory basal area by > 90 percent. No significant differences in the understory and midstory basal area were observed between annual and random fire treatments. The net effect on stand structure was similar under either annual or random fire treatments. Thus, the restoration of closed woodland structure does not require annual burning when more than 14 $m^2$/ha of overstory basal area exists. Overstory basal area was able to increase under a frequent-to-annual fire regime to levels approaching that observed in unburned mature forests. Frequent fire does not add to overstory mortality above what was observed in the control forests, and it may even provide a benefit to the growth and survival of maturing red oak species. There was a subtle but ecologically significant increase in white oak in the overstory of burned and unburned forests. White oaks are more shade tolerant than any of the red oak species, and they dominate in the midstory size class, which supplies recruitment into the overstory when canopy gaps form stochastically in the overstory. Increased dominance of oaks in the fire treatments were associated with increased diameter growth rates in the white oak group tree growth and reduced mortality in red oak group. The increase in overstory basal area following the fire treatments was attributed to (1) ingrowth of midstory stems, (2) reduction of overstory mortality, and (3) growth of overstory trees. The difference in relative change of overstory basal area between the annual and random fire treatments was statistically significant for all species combined in 2001 and 2007, with the annual fire treatment having larger increases, but the significance varied for different species groups and inventory years.

The effect of fire treatments on the advance regeneration has become less and less significant over time based on CART analysis. After 10 years of fire treatments, basal diameter and total height were identified as the two most important contributing factors related to species-specific stem mortality. A new morphological variable, *HBR*—the ratio of the total height to the square of basal diameter—was found to be statistically significantly related to the tree mortality rate for most of the species. The logistic regression models for selected species using the morphological variable did a good job of predicting mortality based on the initial stem size of advance regeneration. These logistic regression models can be useful tools for comparing and quantifying species' responses to fires. The logistic regression analysis indicated that advance regeneration of oaks and hickories was favored more by frequent burning compared with other species, such as flowering dogwood and blackgum, as indicated by the higher intercept values in the logistic models. Fires historically occurred frequently in the Ozark forests. Use of low-intensity prescribed

fire to restore oak woodlands in the Ozarks is effective in managing ecosystem structure and composition. Prescribed burning can be used without aggravating forest health problems, or it may even reduce the risk of threats such as oak decline by favoring white oak growth and dominance and improving red oak vigor. Timber harvesting or thinning may be needed in combination with low-intensity, dormant-season burns to reduce overstory density if open woodland or savanna structures are desired.

## LITERATURE CITED


Canadell, J.; Roda, F. 1991. Root biomass of *Quercus ilex* in a montane Mediterranean forest. Canadian Journal of Forest Research. 21: 1771-1778.

Dey, D.C.; Hartman, G. 2005. Returning fire to Ozark Highland forest ecosystems: effects on advance regeneration. Forest Ecology and Management. 217: 37-53.

Dey, D.C.; Jensen, R.G. 2002. Stump sprouting potential of oaks in Missouri Ozark forests managed by even- and uneven-aged silviculture. In: Shifley, S.R.; Kabrick, J.M., eds. Proceedings of the second Missouri Ozark forest ecosystem project symposium: post-treatment results of the landscape experiment. Gen. Tech. Rep. NC-227. St. Paul, MN: U.S. Department of Agriculture Forest Service, North Central Forest Experiment Station. 102-113.

Dey, D.C.; Parker, W.C. 1997. Overstory density affects field performance of underplanted red oak (*Quercus rubra* L.) in Ontario. Northern Journal of Applied Forestry. 14: 120-125.

Fan, Z.; Kabrick J.M.; Spetich M.A. 2006. Classification and regression tree based survival analysis in oak-dominated forests of Missouri's Ozark highlands. Canadian Journal of Forest Research. 36: 1740-1748.

Fan, Z.; Kabrick J.M.; Spetich M.A. [and others]. 2008. Oak mortality associated with crown dieback and oak borer attack in the Ozark Highlands. Forest Ecology and Management. 255: 2297-2305.

Flader, S.L. 2008. History of Missouri forests and forest conservation. In: Guldin, J.M.; Iffrig, G.F.; Flader, S.L., eds. Pioneer forest—a half century of sustainable uneven-aged forest management in the Missouri Ozarks. Gen. Tech. Rep. SRS-108. Asheville, NC: U.S. Department of Agriculture Forest Service, Southern Research Station: 20-59.

Guyette, R.P.; Muzika, R.M.; Dey, D.C. 2002. Dynamics of an anthropogenic fire regime. Ecosystems 5(5): 472-486.

Hartman, G.W.; Heumann, B.H. 2003. Prescribed fire effects in the Ozarks of Missouri: the Chilton Creek project 1996–2001. In: Proceedings of the second international wildland fire ecology and fire management congress, November 16-22, 2003, Orlando FL. CD-ROM, American Meteorological Society, Boston MA.

Johnson, P.S.; Shifley, S.R.; Rogers, R. 2009. The ecology and silviculture of oaks. New York: CABI Publishing. 580 p.

Kabrick, J.M.; Dey, D.C.; Jensen, R.G.; Wallendorf, M. 2008. The role of environmental factors in oak decline and mortality in the Ozark Highlands. Forest Ecology and Management. 255: 1409-1417.

Record, S.J. 1910. Forest conditions of the Ozark region of Missouri. University of Missouri Agricultural Experiment Station Bulletin No. 89.

Sasseen, A.N. 2003. Using ecological land type phase (ELTp) to evaluate the effect of management on Missouri Ozark vegetation. Columbia, MO: University of Missouri. 185 p. M.S. thesis.

Shifley, S.R.; Brookshire, B.L. 2000. Missouri Ozark forest ecosystem project: site history, soils, landforms, woody and herbaceous vegetation, down wood, and inventory methods for the landscape experiment. Gen. Tech. Rep. NC-208. St. Paul, MN: U.S. Department of Agriculture Forest Service, North Central Forest Experiment Station. 314 p.

Shifley, S.R.; Fan, Z.; Kabrick, J.M.; Jensen, R.G. 2006. Oak mortality risk factors and mortality estimation. Forest Ecology and Management. 229: 16-26.

Spetich, M.A.; He, H.S. 2008. Oak decline in the Boston Mountains, Arkansas, USA: spatial and temporal patterns under two fire regimes. Forest Ecology and Management. 254: 454-462.

# CHAPTER 9.

# Assessment and Etiology of Hickory (*Carya* spp.) Decline in the Midwest and Northeastern Regions

## (Project NC-EM-07-01)

Jennifer Juzwik
Ji-Hyun Park
Linda Haugen

## INTRODUCTION

Hickory decline, particularly decline in bitternut hickory (*Carya cordiformis*) and to a lesser extent in shagbark hickory (*C. ovata*), has recently been noted in Iowa, Maryland, Missouri, New York, Pennsylvania, West Virginia, and Wisconsin (Steinman 2004). Periodic episodes of hickory mortality have been recorded from Wisconsin to Vermont and south-central Georgia since the early part of the 20th century (Hopkins 1912; St. George 1929; USDA Forest Service 1956, 1972). Within the first decade of that century, thousands of hickory trees died in central New York State (Hopkins 1912). Subsequent periodic episodes were reported through the rest of the century. For example, in Wisconsin, episodes of hickory decline or dieback were reported in the late 1960s, late 1980s, and early 2000s (Wisconsin Department of Natural Resources 2005).

Widespread mortality of hickory has historically been attributed to outbreaks of the hickory bark beetle (*Scolytus quadrispinosus*) during extended periods of drought. This insect is considered the most important pest of the species group. In 1994, a fungus species new to science was reported in discolored wood and sunken bark cankers associated with hickory bark beetle attacks. This fungus and a related species were recently described as *Ceratocystis smalleyi* and *C. caryae*, respectively (Johnson and others 2005). Both species were pathogenic on 2-year-old *Carya* spp. in greenhouse studies.

This project was conducted between 2007 and 2011. The planned objectives of the overall project were to (1) conduct field evaluations to (a) determine frequencies of decline and mortality of bitternut, shagbark, and other hickory species in appropriate forest cover types where deviations from expected levels of mortality have been observed; (b) quantify relationships between decline incidence and pathogen, insect pest presence, or both; and (c) quantify relationships between decline incidence and prior land use, fire history, soil fertility, drought, or some combination of the four; and (2) determine the role of two newly described *Ceratocystis* spp. in decline and mortality of hickory.

In this summary, we will briefly describe the findings under the assessment objective (1) and in more detail describe the results of the etiology objective (2). The specific objectives of the etiology portion of these investigations were expanded to include (a) determine the predominant fungi isolated from stem damage observed on hickory trees with declining crowns in surveyed stands, (b) determine the pathogenicity of the predominant fungi, (c) characterize the interactions between the hickory bark beetle and *C. smalleyi* on bitternut hickory exhibiting active crown decline, and (d) determine the role of *C. smalleyi* in development of hickory crown decline. Portions of these results have been published (Juzwik and Banik 2011; Juzwik and others 2008a, 2008b; Park 2011; Park and Juzwik 2012; Park and others 2009, 2010, 2013).

## METHODS AND RESULTS

### Assessment (objective 1)

Survey methods and results of the assessment portion of the project were summarized in the synthesis of evaluation monitoring projects for 1998–2007 (Ambrose 2012). A survey of 27 stands in six States (Indiana, Iowa, Minnesota, New York, Ohio, and Wisconsin) was conducted between 2007 and 2009. The most widespread and predominant insect pest associated with declining bitternut and pignut (*C. glabra*) hickory was the hickory bark beetle. The hickory timber beetle, *Xyleborus celsus*, was the second most common pest documented. Of 1,334 insects that emerged from sections taken from 33 felled declining hickories in 2008, 91 percent were hickory bark beetle and 8 percent were hickory timber beetle. Entry or exit holes of different diameters were the most common type of stem damage observed during point-plot surveys in 21 stands with actively declining bitternut hickory. Cankers and globose galls were the second most common type of stem damage (12 and 11 percent, respectively). Fungi were suspected to be the cause of the cankers and galls observed based on related reports in the literature.

### Etiology: determination of predominant pathogens associated with stem cankers and galls (objective 2a)

***Methods*—**Stem sections for fungal isolation were cut from felled hickory trees in 27 stands in six States (fig. 9.1). Three trees were felled in each stand; in total, 299 sections were obtained from 87 trees. Stem sections were examined for the presence of cankers, galls, xylem discoloration, and insect damage. Subsamples of the damaged stems from diseased bark, sapwood, or both were used for fungal isolation. Isolations were attempted in two ways. Small wood cubes placed in moist chambers fostered sporulation of some fungi, from which some isolates were obtained. Other isolates were obtained by plating wood or bark chips from margins of the diseased-healthy tissue following surface sterilization. Identification of pure isolates was based on cultural and morphological characteristics as well as results of DNA sequencing of the internally transcribed spacer region, the translation elongation factor 1-$\alpha$ gene, or both.

***Results*—**Most sections were taken from trees with either diffuse cankers (50 percent) or annual cankers (38 percent), regardless of insect damage occurrence. Stem galls were present

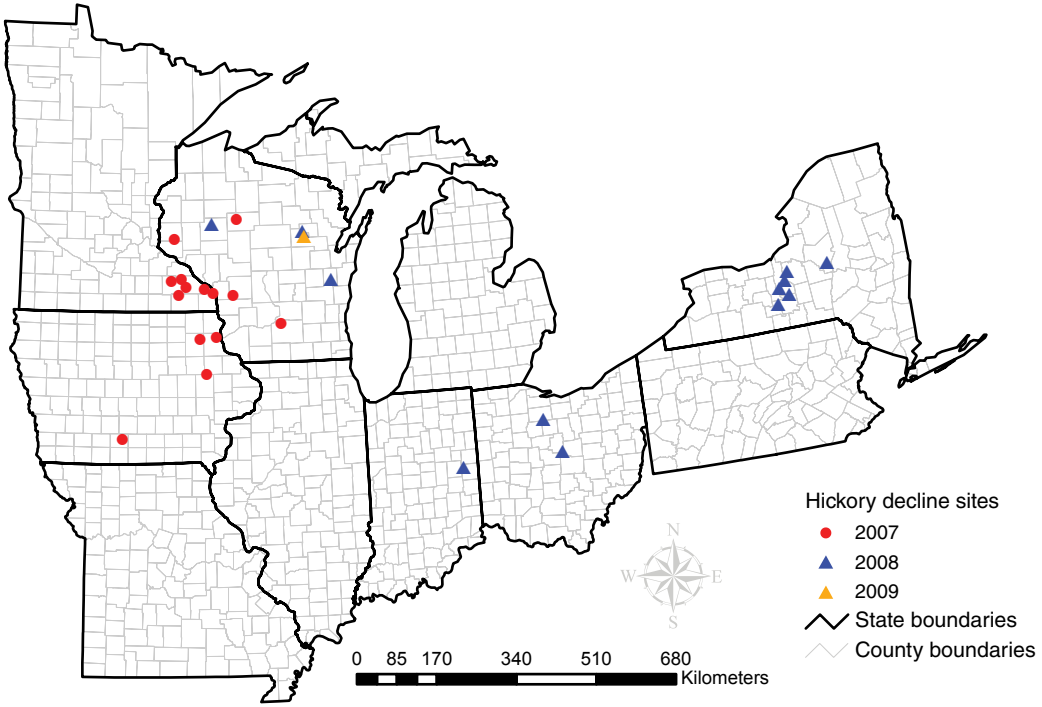


*Figure 9.1—Geographical distribution of forest stands surveyed for hickory decline in six of the North Central and Northeastern States between 2007 and 2009. Source: Paul Castillo (USDA FS).*



on 9 percent of the stem samples while hickory bark beetle damage only (no cankers) was present on 4 percent of the samples. *C. smalleyi* and *Fusarium solani* were commonly isolated while *Phomopsis* sp. was infrequently isolated from the stem samples. One or more of these fungal species were obtained from 132 of the 299 stem sections assayed. *Ophiostoma quercina* and *Penicillium* spp. were found infrequently. Incidences of *C. smalleyi* and *F. solani* were similar for surveyed stands in the six States. *C. smalleyi* was the most commonly isolated fungus from diffuse cankers (149 sections) obtained from 33 trees with declining crowns. *F. solani* was the most commonly isolated fungus from annual cankers (113 sections) obtained from 23 trees

exhibiting top dieback. The isolation frequencies of *C. smalleyi* and *F. solani* were significantly associated with different stem canker types ($p < 0.0001$). *Phomopsis* sp. was the most commonly isolated fungus from upper main stem galls (26 sections) from 7 trees; crown galls typically were not associated with top dieback.

### Etiology: pathogenicity of predominant fungi (objective 2b)

***Methods*—**Pathogenicity tests with *C. smalleyi* were conducted with local isolates on healthy bitternut hickory (13 to 18 cm diameter at breast height [d.b.h.]) in forest stands in Iowa, Minnesota, and Wisconsin. Either fungus-colonized agar plugs (Iowa) or spores suspensions (Minnesota and Wisconsin) were placed in drilled holes to the outer sapwood of study trees and the holes were covered with sterile moist cotton and laboratory film. Water agar plugs (Iowa) or sterile water (Minnesota and Wisconsin) served as a control treatment. Similar pathogenicity tests with *F. solani* were conducted in the same States and sites. Pathogenicity of *Phomopsis* sp. was tested in only the Iowa sites, using fungus-colonized agar disks inoculated into 2- to 4-cm diameter branches of 10- to 15-cm d.b.h. bitternut hickory trees.

***Results*—**Inoculations with *C. smalleyi* resulted in reddish brown bark necrosis and sapwood discoloration typical of the diffuse cankers found on trees with declining crowns. *C. smalleyi* was re-isolated from all fungus-inoculated trees but not from the controls. Stem inoculations with two haplotypes (BB and BC) of *F. solani* resulted in inner bark lesions whose length varied by study site (Park and Juzwik 2012). Sunken or open cankers (average 30 and 38 mm long for Minnesota and Wisconsin, respectively) resulted from all BC isolate inoculations and cankers were similar to those found on trees with top dieback. The BB isolate inoculations resulted in relatively small and callus-bounded cankers (average 20 and 34 mm long for Minnesota and Wisconsin, respectively). We reisolated the same haplotype fungus from cankers in each location; no *F. solani* was obtained from the control wounds. No cankers or galls resulted within 12 months following branch inoculation with *Phomopsis* sp.

### Etiology: *S. quadrispinosus*-*C. smalleyi* interaction on declining trees (objective 2c)

***Methods*—**Two bitternut hickory with 40 and 55 percent crown decline in Marathon County, Wisconsin, and one with 80 percent decline in Chippewa County, Wisconsin, were felled in June 2009. The bark was stripped from the main stem of each tree using a drawknife. Presence and extent of stem colonization by hickory bark beetles and presence of visible bark cankers and xylem lesions with or without associated beetle damage were recorded. In addition, attacking beetles were collected directly from trees in Minnesota and Wisconsin locations in late August and early September, and stem sections from trees felled in late May or early June were placed in emergence tubes to yield "emerged beetles." Teneral adult bark beetles collected by excavation also were obtained from one site.

Serial dilution plating and DNA-based assays (DNA extraction, polymerase chain reaction, and cloning) of attacking and of emerged hickory bark beetles were used to detect presence of *C. smalleyi* on the beetles.

***Results—***The extent of hickory bark beetle colonization of the main stems of the three actively declining trees ranged from aborted attacks (probing holes only) to successful colonization; i.e., egg gallery with radiating larval tunnels. Successful colonization accounted for 92, 53, and 80 percent of the documented hickory bark beetle damage on the declining trees (40, 55 and 80 percent decline rating, respectively). Fewer than 40 percent of the documented bark beetle attacks had accompanying bark cankers, xylem lesions, or both. The margins of the measured lesions always extended beyond the ends of the bark beetle larval tunnels when the damage types co-occurred. The average lengths of the xylem lesions of each tree were 8.2, 5.1, and 7.1 cm, respectively, on the bark-stripped trees. Numbers of bark cankers and xylem lesions varied by tree; i.e., 113 for the 80-percent decline rating tree, 585 for the 55-percent decline rating tree, and 26 for the 40-percent decline rating tree.

*C. smalleyi* was commonly isolated (88 and 93 percent, respectively, for 60 and 61 adult bark beetles from two sites) from hickory bark beetles captured by probing entry tunnels on six bitternut hickories in northern Wisconsin locations. The pathogen was isolated from fewer (11 percent of 21 adults) bark beetles obtained from the Minnesota site. Although the DNA assay was conducted with only a subset of bark beetles from the Wisconsin sites, similar results (92 percent of 24 assayed adults) to the serial dilution plating results were obtained. In contrast, *C. smalleyi* was infrequently isolated from the excavated bark beetle adults (7 percent of 43 beetles) and not isolated from any of the 120 emerged bark beetles. The same result (i.e., 0 percent positive for *C. smalleyi)* was found when molecular assay for DNA of *C. smalleyi* was conducted for 21 emerged bark beetles.

## Etiology: Role of *C. smalleyi* in crown decline (objective 2d)

***Methods—***For sap-flow experiments, healthy bitternut hickory between 13 and 28 cm d.b.h. were inoculated at 50 points with either a spore suspension of *C. smalleyi* or sterile water. Stems of study trees (6 trees in Minnesota, 11 in Wisconsin) were examined for presence of visible cankers 13 to 14 months later. Granier-type thermal dissipation probes and their associated system were used to monitor sap-flow rate of each study tree. In Minnesota, probes were installed at 4.3 to 4.6 m height on three fungus-inoculated, one water-inoculated, and two noninoculated trees in mid-September 2009. Signals from the probes were recorded by a datalogger for 18 days. In Wisconsin, probes were installed above inoculated columns at 4.3 to 4.6 m height on five fungus-inoculated, three water-inoculated, and three noninoculated trees in late July 2010. Following sap-flow measurement, the bark around each inoculation point was stripped using a drawknife and the extent of inner bark necrosis recorded. The

proportion of the total stem area (between 1.8 and 4.0 m) with cankered tissues was calculated for each tree. The presence of *C. smalleyi* in necrotic tissue was verified by isolation. Two sapwood cubes were taken from above and below each probe location, and thin cross sections were obtained using a sliding microtome. For each probe location, 250 vessels for each cube were examined, diameter was measured, and tylose presence or absence was recorded for each vessel.

***Results—***The fungus-inoculated sap-flow study trees exhibited large bark cankers and accompanying xylem lesions compared with very small necrotic areas on water-inoculated trees 13 to 14 months after inoculation in both sites. Differences in canker sizes, however, were found between study sites. The mean size (area) of the cankers on trees in Wisconsin (64.3 ± 2.2 $cm^2$) was larger than that on trees in Minnesota (15.3 ± 0.6 $cm^2$) ($p < 0.0001$). The calculated proportions of *C. smalleyi*-inoculated stems with bark cankers (≤ 11.5 percent in Minnesota and ≤ 41.3 percent in Wisconsin) were much larger than necrotic bark areas on water-inoculated control trees in both sites (< 2.2 percent). Diurnal trends in sap-flow rate were similar for all the trees in both sites (fig. 9.2). Rates were highest in early afternoon and lowest at night. Maximum sap-flow rates, however, were lower for fungus-inoculated trees compared with maximum rates for water-inoculated and noninoculated control trees. Specifically, the maximum sap-flow rates for fungus-inoculated trees were 10.7 to 18.1 g $m^{-2}s^{-1}$ in Minnesota and 5.7 to 27.2 g $m^{-2}s^{-1}$ in Wisconsin, whereas those of the control trees were in the range of 26.3 to 30.0 g $m^{-2}s^{-1}$ in Minnesota and 34.2 to 49.3 g $m^{-2}s^{-1}$ in Wisconsin. In more general terms, the average maximum sap-flow rate for four fungus-inoculated trees (14.0± 2.1 g $m^{-2}s^{-1}$) was 51 percent lower than the average maximum rate for three control trees (28.6 ± 1.1 g $m^{-2}s^{-1}$ ) ($p = 0.009$) in Minnesota. Similarly, the average maximum sap-flow rate for five fungus-inoculated trees (15.3 ± 3.8 g $m^{-2}s^{-1}$) was 64 percent lower than the average maximum rate for six control trees (41.9 ± 2.2 g $m^{-2}s^{-1}$) ($p= 0.0001$) in Wisconsin. The consistently lower sap-flow rates obtained in Minnesota compared with rates in Wisconsin were attributed to the timing of the measurements, which were done in early fall in Minnesota and mid-summer in Wisconsin (Park 2011, Park and others 2013).

For all fungus-inoculated trees in both studies, *C. smalleyi* was isolated from margins of necrotic tissue after sap-flow measurements were completed. The fungus was not isolated from inoculation wounds on any of the water-

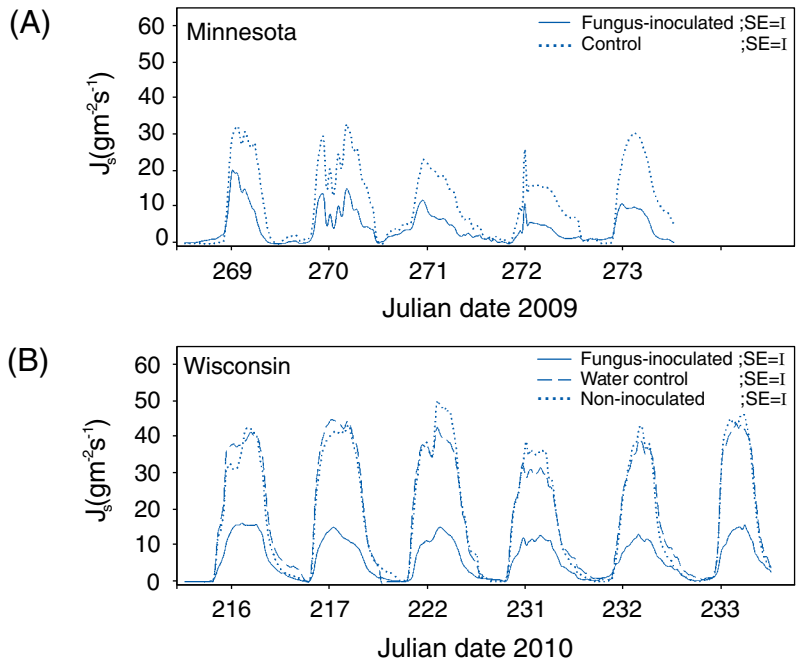


*Figure 9.2—Diurnal changes in sap flow velocity ($J_s$) in* Ceratocystis smalleyi*-inoculated trees versus water-inoculated and non-inoculated controls on selected days during the study period (Park 2011). (A) In Minnesota, data were averaged for fungus-inoculated trees and for one water-inoculated and two non-inoculated trees (= control). (B) In Wisconsin, data were averaged for five fungus-inoculated trees, three water-inoculated trees, and three non-inoculated healthy trees for each treatment. Ticks in x-axis indicate noon on each day. Bars indicate standard errors of the mean peak sap flow velocity values for each treatment.*

inoculated control trees. Vessel diameters and vessel diameter distributions were similar ($p = 0.23$) for the fungus-inoculated and the control trees in each location. As expected, tyloses were observed within vessels of all the study trees. They were more abundant in the fungus-inoculated trees, however, than in the control trees ($p < 0.006$) in both the 2 outer annual rings (30 to 56 percent, fungus-inoculated; 9 percent, controls) and the 9 to 10 outer annual rings (37 to 59 percent, fungus-inoculated; 25 to 42 percent, controls). Within the treatments, tyloses were more abundant in the deeper sapwood location than the outer sapwood annual rings. In addition, more vessels were found plugged in the 9 to 10 outer annual rings of *C. smalleyi*-inoculated trees than in the control trees ($p < 0.006$) for both sites. Significant interactions were found between (1) the average maximum sap-flow rate and tylose abundance in the two outer annual rings ($p = 0.0084$) for both sites combined, and (2) tylose abundance in the same sapwood location and the proportion of cankered bark area ($p = 0.0045$) based on correlation analyses. Based on linear regression analyses, an inverse relationship was found between the proportion of cankered bark area and average maximum flow rates in both sites ($R^2 = 0.90$, $p = 0.0042$, Minnesota; $R^2 = 0.90$, $p < 0.0001$, Wisconsin).

## DISCUSSION AND CONCLUSIONS

Hickory decline—i.e., unhealthy crowns, per Steinman (2004)—is a complex of at least three diseases, two of which involve insect interactions. In one of these diseases, top dieback is caused by heavy gall formation attributed to *Phomopsis* sp. on branches and main stems of smooth-bark hickories. In a second disease, numerous annual cankers caused by *F. solani* on the upper stem and main branches cause top dieback. Ambrosia beetles (e.g., hickory timber beetles) and hickory bark beetles are known to carry *F. solani*. These insects may create infection courts for the fungus and serve as transmitters as well. In the third and most common disease scenario observed in our study, hickory bark beetles and *C. smalleyi* are the predominant biotic agents that cause rapid declining crowns and tree mortality.

The synergistic interaction between hickory bark beetles and *C. smalleyi* results in numerous bark cankers and debilitating xylem lesions on stems of bitternut hickory that we hypothesize leads to rapid crown decline and tree death, especially following predisposing abiotic events such as drought. The bark beetle provides the entry and infection court for *C. smalleyi* on susceptible hickories and is hypothesized to be responsible for disseminating and inoculating the fungus into the wounded tissues. Anatomical observations of fungus-inoculated trees in the sap-flow studies revealed *C. smalleyi* infections in the sapwood of bitternut hickory are correlated with increased tylose formation in xylem vessels. Reduced sap-flow rates in bitternut hickory with numerous (tens to hundreds) stem infections are attributed to waterflow obstruction induced by tyloses in outer annual ring vessels and accumulation of gels in late-wood vessels and adjacent parenchyma cells. Numerous fungus infections and resulting host response can logically explain the symptoms of rapid crown decline, including foliage wilt, observed in affected trees.

We hypothesize that the most recent occurrences of hickory decline we investigated are similar in causes to those of historical episodes reported in the literature. The presence of bark cankers and xylem lesions associated with hickory bark beetle-attacked trees was likely overlooked or considered insignificant in historical investigations. Furthermore, the discovery of the new pathogen, *C. smalleyi*, was made only after the first report of the cankers on such trees (USDA Forest Service 1994). The relatively widespread occurrence of *C. smalleyi* (Park and others 2010) and the occurrence of a sister species suggests that the pathogen is native to the two regions.

## LITERATURE CITED


Ambrose, M.A. 2012. Tree species 'declines' that may be associated with large-scale mortality. In: Bechtold, W.A.; Bohne, M.J.; Conkling, B.L. [and others], eds. A synthesis of evaluation monitoring projects sponsored by the Forest Health Monitoring Program (1998–2007). Gen. Tech. Rep. SRS-159. Asheville, NC: U.S. Department of Agriculture Forest Service, Southern Research Station: 82-88.

Hopkins, A.D. 1912. The dying hickory trees: cause and remedy. Circ. 144. Washington, DC: U.S. Department of Entomology, Bureau of Entomology. 5 p.

Johnson, J.A.; Harrington, T.C.; Engelbrecht, C.J.B. 2005. Phylogeny and taxonomy of the North American clade of the *Ceratocystis fimbriata* complex. Mycologia. 97: 1067-1092.

Juzwik, J.; Banik, M. 2011. Nature of *Ceratocystis smalleyi*—*Scolytus quadrispinosus* interactions on stems of bitternut hickory with declining crowns. Phytopathology. 101: S86.

Juzwik, J.; Haugen, L.; Park, J.-H. 2008a. Bitternut hickory stem cankers and bark necrosis resulting from inoculations with *Ceratocystis* spp. and *Fusarium solani*. Phytopathology. 98: S77.

Juzwik, J.; Haugen, L.; Park, J.-H.; Moore, M. 2008b. Fungi associated with stem cankers and coincidental scolytid beetles on declining hickory in the Upper Midwest. In: Jacobs, D.F.; Michler, C.H., eds. Proceedings of the 16th Central Hardwood Forest Conference. Gen. Tech. Rep. NRS-P-24. Newtown Square, PA; U.S. Department of Agriculture Forest Service, Northern Research Station: 476-482.

Juzwik, J.; Park, J.-H.; Banik, M.T.; Haugen, L. 2012. Biotic agents responsible for rapid crown decline and mortality of hickory in Northeastern and North Central USA. In: Gottschalk, K. [and others], eds. Proceedings of the 18th Central Hardwood Forest Conference. Gen. Tech. Rep. NRS-P-117. Newtown Square, PA; U.S. Department of Agriculture Forest Service, Northern Research Station: 152-168.

Park, J.-H. 2011. Etiology of crown decline and dieback in bitternut hickory. St. Paul: University of Minnesota. 122 p. Ph.D. dissertation.

Park, J.-H.; Juzwik, J.; Cavender-Bares, J. 2013. Multiple *Ceratocystis smalleyi* infections associated with reduced stem water transport in bitternut hickory. Phytopathology. 103: 565-574.

Park, J.-H.; Juzwik, J. 2012. Fusarium canker of bitternut hickory caused by *Fusarium solani* in the North-Central and Northeastern United States. Plant Disease. 96: 455.

Park, J.-H.; Juzwik, J.; Haugen, L.M. 2010. *Ceratocystis* canker of bitternut hickory caused by *Ceratocystis smalleyi* in the North-Central and Northeastern United States. Plant Disease 94: 277.

Park, J-H.; Juzwik, J.; Shaw, C. 2009. Fungi isolated from cankers and galls on hickories exhibiting crown decline or dieback. Phytopathology. 99: S99.

St. George, R.A. 1929. Weather, a factor in outbreaks of the hickory bark beetle. Journal of Economic Entomology. 22: 573-580.

Steinman, J. 2004. Forest health monitoring in the Northeastern United States: disturbances and conditions during 1993–2002. NA-TP-01-04. Newtown Square, PA: U.S. Department of Agriculture Forest Service, Northeastern Area State and Private Forestry. 46 p. http://fhm.fs.fed.us/pubs/tp/dist_cond/hardwoods/hickory.pdf. [Date accessed: July 5, 2011].

U.S. Department of Agriculture (USDA) Forest Service. 1956. Forest insect conditions in 1955: a status report. Washington, DC: U.S. Department of Agriculture Forest Service. 16 p.

U.S. Department of Agriculture (USDA) Forest Service. 1972. Forest insect and disease conditions in the United States in 1971. Washington, DC: U.S. Department of Agriculture Forest Service. 65 p.

U.S. Department of Agriculture (USDA) Forest Service. 1994. Pest alert: hickory mortality. NA-FR-02-94. Radnor, PA: U.S. Department of Agriculture Forest Service, Northeastern Area, State and Private Forestry. 1 p.

Wisconsin Department of Natural Resources. 2005.Wisconsin forest health highlights, December 2005. Fitchburg, WI: Wisconsin Department of Natural Resources, Division of Forestry. 10 p.

# CHAPTER 10.

# The Roles of Fire, Overstory Thinning, and Understory Seeding for the Restoration of Iowa Oak Savannas

## (Project NC-F-07-1)

Lars A. Brudvig
Heidi Asbjornsen

## INTRODUCTION

Savanna ecosystems historically comprised more than 10 million ha of the Midwestern United States, forming a transition zone between western prairies and eastern deciduous forest that extended from Texas into Canada (Nuzzo 1986). These ecosystems were characterized by frequent understory fires, scattered (frequently oak) overstory trees, and a dense, diverse understory layer of grasses, forbs, and shrubs (Nuzzo 1986). With fire suppression, Midwestern savannas can convert to a woodland state through encroachment by disturbance-intolerant shrubs and trees (Brudvig and Asbjornsen 2007, Karnitz and Asbjornsen 2006), leading to reductions in understory diversity (Brudvig 2010, Brudvig and Asbjornsen 2009a), oak regeneration (Brudvig and Asbjornsen 2008, 2009b), and overstory oak tree growth rates (Brudvig and others 2011). Following settlement, most Midwestern savannas were converted to agriculture or were fire suppressed and, although less than 1 percent of historic savannas remain relatively pristine, a large amount may exist in the fire-suppressed, encroached state, and these savannas may be restorable (Asbjornsen and others 2005, Nuzzo 1986). Oak savanna restoration generally involves overstory thinning (i.e., clearing of nonsavanna trees and shrubs) and reintroduction of fire (McCarty 1998); however, little is known about the impacts of such restoration activities on biotic and abiotic ecosystem attributes or the importance of reintroducing native understory species for achieving restoration goals.

In 2008, we initiated an experiment to address these research needs using fire-suppressed, encroached oak savannas in Iowa. Here, we report on the three core objectives for this project: (1) initiate a new, large-scale experiment to evaluate overstory thinning, prescribed fire, and understory species reintroductions as restoration protocols in Midwestern oak savannas; (2) evaluate the effects of these treatments on understory and overstory indicators of forest health; and (3) compare assessments of ecosystem function and restoration success obtained from the measurements in objective 2 with concurrent Forest Inventory and Analysis (FIA) plot measurements.

## METHODS, RESULTS, AND DISCUSSION

### Site description and study design

The study was conducted in eight 1.5- to 3.3-ha white oak (*Quercus alba*) savanna sites near Saylorville Lake in central Iowa, United States. Following decades of fire suppression, these sites were invaded by (generally native) fire-intolerant trees and shrubs (e.g., *Fraxinus americana*, *Ulmus* sp., *Ostrya virginiana*), leading to conversion of the once open-canopied savannas to closed-canopy woodlands (Asbjornsen and others 2005, Brudvig and Asbjornsen 2007).

## Objective 1

To accomplish objective 1, we initiated an oak savanna restoration experiment, implementing thinning, burning, and seeding treatments at the eight study sites. In 2002–03, all nonoak woody stems greater than 1.5 m in height were cut with chainsaws and removed from four randomly selected sites; these four sites were recleared during early 2008 in preparation for the current study. The other four sites remained encroached, as controls. Within each thinned and unthinned site, a 30-by-50 m prescribed burn treatment area was established and paired with an unburned area of equal size. Prescribed fires were conducted during the spring of 2009 and 2010. Although fires historically occurred during many times of year, our approach was to match our experiment with common restoration practice, and Midwestern restoration practitioners commonly conduct prescribed fires during spring in oak savannas (Packard and Mutel 2005). Within each burned or unburned area, we established three 10-by-10 m seed-addition plots. Plots received either a diverse seed mix containing 75 percent forb seeds and 25 percent graminoid seeds by weight (high forb), 25 percent forb seeds and 75 percent graminoid seeds by weight (low forb), or an unseeded control. Seeded plots received seeds of 30 native oak savanna understory forbs and grasses (table 10.1), at a rate of 10 pounds of seed per acre, in late winter of 2008. Species for seed additions (table 10.1) were selected based on Brudvig and Mabry (2008).

**Table 10.1—Species added via seed addition in 2008 and number of study plots inhabited in 2011**

| Species | Family | Habit | Number of plots |
|---|---|---|---|
| *Bromus kalmia* | Poaceae | C3 grass | 0 |
| *Andropogon gerardii* | Poaceae | C4 grass | 2 |
| *Bouteloua curtipendula* | Poaceae | C4 grass | 0 |
| *Schizachyrium scoparium* | Poaceae | C4 grass | 0 |
| *Sorghastrum nutans* | Poaceae | C4 grass | 5 |
| *Spartina pectinata* | Poaceae | C4 grass | 2 |
| *Sporobolus cryptandrus* | Poaceae | C4 grass | 0 |
| *Allium canadense* | Liliaceae | Forb | 0 |
| *Allium cernuum* | Liliaceae | Forb | 0 |
| *Asclepisa tuberosa* | Asclepiadaceae | Forb | 0 |
| *Aster laevis* | Asteraceae | Forb | 0 |
| *Echinacea pallida* | Asteraceae | Forb | 0 |
| *Eryngium yuccifolium* | Apiaceae | Forb | 1 |
| *Liatris pycnostachya* | Asteraceae | Forb | 0 |
| *L. squarrosa* | Asteraceae | Forb | 0 |
| *Monarda punctata* | Lamiaceae | Forb | 2 |
| *Parthenium integrifolium* | Asteraceae | Forb | 0 |
| *Penstemon digitalis* | Scrophulariaceae | Forb | 8 |
| *Potentilla arguta* | Rosaceae | Forb | 0 |
| *Ratibida pinnata* | Asteraceae | Forb | 0 |
| *Rudbeckia subtomentosa* | Asteraceae | Forb | 7 |
| *Silphium integrifolium* | Asteraceae | Forb | 0 |
| *Silphium laciniatum* | Asteraceae | Forb | 0 |
| *Solidago rigida* | Asteraceae | Forb | 0 |
| *Zigadenus elegans* | Liliaceae | Forb | 0 |
| *Baptisia lactea* | Fabaceae | N-fixing forb | 0 |
| *Dalea candida* | Fabaceae | N-fixing forb | 0 |
| *D. purpurea* | Fabaceae | N-fixing forb | 0 |
| *Lupinus perennis* | Fabaceae | N-fixing forb | 0 |
| *Tephrosia virginiana* | Fabaceae | N-fixing forb | 0 |

N = nitrogen.

## Objective 2

To accomplish objective 2, we established monitoring in each seed-addition plot in 2008. Our nested experimental design enabled us to evaluate each combination of canopy thinning (thinned or unthinned), prescribed fire (burned or unburned), and seed addition (high forb, low forb, or control). In each seed-addition plot (total n = 48), we sampled understory species in four permanently marked 1-by-1 m quadrats, saplings (woody stems > 1.4 m height; < 5 cm diameter at breast height [d.b.h.]) and trees (woody stems > 5 cm d.b.h.) in the full 10-by-10 m plot, individuals of seeded species in the full 10-by-10 m plot, and fire temperature at the 10-by-10 m plot center during prescribed burns. We monitored fire temperature using three "pyrometers"—temperature-sensitive paints affixed to copper tags—per plot, which were deployed prior to prescribed fires. Because establishment of seeded individuals was relatively low, our statistical analyses focus on the effects of thinning and burning, though we qualitatively evaluate species' establishment from seed. To evaluate effects of these treatments on biotic indicators of forest health, we compared thinning and burning treatment effects on understory species richness and tree basal area using two-way analysis of variance (ANOVA). We evaluated the seeding treatments by investigating the number of 10-by-10 m plots in which each species established. To evaluate effects of these treatments on prescribed fire dynamics, we tested the effects of thinning on fire during the 2010 burns using t-tests (mean fire temperature and percent of pyrometers that burned in each burn plot).

Overstory thinning increased understory species richness by ~80 to 160 percent (fig. 10.1A; thinning effect $F_{1,6} = 38.5$, $p = 0.0008$), due to a ~20 to 60 percent reduction in overstory basal area in thinned plots (fig. 10.1B; $F_{1,6} = 3.3$, $p = 0.12$). Conversely, we found little evidence of an effect of thinning on sapling densities (thinning effect $F_{1,6} = 0.0$, $p = 0.97$) or effects of prescribed burning on understory richness (fig. 10.1A; burning effect $F_{1,6} = 0.7$, $p = 0.44$), sampling densities ($F_{1,6}$, $p = 0.32$), or overstory basal area (fig. 10.1B; $F_{1,6} = 0.06$, $p = 0.82$), in spite of the fact that 75 percent of pyrometers registered fire temperatures at greater than 121 °C during 2010 burns (mean temperature was 286 °C). There was no interaction between overstory thinning and fire on understory richness ($F_{1,6} = 1.6$, $p = 0.26$), sapling densities ($F_{1,6} = 0.0$, $p = 0.96$), basal area ($F_{1,6} = 1.3$, $p = 0.30$), or fire during burns; plots in thinned and unthinned sites burned with similar probability ($t = 0.75$, $p = 0.48$) and at similar temperatures ($t = 0.29$, $p = 0.78$). Of interest are effects of thinning and burning on oak regeneration. We recorded 7 oak saplings within our plots before prescribed fires (in 2008; of 466 total saplings) and after two prescribed fires (in 2010; of 824 total saplings). This suggests that, anecdotally, burning did not have a pronounced effect on oak sapling densities; however, we are unable to answer this hypothesis statistically with our dataset. We recorded established individuals of seven seeded species in 2011. Many species did not establish from seed (table 10.1); however, some species had become quite abundant by the final year of study (e.g., *Penstemon digitalis* and *Rudbeckia*

*subtomentosa*, which we found in ~25 percent of seeded plots), suggesting successfully established populations.

Together, these results suggest that overstory thinning elicits the largest restoration benefits for forest health during the short term, through increased understory diversity and decreased overstory density—both noted restoration goals for Midwestern oak savannas (Asbjornsen and others 2005). While prescribed fire had little impact during the course of this study, frequent burning will be critical for maintaining thinned conditions through prevention of reencroachment by fire-sensitive tree and shrub species (Brudvig and Asbjornsen 2007), and we note the success of both thinned and unthinned plots at carrying fire, producing burns of reasonably high temperature. We suggest that understanding the reestablishment of key understory species—particularly those that did not establish in this study (table 10.1)—should continue to be a priority, due to the potential for oak savannas to harbor high understory diversity (Brudvig and Mabry 2008).

## Objective 3

To accomplish objective 3, we established FIA phase 2 plots at each savanna site. Plots were established between 2002 and 2006 and arranged linearly, to coincide with co-occurring sampling transects (Brudvig and Asbjornsen 2007) and to fit within savanna site boundaries. During the summer of 2008, woody species were recorded in each plot using standard FIA methodology for seedling, sapling, and tree

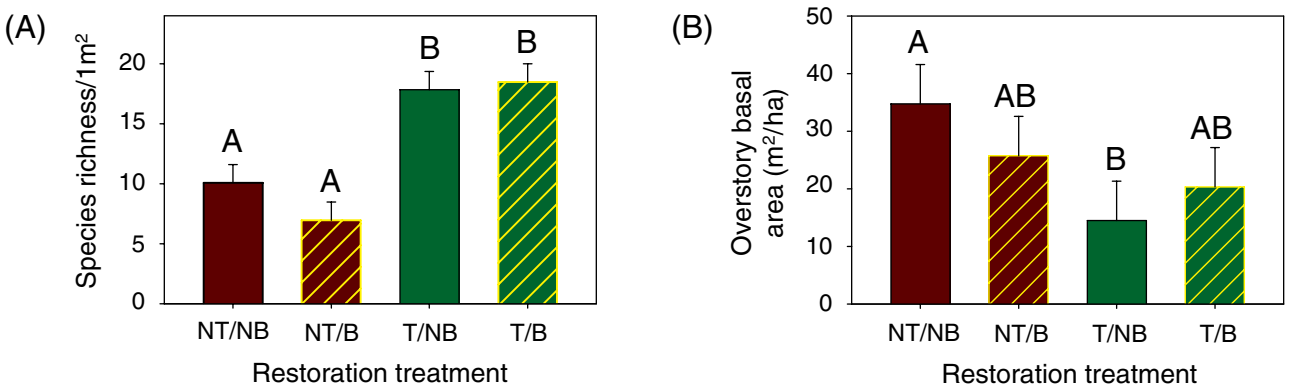


*Figure 10.1—Effects of overstory thinning and prescribed fire on (A) understory species richness and (B) overstory tree basal area (stems > 5 cm). Treatments were: no thinning/no burning (NT/NB), no thinning/burning (NT/B), thinning/no burning (T/NB), and thinning and burning (T/B). Bars with different letters were statistically different (*$p < 0.05$*, based on two-way analysis of variance).*

size classes. We used FIA data to evaluate the effects of mechanical encroachment removal with ANOVA.

FIA sampling during 2008 illustrated clear effects of overstory thinning (fig. 10.2). Relative to encroached control sites, sites restored by mechanical thinning supported reduced tree density (fig. 10.2A; $F_{1,6} = 22.2$, $p = 0.003$), reduced sapling density (fig. 10.2C; $F_{1,6} = 103.7$, $p < 0.0001$), and greater seedling density (fig. 10.2D; $F_{1,6} = 9.6$, $p = 0.2$). We found no evidence of a change in overstory basal area with restoration thinning (fig. 10.2B; $F_{1,6} = 1.4$, $p = 0.29$). These FIA-derived data illustrate similar patterns to data derived from transect-based sampling for sapling and overstory components; however, the FIA plot approach was sensitive to a change in seedling densities, whereas a transect-based approach was not (Brudvig and Asbjornsen 2007). Conversely, plots related to objective 2 illustrated a reduction in overstory basal area with thinning (fig. 10.1B), whereas FIA data did not resolve this difference (fig. 10.2B).

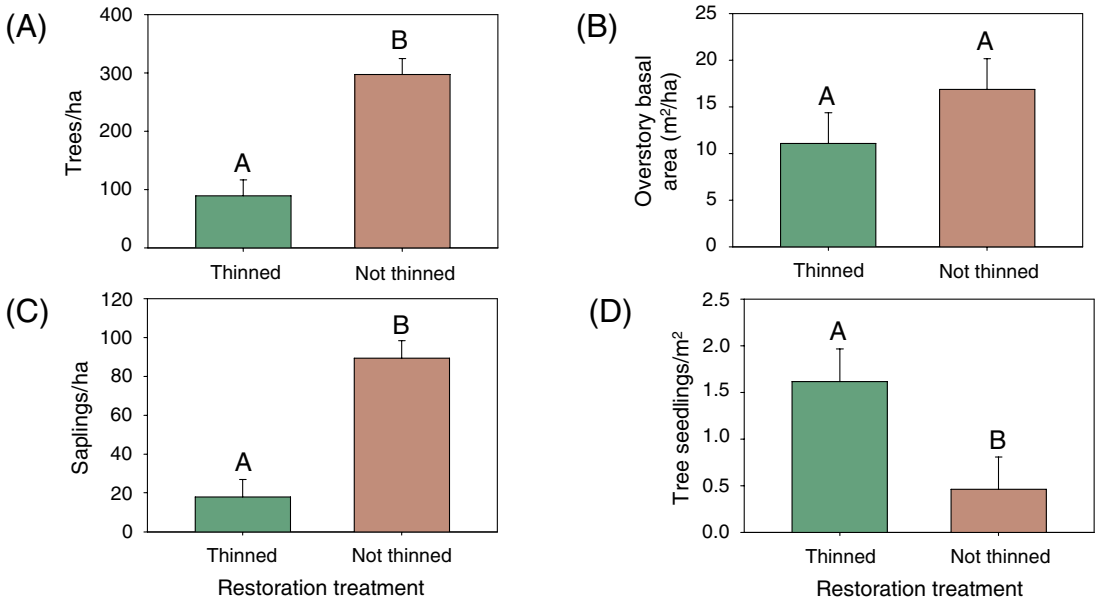


*Figure 10.2—Effects of overstory thinning on (A) overstory tree density, (B) overstory basal area, (C) sapling density, and (D) tree seedling density, as assessed by Forest Inventory and Analysis phase 2 plot data. Bars with different letters indicate statistical differences between restoration treatments* ($p < 0.05$, *based on two-way analysis of variance).*

Data from FIA phase 2 plots were effective at documenting changes in stand structure following oak savanna restoration. Decreased overstory tree and sapling densities, coupled with increased seedling density, illustrate positive benefits of thinning for oak savanna health through a reestablishment of scattered overstory trees and elevated understory light levels (Brudvig and Asbjornsen 2009a), decreased midstory encroachment (Brudvig and Asbjornsen 2007), and the potential for increased tree regeneration, including of oak species (Brudvig and Asbjornsen 2008, 2009b). FIA phase 2 plots may be broadly useful for documenting stand-scale changes in woody species abundance and stand structure following restoration; however, rearrangement of subplots to fit within sites may be necessary.

## CONTACT INFORMATION

Lars Brudvig: brudvig@msu.edu; 517–355–8262.

Heidi Asbjornsen: heidi.asbjornsen@unh.edu; 603–862–1011.

## LITERATURE CITED

Asbjornsen, H.; Brudvig, L.A.; McMullen-Mabry, C. [and others]. 2005. Defining appropriate reference conditions for restoring ecologically rare oak savanna ecosystems in the Midwest, USA. Journal of Forestry. 103: 345-350.

Brudvig, L.A. 2010. Woody encroachment removal from Midwestern oak savannas alters understory diversity across space and time. Restoration Ecology. 18: 74-84.

Brudvig, L.A.; Asbjornsen, H. 2007. Stand structure, composition and regeneration dynamics following removal of encroaching woody vegetation in Midwestern oak savannas, Iowa, USA. Forest Ecology and Management. 224: 112-121.

Brudvig, L.A.; Asbjornsen, H. 2008. Patterns of oak regeneration in a Midwestern oak savanna restoration experiment. Forest Ecology and Management. 255: 3019- 3025.

Brudvig, L.A.; Asbjornsen, H. 2009a. The removal of woody encroachment restores biophysical gradients in Midwestern oak savannas. Journal of Applied Ecology. 46: 231-240.

Brudvig, L.A.; Asbjornsen, H. 2009b. Dynamics and determinants of *Quercus alba* seedling success following savanna encroachment and restoration. Forest Ecology and Management. 257: 876-884.

Brudvig, L.A.; Blunck, H.M.; Asbjornsen, H. [and others]. 2011. Influences of woody encroachment and restoration thinning on overstory savanna oak tree growth rates. Forest Ecology and Management 262: 1409-1416.

Brudvig, L.A.; Mabry, C.M. 2008. Trait-based filtering of the regional species pool to guide understory plant reintroductions in Midwestern oak savannas, USA. Restoration Ecology. 16: 290-304.

Karnitz, H.M.; Asbjornsen, H. 2006. Composition and age structure of a degraded tallgrass oak savanna in central Iowa, USA. Natural Areas Journal. 26: 179-186.

McCarty, K. 1998. Landscape-scale restoration in Missouri savannas and woodlands. Restoration and Management Notes. 16: 22-32.

Nuzzo, V.A. 1986. Extent and status of Midwest oak savanna: presettlement and 1985. Natural Areas Journal. 6: 6-36.

Packard, S.; Mutel, C.F. 2005. The tallgrass restoration handbook for prairies, savannas, and woodlands. Washington, DC: Island Press; Society for Ecological Restoration International Edition. 463 p.

# CHAPTER 11.

# Progression of Laurel Wilt Disease in Georgia: 2009—11

## (Project SC-EM-08-02)

R. Scott Cameron
Chip Bates
James Johnson

## INTRODUCTION

Laurel wilt disease (LWD) is caused by the fungus *Raffaelea lauricola* and vectored by the redbay ambrosia beetle (RAB), *Xyleborus glabratus* (Fraedrich and others 2008). The pathogen and vector were apparently introduced from Asia through the Port of Savannah, and the disease has spread rapidly throughout the lower coastal plains forests in Georgia, killing nearly all large, previously abundant redbay (*Persea borbonia*)[1] trees in its path. Although research and prior surveys have revealed much about this disease, little is known about how it will progress in more diverse habitats with more scattered and smaller redbay trees and other hosts in the laurel family, particularly sassafras (*Sassafras albidum*).

The goals of this monitoring project are to (1) follow the progression of the disease in Georgia; (2) monitor mortality of redbay and sassafras sprouts and trees in areas through which LWD has already moved; (3) establish a methodology and document changes in vegetation composition resulting from the elimination of redbay and associated hosts by this disease; (4) monitor the rate of mortality in redbay, sassafras, and other host plants as the disease spreads inland; and (5) monitor the relative numbers of RAB in areas with varying stages of disease progression.

[1] Some taxonomists distinguish redbay (*P. borbonia*) and swamp bay (*P. palustris*) as separate species. For this study, these taxa are both rescognized as redbay.

## METHODS

### LWD distribution and spread in Georgia

The advance of LWD in Georgia from early 2009 through the end of 2011 was documented by noting dead and dying redbay and sassafras trees through contacts with landowners, directed road surveys, and assessments of monitoring plots by Georgia Forestry Commission Forest Health personnel. The presence of LWD in previously uninfected counties was confirmed by submitting samples from symptomatic trees to Steve Fraedrich, U.S. Department of Agriculture Forest Service, Athens, GA, for laboratory culture of the pathogen, *R. lauricola*.

### LWD long-term monitoring plots

Standardized permanent plots were established using modified Carolina Vegetation Survey protocol (Wentworth and others 2008) procedures in redbay and sassafras habitats to document the LWD process, vegetation changes, and host regeneration survival within sites and across the landscape in southeast Georgia. Sixteen redbay plots were established in the spring of 2009 and revisited six times through early spring of 2012. Each plot consisted of four contiguous 10-by-10 m modules (total 400 $m^2$) in which all host trees > 2.5 cm diameter at breast height (d.b.h.) were marked, measured,

and assessed for tree health status and numbers of live and dead sprouts. Redbay and sassafras regeneration (< 2.5 cm d.b.h.) was tallied in 10-$m^2$ subplots in each module. Vegetation composition in each plot was characterized by estimating the percentage of overstory and understory cover by plant species. Eight sassafras plots were installed using similar procedures, with one or two modules instead of four, and, on three plots with dense thickets of sassafras, trees were tallied by diameter class and not followed individually.

Redbay plots were established in three disease status categories: (1) **absent**—ahead of the advancing front where no disease was known to be present (five plots), (2) **active**—where RAB and the laurel wilt pathogen were present and killing trees (six plots), and (3) **inactive**—areas where large host trees had died and begun to decay and where RAB had presumably emerged from dead host material (five plots). Five sassafras plots were established on absent sites and three plots were established on active sites. Three of the sassafras plots were located adjacent to redbay plots where redbay and sassafras were growing together. All of the absent redbay monitoring plots were located within 15 km of areas known to have LWD and RAB in redbay, sassafras, or both. The location and host species present for each long-term monitoring plot are illustrated in figure 11.1 (two sassafras plots established less than 100 m apart at two locations are represented by single symbols on the map).

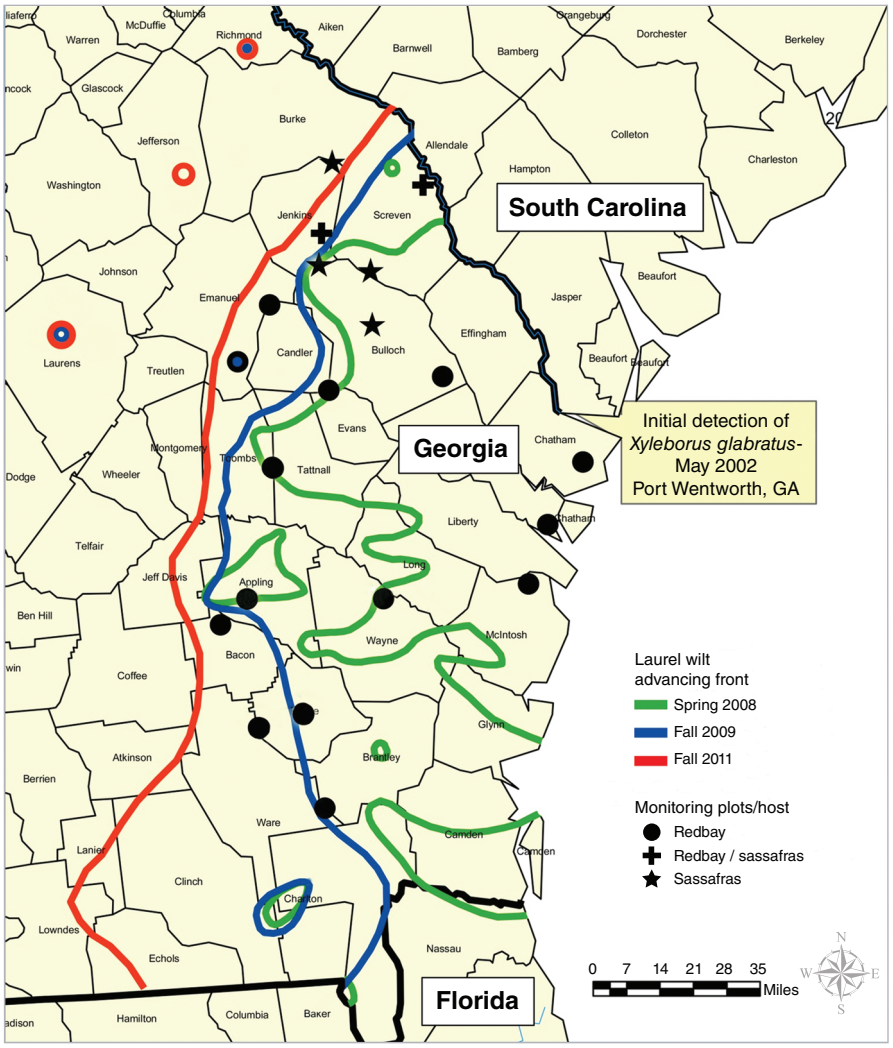


*Figure 11.1—Georgia laurel wilt monitoring plot locations and host species, and delineation of the westward-advancing disease fronts in the spring of 2008 (determined by a grid survey), fall of 2009, and fall of 2011 (estimated from progression in monitoring plots and directed road surveys).*

### RAB monitoring

The relative abundance of RAB in redbay and sassafras habitats with varying stages of disease development (absent, active, or inactive) was assessed by deploying Lindgren 8-funnel traps baited with commercial manuka oil lures (Synergy Semiochemicals Co. P385-Lure M) throughout the month of August (30 days) at 22 sites in 2009 and 23 sites in 2010. Disease development stage designations were determined for each site depending on the status during the trapping period. Dr. Jim Hanula (Forest Service, Athens, GA) sorted trap catches and reported numbers of RAB caught in each trap for both trapping intervals.

## RESULTS AND CONCLUSIONS

### Distribution and spread

The expanding distribution of LWD in Georgia from the spring of 2008, based on a systematic grid survey (Cameron and others 2008), through the end of 2011, based on assessments of LWD monitoring plots and directed road surveys (Cameron and others 2010), is illustrated in figure 11.1. The rate of spread varied greatly along the disease front in Georgia from less than 10 km/year in the upper coastal plain in the north to more than 35 km/year in the southern coastal plain, where large numbers of more uniformly distributed redbay trees have been killed across a broad area behind the advancing front. At least five isolated disease incidents have been documented well beyond the previously known distribution of LWD and likely originated from human-assisted dispersal of the RAB vector via movement of infested wood.

During the past 3 years, most new disease infections along the northern advancing front in Georgia have occurred in isolated pockets of redbay and in scattered groups (thickets) of sassafras trees, where redbay is relatively scarce or absent. Although LWD has not spread rapidly through this area, it has steadily infected additional dispersed groups of sassafras, indicating that LWD can infect sassafras in the absence of redbay and may spread beyond previously predicted limits (Koch and Smith 2008).

### Disease process in redbay

The LWD process in redbay habitat initially develops slowly, starting in one to a few infected (symptomatic) trees. Once a tree becomes symptomatic, it generally wilts rapidly and is colonized by ambrosia beetles within a few months. The rate at which the remaining trees become infected depends in part on host size and density in the area, but the process usually takes a year or more. LWD progression is most rapid in areas with high volumes of redbay, and it is slower in the presence of fewer, smaller, and more scattered redbay trees. The time for the disease to run its course through an area with abundant host (from the first symptomatic trees to inactivity, when all large redbay are dead and have fallen to the ground) ranges from about 3.0 to 4.5 years.

LWD kills nearly all redbay trees greater than a few centimeters d.b.h.; however, abundant sprouts and seedling regeneration are present on most sites after the disease runs its course (fig. 11.2). Sprouts attached to the base of dead redbay trees generally die, but those further out on the root flare often remain alive, although many die back from attacks by *Xylosandrus compactus*, another Asian ambrosia beetle. A few areas have been observed on the coastal plain in Georgia where numerous redbay trees greater than 2.5 cm ranging up to 12 cm d.b.h. are still healthy; however, the continued presence of scattered trees and clumps of sprouts with LWD indicate that the disease and RAB are still active at low levels many years after the initial epidemic.

## Disease process in sassafras

LWD infects sassafras in an apparently haphazard fashion, killing some individual trees and entire thickets while others remain apparently healthy. The largest sassafras trees tend to be affected first, and spread is sometimes rapid in dense thickets, apparently through interconnected lateral roots (fig. 11.3). Leaves on sassafras trees with LWD droop, shrivel, or turn shades of yellow, orange, or red and fall off shortly after symptoms are first manifested, leaving crowns bare within months (fig. 11.4). Infected sassafras will often leaf out in the spring with small leaves that soon shrivel and die. Characteristic black staining in the wood can be present on the surface of the outer sapwood and can be embedded beneath a nonsymptomatic current year's growth ring (fig. 11.3). Epicormic

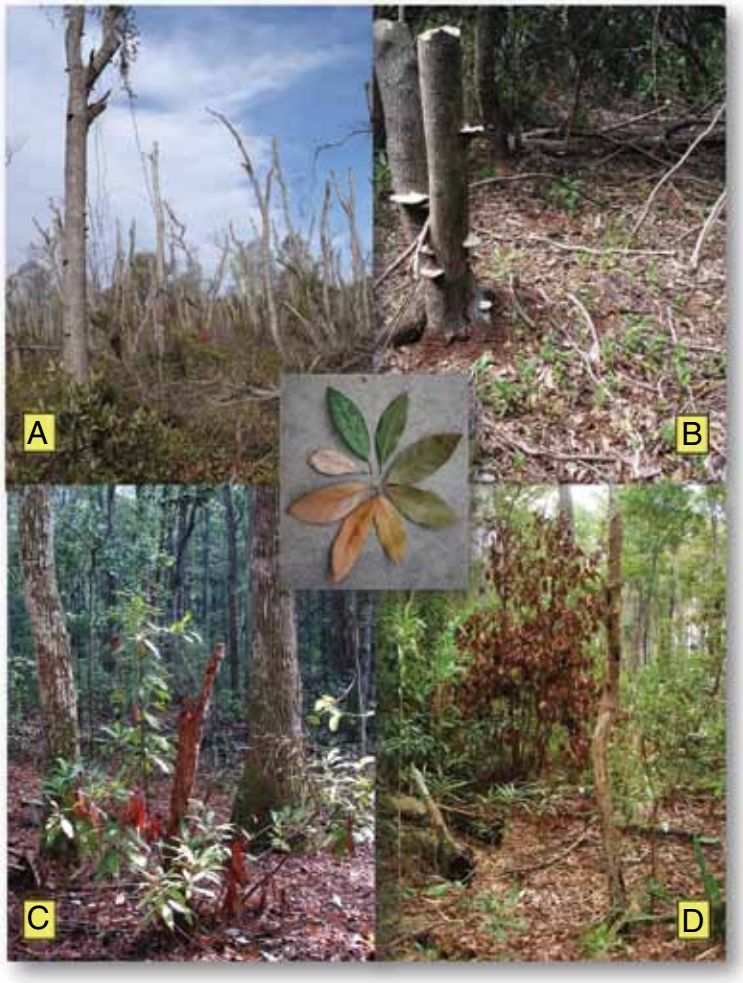


*Figure 11.2—Laurel wilt disease, or LWD, in redbay illustrating progression of leaf symptoms (center) and (A) total mortality and collapse in a dense stand of large redbay, (B) seedling regeneration after the overstory was killed, (C) sprouts around long-dead redbay, and (D) stump sprouts killed by laurel wilt years after the first wave of LWD. (Photos A, B, C, and D courtesy of Scott Cameron, Georgia Forestry Commission; center inset photo courtesy of Chip Bates, Georgia Forestry Commission.)*

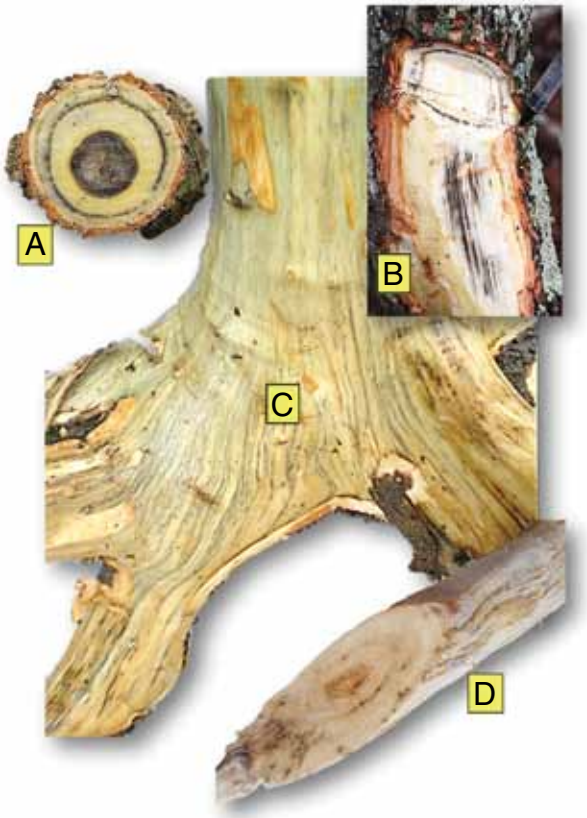


*Figure 11.3—Portions of four separate sassafras trees infected with* Raffaelea lauricola, *illustrating black staining resulting from a reaction of the host to the presence of the fungus: (A and B) embedded within the growth ring of the previous growing season; (C) visible on the outside of the wood exposed by removing the bark at the base of a tree, root flare, and roots; and (D) in a long lateral root through which the fungus apparently infected a small symptomatic tree at the edge of an expanding disease center. (Photos A and C courtesy of Chip Bates, Georgia Forestry Commission; photos B and D courtesy of Scott Cameron, Georgia Forestry Commission.)*

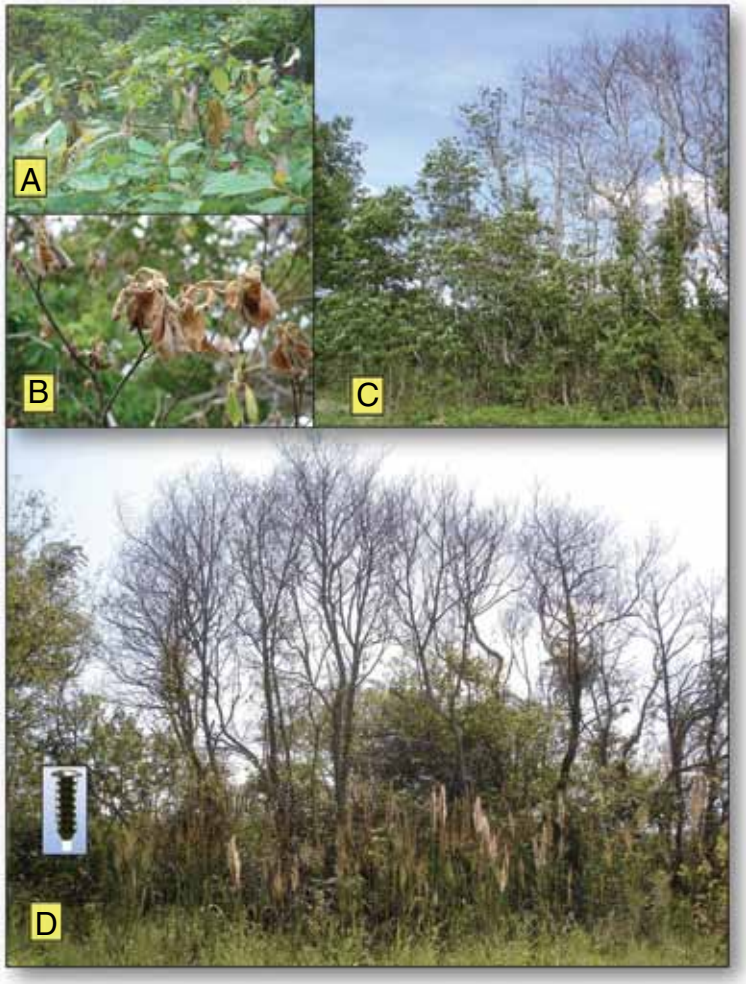


*Figure 11.4—Progression of laurel wilt disease in groups (thickets) of sassafras illustrating (A) initial leaf symptoms, (B) nonpersistent dead leaves, (C) rapid spread through thicket, and (D) 1 year following collective mortality, and position of a Lindgren funnel trap used to monitor redbay ambrosia beetles associated with disease centers in different stages of development. (Photo A courtesy of Chip Bates, Georgia Forestry Commission; photos B, C, D, and inset courtesy of Scott Cameron, Georgia Forestry Commission.)*

shoots are common on the lower stems of diseased sassafras trees, and ambrosia beetle attacks are most abundant at the base of sassafras trees killed by LWD.

## Vegetation changes associated with LWD

Redbay trees killed by LWD decay quickly and begin falling apart within 1 to 2 years. Major, rapid canopy cover changes occur on sites that have a large redbay overstory component before being impacted by LWD (fig. 11.2). Basal sprouts were abundant and persisted around the majority of redbay trees killed by LWD on all monitoring sites. However, redbay seedlings only proliferated on two sites where redbay was a significant component in the overstory and where there was little understory vegetation prior to the LWD epidemic. The impact of LWD on the original vegetation composition is far less on sites with small or sparse redbay in the overstory. When sites have a dense overstory and/or understory of other species, redbay regeneration remains sparse after the passage of LWD.

## Redbay ambrosia beetle trapping

Traps baited with manuka oil and deployed throughout August 2009 and August 2010 were effective for monitoring and comparing relative numbers of RAB among the three disease status categories. RAB were rarely captured in absent (apparently disease-free) locations in advance of the disease front (table 11.1). Numbers of RAB caught near active LWD sites varied greatly but were roughly correlated with the number and size (volume) of dead host trees in the vicinity of the trap, similar to the findings of Hanula and others (2011). Few RAB were trapped on sites where host trees were recently symptomatic and ambrosia beetles were beginning to colonize the trees, while large numbers of RAB were captured on a few sites where new brood beetles were apparently emerging from large volumes of dead host trees. Small numbers of RAB were frequently caught in traps deployed in inactive areas where the disease had moved through many years before, indicating that low populations are being maintained in small redbay trees, or possibly in other, undetermined host material. Few RAB were caught in most traps located near groups of small sassafras trees infected with LWD in the absence of nearby redbay trees. Numerous RAB, however, were caught in one trap adjacent to a large group of sassafras recently killed by LWD (fig. 11.4), supporting the conclusion that RAB attack,

**Table 11.1—Numbers of redbay ambrosia beetles, *Xyleborus glabratus*, caught in manuka oil-baited traps located adjacent to redbay and sassafras stands experiencing varying stages of laurel wilt disease development during August 2009 and August 2010**

| Host type | Disease stage[a] | Number of traps | Total number RAB | Mean number RAB/trap | Standard deviation |
|---|---|---|---|---|---|
| Redbay | | | | | |
| | Absent | 12 | 3 | 0.3 | 0.6 |
| | Active | 15 | 650 | 43.3 | 104.0 |
| | Inactive | 10 | 13 | 1.3 | 1.6 |
| Sassafras | | | | | |
| | Absent | 2 | 0 | 0.0 | 0.0 |
| | Active | 6 | 121 | 20.2 | 43.6 |

RAB = redbay ambrosia beetles.
[a] Disease stage assigned at the time of trap deployment.

transmit LWD, and produce brood in sassafras, although it may not be a favored host (Hanula and others 2008; Mayfield and Hanula 2012).

This summary represents the data collection and analyses completed under the funding of the evaluation monitoring project. Since the preparation of this summary, additional research and analyses have been conducted and an updated, more detailed paper is in preparation.

## LITERATURE CITED


Cameron, R.S.; Bates, C.; Johnson J. 2008. Distribution and spread of laurel wilt disease in Georgia: 2006–08 survey and field observations. Georgia Forestry Commission Report. September 2008. 28 p.

Cameron, R.S.; Bates, C.; Johnson, J. 2010. Evaluation of laurel wilt disease in Georgia: progression in redbay and sassafras—2008–2010. Georgia Forestry Commission Report. December 2010. 36 p.

Fraedrich, S.W.; Harrington, T.C.; Rabaglia, R.J. [and others]. 2008. A fungal symbiont of the redbay ambrosia beetle causes a lethal wilt in redbay and other Lauraceae in the Southeastern United States. Plant Disease. 92: 215-224.

Hanula, J.L.; Mayfield, III, A.E.; Fraedrich, S.W.; Rabaglia, R.J. 2008. Biology and host associations of the redbay ambrosia beetle, *Xyleborus glabratus* (Coleoptera: Curculionidae: Scolytinae), exotic vector of laurel wilt killing redbay (*Persea borbonia*) trees in the Southeastern United States. Journal of Economic Entomology. 101(4): 1276-1286.

Hanula, J.L; Ulyshen, M.D.; Horn, S. 2011. Effect of trap type, trap position, time of year, and beetle density on captures of the redbay ambrosia beetle (Coleoptera: Curculionidae: Scolytinae). Journal of Economic Entomology. 104(2): 501-508.

Koch, F.H.; Smith, W.D. 2008. Spatio-temporal analysis of *Xyleborus glabratus* (Coleoptera: Circulionidae: Scolytinae) invasion in Eastern U.S. forests. Environmental Entomology. 37(2): 442-452.

Mayfield, A.E., III; Hanula, J.L. 2012. Effect of tree species and end seal on attractiveness and utility of cut bolts to the redbay ambrosia beetle and granulate ambrosia beetle (Coleoptera: Curculionidae: Scolytinae). Journal of Economic Entomology. 105(2): 461-470.

Wentworth, T.R.; Peet, R.K.; Lee, M.T.; Roberts, S.D. 2008. Woody plant inventories, CVS-EEP Protocol. Carolina Vegetation Survey. 4 p. http://cvs.bio.unc.edu/protocol/woody-stems-protocol-summary-v4.2.pdf. [Date accessed: May 6, 2012].

# CHAPTER 12.

# Bark Beetle Outbreaks in Ponderosa Pine Forests: Implications for Fuels, Fire, and Management

## (Project INT-F-09-01)

Carolyn Sieg
Kurt Allen
Joel McMillin
Chad Hoffman



## INTRODUCTION

Landscape-scale bark beetle outbreaks have occurred throughout the Western United States during recent years in response to dense forest conditions, climatic conditions, and wildfire (Fettig and others 2007, Bentz and others 2010). Previous studies, mostly conducted in moist forest types (such as lodgepole pine [*Pinus contorta*]) suggest that bark beetle outbreaks alter stand structural attributes and fuel profiles, and thus affect potential fire hazard (Jenkins and others 2008), where hazard is defined as the ease of ignition and resistance to control (Hardy 2005). A number of factors influence postoutbreak fire hazard, including the time since mortality and the proportion of trees killed (Hicke and others 2012, Hoffman and others 2013). In the first few years following tree mortality, canopy fuels are expected to decrease as needles fall to the ground. Lower canopy fuels are assumed to decrease the potential for crown fire spread but allow for greater wind penetration into the stand. Surface fuel accumulation, first from needles and eventually from larger woody fuels, can increase the probability of surface fires transitioning to crowns. There is also a concern that accumulation of heavy woody fuels as dead trees fall to the ground can lead to accumulations above recommended amounts for both fireline construction and for sustaining ecosystem services such as soil protection and wildlife habitat (Brown and others 2003). In some forest types, postoutbreak logging (salvage) of dead trees has been used to recuperate the value of the trees and to potentially reduce fire hazard and enhance forest recovery (Collins and others 2011, Fettig and others 2007). Yet, how postoutbreak logging alters fuel complexes, tree regeneration, and subsequent fire behavior is largely understudied, especially for drier forest types such as those dominated by ponderosa pine (*P. ponderosa*) or Douglas-fir (*Pseudotsuga menziesii*).

Forest Health Monitoring aerial detection surveys (ADS) documented more than 150,000 acres of ponderosa pine forest impacted by mountain pine beetle (*Dendroctonus ponderosae*) in the Black Hills National Forest between 2002 and 2008. Douglas-fir beetle (*D. pseudotsugae*) outbreaks have been detected by ADS in both the Shoshone National Forest (120,000 acres) and Bighorn National Forest (10,000 acres) during the same period. The objectives of this project were to (1) quantify fuels in forest stands with (a) high levels of bark beetle-caused ponderosa pine or Douglas-fir mortality, (b) high tree mortality followed by logging that removed dead trees, and (c) no tree mortality; and (2) model fire behavior in these stands under severe weather scenarios. To accomplish these objectives, we established 60 plots in ponderosa pine stands in the Black Hills National Forest in 2007 and an additional 75 plots in Douglas-fir stands in 2010: 30 in the Bighorn National Forest and 45 in the Shoshone National Forest. We have sampled all 135 plots since either 2009 or 2010 to quantify changes in the fuel

complexes through time. This chapter presents data collected in the Black Hills National Forest 2 years after tree mortality following a mountain pine beetle outbreak, and it contrasts fuel complexes in ponderosa pine stands with and without mortality and in logged mortality stands. Our aim here is to characterize canopy fuel loadings relative to preoutbreak levels, tally surface woody fuel loadings, and simulate two fire behavior metrics in these stand types. This baseline information is critical to addressing our ultimate question about how fuel complexes in these forest types change through time with and without postmortality logging.

## METHODS

The data presented here were collected on 60 plots we established in 2007 on the Black Hills National Forest and sampled in 2009. At the time we established the plots, infested trees were green. We established 15 0.05-acre plots in each of four treatments in ponderosa pine stands. The four treatments included (1) bark beetle-caused mortality, (2) bark beetle-caused mortality with logging leaving moderate postlogging basal area (24 to 72 square feet per acre), (3) bark beetle-caused mortality with logging leaving low basal area (3 to 24 square feet per acre), and (4) no bark beetle-caused mortality controls. In mortality/logged plots, trees killed by bark beetles were removed by whole-tree harvesting in the winter of 2007–08, and nonmerchantable portions of harvested trees were removed offsite.

We quantified stand structure attributes by measuring the diameter at breast height (d.b.h.; measured at 4.5 feet height) for trees greater than 2 inches d.b.h., height, and lowest live branch of each tree, and recorded whether it was alive or dead. We measured stump diameters for recently cut trees in mortality/logged treatments. We calculated basal area and tree density and estimated canopy base height as the average of the lowest live branch heights for each plot. We reconstructed preoutbreak basal area and tree density by including trees killed by the bark beetles into totals. For logged stands, we converted stump diameters into d.b.h. based on locally derived algorithms from 130 trees we measured on the study site. Using stand level average basal area, tree density, and tree height, we estimated canopy fuel loading and canopy bulk density for each treatment and for preoutbreak conditions using equations from Cruz and others (2003).

We tallied surface fuels along two 50-foot transects per plot by time-lag size diameter classes following Brown's (1974) protocols. Size diameter classes included 1-hour (< 0.25 inches), 10-hour (0.25 to 1.00 inches), 100-hour (1.10 to 3.00 inches), and 1,000-hour (> 3 inches) fuels. We tallied 1- and 10-hour fuel classes along 12 feet of each transect (0 to 6 and 44 to 50 feet), 100-hour fuels along 24 feet per transect (0 to 12 and 38 to 50 feet), and 1,000-hour fuels along the entire length of each transect. In addition, we classified 1,000-hour fuels as either sound or rotten. Woody

fuel loading by size classes on each plot was calculated using Brown's (1974) algorithms. Total coarse woody debris (CWD) was calculated as the sum of sound and rotten 1,000-hour fuels, and total woody fuel load was the sum of loadings in all size classes.

We used NEXUS (Scott 1999) to simulate two fire behavior metrics for each treatment: torching index, or the wind speed at which a surface fire is expected to transition into the canopy, and crowning index, or the wind speed at which active crowning is possible (Scott and Reinhardt 2001). Given that total surface fuel loadings averaged less than 10 tons per acre on all treatments, we represented the surface fuels as a fuel model 9 (Anderson 1982) for all simulations. Dead fuel moisture contents were set at 3, 4, and 5 percent respectively for 1-, 10- and 100-hour fuel time lag size classes. Given that considerable differences existed in posttreatment tree densities, we altered the wind reduction factor across treatments to account for greater wind penetration into stands with fewer trees. We used a wind reduction factor of 0.1, which reduces the 20-foot wind speed by 90 percent for no-mortality stands, and factors of 0.2, 0.3, and 0.4 (or wind reductions of 80, 70, and 60 percent, respectively) for the mortality only, mortality/logged moderate basal area, and mortality/logged low basal area treatments, respectively.

## RESULTS

Ponderosa pine stands in the Black Hills National Forest averaged between 164 and 325 trees per acre, with basal areas between 129 and 174 square feet per acre before the mountain pine beetle outbreak. Stands were 100 percent dominated by ponderosa pine trees, which averaged 11 to 12 inches d.b.h. and 48 to 65 feet tall. Comparing postmortality stand structure with reconstructed preoutbreak levels, basal area was reduced 71 percent and tree density 41 percent in bark beetle mortality plots without logging. Mountain pine beetle-caused mortality and postoutbreak logging reduced the basal area 74 percent (to 37.7 square feet per acre) in moderate residual basal area plots and 89 percent (to 14.6 square feet per acre) in low residual basal area plots. Snag density was highly variable among the treatments and mostly the result of recent bark beetle-induced tree mortality. Snag density averaged 28 snags per acre on no-mortality plots compared with 191 per acre on mortality plots without logging. Logged plots had very low snag densities, averaging less than 6 snags per acre across all plots.

Canopy base height averaged 27.9 feet in no-mortality plots. After the bark beetle-caused mortality occurred, canopy base height averaged 23.67 feet in unlogged plots and averaged 24.40 and 20.95 feet in moderate and low residual basal area logged plots, respectively. Compared

with preoutbreak levels, average canopy fuel loading was reduced 66.8 percent in mortality plots without logging, 71.6 percent in mortality/logged moderate residual basal area plots, and 86.0 percent in mortality/logged low-residual basal area plots.

Total woody surface fuel loadings averaged between 5.1 and 9.3 tons per acre on the four treatments (fig. 12.1A). CWD, or woody material greater than 3 inches in diameter, ranged from an average of 2.6 tons per acre on no-morality plots to 5.1 tons per acre on moderate residual basal area logged plots (fig. 12.1B), and in all plot types was dominated by rotten material.

Fire behavior simulations predicted that crowning index increased with decreasing stand density (fig. 12.2A). That is, the simulations indicated that crowning would occur in no-mortality stands under lower wind speeds compared with stands with bark beetle mortality and that even higher wind speeds were required for crowning to occur in mortality/logged stands. Torching indices showed the opposite trend (fig. 12.2B), where higher wind speeds were required for torching to occur in no-mortality stands, and lower wind speeds in the more open mortality and mortality/logged stands.

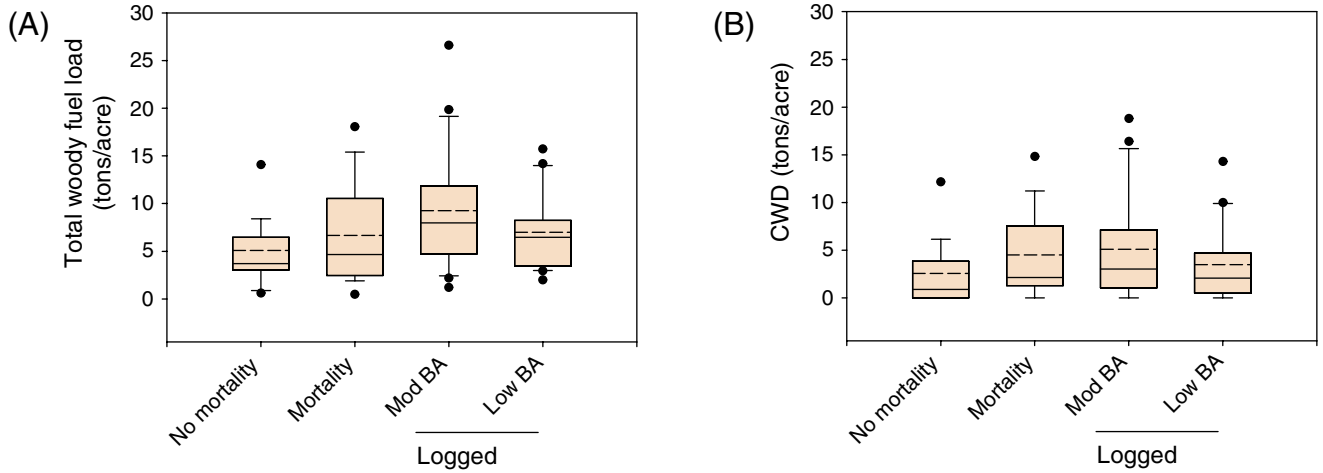


*Figure 12.1—Total woody surface fuel loading (A) and coarse woody debris (B) for no-mortality stands, unlogged mortality stands, mortality/logged stands with moderate postlogging residual basal areas, and mortality/logged stands with low residual basal areas. Boxes indicate 25$^{th}$ and 75$^{th}$ percentiles with medians (solid line), whiskers above and below boxes show 90$^{th}$ and 10$^{th}$ percentiles, and dots indicate outliers.*

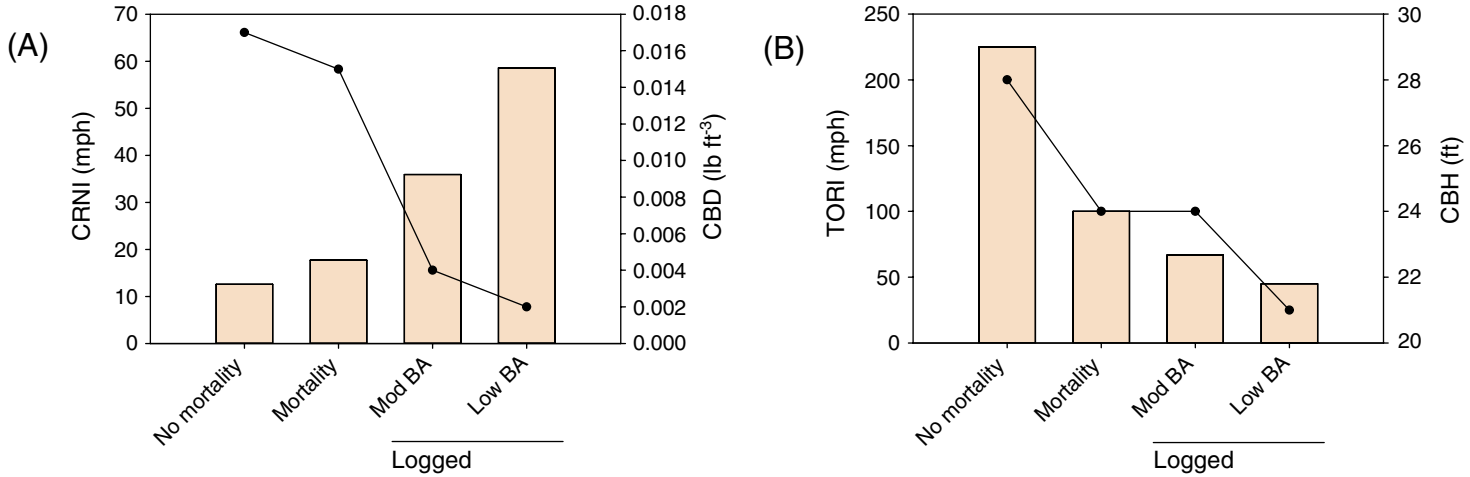


*Figure 12.2—(A) Crowning index (bars; CRNI; left axis) and canopy bulk density (dots; CBD; right axis), and (B) torching index (bars; TORI; left axis) and canopy base height (dots; CBH; right axis) for no-mortality stands, unlogged mortality stands, mortality/logged stands with moderate postlogging residual basal areas, and mortality/logged stands with low residual basal areas stands. Fuel models were held constant (model 9) and wind reduction factor was 0.1, 0.2, 0.3, 0.4, respectively, for the four treatments.*

## DISCUSSION

Bark beetles alone and in combination with postoutbreak logging greatly reduced overly dense stands of ponderosa pine in the Black Hills National Forest. Preoutbreak basal areas in many plots were above 120 square feet per acre, thus making them highly favorable for mountain pine beetle infestations (Schmid and others 1994). High levels of tree mortality resulted in stands with lower canopy fuel loading, similar to trends following bark beetle tree mortality in ponderosa pine forests in the Southwest (Hoffman and others 2012) and lodgepole pine forests in Yellowstone National Park (Simard and others 2011). Another consequence of the tree mortality was a trend of lower canopy base height in mortality plots compared with no-mortality plots, which we attributed to higher mortality of larger trees, leaving smaller trees with crowns closer to the ground.

Total surface woody fuel loadings were relatively similar among stand types. The generally low input of woody material on logged plots was a reflection of the harvesting technique used. Trees were whole-tree harvested when the needles were still green and limbed at landings adjacent to the plots. It is also interesting to note that only 5 (out of 60) plots across all treatments had CWD loadings within recommended ranges (10 to 20 tons per acre) for

dry coniferous forests (Brown and others 2003). The remainder, or nearly 90 percent of the plots, had CWD loadings below recommended ranges. As remaining snags fall to the ground in the future in unlogged mortality plots, target levels of CWD will likely be reached, and perhaps exceeded. In a previous study in the Southwest, 20 percent of ponderosa pine stands killed by both *Ips* and *Dendroctonus* beetles had CWD loadings above recommended levels 5 years after outbreak (Hoffman and others 2012). In our unlogged stands, the large number of dead trees will likely fall within 7 to 10 years, as Schmid and others (1985) found in Colorado. Additional contributions of large woody fuels as well as inputs of smaller twigs and needles will likely raise concerns about increasing surface fuels in the future.

Fire simulations based on fuel complexes 2 years after bark beetle-caused tree mortality suggest that changes in canopy fuels and canopy base heights led to altered fire behavior attributes. Dense no-mortality stands with high canopy fuel loading were predicted to require less wind for crowning to occur, followed by mortality stands and then logged stands. In contrast, due to lower wind penetration and slightly higher canopy base heights, greater wind speeds were predicted to be needed for torching to occur in no-mortality stands. The gradient of increasing wind penetration and decreasing canopy base heights across mortality, mortality/logged moderate basal area, and mortality/logged low basal area plots corresponded to torching predicted to occur at decreasing wind speeds along this gradient.

In summary, 2 years after mountain pine beetle-caused mortality in ponderosa pine stands in the Black Hills National Forest, the major impact on the fuel complex was the loss of at least two-thirds of the basal area and canopy bulk density compared with preoutbreak levels. Removal of the dead trees by logging reduced the basal area and canopy bulk density by an additional 3 to 20 percent. Woody surface fuel loadings in the majority of plots, regardless of treatment, were below recommended ranges for these dry coniferous forests. Fire behavior simulations suggest that stands without bark beetle-caused mortality would require less wind to carry crown fires, whereas the more open stands with mortality, and especially following logging, were less vulnerable to crown fire. Surface fires were predicted to transition into the canopies under lower wind speeds in more open stands after bark beetle mortality, however, due to lower canopy base heights. By continuing to monitor these plots through time, we will be able to test how fuel accumulation patterns through time align with various conceptual models such as Hicke and others (2012). As remaining snags fall in unlogged stands, and seedlings and other vegetation establish in all mortality plots, concerns about fuel continuity and increased potential for fire spread will likely be heightened.

## ACKNOWLEDGMENTS

Funding was provided by Forest Health Monitoring Evaluation Monitoring grant INT-F-09-01. Chris Hoffman, Chris Looney, Emma Gustke, Al Dymerski, Brittany Deranleau, John Wilson, James Wilson, Tania Begaye, and Addie Hite helped with fieldwork and data entry. We appreciate the constructive comments Chris Fettig and John Paul Roccaforte provided on a previous version.

## LITERATURE CITED

Anderson, H.E. 1982. Aids to determining fuel models for estimating fire behavior. Gen. Tech. Rep. INT-122. Ogden, UT: U.S. Department of Agriculture Forest Service, Intermountain Forest and Range Experiment Station. 22 p.

Bentz, B.J.; Régnière, J.; Fettig, C.J. [and others]. 2010. Climate change and bark beetles of the Western United States and Canada: direct and indirect effects. Bioscience. 60: 602–613.

Brown, J.K. 1974. Handbook for inventorying downed woody material. Gen. Tech. Rep. INT-16. Ogden, UT: U.S. Department of Agriculture Forest Service, Intermountain Forest and Range Experiment Station. 24 p.

Brown, J.K.; Reinhardt, E.D.; Kramer, K.A. 2003. Coarse woody debris: managing benefits and fire hazard in the recovering forest. Gen. Tech. Rep. RMRS-105. Fort Collins, CO: U.S. Department of Agriculture Forest Service, Rocky Mountain Research Station. 16 p.

Collins, B.J.; Rhoades, C.C.; Hubbard, R.M.; Battaglia, M.A. 2011. Tree regeneration and future stand development after infestation and harvesting in Colorado lodgepole pine. Forest Ecology and Management. 261: 2168-2175.

Cruz, M.G.; Alexander, M.E.; Wakimoto, R.H. 2003. Assessing canopy fuel stratum characteristics in crown fire prone fuel types of western North America. International Journal of Wildland Fire. 12: 39-50.

Fettig, C.J.; Klepzig, K.D.; Billings, R.F. [and others]. 2007. The effectiveness of vegetation management practices for prevention and control of bark beetle infestations in coniferous forests of the Western and Southern United States. Forest Ecology and Management. 238: 24-53.

Hardy, C. 2005. Wildland fire hazard and risk: problems, definitions, and context. Forest Ecology and Management. 211: 73-82.

Hicke, J.A.; Johnson, M.C.; Hayes, J.L.; Preisler, H.K. 2012. Effects of bark beetle-caused tree mortality on wildfire. Forest Ecology and Management. 217: 81-90.

Hoffman, C.; Morgan, P.; Mell, W. [and others]. 2013. Numerical simulation of crown fire hazard immediately following bark beetle-caused tree mortality in lodgepole pine forests. Forest Science. 59: 390-399.

Hoffman, C.; Sieg, C.H.; McMillin, J.D.; Fulé, P.M. 2012. Fuel loadings five years after a bark beetle outbreak in Southwestern USA ponderosa pine forests. International Journal of Wildland Fire. 21: 306-312.

Jenkins, M.J.; Hebertson, E.; Page, W.; Jorgensen, C.A. 2008. Bark beetles, fuels, fires and implications for forest management in the Intermountain West. Forest Ecology and Management. 254: 16-34.

Schmid, J.M.; Mata, S.A.; McCambridge, W.F. 1985. Natural falling of beetle-killed ponderosa pine. RN-RM-454. Fort Collins, CO: U.S. Department of Agriculture Forest Service, Rocky Mountain Forest and Range Experiment Station. 3 p.

Schmid, J.M.; Mata, S.A.; Obedzinski, R.A. 1994. Hazard rating ponderosa pine stands for mountain pine beetles in the Black Hills. Res. Note RM-529. Fort Collins, CO: U.S. Department of Agriculture Forest Service, Rocky Mountain Forest and Range Experiment Station. 4 p.

Scott, J.H. 1999. NEXUS: a system for assessing crown fire hazard. Fire Management Notes. 59: 20–24.

Scott, J.H.; Reinhardt, E.D. 2001. Assessing crown fire potential by linking models of surface and crown fire behavior. Res. Pap. 29. Fort Collins, CO: U.S. Department of Agriculture Forest Service, Rocky Mountain Research Station. 59 p.

Simard, M.; Romme, W.H.; Griffin, J.M.; Turner, M.G. 2011. Do mountain pine beetle outbreaks change the probability of active crown fire in lodgepole pine forests? Ecological Monographs. 81: 3-24.

# CHAPTER 13.

# Searching High and Low: Patterns of White Ash Health across Topographic Gradients in the Allegheny Region

## (Project NE-EM-09-02)

Kathleen S. Knight
Alejandro A. Royo

## INTRODUCTION AND PROJECT OBJECTIVES

White ash (*Fraxinus americana*) is an important species in eastern forests that is currently threatened by an introduced insect pest, the emerald ash borer (EAB) (*Agrilus planipennis*). Understanding the patterns of white ash health across the landscape prior to the arrival of EAB will enable us to better understand factors that affect forest health in general and will provide information on the ecology of a tree species of particular current interest. As EAB is known to be attracted to stressed ash trees, this knowledge may lead to improved risk maps and monitoring and detection strategies.

White ash decline has been a regional concern for many years, and recent decline episodes have increased interest in this problem. It is of particular interest within the Allegheny National Forest (ANF) in northwestern Pennsylvania. At the ANF, white ash is found at moderate abundances (< 5 percent of live basal area) mixed with other tree species, but it experiences the second highest levels of crown dieback (following sugar maple, *Acer saccharum*) of all the major tree species regionally. Drought and pathogens have been identified as factors contributing to and inciting ash decline (Han and others 1991), but nutrient deficiencies may play a role in predisposing ash trees to decline. White ash is a base cation-demanding species and is associated with soils with higher pH and greater base cation availability (Finzi and others 1998). Another base cation-demanding species, sugar maple, exhibits strong relationships between soil nutrition and decline (Horsley and others 2000). Within the unglaciated portion of the ANF, topographic position is related to nutrient deficiencies. Upper slope positions generally exhibit lower availability of base cations calcium (Ca) and magnesium (Mg) compared with levels at lower slope positions, which have good nutrition (Bailey and others 2004). Finally, based on observations of Morin and others (2006) and trends in the Forest Inventory and Analysis (FIA)/Forest Health Monitoring (FHM) data for the ANF, ash decline and mortality appears to be concentrated on ridgetops and upper slopes.

The objectives of this project were to assess white ash health status in the Allegheny Plateau region using an intensified ash health plot network to enhance existing FIA/FHM data. This enhanced sampling will enable us to explore how topographic position, elm spanworm

(*Ennomos subsignarius* [Hubner]) defoliation history, and other site characteristics are related to ash decline and mortality patterns across the landscape. In addition, we will create a formula to convert between FHM canopy health ratings (dieback, crown density, etc.) and a user-friendly health rating system developed for use by managers and based on the typical decline progression of ash trees infested by EAB. Finally, this enhanced ash monitoring plot system will serve as a basis to monitor future ash mortality with the anticipated arrival of EAB within the next 5 to 10 years.

## BRIEF METHODS

We established new plots to enhance existing FIA/FHM spatial coverage across the ANF and capture a wide gradient of soil fertility (e.g., topographic gradient and soil parent materials). In cooperation with our collaborators from the ANF, we divided the entire forest ownership into a 1.88-by-1.44 mile grid and identified grid squares containing ash based on inventory data. Within each grid square, we systematically searched the area to locate a pair of plots containing white ash where one plot in the pair was established on a lower slope position and the other an upper slope position. We established a total of 193 plots across the entire ANF ownership. At each plot, we conducted an overstory inventory and an herbaceous species inventory (presence or absence) with an emphasis on indicator species strongly associated with base cation-rich sites. As part of the overstory inventory, we rated ash crown health of 538 white ash trees using two different methods:

1. A simple 1–5 categorical rating system developed for easy use by managers and based on the typical decline progression of EAB-infested ash trees (Smith 2006). In this system, a rating of 1 represents a healthy canopy, 5 is a dead canopy, and 2–4 are specific stages of thinning and dieback.

2. The standard numerical FHM phase 3 crown measurement methodology, including uncompacted live crown ratio, crown density, crown transparency, and crown dieback.[1]

A formula relating the two crown health methods was derived and tested on an independent dataset of ash stands in Ohio that

[1] U.S. Department of Agriculture Forest Service. 2007. Crowns: Measurement and Sampling. Section 12 in Forest Inventory and Analysis national core field guide, volume 2: field data collection procedures for phase 3 plots, version 4.0. U.S. Department of Agriculture Forest Service, Washington Office. Internal report. On file with: U.S. Department of Agriculture Forest Service, Forest Inventory and Analysis, Rosslyn Plaza, 1620 North Kent Street, Arlington, VA 22209.

were in various stages of infestation by EAB. To assess whether health ratings were related to deficiencies in base cations, we collected leaves from the focal ash tree in each plot to assess foliar nutrition. Leaves were dried and analyzed for macronutrients and micronutrients, including Ca and Mg. To assess whether health ratings were related to past infestation by insects, defoliation records from aerial surveys were used to determine the number of times each stand was defoliated by elm spanworm, a species known to defoliate ash.

## RESULTS AND CONCLUSIONS

### Conversion formula

The FHM measures of ash tree health most closely related to the categorical health rating system were canopy density and canopy dieback. The full details of this analysis and the conversion formulas are published in Royo and others (2012). The relationship between FHM crown density and categorical crown health ($R^2 = 0.65$) gave correct predictions with the independent dataset from Ohio 71 percent of the time when dead trees were excluded (82 percent when dead trees were included). The relationship between FHM crown dieback and categorical crown health ($R^2 = 0.91$) gave correct predictions with the independent dataset 93 percent of the time when dead trees were excluded (97 percent including the dead trees). The latter model gave poor predictions for crown health category 4 trees, however, due to differences in considering only recent dieback of twigs for FHM and all dead branches in the tree for the categorical ratings.

### Nutrient differences

Foliar nutrient data showed that Ca and Mg foliar concentrations were greater on lower slope positions than upper slope positions. The incidence of herbaceous plants known to track base cation availability was also greater on lower slope positions and was correlated with the foliar base cation data. This relationship between topographic position and base cation availability is a known phenomenon in unglaciated areas of the ANF, likely caused by leaching of nutrient-rich stratigraphic layers.

## Ash health

Ash health was related to topographic position, base cation concentrations, insect defoliation history, and tree diameter at breast height. Crown dieback was greater on upper slope positions than on lower slope positions (fig. 13.1). Greater crown dieback was associated with lower base cation concentrations on the upper slope positions. Categorical crown health ratings also showed poorer crown health on upper slope positions. Upper slope positions with lower base cation concentrations or with a history of defoliation by elm spanworm had the poorest crown health. In addition, crown health was poorer for smaller trees. Standing dead ash trees showed similar relationships to site characteristics. The relative abundance of dead ash trees was greater on sites with upper slope positions, lower base cation concentrations, smaller trees, and a history of elm spanworm defoliation (fig. 13.2). A manuscript including the full details of the ash health, nutrient, and defoliation findings has been published (Royo and Knight 2012).

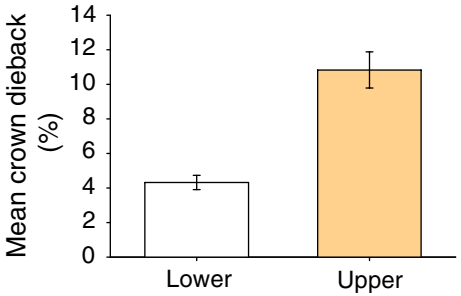


*Figure 13.1—Crown dieback of white ash trees was greater on upper slope positions than lower slope positions. (Reproduced from Royo and Knight 2012.)*

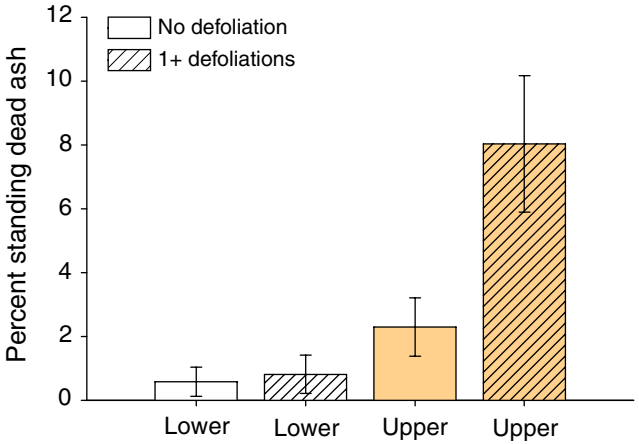


*Figure 13.2—Percent standing dead white ash was greater on upper slope positions, especially in areas with a history of defoliation by elm spanworm. (Reproduced from Royo and Knight 2012.)*

Our data show that multiple factors may interact to influence ash crown health, dieback, and mortality and that there are particular sites where a "perfect storm" of poor nutrition and defoliation stress may lead to especially poor health and greater ash mortality. Topographic position appears to stress ash trees due to low base cation availability on upper slope conditions. Elm spanworm defoliation further exacerbates the poor health of the already stressed trees.

## CONCLUSIONS AND MANAGEMENT IMPLICATIONS

This study provided a landscape-level picture of white ash health and its relationship to topographic position, past defoliation events, and nutrient availability. The synergistic interactions among these factors can create conditions that lead to dieback and death of ash trees. Our results suggest that management of upper slope areas with low nutrient availability to favor nonash species that may have better health and survival in these conditions could lead to improvements in forest health.

As future stressors occur in forest landscapes, their distribution and effects on trees will be affected by the underlying patterns of tree stress that already exist. Understanding these patterns can help us predict the effects of and possibly respond to future threats. For example, EAB, an introduced pest that kills ash trees, is known to be attracted to stressed ash trees, and stressed ash trees are known to die more rapidly than healthy trees in EAB-infested areas. The results of our study could assist in management planning and improve EAB detection by targeting high-risk areas.

## CONTACT INFORMATION

Kathleen Knight: ksknight@fs.fed.us.

## LITERATURE CITED

Bailey, S.W.; Horsley, S.B.; Long, R.P.; Hallett, R.A. 2004. Influence of edaphic factors on sugar maple nutrition and health on the Allegheny Plateau. Soil Science Society of America Journal. 68: 243-252.

Finzi, A.C.; Canham, C.D.; Van Breemen, N. 1998. Canopy tree-soil interactions within temperate forests: species effects on pH and cations. Ecological Applications. 8: 447-454.

Han, Y.; Castello, J.D.; Leopold, D.J. 1991. Ash yellows, drought, and decline in radial growth of white ash. Plant Disease. 75: 18-23.

Horsley, S.B.; Long, R.P.; Bailey, S.W. [and others]. 2000. Factors associated with the decline disease of sugar maple on the Allegheny Plateau. Canadian Journal of Forest Research. 30: 1365-1378.

Morin, R.S.; Liebhold, A.M.; Gottschalk, K.W. [and others]. 2006. Analysis of Forest Health Monitoring surveys on the Allegheny National Forest (1998–2001). Gen. Tech. Rep. NE-339. Newtown Square, PA: U.S. Department of Agriculture Forest Service, Northeastern Research Station. 102 p.

Royo, A.A.; Knight K.S. 2012. White ash (*Fraxinus americana*) decline and mortality: the role of site nutrition and stress history. Forest Ecology and Management. 286: 8-15.

Royo, A.A.; Knight, K.S.; Himes, J.M.; Will, A.N. 2012. White ash (*Fraxinus americana*) health in the Allegheny Plateau region, Pennsylvania: evaluating the relationship between FIA phase 3 crown variables and a categorical rating system. In: McWilliams, W.; Roesch, F.A., eds. Monitoring across borders: 2010 joint meeting of the Forest Inventory and Analysis (FIA) symposium and the Southern Mensurationists. e-Gen. Tech. Rep. SRS-157. Asheville, NC: U.S. Department of Agriculture Forest Service, Southern Research Station. 123-129.

Smith, A. 2006. Effects of community structure on forest susceptibility and response to the emerald ash borer invasion of the Huron River watershed in southeast Michigan. Columbus: The Ohio State University. 122 p. M.S. thesis.

# CHAPTER 14.

## Use of Forest Inventory Data to Document Patterns of Yellow-Cedar Occurrence, Mortality, and Regeneration in the Context of Climate

(Project WC-EM-09-02)

P. Hennon
J. Caouette
T. Barrett
D. Wittwer



This chapter was previously published as Hennon, P.; Caouette, J.; Barrett, T.M.; Wittwer, D. 2011. Use of forest inventory data to document patterns of yellow-cedar occurrence, mortality, and regeneration in the context of climate. In: Forests of southeast and south-central Alaska, 2004–2008. Gen. Tech. Rep. PNW-GTR-835. Portland, OR: U.S. Department of Agriculture Forest Service, Pacific Northwest Research Station: 57-62.

## BACKGROUND

Yellow-cedar (*Callitropsis nootkatensis*) has great cultural and economic value but has experienced widespread mortality for about 100 years in southeast Alaska (Hennon and Shaw 1997). The tree mortality, known as yellow-cedar decline, appears as dense concentrations of dead yellow-cedar trees (fig. 14.1), which are readily detectable by aerial survey or other forms of remote sensing. Yellow-cedar decline occurs primarily in unmanaged forests on wet soils where trees of various sizes and ages die and remain standing long after death. The cause of yellow-cedar decline appears to be freezing injury of shallow fine roots when they are not protected by snow in late winter or spring (Hennon and others 2012, Schaberg and others 2008). The Forest Service Forest Health Protection team has developed a fairly complete distribution map for yellow-cedar decline; it occurs in more than 2,000 locations totaling over 500,000 acres (Lamb and Winton 2010). Producing maps and geographic information system layers for healthy yellow-cedar forests has proven more difficult, however, because cedar trees are not easily distinguished from hemlocks and other trees in mixed-species forests. Thus, there is no reliable information on the current distribution of healthy yellow-cedar forests to place the decline issue into some spatial context.

*Figure 14.1—Yellow-cedar decline results in more than 70-percent mortality of yellow-cedar, which can be detected by aerial surveys and other forms of remote sensing. Evaluating healthy yellow-cedar forests requires the use of inventory data. (Photo: USDA Forest Service)*

## METHODS

We used Forest Inventory and Analysis (FIA) and other inventory plot data and personal field observations in selected areas to produce a coarse distribution map of yellow-cedar forests for southeast Alaska. For this coarse map, entire watersheds were designated as having yellow-cedar if yellow-cedar was present in an inventory plot or was observed there. We overlaid the map of dead cedar forests generated from the forest health detection aerial survey to determine how yellow-cedar decline fits into the general distribution of the tree.

We also analyzed FIA inventory data on the occurrence of live, dead, and regenerating yellow-cedar by elevation classes to evaluate our observations that the tree is dying at low elevations but thriving and regenerating at higher elevations in the region. We calculated ratios of live trees to dead trees and live trees to live saplings using a 5-inch diameter threshold to separate trees and saplings, and then charted these ratios by elevation to explore trends of how yellow-cedar populations may be changing by elevation. Results that relate numbers of yellow-cedar trees to elevation used FIA plots that were measured between 1995 and 1998; there were 625 forested plots with yellow-cedar trees in that inventory. For information about net change of yellow-cedar in the region, we used 307 of these plots that were remeasured from 2004 through 2008.

## RESULTS

The map showing the occurrence of yellow-cedar in southeast Alaska (fig. 14.2) is the most detailed view of yellow-cedar's natural range within the region. Yellow-cedar is present throughout most of southeast Alaska, but there are areas where it is rare or absent. For example, yellow-cedar is apparently missing from large areas in the northeastern portion of the panhandle, even though there is abundant

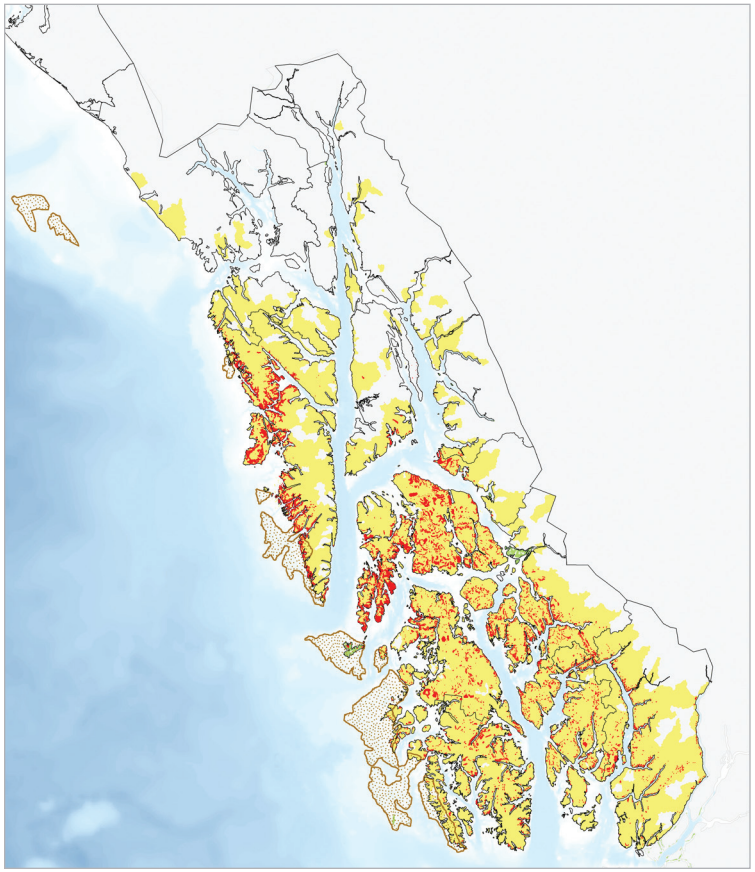

*Figure 14.2—Occurrence map of yellow-cedar in southeast Alaska (yellow) from Forest Inventory and Analysis and other inventory data and several personal observations, and the distribution of yellow-cedar decline (red) mapped during forest health aerial detection surveys. Note that yellow-cedar decline occurs within most, but not all, of the range of yellow-cedar in southeast Alaska. The speckled areas along the outer west coast of the region indicate glacial refugia during the late Pleistocene Epoch (Carrara and others 2007) and may represent the origins for yellow-cedar for subsequent Holocene migration.*

suitable habitat present in the form of bog and forested wetland complexes. This regional map of yellow-cedar is useful for a variety of purposes; for example, it has already been used to illustrate where yellow-cedar is present as a resource for bark and wood collection by native people near each of the villages or towns. Also, we used this map as the basis for sampling in a new regionwide population genetics study for yellow-cedar.

Overlaying the yellow-cedar decline on this map reveals that the intensive mortality problem covers only part of yellow-cedar's regional distribution. Yellow-cedar decline is present in the southern and northwestern portions of the panhandle, but yellow-cedar growing in the northeastern portion of the panhandle appears to be free of the intensive mortality.

Although yellow-cedar can be found from shoreline forests to timberline in southeast Alaska, inventory data reveal that the

abundance of this tree peaks at mid-elevation range (fig. 14.3). Tree death and regeneration of yellow-cedar show somewhat of a departure by elevation from this pattern of live trees. The ratio of dead trees to live trees was greatest at lower elevation and then diminished upslope, but the ratio of live trees to live saplings showed the opposite relationship, with a greater proportion of regeneration at higher elevations (fig. 14.4).

Overall, change in net live tree biomass of yellow-cedar between the 1995–98 and 2004–08 inventories showed an increase of 0.61 percent, which was not significantly different from 0 ($p = 0.4064$). Average annual mortality of trees greater than 5 inches diameter at breast height (d.b.h.) was 0.30 percent (standard error = 0.04 percent). Average annual harvest rate was 14 percent of average annual mortality, for a total tree death rate of 0.34 percent. Total number of live yellow-cedar trees greater than or equal to 5 inches d.b.h. did not show significant change in biomass between the 1995–98 and 2004–08 inventories ($p = 0.7443$).

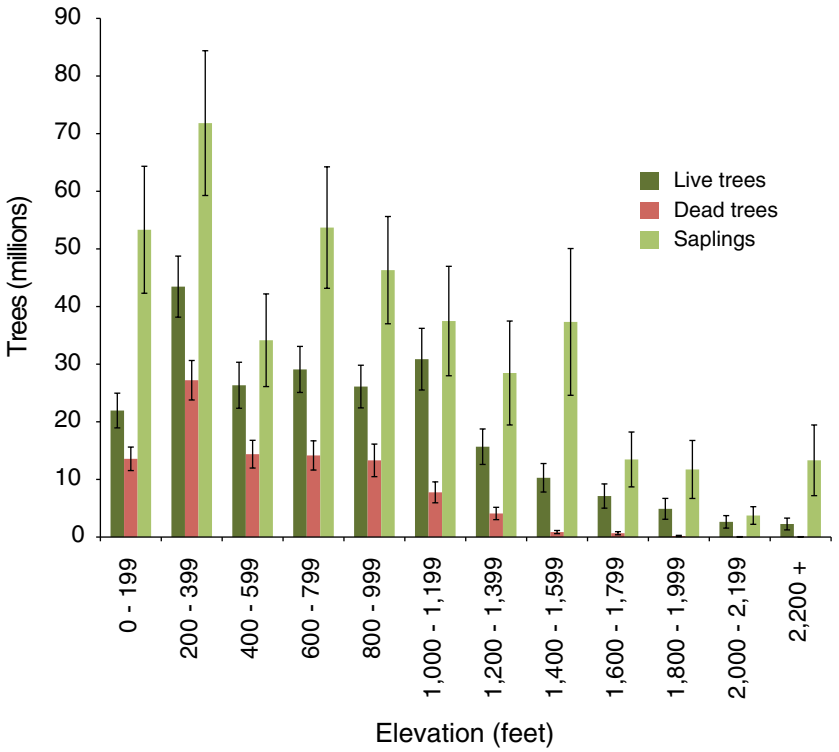


*Figure 14.3—Numbers of yellow-cedar trees (live trees ≥ 5 inches diameter at breast height [d.b.h.], dead trees ≥ 5 inches d.b.h., and live saplings < 5 inches d.b.h.) by elevation. Lines at end of bars represent ± standard error.*

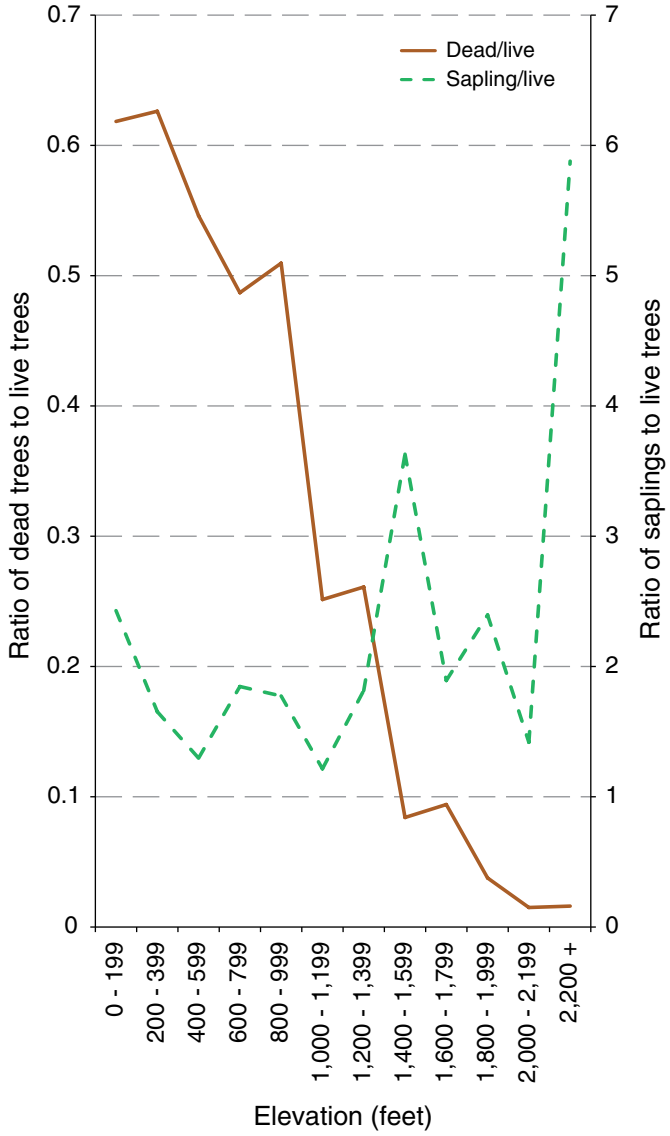


*Figure 14.4—Ratio of yellow-cedar dead trees to live trees and live saplings to live trees for 200-foot elevation classes from Forest Inventory and Analysis inventory plot data.*

## INTERPRETATION

The general occurrence of yellow-cedar in southeast Alaska may be the result of long-term climate change in the region combined with yellow-cedar's low reproductive capacity. We hypothesize that yellow-cedar survived the late Pleistocene Epoch in forested refugia along the outer western coast of the panhandle when most of the region was covered by ice sheets (Carrara and others 2007). Yellow-cedar likely began to colonize much of southeast Alaska during favorable climate conditions in the last 4,000 years, but our data suggest that the species is still actively migrating toward the northeast. This scenario may explain the absence or rarity of the tree in the northeast portion of southeast Alaska. The above-mentioned population genetics study based on our yellow-cedar map is designed to evaluate this hypothesis. Yellow-cedar also grows farther to the northwest in Prince William Sound. Populations are so small there that we were able to produce a map of the tree's range there by observations from a boat (Hennon and Trummer 2001).

The pattern of yellow-cedar decline within the general distribution of yellow-cedar is consistent with our interpretation that seasonal snow depth is a controlling factor for yellow-cedar decline. The lowest snow zone on a regional snow map shows a remarkably close association with yellow-cedar decline (Hennon and others 2008). Areas with more annual accumulation of snow are generally those that have healthy yellow-cedar populations. Snow protects yellow-cedar from the proximal injury leading to tree death—freezing injury of shallow-growing fine roots in late winter (Schaberg and others 2008).

Yellow-cedar death in FIA plots is more common at low elevations. This is consistent with the same finding from aerial surveys, where the acreage of yellow-cedar decline mapped was clearly skewed toward lower elevations (Lamb and Winton 2010). The association of yellow-cedar decline with lower elevations is consistent with the role of snow in protecting yellow-cedar from the freezing scenario mentioned above.

Tree species that show different elevational patterns of occurrence among live trees, dead trees, and regeneration may be considered relatively unstable with regard to climate. More stability for a tree species would be exhibited by a pattern where live trees, dead trees, and regeneration had similar elevational trends. Yellow-cedar appears to be a species in flux, however, as our data indicate the trees are dying at low elevation, surviving as live trees at mid-elevation, and regenerating at higher elevation. Thus, under the recent-past and current climate, yellow-cedar populations appear to be shifting to higher elevations.

The relatively low rate of recent tree mortality is interesting given the large acreage of dead yellow-cedar in southeast Alaska. Our reconstruction of yellow-cedar mortality through the 1900s shows that tree death peaked during the 1970s and 1980s (Hennon and Shaw 1994). We have observed recent mortality in specific areas, despite the fairly low regional mortality rate. Although pollen records clearly show that tree species migrate over time in response to climate, little is known about the process of migration. The long-term occurrence of yellow-cedar is not well known because the species was omitted from the classic pollen profile studies conducted in the region (Heusser 1960). Spatially differentiated mortality and regeneration could occur either gradually or in

pulses. If mortality is caused by the combination of low snow cover and spring freezing, both episodic events, then mortality would occur in pulses. However, yellow-cedar trees may take a long time to die after they are injured, as root damage from weather can have cumulative effects on tree growth and health (Beier and others 2012). These possibilities suggest that monitoring needs to be long term to capture temporal variability as well as spatial variability.

These findings can contribute to development of an adaptive strategy for the conservation and management of yellow-cedar (Hennon and others 2012). Continued analysis of inventory plot data for yellow-cedar habitat preferences would aid in the construction of a high-resolution distribution map. A distribution map could be combined with aerial surveys of dead cedar and snow modeling to partition the landscape of coastal Alaska into areas that are unsuitable and suitable for yellow-cedar. Inventory plot data should be queried to evaluate successional trends in forests impacted by yellow-cedar decline to project the future composition and productivity of these forests. Inventory data could also be used to document the resource (e.g., diameter classes and volume) of dead yellow-cedar that might be available for salvage recovery on the roughly 500,000 acres of yellow-cedar decline.

## LITERATURE CITED


Beier, C.M.; Sink, S.E.; Hennon, P.E. [and others]. 2008. Twentieth-century warming and the dendroclimatology of declining yellow-cedar forests in southeastern Alaska. Canadian Journal of Forest Research. 38: 1319-1334.

Carrara, P.E.; Ager, T.A.; Baichtal, J.F. 2007. Possible refugia in the Alexander Archipelago of southeastern Alaska during the late Wisconsin glaciation. Canadian Journal of Earth Sciences. 44: 229-244.

Hennon, P.E.; D'Amore, D.V.; Schaberg, P.G.; Witter, D.T.; Shanley, C.S. 2012. Shifting climate, altered niche, and a dynamic conservation strategy for yellow-cedar in the North Pacific coastal rainforest. Bioscience. 62(2): 147-158

Hennon, P.E.; Shaw, C.G., III. 1994. Did climatic warming trigger the onset and development of yellow-cedar decline in southeast Alaska? European Journal of Forest Pathology. 24: 399-418.

Hennon, P.; Shaw, C.G., III. 1997. The enigma of yellow-cedar decline: what is killing these defensive, long-lived trees in Alaska? Journal of Forestry. 95(12): 4-10.

Hennon, P.E.; Trummer, L.M. 2001. Yellow-cedar (*Chamaecyparis nootkatensis*) at the northwest limits of its range in Prince William Sound, Alaska. Northwest Science. 75: 61-72.

Heusser, C.J. 1960. Late Pleistocene environments of North Pacific North America. New York: American Geographical Society. Special Publication 35. 308 p.

Lamb, M.; Winton, L., comps. 2010. Forest health conditions in Alaska—2009. Protection Report R10-PR21. Anchorage, AK: U.S. Department of Agriculture Forest Service, Alaska Region, Forest Health Protection. 73 p.

Schaberg, P.G.; Hennon, P.E.; D'Amore, D.V.; Hawley, G.J. 2008. Influence of simulated snow cover on the cold tolerance and freezing injury of yellow-cedar seedlings. Global Change Biology. 14: 1282-1293.

# CHAPTER 15.

# Thousand Cankers Disease in Tennessee: For How Long?

## (Project SO-EM-B-11-01)

KaDonna Randolph

## INTRODUCTION

In August 2010, the Tennessee Department of Agriculture (TDA) announced the discovery of the walnut twig beetle (WTB) (*Pityophthorus juglandis*) and associated fungus *Geosmithia morbida* in Knox County (TN.gov Newsroom 2010). This find, the first east of Colorado, incited alarm due to the potentially devastating effects on black walnut (*Juglans nigra* L.), an extremely valuable tree species that is highly susceptible to the thousand cankers disease (TCD) caused by *G. morbida*. After the initial discovery in Knox County, TCD was identified in five other Tennessee counties: Anderson, Blount, Loudon, Sevier, and Union (TN.gov Newsroom 2011). All six counties were quarantined by TDA to limit the movement of black walnut material out of the infested areas.

Symptoms of TCD include yellowing leaves and thinning foliage in the upper part of the crown. As the disease progresses, crown dieback continues with progressively larger branches dying until the tree completely succumbs to mortality, often within 2 to 4 years of the earliest visible symptoms (Hansen and others 2011, Kolařík and others 2011, Seybold and others 2010). TCD may have been present in Tennessee 10 to 20 years prior to its discovery (Haun and others 2010). If this is indeed the case, then it is possible that evidence of its presence might exist in the data collected by the Forest Inventory and Analysis (FIA) Program. Among the data collected by FIA are descriptions of individual tree crown condition and tree status (live or dead); therefore, the objectives of this project were to (1) analyze black walnut crown conditions from the past 10 years to determine if symptoms of TCD were present, (2) locate areas that have black walnut trees with poor crown conditions that might suggest the presence of TCD, and (3) evaluate the effectiveness of the FIA plot network for detecting localized forest health problems (Randolph and others 2010).

## METHODS

Data included in this study were collected by the Southern FIA Program in Tennessee between 2000 and 2009. Under the current inventory, FIA has two phases of on-the-ground data collection. Traditional timber inventory variables are collected in what is known as the phase 2 (P2) inventory, and additional forest health variables are collected in the phase 3 (P3) inventory (Bechtold and Patterson 2005). FIA plots are located across the United States in such a way that each P2 plot represents about 2428 ha. P3 plots, a 1/16 subset of the P2 plots, represent about 38 850 ha each. Both P2 and P3 plots consist of four 7.32-m fixed-radius subplots spaced 36.6 m apart in a triangular arrangement.

Variables included in the analysis were tree status (live or dead), four assessments of crown condition, and cause of death. The crown assessments were crown density (the amount of crown branches, foliage, and reproductive structures that blocks light visibility through the projected crown outline), crown dieback (recent mortality of branches with fine twigs, which begins at the terminal portion of a branch and proceeds inward toward the trunk), foliage

transparency (the amount of skylight visible through the live, normally foliated portion of the crown, excluding dieback, dead branches, and large gaps in the crown), and hardwood dieback incidence (hereafter, "SRS dieback;" recorded as present if 10 percent or more of the crown area is affected with dieback that has occurred from the branch tips inward or as absent if otherwise) (Schomaker and others 2007, USDA Forest Service 2008). Possible causes of death were insect, disease, fire, animal, weather, vegetation (includes suppression, competition, and vines; e.g., kudzu), silvicultural or land clearing activity, or unknown (USDA Forest Service 2008). Tree status was recorded for all trees and SRS dieback for all hardwood trees measured on both P2 and P3 plots. Cause of death was recorded for all dead trees on both P2 and P3 plots. Crown density, crown dieback, and foliage transparency were assessed for all live trees on all P3 plots, and crown density and crown dieback additionally on all P2 plots included in the Tennessee urban FIA pilot study (Nowak and others 2012). Trees were categorized as "recent mortality" if the status was "live" at the previous inventory but "dead" at the most recent inventory, between 2005 and 2009. Only trees ≥ 12.7 cm diameter at breast height (d.b.h.) were included.

Black walnut crown density, crown dieback, and foliage transparency were averaged for the entire State and by plot for the years 2005–09. Frequency of SRS dieback was summarized by year, 2000–09, for black walnut individually and for all other hardwood species combined. Plot maps of the crown condition averages and occurrences of SRS dieback, recent black walnut mortality, and mortality causes between 2005 and 2009 were examined visually for spatial correlation.

## RESULTS

Between 2005 and 2009, 23 black walnut trees were assessed for crown condition on 17 P3 plots across Tennessee. During this time, crown conditions averaged 44.3 percent crown density, 0.4 percent crown dieback, and 21.7 percent foliage transparency. The percentage of trees with SRS dieback fluctuated annually between 0.0 percent in 2000, 2006, and 2008 and 10.2 percent in 2002. This annual variation was greater than that observed for all other hardwoods, which ranged from 0.0 percent in 2000 to 2.7 percent in 2003. There were 31 live black walnut trees assessed for crown condition across 20 P2 urban plots. Crown conditions for those trees averaged 36.0 percent crown density and 16.3 percent crown dieback. At the plot level, most crown density and foliage transparency averages were generally "normal and healthy" (fig. 15.1). The plots that were marginally healthy in terms of crown density (i.e., ≤ 35 percent crown density) were scattered throughout the State. Only one plot had a crown dieback average at the marginal health level, and that was a P2 urban plot observed in Knox County (fig. 15.1B).

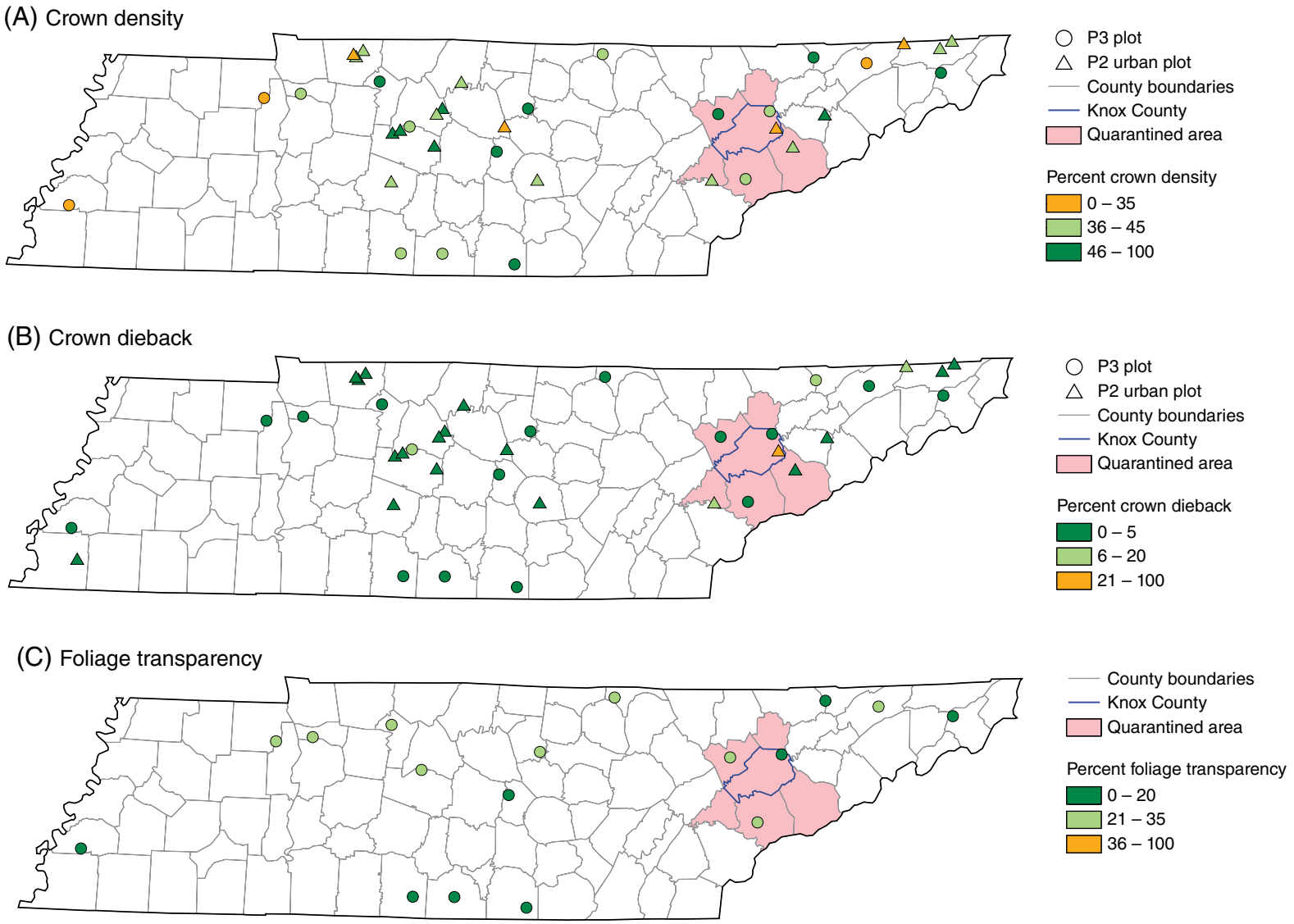


*Figure 15.1—Thousand cankers disease quarantined counties and mean crown conditions by plot for black walnut trees in Tennessee between 2005 and 2009: (A) crown density, (B) crown dieback, and (C) foliage transparency. Plot locations are approximate.*

Recent mortality was scattered throughout Tennessee but occurred most often in middle Tennessee. Vegetation was the most frequently recorded cause of death for black walnut (fig. 15.2). In the six quarantined counties in particular, 35 live and 12 dead black walnut trees (d.b.h. ≥ 12.7 cm) were observed on 23 of the 161 forested P2 plots between 2005 and 2009. The dead trees were observed in Blount (1 tree), Knox (5 trees), and Sevier (6 trees) Counties. Cause of death was recorded for 9 of these 12 dead walnuts as vegetation (4 trees), disease (2 trees), silviculture/land clearing (2 trees), or weather (1 tree). Only 4 of these trees, 2 killed by disease and 2 by vegetation and both in Knox County, were classified as recent mortality. All of the dead walnuts observed in Sevier County were dead upon their first encounter in 2000 or 2001, as was the one dead walnut in Blount County, first observed in 1999.

## DISCUSSION

Williams (1990) noted that black walnut typically occurs as individual trees or small clusters scattered throughout the mixed hardwood forest. This pattern was supported by the plot data collected in Tennessee. When occurring on a plot, the number of live black walnut trees ranged between 1 and 7, with an average of 1.4 live trees per P3 plot. This infrequent occurrence across the landscape in conjunction with the P3 sampling intensity makes it difficult to capture an adequate sample for rigorous estimation of black walnut crown conditions in Tennessee. Indeed, the number of plots with black walnut trees in the P3 sample falls short of the number of plots recommended by Bechtold and others (2009) for estimating changes over time. Nevertheless, some general observations about black walnut and the possible extent of TCD in Tennessee can be gleaned from

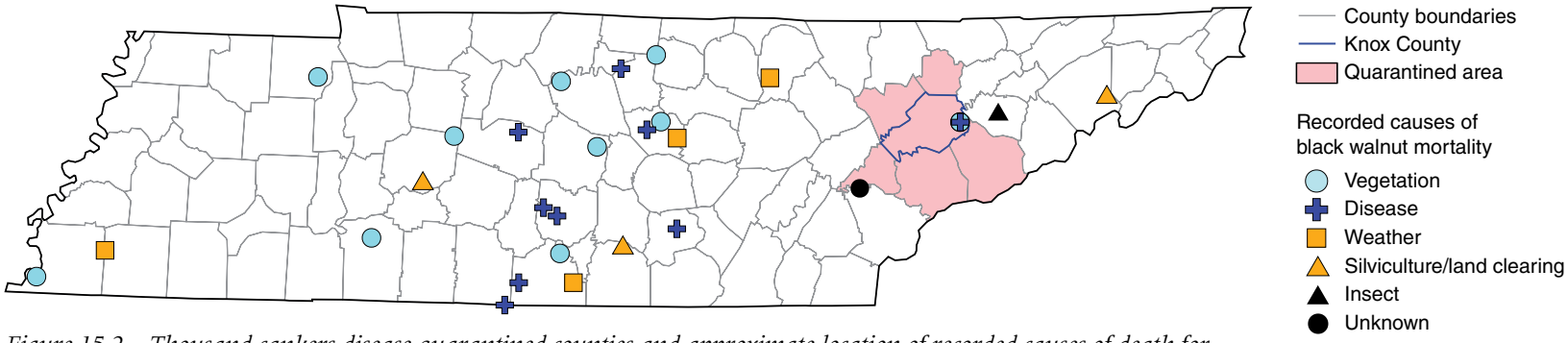


*Figure 15.2—Thousand cankers disease quarantined counties and approximate location of recorded causes of death for recent black walnut mortality in Tennessee, 2005 to 2009.*

the FIA data. Most notably is that within the six quarantined counties, recent mortality and extremely poor crown conditions were confined to the same one plot in Knox County. Further, Nowak and others (2012) noted that 14 percent of the black walnut urban sample was standing dead, all of which occurred on this same P2 urban plot in Knox County. Crown conditions on the remaining plots in the quarantined counties, and for the State overall, were within the range of what is typically considered normal and healthy for hardwood trees. This seems to suggest that the WTB may not have invaded the forest at large or has not progressed far enough to be detected.

During the course of this project, WTB and TCD were discovered in Virginia and Pennsylvania, and the investigation was expanded to include the entire native range of black walnut in the Eastern United States. A comprehensive treatment of the findings for the expanded investigation is given by Randolph and others.[1] The same general conclusions found in this Tennessee-specific investigation were concluded in the expanded project. That is, overall crown conditions were generally within the normal range for hardwood trees and were relatively stable between 2000 and 2010, with no obvious clustering of poor crown conditions or recent mortality due to unknown causes.

[1]Randolph, K.C.; Rose, A.K.; Oswalt, C.M.; Brown, M.J. Manuscript in preparation. Status of black walnut (*Juglans nigra* L.) in the Eastern United States. Authors can be reached at Southern Research Station, Forest Inventory and Analysis, 4700 Old Kingston Pike, Knoxville, TN 37919.

## CONCLUSION

Across Tennessee, black walnut crown conditions were within the range of what is typically considered normal and healthy for hardwood trees. Overall, little in the FIA data suggested the presence of WTB and TCD in the forested landscape of Tennessee. This could be due to the actual absence of WTB or perhaps an insufficient inventory and monitoring system to detect its presence. Given the distribution of recent mortality, middle Tennessee may be an area for special WTB and TCD surveys.

## CONTACT INFORMATION

KaDonna Randolph: krandolph@fs.fed.us; 865–862–2024.

## LITERATURE CITED

Bechtold, W.; Randolph, K.; Zarnoch, S. 2009. The power of FIA phase 3 crown-indicator variables to detect change. In: McWilliams, W.; Moisen, G.; Czaplewski, R., comps. Forest Inventory and Analysis (FIA) symposium 2008. Proc. RMRS–P–56CD. Fort Collins, CO: U.S. Department of Agriculture Forest Service, Rocky Mountain Research Station: 21 p.

Bechtold, W.A.; Patterson, P.L., eds. 2005. The enhanced Forest Inventory and Analysis Program—national sampling design and estimation procedures. Gen. Tech. Rep. SRS-80. Asheville, NC: U.S. Department of Agriculture Forest Service, Southern Research Station. 85 p.

Hansen, M.A.; Bush, E.; Day, E. [and others]. 2011. Walnut thousand cankers disease alert. Virginia Cooperative Extension. http://www.ppws.vt.edu/~clinic/alerts/07-22-11_TCD_alert.pdf. [Date accessed: September 19].

Haun G.; Powell, S.; Strohmeier, C.; Kirksey, J. 2010. State of Tennessee thousand cankers disease action plan. http://www.tn.gov/agriculture/publications/regulatory/TN_TCD_ActionPlan.pdf. [Date accessed: October 25].

Kolařík, M.; Freeland, E.; Utley, C.; Tisserat, N. 2011. *Geosmithia morbida* sp. nov., a new phytopathogenic species living in symbiosis with the walnut twig beetle (*Pityophthorus juglandis*) on *Juglans* in USA. Mycologia. 103(2): 325–332.

Nowak, D.J.; Cumming, A.B.; Twardus, D.T. [and others]. 2012. Urban forests of Tennessee, 2009. Gen. Tech. Rep. SRS-149. Asheville, NC: U.S. Department of Agriculture Forest Service, Southern Research Station. 52 p.

Randolph, K.; Oswalt, C.; Rose, A.; Brown, M. 2010. Thousand cankers disease in Tennessee: for how long? (project proposal). http://fhm.fs.fed.us/em/funded/11/SO-EM-B-11-01.pdf. [Date accessed: February 15, 2012].

Schomaker, M.E.; Zarnoch, S.J.; Bechtold, W.A. [and others]. 2007. Crown-condition classification: a guide to data collection and analysis. Gen. Tech. Rep. SRS-102. Asheville, NC: U.S. Department of Agriculture Forest Service, Southern Research Station. 78 p.

Seybold, S.; Haugen, D.; O'Brien, J.; Graves, A. 2010. Pest alert: thousand cankers disease. NA–PR–02–10. Newtown Square, PA: U.S. Department of Agriculture Forest Service, Northeastern Area State and Private Forestry. 2 p.

TN.gov Newsroom. 2010. Thousand cankers disease discovered in East Tennessee. Press release. August 5, 2010. Nashville, TN: State of Tennessee Government. http://news.tn.gov/node/5684. [Date accessed: September 13, 2011].

TN.gov Newsroom. 2011. Walnut tree quarantine expanded due to thousand cankers disease. Press release. August 29, 2011. Nashville, TN: State of Tennessee Government. http://news.nt.gov/node/7691. [Date accessed: September 12].

U.S. Department of Agriculture (USDA) Forest Service. 2008. Forest Inventory and Analysis national core field guide: field data collection procedures for phase 2 plots, version 4.0. Vol.: SRS MIDAS version, updated October 1, 2008. Knoxville, TN: U.S. Department of Agriculture Forest Service, Forest Inventory and Analysis Program, Southern Research Station. [Pages unknown].

Williams, R.D. 1990. Black walnut. In: Burns, R.M.; Honkala, B.H., tech. cords. Silvics of North America. Vol. 2: hardwoods. Agric. Handb. 654. Washington, DC: U.S. Department of Agriculture Forest Service. [Pages unknown].

# CHAPTER 16.

# Impacts of Swiss Needle Cast in the Cascade Mountains of Northern Oregon: Monitoring of Permanent Plots After 10 Years

(Project WC-EM-B-11-01)

Gregory M. Filip
Alan Kanaskie
Will R. Littke
John Browning
Kristen L. Chadwick
David C. Shaw
Robin L. Mulvey



## INTRODUCTION

Swiss needle cast (SNC), caused by the fungus *Phaeocryptopus gaeumannii*, is one of the most damaging diseases of coast Douglas-fir (*Pseudotsuga menziesii* var. *menziesii*) in the Pacific Northwest (Hansen and others 2000, Mainwaring and others 2005, Shaw and others 2011). Biological impact is particularly acute on the Oregon and Washington coasts, one of the most productive regions for temperate forest growth. In 2011, an aerial detection survey of coastal Oregon mapped more than 444,000 acres of Douglas-fir forest with obvious symptoms of SNC, the highest acreage recorded since surveys started in 1996. Annual Douglas-fir volume-growth losses from SNC are estimated at about 23 percent over 187,000 acres, with some stand-level volume losses as high as 52 percent in northwest Oregon (Maguire and others 2002, 2011).

Although defoliation from SNC occurs in the northern Cascade Mountains of Oregon, it is believed to be less damaging than in the Oregon Coast Range probably because of differences in sites, stands, and the pathogen. In particular, persistent wet conditions in the spring and early summer, during the sporulation and infection period, and mild winter temperatures are believed to provide ideal conditions for disease development. In 2001, baseline monitoring plots were established in 59 stands representing 2 million acres in the Cascade Mountains in Oregon using Forest Health Monitoring Program funding. These plots must be remeasured after 5 and 10 years in order to determine the impact of SNC on Douglas-fir growth. These plots currently are the only source of data for SNC impact in the Oregon Cascade Range.

Primary objectives of our project were to determine changes after 5 and 10 years (2001 to 2011) in (1) tree diameter, (2) total-height growth, (3) live-crown ratio (LCR), and (4) SNC severity as estimated by needle retention and density of stomata occlusion in 59 stands in the northern Oregon Cascade Mountains. In 2011, our secondary objective was to compare foliage retention estimates in the field with those in the laboratory.

## METHODS

From April to June 2001, prior to Douglas-fir budbreak, transects were installed in 59 stands. Sampled stands were initially 10 to 23 years old and contained more than 50 percent Douglas-fir. Stands were systematically located on public and private lands in the western Oregon Cascade Mountains (Freeman 2001).

Ten Douglas-fir trees were sampled per stand, for a total of 590 trees. Branches were sampled at mid-crown for foliage retention and needle stomata occlusion associated with SNC. Each stand had one transect with five sample plots located at 50-foot intervals. Transects were established in a location representative of each stand, based on aerial photos. Stand data collected in 2001 included (1) elevation, (2) slope aspect (eight cardinal points), (3) slope percent, and (4) Global Positioning System (GPS) coordinates at the reference point at the start of each transect.

At each plot, the nearest codominant or dominant Douglas-fir on each side of the transect was selected. Data collected for each tree in 2001 included (1) stand, plot, and tree number; (2) diameter at breast height (d.b.h., at 4.5 feet aboveground, nearest 0.1 inch); (3) total height (nearest foot); (4) height to lowest live branch (nearest foot); (5) ocular estimation of foliage retention in the mid-crown (0 to 8 years); and (6) foliage-retention index, calculated for each sampled branch. For estimating foliage retention in the mid-crown (0 to 8 years), a tree that had 100 percent of 1-year-old needles, 100 percent of 2-year-old needles, 60 percent of 3-year-old needles, and 20 percent of 4-year-old needles would be rated 2.7 years. Heights were measured in 2001 with a clinometer. LCRs were calculated by subtracting height to lowest live branch from total tree height to get live-crown length, and then dividing live-crown length by total tree height and multiplying by 100.

Foliage-retention index was calculated for each sample tree as follows. A live branch at mid-crown was selected on the south side of the sample tree and cut from the stem with a pole pruner. For trees with a mid-crown height greater than 25 feet (most trees in 2011), the tree was climbed by a certified climber, and the selected branch was severed at the trunk with a hand saw. From the cut branch, a secondary lateral branch that was at least 4 years old was selected, and the amount of foliage remaining in each needle age class (up to 4 years) was rated and recorded as: 0 = 0 to 10 percent of full complement present, 1 = 11 to 20 percent present, 2 = 21 to 30 percent present, … 9 = 90 to 100 percent present. Ratings were summed for a minimum score of 0 and a maximum of 36 for each branch. Foliage retention has been shown to be the most reliable and efficient variable when estimating SNC severity in terms of tree volume-growth loss (Filip and others 2000, Hansen and others 2000, Maguire and others 2002). Foliage retention estimates from the mid-crown are considered more reliable than upper or lower crown estimates, especially in larger trees.

From April to July 2006 and 2011, the 59 stands sampled in 2001 were relocated using reference maps, aerial photos, and GPS coordinates. The same data collected in 2001 were collected for each tree in the 59 stands. If a sample tree was dead or severely broken, the cause was recorded and the nearest live Douglas-fir tree was selected as a replacement. Data from replacement trees, however, were not used in our analyses. Total height and height of the lowest live branch were measured with a laser height measurer (Laser Technology, Inc.).

In 2006 and 2011, for all 10 sample trees per stand, foliage from severed branches was placed in a sample bag, labeled with stand and tree number, and processed in the Weyerhaeuser Corp. laboratory (Centralia, WA) for pseudothecial counts and foliage retention (2011 only). Pseudothecial density, measured as the percentage of needle stomata occluded, is a direct method of determining the presence of *Phaeocryptopus gaeumannii* and severity of the disease. Measurements were made on 2-year-old needles only. In 2002, foliage from 10 of 37

stands was sampled for fungal DNA to determine fungal lineage (Freeman 2002, Winton and Stone 2004).

For pseudothecial counts in 2006 and 2011, sampled needles were placed under a camera (Big-C Dino-Lite Pro AD413T [USB] 12x~200X) connected to a laptop computer, and the percentage of occluded stomata was recorded at 200X magnification. Foliage retention during the last 4 years also was calculated in the lab in the same manner as was done in the field on a scale of 0 to 36.

Because some stands were thinned and stand density can influence tree growth, total basal area per acre and basal area per acre of Douglas-fir were calculated in 2006 and 2011 around one tree at each of the five sample points. Total plot basal area was measured around each sample tree by counting all in-trees with a 10-factor prism and multiplying by a basal-area factor of 10. All trees greater than or equal to 1.0 inch d.b.h. of any species were counted. All data were entered into an Excel spreadsheet where $R^2$ values were calculated from selected graphed data.

## RESULTS AND DISCUSSION

From the 59 sampled stands, numbers of stands by each management agency were: Salem Bureau of Land Management = 16; Willamette National Forest = 12; Weyerhaeuser Corp. = 9; Mt. Hood National Forest = 7; Eugene Bureau of Land Management = 6; Port Blakely = 6; Longview Fibre Co. = 2; and Oregon Department of Forestry = 1. Stands ranged in elevation from 500 to 4,200 feet and percent slope from 0 to 60. Total basal area per acre in 2011 averaged 108 square feet (range = 34 to 198). Douglas-fir basal area per acre averaged 95 square feet (range = 34 to 198).

Some stands had been precommercially thinned either before or after initial plot establishment in 2001. Between 2001 and 2011, 46 plot trees (8 percent) were accidentally felled, broke, or died; these plot trees were replaced with other trees. The plot trees and their replacements were not included in stand means. Other major stand species besides Douglas-fir included western hemlock (*Tsuga heterophylla*) at the lower elevations and noble fir (*Abies procera*) at the upper elevations.

Mean 10-year d.b.h. growth was 4.2 inches (range = 1.8 to 6.0) and total-height growth was 24.7 feet (range = 8.3 to 31.8). Mean LCR decreased by 15.5 percent (range = 3.7 percent increase to 40.8 percent decrease) over 10 years; 6 of 43 (14 percent) stands increased in mean LCR. Sixteen trees were not measured for LCR in 2001. Correlations between total plot basal area and tree growth were poor, at $R^2 = 0.004$ for d.b.h. growth and 0.15 for height growth.

From field measurements, mean foliage-retention index decreased by 0.4 (range = -15.8 to 8.6) over 10 years. If lab measurements are used, however, foliage-retention index increased by 3.2 in 10 years. Ground-based estimates of

mid-crown foliage retention increased by 1.2 years (range -0.7 to 3.1) from 2001 to 2011. In 2006 and 2011, many trees had a partial 5th- year complement of needles and some trees as many as 8 years of needles, but these were not reflected in retention indices that scored only the last 4 years of needles. Mid-crown foliage ratings did capture 5- to 8-year-old needles. Correlations between field foliage-retention index and mid-crown foliage retention years were moderate, at $R^2 = 0.68$ in 2001, 0.54 in 2006, and 0.46 in 2011. Mid-crown foliage retention averaged 4.7 years, and only three stands had less than 3 years of foliage in 2011.

In 2011, foliage-retention index was measured in the field and again in the lab on a scale of 0 to 36. Correlation between the two sampling methods was moderate ($R^2 = 0.31$). Foliage-retention index measured in the lab was generally higher than measured in the field. We speculate that the lab estimates probably are more accurate than the field estimates because they were supervised by trained pathologists, while the field estimates mainly were conducted by the newly hired tree-climbing crew. Also, the lab estimate of an increase in 10-year foliage-retention index was in the same positive direction as the 10-year mid-crown foliage-retention ratings ocularly estimated from the ground.

Mean percentage of stomata occluded by pseudothecia was 8.7 percent for 2-year-old needles sampled in 2011; this needle cohort initially was infected as new growth after budbreak in 2009. No stands had mean stomata-occlusion densities greater than 34 percent in 2011. Correlation between 2011 field foliage-retention index and 2-year-old needle stomata occlusion was moderate, at $R^2 = 0.25$ (fig. 16.1). Correlation between 2011 lab foliage-retention

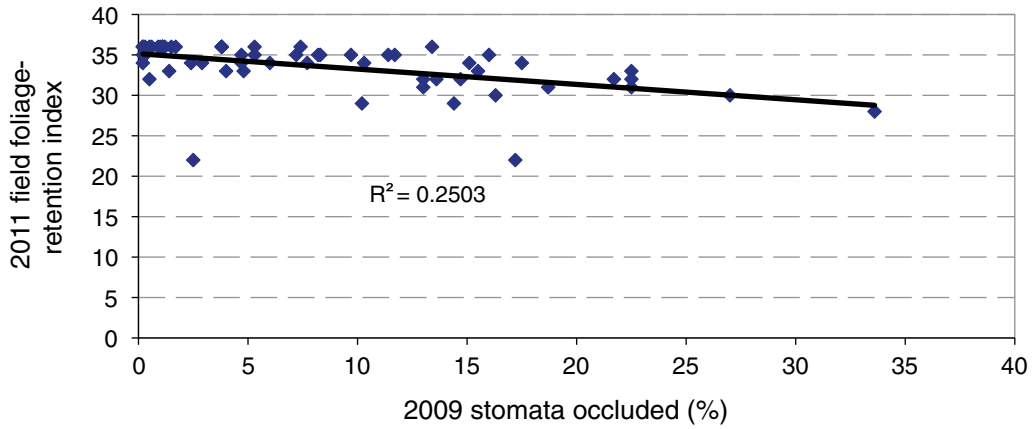


*Figure 16.1—2011 field foliage-retention index vs. 2009 (2-year-old) needle-pseudothecial density (stomata occluded). From Filip and others (2012).*

index and 2009 needle stomata occlusion also was moderate, at $R^2 = 0.25$. Other factors besides occluded stomata, such as tree genetics and soil-nutrient levels, are known to affect foliage retention.

In the Oregon Coast Range, Hansen and others (2000) showed that increasing proportions of stomata occupied by pseudothecia were associated with increasing defoliation. They recorded mean pseudothecial densities up to 50 percent in 1-year-old foliage and foliage retention as low as 1 year. In contrast, in 2011, our highest mean pseudothecial density was 33.6 percent in 2-year-old needles, and our lowest mean foliage retention was 2.3 years. All pseudothecia collected in the Cascade Range in 2002 were from lineage 1 (Winton and Stone 2004).

There was a moderate correlation between stand elevation and either 2011 foliage-retention index ($R^2 = 0.52$) or 2009 (2-year-old) needle-stomata occlusion ($R^2 = 0.52$; fig. 16.2). In general, there was more foliage and fewer pseudothecia at the higher elevations.

There were poor correlations between 2011 mid-crown foliage (yrs) and either 10-year d.b.h. growth ($R^2 = 0.05$; fig. 16.3) or total height growth ($R^2 = 0.01$; fig. 16.4). There were also poor correlations between diameter and height growth and 2011 foliage-retention index ($R^2 = 0.02$ and 0.06). Poor correlations occurred between 2009 (2-year-old) needle-stomata occlusion and either 10-year d.b.h. growth ($R^2 = 0.00$) or total height growth ($R^2 = 0.11$).

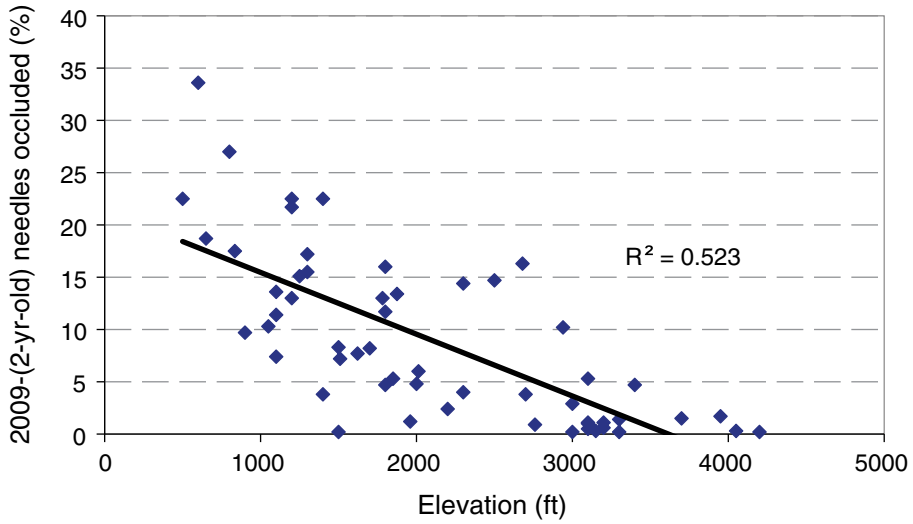


*Figure 16.2—2009 (2-year-old) needle-pseudothecial density (stomata occluded) and elevation. From Filip and others (2012).*

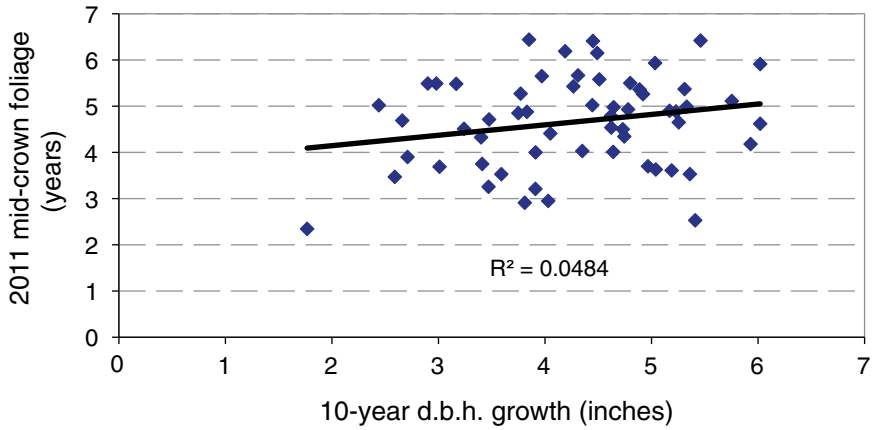


*Figure 16.3—2011 mid-crown foliage retention and 10-year diameter-at-breast-height growth. From Filip and others (2012).*

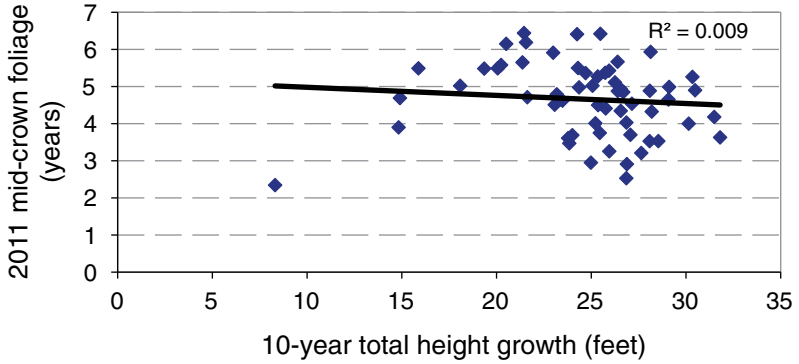


*Figure 16.4—2011 mid-crown foliage retention and 10-year total height growth. From Filip and others (2012).*

## CONCLUSIONS

No effect of SNC on Douglas-fir growth is apparent from 2001 to 2011 in the stands sampled in the Cascade Range. There are at least three possible reasons why this is so:

1. SNC levels during the past 10 years in the Cascade Range are not as severe as in the Oregon Coast Range. Only a few stands sampled in the Cascades have mean foliage retention of less than 3 years. There were no stands with mean stomata occlusion densities greater than 50 percent on 2-year-old needles in 2001, 2006, and 2011.

2. Oregon Cascade Range site characteristics, including plant associations, soil chemistry and parent material, air temperatures, and monthly precipitation and leaf wetness may not be as conducive to elevated populations of the causal fungus, *Phaeocryptopus gaeumannii*, and subsequent severe defoliation as in the Coast Range.

3. The genetics (lineage 1) of isolates of the causal fungus in the Oregon Cascades more closely resemble isolates from Idaho, Europe, and New Zealand than isolates from the Oregon Coast Range (Winton and Stone 2004). Also, lineage 2, which is abundant in the Oregon Coast Range, has not been reported in the Cascade Mountains.

Based on our results, forest managers do not need to change their current practices in the northern Oregon Cascades because of SNC. Managing a mix of Douglas-fir and western hemlock (at lower elevations) and noble fir (at higher elevations), however, will help offset any future stand-growth declines due to SNC or other pest outbreaks should such develop.

## ACKNOWLEDGMENTS

We thank Mike McWilliams, Oregon Department of Forestry; Floyd Freeman, U.S. Department of Agriculture Forest Service; and Bob Ohrn and Charlie Thompson, Salem and Eugene Bureau of Land Management. We also thank Jon Laine, Kevin Nelson, and Michael Thompson from Oregon Department of Forestry and field crews from the Salem and Eugene Bureau of Land Management and the Mt. Hood and Willamette National Forests for data collection and J.T. Marrs Contract Cutting for tree climbing and sampling.

## LITERATURE CITED

Filip, G.M.; Kanaskie, A.; Kavanagh, K. [and others]. 2000. Silviculture and Swiss needle cast: research and recommendations. Corvallis, OR: Oregon State University, Forest Research Laboratory. Research Contribution 30. 16 p.

Filip, G.; Kanaskie, A.; Littke, W. [and others]. 2012. Impacts of Swiss needle cast on Douglas-fir growth in the Cascade Foothills of northern Oregon after 10 years. In: Shaw, D., ed. Swiss Needle Cast Cooperative annual report. Corvallis, OR: College of Forestry, Oregon State University. 93 p.

Freeman, F. 2001. Swiss needle cast monitoring transects in the Oregon Cascades. In: Filip, G., ed. Swiss needle cast cooperative annual report. Corvallis, OR: Oregon State University, College of Forestry: 11-13.

Freeman, F. 2002. Swiss needle cast monitoring in the Oregon Cascades. In: Filip, G., ed. Swiss needle cast cooperative annual report. Corvallis, OR: Oregon State University, College of Forestry: 11-14.

Hansen, E.M.; Stone, J.K.; Capitano, B.R. [and others]. 2000. Incidence and impact of Swiss needle cast in forest plantations of Douglas-fir in coastal Oregon. Plant Disease. 84: 773-778.

Maguire, D.; Kanaskie, A.; Voelker, W. [and others]. 2002. Growth of young Douglas-fir plantations across a gradient in Swiss needle cast severity. Western Journal of Applied Forestry. 17(2): 86-95.

Maguire, D.A.; Mainwaring, D.B.; Kanaskie, A. 2011. Ten-year growth and mortality in young Douglas-fir stands experiencing a range in Swiss needle cast severity. Canadian Journal of Forest Research. 41: 2064-2076.

Mainwaring, D.B.; Maguire, D.A.; Kanaskie, A. [and others]. 2005. Growth responses to commercial thinning in Douglas-fir stands with varying severity of Swiss needle cast in Oregon, USA. Canadian Journal of Forest Research. 35: 2394-2402.

Shaw, D.C.; Filip, G.M.; Kanaskie, A. [and others]. 2011. Managing an epidemic of Swiss needle cast in the Douglas-fir region of Oregon: the role of the Swiss needle cast cooperative. Journal of Forestry. March: 109-119.

Winton, L.M.; Stone, J.K. 2004. Microsatellite population structure of *Phaeocryptopus gaeumannii* and pathogenicity of *P. gaeumannii* genotypes/lineages. In: Mainwaring, D., ed. Swiss needle cast cooperative annual report. Corvallis, OR: Oregon State University, College of Forestry: 42-48.

# ACKNOWLEDGMENTS

This research was supported in part through the projects "Forest Health Monitoring, Assessment, and Analysis" of Research Joint Venture Agreement 11-JV-11330146-090 (July 12, 2011, through May 31, 2013), "Forest Health Monitoring and Assessment" of Research Joint Venture Agreement 12-JV-11330146-063 (June 14, 2012, through April 30, 2014), and "Forest Health Monitoring, Analysis, and Assessment" of Research Joint Venture Agreement 13-JV-11330146-043 (July 23, 2013, through October 15, 2014), all between North Carolina State University (this institution is an equal opportunity provider) and the U.S. Department of Agriculture Forest Service, Southern Research Station, Asheville, NC. This research was supported by funds provided by the U.S. Department of Agriculture Forest Service, Southern Research Station, Asheville, NC.

The editors and authors of this report thank the following for their reviews and constructive comments: Phyllis Adams, Larry Scott Baggett, Margaret Devall, Marla Downing, Mark Fenn, Christopher Fettig, Stephen Fraedrich, Ellen Goheen, Katie Greenberg, Tom Hall, Andrea Hille, Steven Katovich, Olaf Kuegler, Albert "Bud" Mayfield, Bruce McCune, Randy McKenzie, Manfred Mielke, Amy Miller, Randall Morin, Daniel Omdal, KaDonna Randolph, John Paul Roccaforte, Annemarie Smith, Dale Starkey, Borys Tkacz, Denys Yemshanov, Andrew Yost, and Stan Zarnoch.

# AUTHOR INFORMATION

## SECTION 1, Analyses of Short-Term Forest Health Data; and SECTION 2, Analyses of Long-Term Forest Health Trends and Presentations of New Techniques


Mark J. Ambrose, Research Assistant, North Carolina State University, Department of Forestry and Environmental Resources, Raleigh, NC 27695.

John W. Coulston, Research Scientist, U.S. Department of Agriculture Forest Service, Southern Research Station, Knoxville, TN 37919.

Frank H. Koch, Research Ecologist, U.S. Department of Agriculture Forest Service, Southern Research Station, Research Triangle Park, NC 27709.

Sarah Jovan, Research Ecologist, U.S. Department of Agriculture Forest Service, Pacific Northwest Research Station, Portland, OR 97205.

Randall S. Morin, Research Forester, U.S. Department of Agriculture Forest Service, Northern Research Station, Newtown Square, PA 19073.

Jeanine L. Paschke, Geographic Information Systems Analyst, Sanborn, Fort Collins, CO 80526.

Kevin M. Potter, Research Associate Professor, North Carolina State University, Department of Forestry and Environmental Resources, Raleigh, NC 27695.

Kurt H. Riitters, Research Scientist, U.S. Department of Agriculture Forest Service, Southern Research Station, Eastern Forest Environmental Threat Assessment Center, Research Triangle Park, NC 27709.

William D. Smith, Research Scientist, U.S. Department of Agriculture Forest Service, Southern Research Station, Eastern Forest Environmental Threat Assessment Center, Research Triangle Park, NC 27709.

Susan Will-Wolf, Senior Scientist, University of Wisconsin-Madison, Department of Botany, Madison, WI 53706.

*Author Information, cont.*

## SECTION 3, Evaluation Monitoring Project Summaries


Kurt Allen, Entomologist, U.S. Department of Agriculture Forest Service, Forest Health Monitoring, Region 2, Rapid City, SD 57701.

Heidi Asbjornsen, Associate Professor, University of New Hampshire, Department of Natural Resources and the Environment, Durham, NH 03824.

T. Barrett, Research Forester, U.S. Department of Agriculture Forest Service, Pacific Northwest Research Station, Forestry Sciences Laboratory, Anchorage, AK 99503.

Chip Bates, Forest Health Coordinator, Georgia Forestry Commission, Statesboro, GA 30461.

John Browning, Forest Pathologist, Weyerhaeuser Forestry, Centralia, WA 98531.

Lars A. Brudvig, Assistant Professor, Michigan State University, Department of Plant Biology, East Lansing, MI 48824.

R. Scott Cameron, Forest Health Manager (retired), International Paper, and Georgia Forestry Commission, Richmond Hill, GA 31324.

J. Caouette (deceased), Statistician, The Nature Conservancy, Juneau, AK 99801.

Kristen L. Chadwick, Plant Pathologist, U.S. Department of Agriculture Forest Service, Forest Health Protection, Sandy, OR 97055.

Daniel C. Dey, Research Forester, U.S. Department of Agriculture Forest Service, Northern Research Station, Columbia, MO 65211.

Zhaofei Fan, Assistant Professor, Department of Forestry, College of Forest Resources, Mississippi State University, Mississippi State, MS 39672.

Gregory M. Filip, Regional Forest Pathologist, U.S. Department of Agriculture Forest Service, Forest Health Protection, Portland, OR 97208.

Linda Haugen, Plant Pathologist, U.S. Department of Agriculture Forest Service, Northeastern Area State and Private Forestry, St. Paul, MN 55108.

Paul Hennon, Research Pathologist, U.S. Department of Agriculture Forest Service, Pacific Northwest Research Station, Forestry Sciences Laboratory, Juneau, AK 99801.

Chad Hoffman, Assistant Professor, Department of Forest and Rangeland Stewardship, Colorado State University, Fort Collins, CO 80521.

James Johnson, Chief of Forest Management, Georgia Forestry Commission, Macon, GA 31202.

Jennifer Juzwik, Research Plant Pathologist, U.S. Department of Agriculture Forest Service, Northern Research Station, St. Paul, MN 55108.

Alan Kanaskie, Forest Pathologist, Oregon Department of Forestry, Salem, OR 97310.

Kathleen S. Knight, Research Ecologist, U.S. Department of Agriculture Forest Service, Northern Research Station, Delaware, OH 43015.

Will R. Littke, Forest Pathologist, Weyerhaeuser Forestry, Federal Way, WA 98063.

Joel Mcmillin, Entomologist, U.S. Department of Agriculture Forest Service, Forest Health Protection, Region 3, Flagstaff, AZ 86001.

Robin L. Mulvey, Plant Pathologist, U.S. Department of Agriculture Forest Service, Forest Health Protection, Juneau, AK 99801.

Ji-Hyun Park, Post-Doctoral Scientist, Korea Forest Research Institute, Seoul, Republic of Korea.

Kadonna Randolph, Mathematical Statistician, U.S. Department of Agriculture Forest Service, Southern Research Station, Knoxville, Tennessee 37919.

*Author Information, cont.*

Alejandro A. Royo, Research Ecologist, U.S. Department of Agriculture Forest Service, Northern Research Station, Irvine, PA 16329.

David C. Shaw, Forest Health Extension Specialist, Oregon State University, Corvallis, OR 97331.

Carolyn Sieg, Research Ecologist, U.S. Department of Agriculture Forest Service, Rocky Mountain Research Station, Flagstaff, AZ 86001.

Dustin Wittwer, Geospatial Services Specialist, U.S. Department of Agriculture Forest Service, Alaska Region, Juneau, AK 99801.

**Potter, Kevin M.; Conkling, Barbara L., eds**. 2014. Forest health monitoring: national status, trends, and analysis 2012. Gen. Tech. Rep. SRS-198. Asheville, NC: U.S. Department of Agriculture Forest Service, Southern Research Station. 192 p.

The annual national report of the Forest Health Monitoring Program of the Forest Service, U.S. Department of Agriculture, presents forest health status and trends from a national or multi-State regional perspective using a variety of sources, introduces new techniques for analyzing forest health data, and summarizes results of recently completed Evaluation Monitoring projects funded through the national Forest Health Monitoring Program. Survey data are used to identify geographic patterns of insect and disease activity. Satellite data are employed to detect geographic clusters of forest fire occurrence. Data collected by the Forest Inventory and Analysis Program of the Forest Service are employed to detect regional differences in tree mortality. Relationships are assessed between macrolichen species richness and forest density, forest connectivity, and land cover. Macrolichen data are also used to investigate the effects of precipitation on indices used to develop nitrogen critical loads. Nine recently completed Evaluation Monitoring projects are summarized, addressing forest health concerns at smaller scales.

**Keywords**—Drought, fire, forest health, forest insects and disease, lichens, tree mortality.

**Scan this code to submit your feedback, or go to www.srs.fs.usda.gov/pubeval**

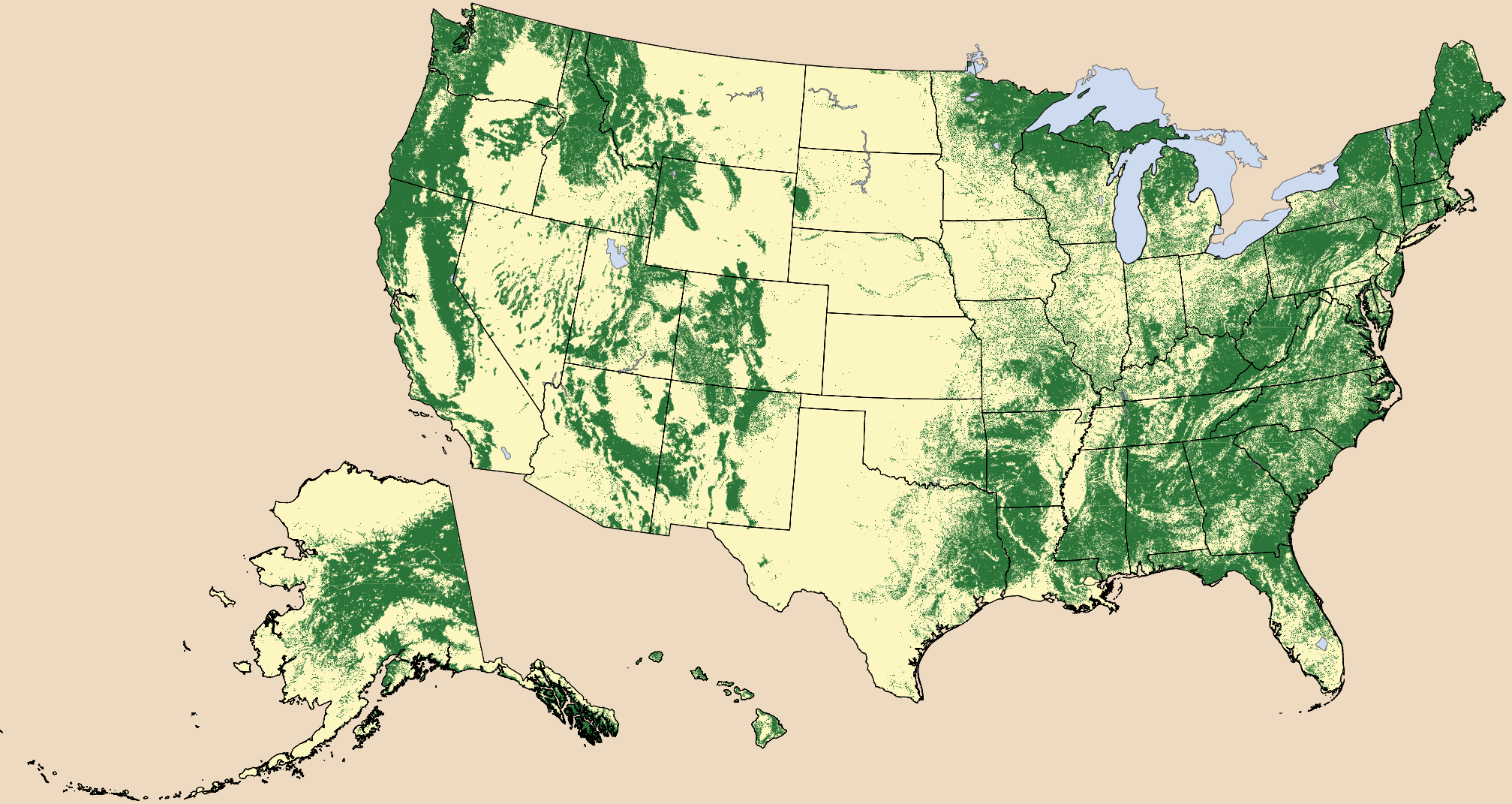

The Forest Service, United States Department of Agriculture (USDA), is dedicated to the principle of multiple use management of the Nation's forest resources for sustained yields of wood, water, forage, wildlife, and recreation. Through forestry research, cooperation with the States and private forest owners, and management of the National Forests and National Grasslands, it strives—as directed by Congress—to provide increasingly greater service to a growing Nation.

**Forest Health Monitoring:** National Status, Trends, and Analysis 2012

2014